Western Australian School of Mines

GLYCINE AS A LIXIVIANT FOR THE LEACHING OF LOW GRADE COPPER-GOLD ORES

Bennson Chemuta Tanda

This thesis is presented for the Degree of

Doctor of Philosophy

of

Curtin University

February 2017

Author's Declaration

To the best of my knowledge and belief, this thesis contains no material previously published by any other person except where due acknowledgment has been made.

This thesis contains no material which has been accepted for the award of any other degree or diploma in any university.

Signature: 

Date: 28-02-2017

List of Publications

Tanda, B. C., Eksteen, J. J., & Oraby, E. A. (2017). An Investigation into the Leaching Behaviour of Copper Oxide Minerals in Aqueous Alkaline Glycine Solutions. *Hydrometallurgy, 167*, 153-162

Tanda, B. C., Oraby, E. A., & Eksteen, J. J. (2017). Recovery of Copper from Alkaline Glycine Leach Solution Using Solvent Extraction. *Separation and Purification Technology, 187*, 389-396

Eksteen, J. J., Oraby, E. A., & Tanda, B. C. (2017). A Conceptual Process for Copper Extraction from Chalcopyrite in Alkaline Glycinate Solutions. *Minerals Engineering*, 108, 53-66

Oraby, E. A., Eksteen, J. J., & Tanda, B. C. (2017). Gold and Copper Leaching from Gold-Copper Ores and Concentrates Using a Synergistic Lixiviant Mixture of Glycine and Cyanide. *Hydrometallurgy, 169*, 339-345

Eksteen, J. J., Oraby, E. A., & Tanda, B. C. (2016). Developing Robust Hydrometallurgical Processes to Recover Metals from Deposits with Large Geometallurgical Variation. Paper presented at the The Third AusIMM International Geometallurgy Conference, Perth-Australia, 15-20

Eksteen, J. J., Oraby, E. A., & Tanda, B. C. (2016). An Alkaline Glycine Based Process for Copper Recovery and Iron Rejection from Chalcopyrite. Proceedings of the 46th Annual Hydrometallurgy Meeting and the 4th International Symposium of Iron Control in Hydrometallurgy. Eds. E.M.L. Peek, M. Buarzaiga, & J.E. Dutrizac. 11-15 September, Quebec City, Quebec, pp. 349-358

Abstract

In gold processing, resources that can be efficiently processed by the well-established cyanide process are in decline. Most recently, research focus has shifted towards the processing of low grade, complex ore bodies that contain impurities such as copper, arsenic, antimony, nickel and zinc which are detrimental to the cyanide process. Copper-containing gold ores are an important source of both copper and gold as they are obtainable in huge deposits in many countries throughout the world. The conventional cyanidation of gold ores is inefficient in the treatment of copper-gold ores since the presence of copper minerals results in increased reagent consumption (cyanide, lime and oxygen) and decreased gold dissolution rate. In addition to these technical challenges, the use of cyanide in the mining industry has been banned or restricted in some parts of the world due to its toxicity and the associated environmental concerns .

Glycine is an environmentally benign reagent which has been reported to form stable complexes with copper and gold. In this research, glycine, was investigated as a potential lixiviant for low grade copper-gold ores at alkaline pH. Although alkaline glycine solutions have been reported to selectively leach copper over gold from a copper flotation concentrate, the leaching behaviour of individual copper minerals in alkaline glycine solutions has not been studied. Also, there are no publications on the leaching kinetics of any copper minerals in the alkaline glycine system. Low grade copper–gold ores have not been leached in the proposed lixiviant system in order to establish the influence of process variables on copper and gold leaching and the deportment of impurity metals. Furthermore, no data has been published on the recovery of copper from alkaline glycine leach system. This research project is thus novel and will present a significant contribution to knowledge as it endeavours to fill the gaps in knowledge mentioned above.

Copper minerals were bottle rolled in alkaline glycine solutions under ambient conditions and the results revealed that, with the exception of chyrsocolla, copper oxide minerals leach more rapidly than their sulfide counterparts. Copper extractions from azurite, malachite, cuprite, chrysocolla, metallic copper, chalcocite and chalcopyrite were 97, 90, 94, 19, 92, 42, 6 %, respectively. However, during the leaching kinetic investigations for malachite, chalcocite and chalcopyrite carried out in a glass reactor whereby process variables could be controlled, higher copper extractions rates were obtained. Up to 99 % Cu was extracted from malachite in just 30 minutes. Leaching of a finely ground chalcocite (P_{80} 18 µm) resulted in

78 % Cu extraction in 48 hours. The leaching of a P_{100} of 10 µm chalcopyrite resulted in 90 % Cu extraction after 96 hours.

Copper speciation in the PLS identified Cu (II) ions as the stable Cu species that form the stable Cu-glycinate complex. Sulfur speciation of chalcopyrite PLS showed that, over 90.0 % of leached sulfur was in the form of sulfate (SO_4^{2-}). It was determined that chalcopyrite leaching was dominantly controlled by diffusion through the product layer. The leaching of copper from malachite and chalcocite was also noted to be controlled by diffusion through the product layer. It was also predicted that chalcocite leaches in two stages; the first stage involves the rapid dissolution of surface chalcocite leaving behind a covellite residue which leaches rather slowly in the second stage.

Copper-gold ores (oxides: Cu-Au ore A, sulfides: Cu-Au B and Cu-Au C) leaching in alkaline glycine solution revealed that, Cu and Au simultaneously leach from both ore types. However, Cu leaches faster than gold. Glycine concentration, temperature, initial leach solution pH, dissolved oxygen had no significant influence on copper dissolution from the gold-copper oxide ore as about 75.0 % was obtained for all variables after 96 hours of leaching. Over the same time, Au dissolution was significantly improved by increased temperature. At 60 °C , 32 % Au was leached while only 0.5 % was leached at 25 °C. Galvanic interactions caused by the addition of 20 g/t pyrite to the Au-Cu oxide ore led to 60 % Au dissolution which is a 36 % increase from that with no added pyrite. During the leaching of the Au-Cu sulfide ore, gold dissolution occurred concurrently with copper dissolution at 25 °C. This observation was attributed to galvanic interactions since the sulfide ore naturally contained pyrite. Increases in glycine concentration also improved the dissolution of both copper and gold from the sulfide ore. Upto 66 and 25 % Cu and Au, respectively, was leached from Cu-Au ore C (sulfide) after 96 hours in the glass reactor.

Copper recoverability from the glycine leached PLS was investigated by solvent extraction and and sulfide precipitation. Solvent extraction experiments using Mextral 84H (oxime) and Mextral 54-100 (diketone) at an Aqueous-to-Organic ratio (A:O) of 2:1, recovered 99 % and 96 % Cu, respectively make up solutions. Glycine was not extracted by either extractants and can thus be recycled to the leaching circuit. Copper was completely stripped with make-up spent electrolyte solution from Mextral 54-100, while only 80.0 % was stripped from Mextral 84H. Copper solvent extraction from ore leachates showed similar results. However, Zn , Co and Ni were simultaneously extracted with Cu although to a much lesser extent. Au is not extracted by either extractant.

Copper precipitation using sodium hydrogen sulfide (NaHS) showed that 99.0 % of copper was precipited at a Cu:S molar ratio of 1:1. The precipitate was identified by XRD analysis to be 100 % covellite with a particle size distribution of P_{80} 66 μm. As was the case with solvent extraction, Zn, Ni and Co that are concomitantly leached with copper are also prepecipited but to a much lesser extent than Cu. The gold content in solution was observed to be reduced by up to 16.2 % during copper precipitation.

The results obtained in this research enabled the development of flowsheets according to the type of ore being processed. Low grade ores are best processed by heap leaching, solvent extraction and electrowinning of copper. Any gold present in ore is simultaneously leached with the copper, and then recovered by activated carbon after solvent extraction of copper. For Cu-Au flotation concentrates, the feed is subjected to ultrafine grinding and then leached at elevated temperatures (60 °C) in tanks.

Acknowledgements

The achievement of this thesis is thanks to the significant contribution of many people. Most particularly, I would like to express my deepest and sincere thanks to my supervisors Professor Jacques Eksteen and Dr Elsayed Oraby for their guidance, tolerance, support, endurance and encouragement during this process. I immensely appreciate their enthusiasm and motivation which inspired me to conduct and complete this research.

My sincere gratitude goes to the all the members of the Gold Technology Group for all their encouragement and assistance throughout this project.

I acknowledge with thanks the financial support from Curtin University and the Gold Technology Group, without which the work presented in this thesis would not have been possible.

Last but not the least, I would like to express my wholehearted gratitude to my wife, Melvice Tanda, my daughter Lumafanwi Tanda, my entire family and friends whose support and love has been invaluable throughout this journey.

Table of Contents

List of Figures

List of Tables

List of Abbreviations

XRD	X-Ray Diffraction
XRF	X-Ray Fluorescence
TIMA	TESCAN Integrated Mineral Analyser
SEM	Scanning Electron Microscopy
XPS	X-Ray Photoelectron Spectroscopy
PLS	Pregnant Leach Solution
UV-Vis	Ultra Violet -Visible
AAS	Atomic Absorption Spectrometry
ICP-OES	Inductively Coupled Plasma- Optical Emission Spectroscopy
ICP-MS	Inductively Coupled Plasma- Mass Spectroscopy
HPLC	High Pressure Liquid Chromatography
Gly	Glycine
PS	Particle Size
SS	Stirring Speed
DO	Dissolved Oxygen
OD	Outside Diameter
WAD	Weak Acid Dissociable
E_A	Energy of Activation

Chapter 1 Introduction

1.1 Background to this study

High grade reserves with readily recoverable gold deposits are gradually being depleted (Zammit et al., 2012), leading to escalated interest in the mining and processing of low grade, complex and refractory resources. Copper can often be a valuable by-product of these ores.

Cyanidation has been the most extensively applied method for the recovery of gold from ores and concentrates for over a century. This is because cyanide forms very stable complexes with gold and is relatively selective leading to high gold recoveries. In addition, the process is robust and relatively low cost (Hilson & Monhemius, 2006b). Despite the popularity of the cyanidation process, it has been recorded to be suboptimal in treating refractory and polymetallic gold ores.

Refractory ores might have gold embedded in a mineral matrix or have components of the ore that adsorb/precipitate the dissolved metal as preg-robbing materials or complex species that consume the leaching agents (La Brooy et al., 1994). As a consequence of the continuous depletion of non-refractory and high grade gold ores, there has been a significant focus on processing complex low grade gold ores especially those containing easily soluble copper minerals. Copper-containing gold ores are an important source of both copper and gold as they are obtainable from many countries throughout the world including Australia, Chile, Philippines, Saudi Arabia, Canada, Argentina, USA, Indonesia, Peru, Mexico, Indonesia and China (Carlile & Mitchell, 1994; Green & Mueller, 1999; Sutulov, 1975; Wang et al., 2013). In Australia, such deposits are found in Boddington-WA; Telfer-WA; Browns Creek, NSW; Gabanintha-WA; and Red Dome-Qld, Olympic Dam-SA and Cadia Valley-NSW(Hsu et al., 1997).

Cyanide is a “one way” reagent that shows poor ability to recovery and re-use; indicating that it can be consumed in large amounts during the leaching of ores containing easily soluble copper minerals. Cu-Au ores typically have high Cu:Au ratios of 500:1 to 5000:1 implying high reagent use, particularly considering that CN:Cu ratios of greater than 4:1 are required to provide free CN for Au dissolution and suppression of Cu co-adsorption onto activated carbon. Due to the Weak Acid Dissociable (WAD) cyanide constraints on tailings, free and WAD cyanide must be detoxified, destroyed at a significant expense (Dai et al., 2012).

In addition to the challenges of cyanidation to treat copper-gold ores, cyanide toxicity is a health and environmental concern. The death of birds, animal and fish resulting from the use of cyanide by gold mines has been extensively reported (Jeffrey et al., 2002; Korte & Coulston, 1998). In the cyanide process, leachable copper has not only resulted in high cyanide consumption causing low recoveries but also forms weak acid dissociable (WAD) cyanide which is not easily amendable to natural degradation (Adams et al., 2008). Copper-cyanide complexes from the Romanian tailings dam disaster were traced for some 2000 km to the mouth of the Danube River(Korte et al., 2000). It is a result of these reported environmental and health issues that, governments and non-governmental organisations have encouraged the mining industry to develop alternatives to the cyanidation process. In Australia, more stringent policies have been put in place to hinder the construction of cyanide leaching plants (Jeffrey et al., 2002). The European Union has also adopted more stringent directives on the use of cyanide while some states in the United States have imposed a complete ban on cyanide usage in the mining industry. Both the technical difficulties of cyanidation of copper-gold ores and the toxicity of cyanide continue to motivate research into cyanide alternatives.

The development of an alternative process to cyanide leaching must therefore address both the health and environmental issues associated with cyanide, and also the difficulties of cyanidation to treat refractory and complex low grade copper-gold ores. Significant research undertaken to develop plausible substitutes to cyanide have cited lixiviants such as thiourea, halides, ammoniacal thiosulfate, nitriles, bisulfite, aqua-regia, and bacteria as potential alternatives (Aylmore, 2005; Hilson & Monhemius, 2006b; Molleman & Dreisinger, 2002; Senanayake, 2004; Sparrow & Woodcock, 1995; Syed, 2012). The applicability of most of the alternatives has been limited due to gaps in knowledge, cost of reagents, toxicity and the corrosive nature of some of the reagents.

The thiosulfate-copper-ammonia system, although considered a viable alternative technology because of its lower toxicity and having gold leaching rate comparable to that of cyanide, has been observed to have a very complex chemistry. Maintaining its stability under variable pH/Eh conditions is a critical draw back to its extensive application in the gold industry (Breuer & Jeffrey, 2000).

Less attention has been given to the use of organic acids as lixiviants in the mining industry and, in particular, gold extraction (Hilson & Monhemius, 2006b). The role of organic acids on the dissolution and transportation of gold in the soil, leading to the formation of gold

deposits has been reported by geochemists (Fetzer, 1934). Humic acid has been reported to act as a solvent for copper and gold by forming complexes with the metals (Baker, 1973, 1978; Fetzer, 1946).

It has also been noted (Groudev et al., 1995) that, during the biological leaching of gold from ores, the dissolution of gold occurred via gold-oxidising (peroxides) and gold complexing (amino acids) agents secreted by the bacteria. Some of the identified micro-bacterial synthesised amino acids are asparagine, glycine, aspartic, histamine, serine and phenylamine and alanine (Korobushkina et al., 1974). A study of the dissolution mechanism of gold and silver in glycine with peroxide as oxidising agent revealed that the reaction between glycine and gold produces a complex anion and the bonding was postulated to be between the carboxylic anions and the amino group nitrogen as a donor-acceptor (Mineev & Syrtlanova, 1984). It was established by Bogdanovskaya et al. (1986) that there is a chemical interaction between a gold electrode and glycine through the adsorption of glycine on the gold electrode in an alkaline environment. In the same way, amino acids have been reported to electrochemically dissolve silver through the formation of a silver amino acid complex (Safronov et al., 1983).

In the case of metallic copper, its interaction with amino acids (especially glycine) has been extensively reported in the electronics industry and biological systems, but such interactions are yet to be considered in the mining industry (where the copper is mineralised as oxides and sulfides). The chemical-mechanical planarization of copper in the presence of glycine and peroxide has drawn a lot of research in the production of copper interconnect semiconductors for integrated circuit boards (Aksu & Doyle, 2001, 2002; Chen et al., 2013; Seal et al., 2003; Zhang & Shankar, 2001). It has been shown that glycine acts as a chelating agent; rapidly forming irreversible complexes with copper ions oxidised by the peroxide. In a similar manner, the interaction between copper ions and proteins in biological systems has been established to be through the formation of coordinate bonds between copper and the functional groups on amino acids (Nunn et al., 1989; O'Brien & Nunn, 1982; Rubino & Franz, 2012; Thimann, 1932).

From the understanding that a prospective lixiviant for gold should be cheap or recyclable, selective, non-toxic and compatible to downstream recovery processes (Avraamides, 1982), glycine presents itself as a potential candidate to partially replace cyanide in the gold industry. Glycine is the smallest amino acid with the formula NH_2CH_2COOH. It is an odourless, sweet tasting crystalline solid with a solubility of 25g/100ml at 25°C. Toxicology information

on glycine via MSDS reports show that it is not toxic to humans or to the environment and there are no special requirements for its transportation as is the case with cyanide. It is used in food, pharmaceuticals and animal feed. Glycine can be synthesised industrially from chloro-acetic acid and ammonia.

In an aqueous medium, glycine generally exists as a zwitterion (Tortonda et al., 1996) making it stable in both acidic and basic environments. Feng and Van Deventer (2011) investigated the effects of amino acids L-valine, glycine, DL-α- alanine, L-histidine on the stability of the ammonical-thiosulfate system and observed that gold extraction from a pyrite concentrate was (using thiosulfate as the lixiviant) improved in the presence of these amino acids as they tend to form stronger complexes with copper than ammonia.

Scoping experiments done by Oraby and Eksteen (2013) to establish a frame work for glycine-gold leaching showed that the glycine-peroxide system can effectively leach pure gold and silver sheets. Observation, after 48 hours of gold leaching in solutions containing 0.5 M glycine and 1 % peroxide at pH 11, showed a leaching rate of 0.322 µmol/m^2.s. This rate is comparable to the 0.22-0.25 µmol/m^2.s gold leaching in thiosulfate-EDTA or thiosulfate-oxalate systems after six days of leaching. It was also proven that activated carbon could be used to recover gold and silver from the leach liquor. The gold–glycinate complex was found to be effectively loaded on activated carbon up to 13.2 g_{Au}/kg_{carbon} in 4 h (Oraby & Eksteen, 2015). The alkaline glycine system has been shown to selectively leach copper (ambient temperature and pressure) from a copper-gold concentrate (Oraby & Eksteen, 2014). Recently, it has been established that the alkaline glycine solutions can effectively leach copper from its ores while rejecting impurities such as iron, calcium and magnesium which can be detrimental to the leaching process (metal precipitation on heaps) and downstream processes such as solvent extraction (Tanda et al., 2017).

Glycine, with all its advantages mentioned, firmly positions itself as a promising alternative lixiviant for the economical processing of low grade copper-gold ores.

Although alkaline glycine solutions have been reported to leach copper from a float concentrate, no studies have been done on the leaching behaviour of individual copper minerals. The novel contribution of this research will be the studying and reporting of the leaching behaviour of individual copper minerals in alkaline glycine solutions. The response of gold-copper oxide and gold-copper sulfide ores towards varying process variables in the alkaline glycine solution has not previously been investigated. Additionally, the thesis

investigated the recovery of copper from the leach liquor solutions and also determined the deportment of glycine during metal recovery. This research project therefore endeavoured to understand the effect of process conditions and variables on the leaching of copper and gold from their resources using alkaline glycine solutions and also investigated possible methods for recovering gold and copper from their pregnant leach solutions.

1.2 Objectives and significance of this study

The main aim of this research project is to achieve the following objectives:

- To investigate and establish the leaching behaviour of copper minerals in the alkaline glycine solutions. The effects of process variables on the dissolution kinetics of copper from its oxide and sulfide minerals will be studied;
- To study the effects of process variables, additives and impurities on the dissolution of copper and gold from copper-gold ores;
- To evaluate different methods for metal, mainly copper recovery and the possibility to recycle the barren solution;
- To propose a technically feasible high level flow sheet to treat Cu-Au ores using glycine.

The attainment of the above objectives could have a meaningful influence in the copper and gold industry. The main significant outcomes would be:

- To introduce an environmentally benign process for treating various types of copper and gold ores;
- To enable the economic processing of gold ores having more than 0.5 % copper oxides, or 1.0 % copper sulfides;
- To enable treatment of ores which fall below cut-off grades for conventional processes;
- To provide a suitable reagent for the in-situ leaching of lean or placer gold deposits which are difficult to access but also allow the lixiviant to be recycled and reused and thereby significantly lowering costs.

1.3 Scope of this study

The scope of this research includes a range of topics related to the discipline of hydrometallurgy. The mineralogical and elemental assessment of the variety of mineral specimens and ores used was a critical aspect of the research.

As mentioned in Section 1.1, alkaline glycine solutions have been shown to selectively leach copper from its different minerals from a copper-gold concentrate. It was thus paramount to understand the leaching behaviour of different classes of copper minerals (oxides, secondary and primary sulfides) in alkaline glycine solutions under various glycine concentrations and solution pHs. Concomitantly, the metal dissolution-rates associated with leaching behaviour of the various copper minerals is inextricably tied to this leaching behaviour. Therefore, part of this study focuses on the leaching mechanisms and kinetics of a major copper oxide (malachite) as well as secondary (chalcocite) and primary sulfide (chalcopyrite) minerals in alkaline glycine solutions. The successful development and application of the glycine leaching system will depend on a detailed knowledge of the leaching mechanism. Characterization of the copper and sulfur species in solution and leach residues will provide the basis for explaining the reaction steps that contribute to the observed leaching behaviour of the copper minerals.

As the research topic indicates, glycine is being proposed as a lixiviant for copper-gold ores as their traditional processing method (direct cyanidation or acid leaching followed by cyanidation) poses economic and operability challenges. A portion of the research focuses on the effect of process variables such as reagent concentration, solution pH, and temperature on the dissolution of copper and/or gold from oxide and sulfide based copper-gold ores. Literature (European Innovation Partnership on Raw Materials, 2014; Norgate & Jahanshahi, 2010; VTT, 2016) has, however, indicated that, due to the continuous decline of high grade ores deposits, low grade complex ores have drawn a lot of research interests. One of the most economical method for processing such low grade ores is through heap leaching. Therefore, heap leaching simulation through column leaching experiments was conducted to deduce if the alkaline glycine solution could be used on heaps. The scope of the column experiments was restricted to preliminary investigations and not extended to the optimum conditions for dissolving copper and/or gold through heap leaching.

In order to consider the feasibility of alkaline glycine systems for leaching of copper and gold from its resources, it is imperative to study both the leachability of copper from its ores and

the recovery of vital metals from the PLS. Solvent extraction and metal sulfide precipitation were investigated as main methods for recovering copper from the pregnant leach solutions.

1.4 Thesis Overview

The thesis is divided into 8 chapters. An outline of the aspects covered by each chapter is given below:

Chapter 2 is dedicated to a detailed review of literature on the major aspects of the thesis. The importance of copper-gold ores and the influence of their mineralogy on processing have been discussed. Challenges of traditional processing techniques and limitations of current technologies to conquer these challenges will be reviewed. Attributes of good lixiviants and the advantages presented by glycine have also been presented. Lastly, leaching techniques applicable to low grade copper-gold ores have also been appraised.

Chapter 3 introduces the materials and reagents used throughout the project. The Chapter discusses experimental setup and methods to achieve the thesis objectives and finally covers the analytical methods used to reach the required results.

Chapter 4 presents the leaching behaviour of major copper minerals in the alkaline glycine solutions. The dissolution behaviour of impurity metals associated with the copper minerals will also be studied and reported.

Chapter 5 investigates the mechanisms and kinetics of copper leaching in the glycine system. It starts by giving a background on the importance of understanding the leaching mechanisms and the rate controlling stages. The effect of process variables on the leaching kinetics of malachite (oxides), chalcocite (secondary sulfide) and chalcopyrite (primary sulfide) are also presented.

Chapter 6 involves the study of the effects of process variables on the leaching of copper and gold from gold-copper oxide and gold-copper sulfide ores. Column leaching will be carried out to simulate the heap leaching technique for the low grade ores.

Chapter 7 explores the possibility of recovering copper from the pregnant leach solutions. The two techniques studied were solvent extraction and metal sulfide

precipitation. The fate of gold and other impurity elements concurrently leached with copper was tracked and reported.

Chapter 8 summarizes the major results obtained during this study and also outlines recommendations for further work.

Chapter 2 Review of Literature

2.1 Chapter Objective

This chapter reviews the available literature on the different aspects relating to the entire project. As the project endeavours to propose and develop a new leach process by utilizing a new lixiviant for low grade copper-gold ores, it is essential to first review the potential of copper-gold ores as a major source of future copper, gold and other valuable metals. The variation in copper-gold deposits and the influence of these variations on ore processing will also be reviewed.

There has been an extensive research on the challenges facing the processing of copper-gold ores and with numerous technological advances being proposed. Both the challenges and the process developments will be critically appraised.

Selecting a lixiviant for leaching a particular ore entails the consideration of ore structure and mineralogy, leaching techniques, the development of flowsheets, and environmental management. The attributes of a good lixiviant and the aspects to be considered for selecting a good leaching agent for a particular ore will be further elaborated in this chapter.

While proposing glycine as an alternative lixiviant for low grade copper-gold ores, it will be vital to indicate the physical and chemical properties of glycine establishing it as a candidate for the leaching of copper and gold from their ores.

Lastly, it is important to critically review the challenges of conventional leaching techniques that are being employed for low grade copper-gold ores.

2.2 Copper-Gold Resources

In an examination of various primary gold deposits, by Schartz (1994) found that native gold was intergrown with chalcopyrite in over 20% of the ores surveyed. Tetrahedrite, tennantite, bornite as well as chalcocite were also found to have significant associations within certain gold ores (Muir et al., 1989). Porphyry copper deposits are among the largest reservoirs of gold in the upper crust and are important potential sources for gold (Kesler et al., 2002; Sutulov, 1975) as they can contain up to 100t of gold (Kerrich et al., 2000). Sillitoe, (2010a) reported that as of 2010, three quarters of the world's Cu, one-fifth of Au and other valuable

metals come from porphyry copper systems. The close association of gold and copper is believed to have occurred due to the introduction of the two metals together during the early stages of alteration and mineralization. Secondary ion mass spectrometry (SIMS) was used at the Advanced Mineral Technology Laboratory in London, Ontario to determine the gold content of sulfide and oxide minerals in porphyry copper-gold deposits. The results indicated that gold is found in porphyry copper deposits as solid solution in both Cu-Fe and Cu sulfides and as small grains of native gold, commonly at bornite boundaries (Kesler et al., 2002). Porphyry copper deposits are obtainable in many regions of the world as shown in Figure 2.1

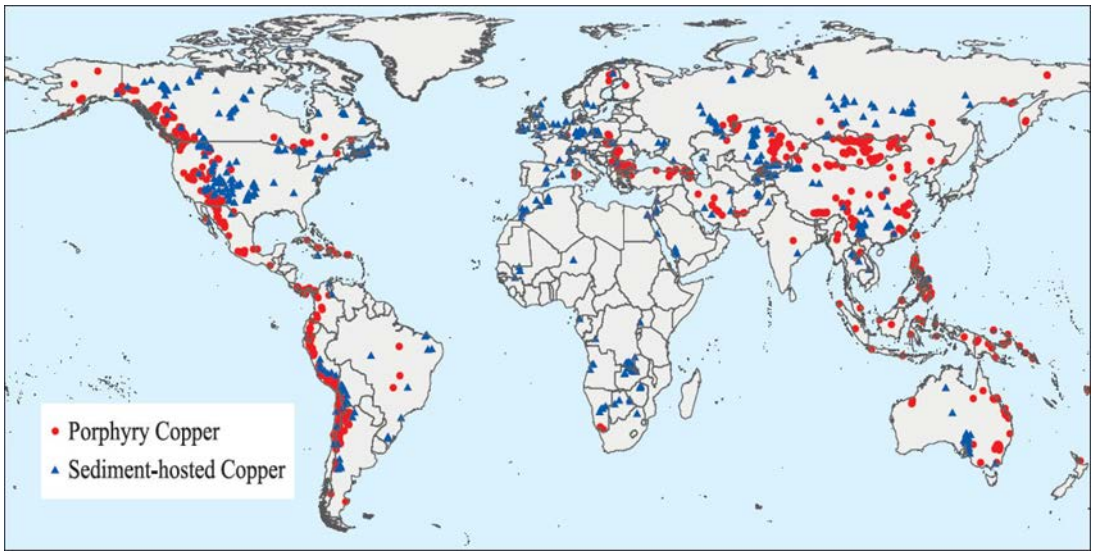

Figure 2.1 Mineralogical World distribution of porphyry copper deposits (Johnson et al., 2015)

According to an assessment of copper resources, the United States Geological Survey (2014), by 2100 million metric tons (Mt) of copper have been discovered with porphyry deposits making up 60% of the identified resources. South America, South central Asia and Indochina, and North America account for approximately 50 % the total global copper resources. However, the world's largest porphyry deposits are mined in South America. Other porphyry deposits are found in Central America and the Caribbean, North-central Asia, Northeast Asia, Eastern Europe, Southwestern Asia and Australia.

In Australia, such deposits are found in Boddington-WA; Telfer-WA; Browns Creek-NSW; Gabanintha-WA; and Red Dome, Qld, Olympic Dam-SA, Northparkes-NSW, Cadia Valley-NSW, Osborne-Qld, Ernest Henry-Qld, Ridgeway (Hsu et al., 1997; Geoscience Australia, 2007). Several large deposits containing significant resources of gold and copper mineralization in Porphyry copper-gold, skarn, and high sulfidation enargite-gold deposits

have also been found in Indonesia, e.g., Grasberg-Ertsberg, Frieda River district, and Wafi-Golpu (Carlile and Mitchell, 1994; Sillitoe, 2010b).

The quantity of undiscovered copper resources is postulated to be about twice the discovered with the mean total of undiscovered resources for porphyry deposits being 3500 million tons (United States Geological Survey, 2014). With porphyry deposits accounting for about 60% of the world's copper, they become a valuable potential for copper-gold extraction. Although porphyry deposits are generally large and contain millions of tonnes of ore, metal grades vary considerably but often average less than 1% for Cu and less than 1 g/t for Au.

2.2.1 Mineralogical variation in porphyry copper-gold deposits

The determination of mineral processing methods and techniques depends most importantly on the features and mineralogy of the ore. These characteristics result from a disparity in metal grain size distribution, mineralogical mode of gold occurrence, host and gangue mineral types, and mineral alterations (Marsden & House, 1992). In order to understand the mineralogical variations in porphyry deposits, many researchers have tried to establish a comprehensive definition for porphyry ores bodies that would incorporate geological, economics and engineering views (Sutulov, 1975). The geological definition of porphyry copper as being a disseminated copper mineralization in an acid igneous porphyric rock has been refuted by many as being incomplete for not incorporating economical and engineering aspects of the ore body. According to a number of publications(Bateman, 1952; Lowell, 1989; Parson, 1957; Titley, 1982), porphyry copper deposits bear common features such as low grade, large tonnage, disseminated replacements in porphyry, similar primary mineralogy, supergene enrichment and overlaid by leached oxide cappings.

The formation of porphyry copper deposits has been attributed to hydrothermal systems that developed in and around felsic intrusions and emplaced at relatively high levels in the crust. As magma rises through the earth's crust, it encounters pressure changes that cause the magma to crystalize releasing mineral rich water which flows into surrounding rocks through cracks and fractures leading to a vein-like mineralization (Briggs, 2014). Different porphyry copper deposits vary in terms of morphology and architecture (irregular, oval, cylindrical and inverted cup shapes), associated structures and mineralization styles (veins, vein sets, stockworks, fractures, crackled zones and breccia pipes), mineralogy, and

alterations (Bateman, 1952; Sinclair, 2007). The mineralogy of porphyry deposits is highly varied leading to the classing of deposits according to their principal component ores and associated minerals. Different porphyry subtypes are: Cu, Cu-Mo, Cu-Mo-Au, Cu-Au, Au, Mo, W-Mo, Sn, Sn-Ag, and Ag deposits. Alteration zones in many porphyry deposits are composed of inner potassic zone, an outer zone of propylitic alteration, phyllic (sericitic) and an argillic alteration zone (Sillitoe, 2000).

The alterations in a porphyry copper-gold deposit model are shown in Figure 2.2. Major zones are accordingly described.

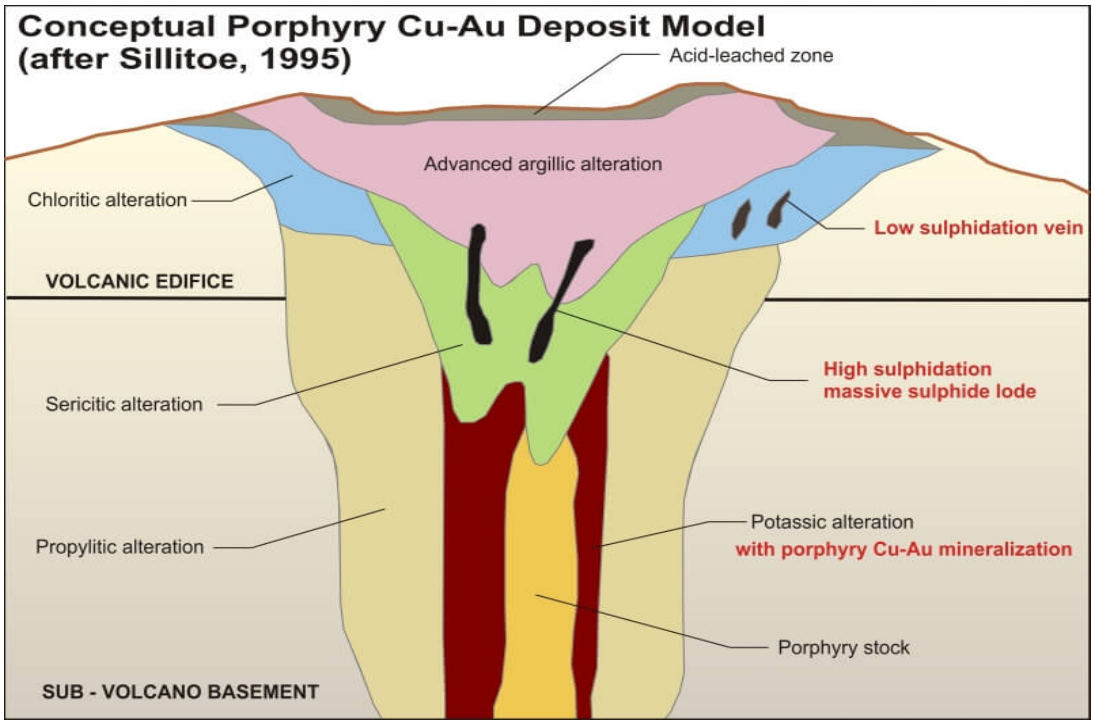

Figure 2.2 Alterations in a porphyry Cu-Au deposit model (Sillitoe, 1995).

- The argillic zone may have undergone weathering or leaching, supergene enrichment depending on the depth and location of the water table. This zone is generally clay-rich composing of quartz, illite, pyrite, kaolinite, smectite, montmorillite and calcite.
- Sericitic zone mostly composed of quartz, sericite and chlorite. Pyrite is associated with the main orebody and the veins are filled with quartz and other silicates.
- Potassic zone, characteriszed by K-feldspar, is composed of secondary biotite-muscovite-sericite-orthoclase feldspar-magnetite, associated with most of the ore in the stockwork as well as along veins and fractures.
- Propylitic zone contains a bigger range of alteration minerals as a result of its typical shallow depth and resultant higher degree of weathering. It is commonly composed of

quartz, sericite, pyrite, epidote-calcite and other clays (Holliday & Cooke, 2007).

These variations in the ore bodies significantly influence the applied mining and metal extraction processes (Sutulov, 1975). The four major zones obtained in porphyry copper deposits portray different mineralogy and textures and therefore require different processing approaches. Deciding on whether to mine a particular ore body by open-pit or underground mining technique depends on the nature and location of the deposit, the size, depth and grade of the deposit (Norgate & Haque, 2010). The influence of textual variation and gangue mineralogy of a porphyry ore on the recovery of copper was reviewed by Cropp et al. (2013). They stated that seven key mineralogical factors:

- The fine-grained copper minerals;
- Locked minerals in composite particles;
- Surface coatings on valuable minerals;
- Gangue composites;
- Entrained gangue;
- Activated gangue, and
- Deleterious element distribution control the flotation recovery of copper from porphyry ores.

Table 2.1, modified from Yildirim et al. (2014), shows the principal alteration and mineralization in a typical porphyry copper deposit and some of their influences on grind and float processes.

Table 2.1 Principal alteration types with mineralogy, impact on a grind float circuit modified from (Yildirim et al., 2014)

Alteration type	Position in system (abundance)	Key minerals	Principal sulfide assemblages (minor)	Expected effect on mill throughput	Expected effect on flotation
Potassic (K-silicate)	Copper zones of porphyry copper deposits	Biotite, K-feldspar	Pyrite, chalcopyrite, bornite, digenite and chalcocite	High	Low
Chlorite-sericite(sericite-clay-chlorite)	Upper parts of porphyry Cu core zone	Chlorite, sericite/illite, hematite	Pyrite, chalcopyrite	Moderate	Moderate
Sericite (phyllic)	Upper parts of porphyry Cu core zone	Quartz, sericite	Pyrite, chalcopyrite, enargite, tennantite, bornite, sphalerite	Moderate	Moderate
Advanced argillic	Above porphyry Cu deposits, constitutes lithocaps	Quartz, alunite, pyrophyllite, dickite, kaolinite	Pyrite, enargite, chalcocite, covellite	Low	High
Propylitic	Marginal parts of systems below lithocaps	Chlorite, epidote, albite, carbonate	Pyrite, sphalerite, galena	N/A	N/A
Sodic-calcic	Deep, including below porphyry Cu deposits (un-common)	Albite/ oligioclase, actinolite, magnetite	Typically absent	N/A	N/A

The geological and mineralogical variation of an ore body at different horizons as noted with porphyry copper deposits can radically influence leaching characteristics (Iasillo et al., 2013). The supergene zone at the top of most porphyry deposits consist of an upper oxidized layer referred to as the cap and an underlying sheet-like zone called the blanket zone. The cap is composed of Cu oxides, Cu carbonates, Cu sulfates, Cu chlorides, Cu silicates and native Cu while the blanket are mostly secondary copper and iron sulfides such as chalcocite, covellite, bornite, and remnants of chalcopyrite (Petruk, 2000). The difference in alterations is significant enough to warrant separate flowsheets for each ore type. The type of leaching agent and method depend on the type of ore. Copper oxide ores are easily leachable by sulfuric acid but when they contain huge amounts of carbonates, sulfuric acid leaching becomes uneconomical due its high reagent demand (Habashi, 1970). Such ores can be

processed by leaching with alkaline lixiviants such as ammonia and its derivatives or generally not exploited at all. Copper sulfide minerals are rather more difficult to leach requiring more aggressive conditions such as strong oxidizing agents and high temperatures. It is well known that chalcopyrite, although being the most abundant copper mineral, is also the most difficult to leach thereby attracting a high volume of research,(Nazari et al., 2011; Turkmen & Kaya, 2009).

2.3 Processing of Copper-Gold Ores

Copper-gold association in ore bodies can either be one that contains predominantly copper minerals with significant levels of gold mineralization or where the presence of copper is at nuisance levels to the gold deposit. Where the copper level dominates and copper can be recovered for its economic value (through grinding, flotation and smelting), gold is generally recovered as a by-product (slime) from the copper smelting and refining process. Gold can also be recovered from the flotation tailings by hydrometallurgical routes. The most economical approach for sulfide ores has been to produce a gold-copper flotation concentrate for metal recovery by smelting (Dunne, 1991).

On the other hand, where copper has no economic value, it poses serious problems to the conventional cyanide leaching of gold by consuming reagents and adversely affecting the downstream processes (Sceresini, 2005). It has been extensively researched and published by many researchers (Abbruzzese et al., 1995; Adams et al., 2008; Bas et al., 2012; Dai et al., 2012; Deschênes & Prud'homme, 1997; Jiang et al., 2013; La Brooy et al., 1991a; Muir, 2011; Muir et al., 1989; Sparrow & Woodcock, 1995) that the presence of copper minerals in gold ores poses significant problems during cyanidation of gold. These problems arise during leaching, recovery and purification stages. Typically, ores containing 0.3%-0.5% Cu in the form of oxide or >1 % Cu in the form of sulfide are not amenable to conventional cyanidation (Deng, 1995).

2.3.1 Copper-Gold Cyanidation Challenges

2.3.1.1 Leaching

During leaching, the presence of cyanide soluble copper can result in high cyanide consumption as well as low dissolution of gold. Most copper minerals are soluble in cyanide (Shantz & Reich, 1978) to various degrees. They form a series of complexes: CuCN, $[Cu(CN)_2]^-$

, $[Cu(CN)_3]^{2-}$, $[Cu(CN)_4]^{3-}$ whose equilibria in free cyanide and un-dissociated hydrocyanic acid is described by Equations 2.1 to 2.5.

$$Cu^{+} + CN^{-} = CuCN_{(s)} \qquad \log K = -20 \qquad (2.1)$$

$$CuCN + CN^{-} = [Cu(CN)_2]^{-} \qquad \log K = +24 \qquad (2.2)$$

$$[Cu(CN)_2]^{-} + CN^{-} = [Cu(CN)_3]^{2-} \qquad \log K = +5.3 \qquad (2.3)$$

$$[Cu(CN)_3]^{2-} + CN^{-} = [Cu(CN)_4]^{3-} \qquad \log K = +1.5 \qquad (2.4)$$

$$H^{+} + CN^{-} = HCN_{(aq)} \qquad \log K = -9.21 \qquad (2.5)$$

Lu et al. (2002) reviewed the aqueous chemistry of copper cyanide and reported that according to published data, the dissociation constants of the various complexes at 25 ° C, as shown in their respective equilibrium equations (2.1 to 2.5), are the most agreeable.

The predominant Cu-CN species in solution depend on the cyanide-copper ratio, temperature and pH. The Eh-pH diagram for Cu-CN-H_2O indicates that, under normal leaching conditions, $[Cu(CN)_3]^{2-}$ is the most common species in solution. As Cu (I) forms a very strong cyanide complex, it is generally recognized that CN:Cu molar ratio must be higher than 3:1 for gold leaching to start. Natural cyanide degradation at the tailing dam depletes free and weakly bound cyanide so that $[Cu(CN)_2]^{-}$ in recycle water will react with more free cyanide in leach liquor to form $[Cu(CN)_3]^{2-}$ and $[Cu(CN)_4]^{3-}$ (Sceresini, 2005). Thus, copper has to be removed from the leach circuit to maintain high amounts of free cyanide in solution. When the copper concentration in the recycling solution is high, the solution is considered to be fouled and its leaching efficiency decreases. This is particularly a problem when the minerals being processed have readily-soluble copper minerals such as azurite, malachite, cuprite, chalcocite and bornite (Alonso-González et al., 2009). It has been statistically shown by Jiang et al. (2001) that gold recovery and cyanide consumption are both linearly related to the soluble copper content (metallic copper, copper oxides and secondary copper sulfides). The solubility of different copper minerals in 0.099% NaCN at 23 and 45 °C is given in Table 2.2 (Hedley & Tabachnick, 1968).

Table 2.2 Solubility of copper minerals in 0.099 % NaCN solution (Hedley & Tabachnick, 1968)

Mineral	Formula	% Cu leached	
		At 23 °C	At 45 °C
Azurite	$2Cu(CO)_3.Cu(OH)_2$	94.5	100
Malachite	$2CuCO_3(OH)_2$	90.2	100
Chalcocite	Cu_2S	90.2	100
Metallic copper	Cu	90	100
Cuprite	Cu_2O	85.5	100
Bornite	$FeS.2Cu_2S.CuS$	70	100
Enargite	Cu_3AsS_4	65.8	75.1
Tetrahedrite	$(Cu, Fe,Ag,Zn)_{12}Sb_4S_{13}$	21.9	43.7
Chrysocolla	$CuSiO_3.nH_2O$	11.8	15.7
Chalcopyrite	$CuFeS_2$	5.6	8.2

Muir (2011) stated that copper bearing ores can consume up to 30 kg/ton NaCN for every 1% of reactive copper present. When copper sulfides such as covellite are present, cyanide consumption can reach 51 kg/ton due to the formation of thiocyanate and cyanate (Lower & Booth, 1965).

2.3.1.2 Recovery

Copper is precipitated along with gold and silver in the Merrill-Crowe process and consequently resulting in higher consumption of zinc dust (Parga et al., 2015). The removal of copper from the precipitate by digesting with sulfuric acid prior smelting is costly, time consuming and produces copper in an acidic medium which must be neutralized before disposal.

During the recovery of gold by CIL or CIP, copper competes with gold to adsorb on carbon and, under certain conditions, copper readily adsorbs onto activated carbon and displaces gold. At low pH values and low free cyanide concentrations, with $Cu(CN)_2^-$ predominant in solution, the kinetics of copper loading on activated carbon is enhanced.

In operations where water is hypersaline, it is impracticable to obtain pH values above 10 due to the magnesium precipitation which starts at pH 9.3 resulting in high alkali consumption to maintain high pH. Copper contamination in such situations presents serious problems due to the evident low pH that would favour copper adsorption (Sceresini, 2005).

Recovery of gold from copper–gold cyanide liquors by electrolysis is problematic due to the contamination of the final gold product by copper impurities.

In gold electrowinning, gold can be selectively electrowon over copper provided the molar ration of CN: Cu exceeds 3:1 (Muir et al., 1989). But if the activated carbon recovered from leach circuits has very high copper/gold ratio resulting from high concentrations of copper cyanide liquors, the clarified carbon eluates will also be rich in copper. The high concentration of copper-cyanide in the electrowinning cell results in the co-deposition of gold and copper which decreases the capacity of the electrowinning cell to plate gold and also affects adherence of deposited metal and flow of electrolyte through the cell by overloading the cathodes (Avraamides et al., 1992).

2.3.1.3 Effluent Treatment

Another problem that arises from the cyanidation of copper bearing gold ores is the level of tailings management. The biggest concern when processing copper containing ores is the discharge of copper cyanide complexes to the tailings dam because most metal complexes, including those of copper, are highly toxic to most forms of life. Copper cyanide complexes are significantly problematic as they are more stable than free cyanide ions (Strizhko et al., 2013) and thus not easily degradable by nature. The death of birds, animal and fish resulting from the use of cyanide by gold mines has been extensively reported (Jeffrey et al., 2002; Korte & Coulston, 1998). A good example of such a report is the collapse of the tailings dams at Omai in Guayana and Baia Mare in Romania leading to a cyanide spill. Copper-cyanide complexes from the Romanian disaster were traced for some 2000 km to the mouth of the Danube River (Korte et al., 2000). Although technological approaches are currently being used in the mineral processing industry for the detoxification of cyanide tailings (Dai et al., 2012), these elevate the overall processing cost and decrease profit margins.

2.3.1.4 Socio Economic – Adherence to the “Cyanide Code”

Apart from the challenges encountered during the cyanidation process, the use of cyanide also poses socio-economic challenges. The international cyanide management code for the gold industry (International Cyanide Management Institue, 2009) has outlined guidelines that must be adhered to during production, transportation, handling, operations, decommissioning, worker safety, emergency, training and dialogue.

Although a mining company may not be directly involved in the production, distribution and transportation of cyanide, it is the operator's responsibility to ensure that its contractors follow the cyanide code. Interruptions on operator's primary purchasing arrangements for cyanide can occur as a result of production or transportation problems beyond its control. It might then be necessary to purchase cyanide from alternate sources for a limited time to ensure continued gold production.

The cyanide code also requires operators to routinely initiate dialogue with stakeholders to discuss their cyanide management procedures and also provide an opportunity for the stakeholders to communicate issues of concern in direct and responsive manner (Logsdon et al., 1999). Mining companies involved in the use of cyanide are required to implement the cyanide code to maintain their licenses. Implementation of the code continues to add to the operational costs of companies.

2.3.2 Coping with Copper-Gold Cyanidation Challenges

Several approaches have been proposed to cope with the noted challenges occurring during the cyanidation of copper-gold ores. These approaches could be classified as those that seek to improve the cyanidation process and those that employ non cyanide based lixiviants to efficiently process copper in the copper-gold ores.

Table 2.3 presents technological solutions to cope with the presence of nuisance copper in copper-gold materials.

Table 2.3 Technological solutions to nuisance copper in gold ore cyanidation

Approach	Technology		Drawback	References
Cyanide based approach	Pre-treatment	Roasting	Added cost	Xu et al., 2014
		Oxidation ([1]chemical, [2]bio-oxidation)	Added cost	1 Dalton et al., 1991 2 Chiacchiarini et al., 2003
		Selective leaching of Cu		Muir, 2011
	Selective gold leaching	Ammoniacal-cyanide leaching	Lower recoveries as compared to cyanide only	Hayes & Corrans, 1992; Vukcevic, 1997; Hunt, 1901
	Selective recovery	Ion flotation of Au		Galvin et al., 1992; Malcolm et al., 1991
		Solvent extraction of Cu		Xie & Dreisinger, 2009
		Zinc cementation of (Cu)		Tran & Hsu, 1996
		Acid precipitation (Au)		Sorensen, 1988a, 1988b
	Tailings treatment	AVR	Added costs	Sceresini, 2005
		SART		Ford et al., 2008
		Cutech		Fleming, 2005
		Inco		Scott, 1981
		Augment		Xie et al., 2013
		Hannah		SGS Minerals Services, 2013
		Vitrokele		Tran et al., 2000
		Membrane filtration		Lombardi, 2008
		electrowinning (Cu)		Dai et al., 2012
Non-Cyanide based	Thiosulfate leaching		Complex chemistry and reagent degradation, problematic gold recovery, high reagent consumption	Breuer & Jeffrey, 2000; Jiang et al., 2013; Langhans Jr et al., 1992
	Thiourea leaching		High reagent use and cost	Hilson & Monhemius, 2006a; Lacoste-Bouchet et al., 1998
	Halides	Bromine-bromide	Un-economical as reagents are expensive. May be considered for concentrates	Muir et al., 1989
		Chlorine-chloride		Sparrow & Woodcock, 1995
		Iodine-iodide		Davis et al., 1993

2.4 Attributes of Good Lixiviants

Leaching is one of the most important unit operations in hydrometallurgical processing of minerals as its efficiency significantly influences the technical and economic success of a business (Crundwell, 2013). The leaching process involves the dissolution of minerals or metals in an aqueous solution. Generally, metals bound in minerals are transformed into metal ions that are released into an aqueous solution, i.e. immobilized metals become mobilized. The major objective of leaching is to maximize the valuable metal distribution to either the leach solution or the residue (solid phase) with desired characteristics (Gupta & Mukherjee, 1990). The choice of lixivant depends first and most importantly on the mineralogical composition of the ore material to be leached. According to Olubambi et al. (2006), the selection of optimum technical and economic routes for minerals requires a complete knowledge of the ore, especially its chemical and mineralogical compositions, relative amounts of minerals, and particle size distribution.

Water alone can solubilize many sulfates, chlorides and nitrates. Acids, however, are the most common leaching agents for oxides and sulfates. Sulfuric acid is the most commonly used acid because of its low cost, availability and low volatility as well as high chemical stability in aqueous solutions. The use of other acids, such as nitric and hydrochloric acids, is limited to specific systems owing to undesirable properties such as high costs, volatility, corrosiveness and indiscriminate gangue dissolution (Burkin, 2001). Alkaline lixivants are also used for leaching and the most common alkaline lixiviant is sodium hydroxide (used in the Bayer process). Alkaline ammonia and its derivatives are used on the basis of their target minerals selective dissolution. Certain salts such as sodium cyanide have been used for more than a century for the leaching of gold and silver (Burkin, 2001). Table 2.4 shows the commonly used leaching agents and their applications.

Table 2.4 Common leaching agents and their applications

Leaching agent type	Leaching agent	Application
Acids	diluted H_2SO_4	Copper oxides, zinc oxides
	diluted H_2SO_4 + oxidant	Copper sulfides, zinc and nickel sulfides, uranium oxide
	concentrated H_2SO_4	Sulfidic copper concentrates, nickel laterites
	HNO_3	Copper sulfides, nickel and molybdenum sulfides, Mo strap, uranium concentrates, zirconium oxides
	HCl	ilmenite, nickel matte, cassiterite
Bases	NaOH	Bauxite
	Na_2CO_3	Uranium oxides, scheelite
	NH_4OH + ammonia salts + oxygen	Copper sulfides, nickel sulfides, reduced laterites (Ni)
Salts	$Fe_2(SO_4)_3$, $FeCl_3$	Sulfidic concentrates of base metals
	$CuCl_2$	Sulfidic concentrates of base metals
	KCN (NaCN) + oxygen	Au and Ag, Cu effluents
	$FeSO_4$ + oxygen	effluents $FeSO_4$ + oxygen nickel sulfide
Chlorine (in water solution)	Aqueous chlorine, Chlorates(I)	Sulfidic concentrates of Ni, Cu, Zn, Pb, Hg, Mo, reduced laterites (Ni)
Water	water	Water soluble sulfates, chlorides, molybdates, vanadates, tungstates, perrhenates.

The selection of a suitable leaching reagent should consider the following factors (Avraamides, 1982):

- It should be selective and have high activity to dissolve components of interest rapidly enough to make commercial extractions possible;
- It should be inexpensive with the possibility to be produced in bulk industrial quantities;
- Compatible with downstream recovery process and also recyclable; and
- Environmentally friendly.

Gos and Rubo, (2001) outlined basic criteria which should be considered for selecting appropriate lixiviants for gold based on technical aspects, toxicity and economics. This is outlined in Table 2.5.

Table 2.5 Outline for selecting appropriate lixiviants for gold (Gos & Rubo)

Economics	Toxicity	Process Applicability
• Capital investment • Extraction economics • Availability • Costs considering detox/recycling	• Emissions • Handling • Environmental toxicity	• Limitations (e.g. ore type, selectivity, control, separation, etc.) • Recyclability • Detoxifiability • Large scale application (proven technology)

As presented in Table 2.5, a perfect lixiviant should therefore be economical, be applicable to most ore types, can be safely transported, handled and easy to detoxify or recycle. According to most researchers, of all the alternative lixiviants that have been proposed for leaching gold for example, there is none that fulfils all the criteria of an ideal lixiviant (Barbetti & Avraamides, 2003; DeVries & Hiskey, 1992; Gos & Rubo, 2001; Hilson & Monhemius, 2006b; Senanayake, 2004; Sparrow & Woodcock, 1995).

2.4.1 Attributes of Copper and/or Gold Ore Lixiviants

2.4.1.1 Acids

Sulfuric acid is the most widely used leaching agent for copper ores due to its affordability, its fast attack on oxidized ores, and the fact that it might be regenerated during the leaching of sulfate and sulfide minerals (Biswas & Davenport, 1976). Acids have rather been observed to be deficient in the leaching of ores containing calcium-magnesium carbonate as gangue material since these carbonates are very soluble in acids. The high dissolution of carbonates leads to the consumption of huge amounts of acid during the leaching of such ores; making the process uneconomical (Habashi, 1970, 1980; You-Cai et al., 2013). For acid leaching of carbonates (dolomite, calcite, ankerite), 1 ton of ore requires about 1 ton of H_2SO_4 (International Atomic Energy Agency, 2001). This makes the use of sulfuric for such ores uneconomical.

2.4.1.2 Ammonia

Ammonia and its derivatives, such as ammonium hydroxide, form stable complexes with some metal cations (cobalt, nickel and copper) through the nitrogen group and this has been observed to significantly enhance both the solubility and stability of the metals in solution

(Greenberg, 1951). It has also been reported that ammoniacal leaching selectively leaches metals of interest over gangue metals. Despite ammoniacal leaching having the advantage of selectivity leaching of target metals over impurities or gold, its use presents technical and environmental challenges which include its unpleasant odour detected even at low concentrations, its toxicity to aquatic organisms, and its adverse health effects such as corrosiveness to the respiratory track, and burning of the skin. According to the National Institute for Occupational Safety and Health (NIOSH), the threshold limit value for ammonia is 25 ppm for a normal 8-hour shift. Additionally, the volatility of ammonia leads to reagent loss. Ammonia can also be oxidised. These challenges have limited the application of the ammoniacal systems to enclosed agitated tank processes and precludes low grade leach options such as in-situ leaching or heap leaching.

2.4.1.3 Cyanide

Cyanidation has been the most extensively applied method for the recovery of gold from ores and concentrates for over a century. This is because cyanide forms very stable complexes with gold. Unlike WAD cyanide, the gold-cyanide complex is a strong acid dissociable (SAD) that requires strong acidic conditions (pH<2) to dissociate and release $HCN_{(g)}$. Also, gold cyanidation is relatively selective and this leads to high gold recoveries. The process is robust and relatively low cost (Hilson & Monhemius, 2006b). Despite the popularity of the cyanidation process, cyanide is a toxic reagent. If cyanide is not properly handled, i.e., solution pH not maintained above 9, HCN gas is produced which can result in human fatality if exposed. The death of birds, animals and fish in surrounding ecosystems to gold mine sites extensively reported (Jeffrey et al., 2002; Korte & Coulston, 1998). Also, the cyanidation process becomes uneconomical for many polymetallic ores.

Technically, the cyanidation process is ineffective in treating refractory and complex gold ores due to preg-robbing and high content of cyanide consuming minerals such as copper oxides (La Brooy et al., 1991b; La Brooy et al., 1994), unless preceeded with some form of ore or concentrate pretreatment.

2.4.1.4 Thiosulfate

The thiosulfate system has been considered the most viable alternative technology to cyanidation because of its low toxicity and also for having comparable gold leaching rate to that of cyanide, but has been noted to have a very complex chemistry. Maintaining its

stability under variable pH/Eh conditions is a critical drawback to its extensive application in the gold industry (Breuer & Jeffrey, 2000). Although thiosulfate is relatively available at reasonable price, the reported high reagent consumption of up 48.6 kg/t indicate that the extraction cost could be significantly higher than that of cyanidation. Also, high oxygen demand of four moles to a mole of thiosulfate increase the operating cost (Gos & Rubo, 2001). However, thiosulfate has its first commercial application at Barrick's Goldstrike operation in Nevada, USA for the processing of preg robbing gold ore (Vaikuntam et al., 2016).

2.4.1.5 Halides

The potential of chlorides, bromides and iodides to leach gold has been well established and pre-dates cyanidation (La Brooy et al., 1994). Gold extraction by halides is generally faster than in cyanide but extraction with halide-based systems comes at a higher cost (Free, 2013). Chloride and bromide systems need special construction equipment for their operation (Hilson & Monhemius, 2006b). The oxidants used in these halide systems are, however, the halogens of the halides themselves that all have lethal and occupational health standards higher than that of hydrogen cyanide. This high toxicity and consumption levels have hindered a significant consideration of halides as favourable alternatives to cyanide (Gos & Rubo, 2001).

2.5 Alkaline Ammoniacal Hydrometallurgy of Copper and Gold

It is well known that large, high grade ores which are normally processed by conventional pyrometallurgical processes are in continuous decline (Ata et al., 2001). Most research in hydrometallurgy is being tilted towards the processing of low-grade polymetallic ores which are normally not exploited due to the non-availability of cost effective technologies. The development of leaching-solvent extraction-electrowinning (L-SX-EW) processing route in the 1970's led to the commercial exploitation of such low grade ores (Prasad & Pandey, 1998). Currently, about 22 % of the world's copper is obtained via the L-SX-EW route (International Copper Study Group, 2013). In hydrometallurgy, acids especially sulfuric acid has been widely accepted as the most effective lixiviant for the extraction of base metals from their ores. However, acid interacts with various altered and layered silicates to solubilise a range of metallic cations (K^+, Na^+, Mg^{2+}, Al^{3+}, Ca^{2+}, Fe^{3+}, Mn^{2+}) as well as anions such as

sulfates (SO_4^{2-}) and halides (Cl^-, F^-) which are corrosive, and may leave behind silica gels. These silica gels, together with the accumulation of ions due to often prevalent water balance constraints, can cause severe operating challenges in solvent extraction circuits due to crud formation, necessitating expensive crud removal and purification systems. The high ion loading may also lead to significant water treatment and neutralisation costs. Many copper minerals are inherently alkaline (oxides, carbonates, hydroxyl-halides and basic sulfates), due to the surrounding host rock of gangue minerals.

Sulfuric acid, which is widely employed as the main lixiviant for leaching copper oxide minerals, has been observed to be infeasible for the leaching of ores containing high calcium-magnesium carbonate as gangue materials since these carbonates are very soluble in acids (Habashi, 1970; Pokrovsky et al., 2005; Vignes, 2013). Table 2.6 shows the acid consumption and estimated time to complete the dissolution of major carbonaceous materials in 10 g/L sulfuric acid solutions. It can be seen that for acid leaching, each 1 ton of carbonate minerals (dolomite, calcite, ankerite) requires about 1 ton of sulfuric acid.

Table 2.6 The acid consumption and estimated time to complete the dissolution of major materials in 10 g/L sulfuric acid solutions (International Atomic Energy Agency, 2001)

Minerals	Formula	Specific acid consumption, kg/t		Time for complete dissolution
		1 day	250 days	
Albite	$Na[AlSi_3O_8]$	0.3	1.6	100-150 years
Microcline	$K[AlSi_3O_8]$	0.6	0.2	100-150 years
Muscovite	$KAl_2(OH)_2 \cdot [AlSi_3O_{10}]$	1.6	7.0	~ 100 years
Biotite	$K(Mg,Fe)_2 \cdot [AlSi_3O_{10}] \cdot (OH,F)_2$	20.1	140.2	2-8 years
Vermiculite (hydromica)	$(Mg,Al,Fe)_3 \cdot (OH)_2$ $[(Si,Al)_4O_{10}] \cdot 4H_2O$	39.3	247.2	2-8 years
Kaolinite	$Al,_4\,(OH)_8[Si_4O_{10}]$	2.6	23.7	30-50 years
Montmorillonite	$(Ca,Na)(Mag,Al,Fe)_2$ $.(OH)_2[(Si,Al)_4O_{10}] \cdot nH_2O$	15.7	64.2	10-20 years
Chlorite	$(Mg,Fe)_{3-n}(Al,Fe^{3+})_n$ $/OH/_4Al_nSi_{2-n}O_5\ \ (n=0.3-1)$	18.9	138.9	1 day to 8 years
Carbonized organics		33.6	60.5	Over 10 years
Pyrite	FeS_2	2.5	2.8	
Calcite	$CaCO_3$	930	998	1-10 days
Dolomite	$Ca(Mg)[CO_3]_2$	980	1065	up to 10 days
Ankerite	$Ca(Mg,Fe)[CO_3]_2$	940	1026	3-8 days
Siderite	$FeCO_3$	262	920	8-10 days
Magnesite	$MgCO_3$	114	1149	3-4 months
Limonite	$Fe_2O_3 \cdot nH_2O(n=1-4)$			1-7 months

The presence of carbonates during acid heap leaching processes also results in the precipitation of gypsum ($CaSO_4 \cdot 2H_2O$) which reduces heap permeability and solution percolation as was observed at the Twin Buttes mine in Arizona (Bartlett, 1998). In addition, the large quantities of gypsum may coat and passivate precious metals. Acid also reacts with sulfide minerals present in the transition zone to form elemental sulfur which is problematic when precious metals are present due to surface passivation (particularly of silver and electrum) and significant cyanide consumption due to the elemental sulfur reacting with

cyanide to form the leaching inactive thiocyanate species. Moreover, the formation of jarosites, which can lock up silver in highly insoluble form, may lead to significant precious metal losses, as well as toxic heavy metal inclusions that may be remobilised during weathering of leach residues. In the recovery of valuable metals from deposits containing high acid consumable materials, an alkaline leaching medium presents lots of advantages over an acidic medium as being more selective, less corrosive, and with lower reagent consumption.

Considering the current trend of declining metals grades in ore deposits, the advantages of alkaline leaching cannot be over-emphasised. The most widely used and industrially applied alkaline leaching reagent for base metals and especially copper is ammonia and its derivatives. Ammonia leaching also serves as an important reference case and basis for comparison to the alkaline glycine leach approach. The ability of ammonia to dissolve metallic copper has been known for more than a century (Meng & Han, 1996; Reilly & Scott, 1977). By 1946, considerable research had been conducted to investigate the direct leaching of copper by aqueous ammonia solutions (Lane & McDonal, 1946). The Sheritt Gordon ammonia pressure leaching process has been extensively used for the leaching of nickel-copper concentrates (Biswas & Davenport, 1994) during which sulfide sulfur is converted to sulfate and copper recovery from PLS is by high pressure hydrogen reduction (Paynter, 1973). A modification of the Sheritt Gordon process, the Arbiter process, was the only commercialised ammoniacal leaching process for treating copper sulfide concentrates (Peters, 1992). It eliminated high pressures by employing the use of oxygen and vigorous agitation in order to achieve good oxygen dissolution. Copper was recovered by solvent extraction and not by precipitation as was the case with the Sheritt process (Paynter, 1973). Recently, MetaLeach Limited, has been testing and evaluating a proprietary ammonia based process, “Ammleach” for the selective extraction of base metals from their concentrates and amenable ore deposits (MetaLeach Limited, 2017). The major difference between the Ammleach process and previous ammoniacal processes is the introduction of the pre-treatment step which will be tailored for a specific ore deposit. It is claimed that the Ammleach process could be modified to cope with changing mineralogy that is often obtained in porphyry copper deposits.

Alkaline ammonia/oxygen processes are ideal when the host rock is acid consuming such (e.g., calcareous or dolomitic minerals) beacause they minimise reagent consumption. Additionally, alkaline leach systems alleviate corrosion problems observed in acidic systems

by limiting dissolution of impurity elements such as Fe and Mn that, if present in significant amounts in the leach liquor, will require adequate purification and controlled methodological recovery of the metals of interest (Bell et al., 1995; Paynter, 1973; Prasad & Pandey, 1998). These additional purification steps would increase operating costs.

In ammoniacal systems, dissolved metal ions have been observed to be stabilised in solution through the formation of soluble ammine complexes via the reactive nitrogen-containing group (Greenberg, 1951). Similarly, glycine, which is being proposed as the main lixiviant in this research is also known to dissolve metals from their ores via the formation of metal-glycinate complexes through its amino group (Aksu & Doyle, 2002; Bukharov et al., 2014). Both alkaline glycine and ammonia solutions (Park et al., 2007) act as buffer solutions further making the two systems very similar.

The similarities between the alkaline ammoniacal and alkaline glycine systems thus make it imperative for this thesis to review and understand the reaction chemistry and kinetics of copper and gold in alkaline ammoniacal systems. The review will elucidate the understanding of the leaching behaviour, mechanisms and kinetics of copper minerals and gold in the alkaline glycine solutions.

2.5.1 Aqueous Chemistry of Copper and Ammonia

Potential-pH diagrams which are used to present the thermodynamic behaviour of leaching systems (Radmehr et al., 2013) show the stability regions of chemical species present in the leaching solution. However, Eh-pH diagrams only illustrate thermodynamic relationships and do not give any information on reaction kinetics (Meng & Han, 1996).

For ammoniacal copper leaching systems, depending on the Eh and pH of the solution, either Cu(I) and Cu(II) amine species can exist in solution as shown in Figure 2.3 (Konishi, 2007; Xi et al., 2011). According to the Eh-pH diagram for $Cu–H_2O-NH_3$, Figure 2.3, the Cu (I) species, $Cu(NH_3)_2^+$, is stable between pH 5 – 12 and Eh between -0.2 to 0.2 V. The Cu(II) species, $Cu(NH_3)_4^{2+}$ is stable between pH 8.5 -11.5 and Eh between -0.15 and 1.3 V. However, on comparing the stability constants of $Cu(NH_3)_2^+$ being $3.8*10^{10}$ and that of $Cu(NH_3)_4^{2+}$ being $4.8 *10^{12}$ (Chmielewski et al., 2009), the cupric ion is thermodynamically more stable in solution.

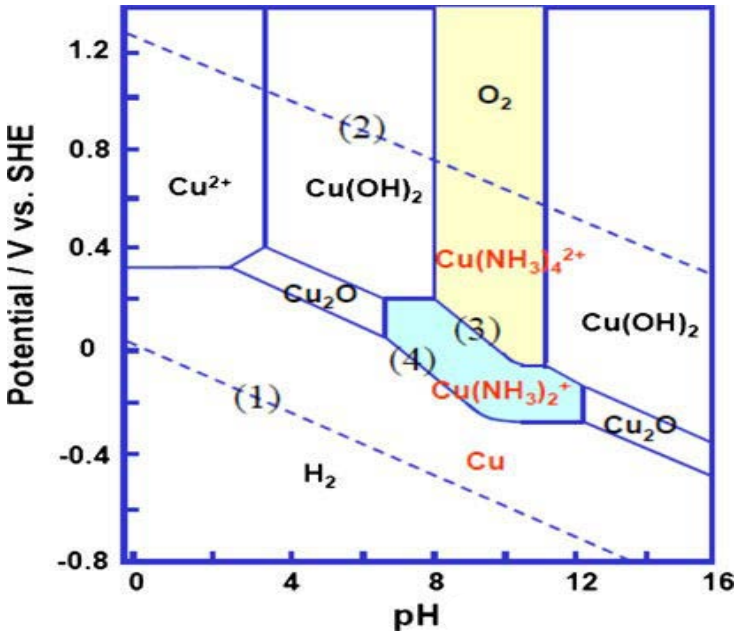

Figure 2.3 Potential-pH diagram of Cu-NH_3-H_2O system: 25 °C, Cu activity of 0.5 and [NH3] of 7 kmol/L (Konishi, 2007)

2.5.1.1 Kinetics of Metallic Copper Dissolution in Ammoniacal Solutions

Copper reacts readily with aqueous ammonia in the presence of oxygen, as shown in Equation 2.6:

$$Cu + ½\ 0_2 + 4NH_3 + H_2O \rightarrow Cu(NH_3)_4^{2+} + 2OH^- \qquad (2.6)$$

Halpern (1953) studied the dissolution kinetics of metallic copper in ammonia –ammonium solutions over a wide range of NH_3 and NH_4^+ concentrations, oxygen pressures, temperatures and stirring speeds. He noted that, at low oxygen pressure, copper dissolution rate was limited by the transport of oxygen to the surface while, at increased oxygen pressure, surface chemical reaction limited copper dissolution rate.

The dissolution rate of metallic copper plate in aqueous cupric ammine solutions was studied by Uchida et al. (1996) at 0.05-1.0 mol $CuSO_4$ concentration, 0-3000 rpm rotation speed and temperatures between 10-90°C. They found that copper dissolution increases with an increase in temperature and rotation speed, while a maximum rate was observed with increasing Cu(II) concentration. They concluded that, at temperatures below 30 °C copper dissolution rate was mainly controlled by chemical reaction while, at temperatures higher than 40 °C, diffusion of cupric complex was the rate controlling step.

2.5.1.2 Kinetics of Malachite Leaching in Ammoniacal Solutions

Malachite, being the most common copper oxide mineral and easily amenable to alkaline leaching, has attracted a substantial amount of research on its leaching kinetics by ammonia/ammonium salt solutions such as $(NH_4)_2CO_3$, $(NH_4)_2SO_4$ or NH_4Cl (Wang et al., 2009).

Bingöl et al. (2005) examined the leaching of malachite with aqueous ammonia/ammonium carbonate solution at 25 °C, solid to liquid ratio of 1:10, stirring speed of 300 rpm, particle size less than 450 µm, and observed that up to 98 % of copper was extracted in 120 minutes with very limited dissolution of impurity gangue minerals. Other researchers (D'Aloya & Nikoloski, 2012; Liu et al., 2012a; Oudenne & Olson, 1983a; Wang etal., 2009; Yartaşi & Çopur, 1996) have also established that ammonia solutions are suitable for leaching carbonaceous copper ores due to their ability to selectively leach copper over the carbonaceous gangue. The leaching kinetics of malachite was examined in water saturated ammonia gas by Arzutug et al. (2004) and it was found that the leaching rate fitted a pseudo-second order kinetic model with an E_a of 85.16 kJ/mol. On investigating the dissolution kinetics of malachite in ammonium chloride solutions, Yartaşi and Çopur (1996) noted that the reaction was controlled by diffusion through the product film with a required E_a of 81.3 kJ/mol.

Oudenne and Olson (1983b) conducted experiments to investigate the leaching kinetics of malachite in ammonium carbonate solutions. They found that the leaching process occurred in two reaction stages with rapid dissolution of malachite occurring in the first 10 % of the first stage which then decreased due to the formation of needle-structured $Cu(OH)_2$ intermediate. Stage two reactions involved the dissolution of the intermediate product which occurs only after all pure malachite has been dissolved. E_a's for the first and second stages were 64 kJ/mol and 75 kJ/mol, respectively. Künkül et al. (1994) observed that the kinetics of malachite leaching in ammonia solutions is controlled by the diffusion through the product layer with the E_a determined to be 22.338 kJ/mol. On evaluating the leaching kinetics of a low-grade copper ore containing Ca-Mg carbonate in ammonia-ammonium sulfate with persulfate, Liu et al. (2012b) used the shrinking core model and showed that the leaching rate is influenced by both interfacial transfer and diffusion across the product layer requiring an E_a of 22.91 kJ/mol. The contribution of process variables on the dissolution kinetics of malachite ore in ammonium chloride solution was studied by Ekmekyapar et al. (2003). The results indicated an increase in the dissolution kinetics when reaction temperature,

ammonium chloride concentration, and stirring speeds were increased. The E_a for the process was stated as 71 kJ/mol and the dissolution model was established to be mixed kinetics.

Recently, copper dissolution from a malachite ore in ammonium nitrate solutions was reported by Ekmekyapar et al. (2012) to be a mixed kinetic model, including both surface chemical control (30 to 50 °C) and diffusion through a porous ash product layer (50 to 70 °C). It was noted that the sequential stages had E_a's of 95.10 kJ/mol and 29.50 kJ/mol, respectively. A kinetic study performed by Künkül et al. (2013) on the dissolution of malachite in ammonium acetate reported the leaching process to follow a mixed kinetic control model with a calculated E_a of 59.6 kJ/mol.

The overall reaction of malachite and ammonia is as illustrated by Equation 2.7:

$$CuCO_3.Cu(OH)_2 + 8NH_3 \rightarrow 2[Cu(NH_3)_4]^{2+} + CO_3^{2-} + 2OH^- \quad (2.7)$$

2.5.1.3 Kinetics of Chalcocite Leaching in Ammoniacal solutions

According to Salvador (1978), chalcocite leaching in a low-pressure, oxygen ammonia system occurs in two stages. In the first stage, chalcocite is rapidly converted to soluble cupric ions and a blue-remaining covellite. The residual covellite material then leaches at a much slower rate in the second stage producing more cupric ions and sulfate. In the first stage and below 35 °C, copper dissolution is initially controlled by surface chemical reaction (E_a of 66.94 kJ/mol) and then by diffusion through the product layer with an E_a of 55.65 kJ/mol. Above 35 °C, and during the first stage, copper dissolution is controlled by a diffusion process with a calculated Ea of 25.94 kJ/mol. In the second stage, copper dissolution is controlled by an electrochemical model in which the rate is proportional to the concentration of oxygen and hydroxide ion concentration and independent of initial surface area. The estimated apparent E_a for the second stage is 46.86 kJ/mol.

Filmer et al. (1979) modelled the kinetics of chalcocite (Cu_2S) to covellite (CuS) in buffered aqueous ammonia solution at pH 10.5 using the shrinking core of the Cu_2S within a thickening shell of $Cu_xS(X\geq1)$. Their main objective was to determine the nature and role of any diffusion-controlling solid state films which are formed on chalcocite and covellite on the dissolution rate. They noted that diffusion of cupric ions through the Cu_xS controls the reaction rate. The oxidation of covellite to cupric ions, sulfur and sulfate is controlled by mixed chemical and

diffusion models. It was noted that the presence of sulfur, if any, does not influence rate or oxidation mechanism.

Chalcocite generally reacts with ammonia according to equation 2.8:

$$Cu_2S + 4NH_3 + ½O_2 + H_2O = CuS + Cu(NH_3)_4^{2+} + 2OH^- \quad (2.8)$$

2.5.1.4 Kinetics of Chalcopyrite Leaching in Ammoniacal Solutions

Chalcopyrite is the most abundant copper containing mineral (Dutrizac, 1978; Watling, 2013) accounting for about 70 % of world copper reserves (Córdoba et al., 2008). Ironically, chalcopyrite is also the most recalcitrant or refractory of the copper minerals to hydrometallurgical processes due to its inertness in aqueous systems (Haver & Wong, 1971). Because of its abundance and difficulties encountered during its processing, chalcopyrite is one of the most investigated copper minerals (Li et al., 2013b).

XPS analysis by Brion (1980) found that when ground chalcopyrite is exposed to air for a few minutes, iron hydroxide/oxyhydroxide is formed. This is followed by the formation of a basic iron sulfate which increases with time. Prolonged exposure results in a reduction of the concentration of surface copper.

Gardner and Woods (1979) noticed that, during the oxidation of chalcopyrite in basic and neutral mediums, ferric hydroxide is the main component of the surface layer. It was also affirmed by Zachwieja et al. (1989) that a hydrated iron hydroxide layer is formed in air-saturated alkaline solutions. Yin et al. (1995), investigated the electrochemical oxidation of chalcopyrite with different electrolytes and concluded from XPS data that, the type of passivation layers formed depended on the solution pH and applied potential. The composition of the surface layer in alkaline solution (pH 9.2) was CuS_2 and Fe_2O_3 at potentials lower than 540 mV SHE while S^0, CuO and Fe_2O_3 were formed at potentials greater than 740 mV SHE. It was, however, noticed that the passivation effect was less noticeable in weakly acidic of pH 6.8 or strongly alkaline solutions of pH 13 (Yin et al., 1995).

Reiley and Scott (1977) investigated the rate of chalcopyrite dissolution in ammoniacal solution under the following conditions 50-95 °C, oxygen pressure of 689 kPa and $[NH_3]$ of 2.5 – 7.0 mol/L. They used an electrochemical surface reaction model to dtermine that oxygen reduction on the solid surface is the rate determining step requiring an E_a of 74.1 kJ/mol.

During a study of the dissolution of chalcopyrite in different ammonium salt solutions, Moyo and Petersen (2016) observed that different surface products arise from different solutions. Ammonium sulfate and ammonium perchlorate solutions resulted in the formation of Fe-oxyhydroxide layer with moderate sulfur, ammonium-ammonium carbonate resulted in no surface layer formation although a marginal amount of iron was found on the mineral surface. The reaction kinetics were influenced by the formation of surface products indicating that reaction kinetics and passivation must be studied concomitantly.

Beckstead and Miller (1977) investigated chalcopyrite leaching using mono-size particles in stirred reactor at dilute solid phase concentration so that oxygen transport at the gas/liquid interface would not limit the rate. They reported that the reaction kinetics is controlled by a catalytic electrochemical surface reaction with a calculated E_a of 41.84 kJ/mol.

The leaching kinetics of chalcopyrite in ammonium iodide solutions with iodine studied by Guan and Han (1997) using the rotating disk method revealed that the leaching rate was limited by an electrochemical reaction. At temperatures between 16 and 35 °C, the E_a of was 50 kJ/mol while between 35 and 60 °C, it was estimated to be 30.3 kJ/mol .

According to Das and Anand (1995), the ability of ammonia-ammonium sulfate solution to leach copper while rejecting iron is believed to occur through the initial leaching of Fe(II) which subsequently oxidises and then precipitates as Fe(III) oxides in sodium hydroxide environments. Reduction of oxygen on the surface was assumed to be rapid with the slow step being the diffusion of dissolved oxygen from the bulk solution phase to the solid surface.

Chalcopyrite leaching in oxygenated ammonia solutions can be presented by Equation 2.9

$$CuFeS_2 + 4NH_3 + 17/4O_2 + 2OH^- \rightarrow Cu(NH_3)_4^{2+} + 1/2Fe_2O_3 + 2SO_4^{2-} + H_2O \quad (2.9)$$

2.5.1.5 Aqueous Chemistry of Gold- Ammonia System and Kinetics of Gold Dissolution in Ammoniacal Solutions

The Eh-pH diagram of Au-NH_3-H_2O in Figure 2.4 shows that Au^+ and Au^{3+} can react with ammonia to form $Au(NH_3)_2^+$ and $Au(NH_3)_4^{3+}$ complexes, respectively. The wide pH stability range of the ionic gold species indicate that gold can be dissolved in ammoniacal solutions even at room temperature (Dasgupta et al., 1997). However, only $Au(NH_3)_2^+$ is predominant

within the stablity region of water (Meng & Han, 1996).

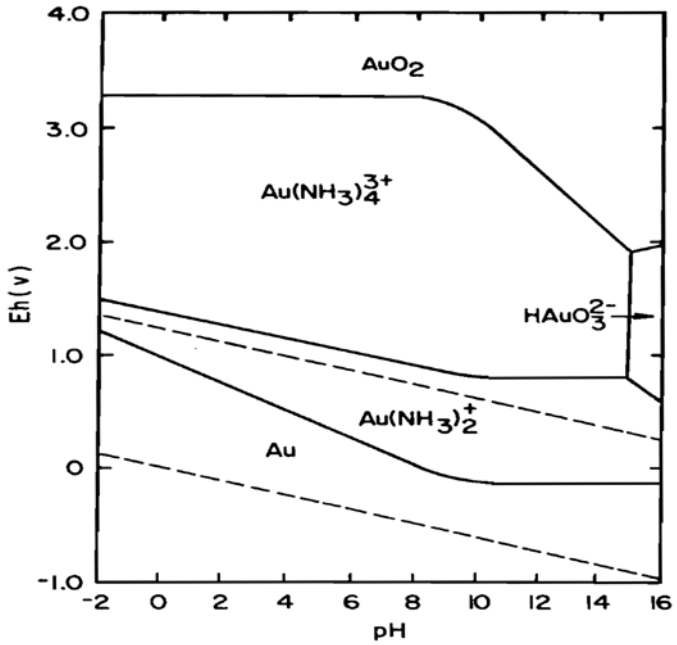

Figure 2.4 Eh-pH diagram for Au- NH_3-H_2O system: 25 °C, 101.3 kPa, activity of ions 10-4, [NH_3] of 1.0 M (Meng & Han, 1996)

A review on gold dissolution in ammoniacal solutions by Meng and Han (1996) indicated that gold dissolution is only significant at temperatures higher than 80 °C. Oxygen was found to be an effective oxidant even though it has a low solubility in aqueous solutions. The order of the oxidation ability for investigated ionic oxidants was $Cu^{2+} > Co^{2+} > OCl^-$. Gold dissolution in the ammonia solution was predicted to be limited by the electrochemical transfer of electrons. Depending on experimental conditions, calculated apparent E_a is in the range of 47.1-86.2 kJ/mol. Han and Fuerstenau (2000) studied the influence of factors on gold dissolution rate in ammoniacal solutions and confirmed that gold dissolution practically does not occur unless the temperature is raised to at least 80 °C and more practically above 120 °C. They also noted that, although cupric ammine is an effective oxidant for gold dissolution, iodine was the most effective because it acts as both an oxidant and a complexing agent. Additionally, iodine could be regenerated in the presence of oxygen. At temperatures between 160-200 °C, up to 95 % gold could be extracted in ammonia/ammonium solutions within 1-2 hours of leaching.

The general reaction equation between gold and ammonia is presented in Equation 2.10

$$2Au + 4NH_3 + 1/2O_2 + H_2O \rightarrow 2Au(NH_3)_2^+ + 2OH^- \quad (2.10)$$

2.5.2 Metal Recovery from Ammoniacal PLS

2.5.2.1 Copper

Copper recovery from alkaline ammoniacal solutions adaptoed the solvent extraction approach. Solvent extraction was first introduced into the mining industry in the late 1940s for the processing of uranium solutions. The success of these operations initiated the transfer of the technology to the treatment of copper pregnant leach solutions (PLS) in 1969. Solvent extraction involves the mixing the PLS (containing the desired metal, usually in low concentrations and accompanied with other impurity metals) with an immiscible organic solution containing an extractant. The reaction between the extractant and the desired metal forms a chemical compound which is soluble in the organic solvent. The immiscible solutions are then separated and the loaded organic solvent is mixed with another aqueous phase to produce a more concentrated and pure aqueous solution of the metal of interest (stripping) while the organic solvent (raffinate) is recovered and recycled back into the extraction process (Gálvez et al., 2004; Gupta & Mukherjee, 1990).

In the solvent extraction of copper from ammoniacal solutions, a variety of extractants have been tested and applied industrially to recover copper (Meng & Han, 1996). In Anaconda's Arbiter Plant and BHP's Coloso plant in Chile, after leaching, the slurry was filtered and copper was solvent extracted by LIX-64N. The loaded organic was then stripped by sulfuric acid and electrowon to give metallic copper. Ammonia was recovered by lime addition to the raffinate with gypsum precipitation (Radmehr et al., 2013; Wang et al., 2009).

LIX64N was noted to have low copper extraction capacity and also significantly transfers ammonia onto the organic phase and this hampered its further application (Jergensen, 1999). LIX84 which has been very successful in extracting copper from acidic solutions has been reported to exhibit high copper extraction from ammonia solutions (more than 50 g/L) but, unfortunately, also picks up ammonia. In such cases, ammonia needs to be scrubbed in order to prevent the accumulation of and precipitation of ammonium sulfate during the electrolytic process (Parija & Sarma, 2000). In 1995, LIX54, a beta diketone which had shown high copper loading ability from its ammoniacal leach solutions with low ammonia transfer, was used at a pilot plant in Escondia-Chile. It was, however, realised that the keto group of the LIX54 extratant deteriorated over time due to its reaction with ammonia to produce a ketamine. Copper stripping from the organic phase became very challenging and the pilot plant was eventually closed down (Hu et al., 2010).

Using sterically hindered beta-diketone, Hu et al. (2010) were able to show that, at 25 °C upwards of 95.09 % of copper could be extracted from ammoniacal solutions while only 14.5 mg/L of ammonia was detected in the organic phase.

2.5.2.2 Gold

Investigations on the recovery of gold from ammoniacal solutions have mostly focused on adsorption by activated carbon and ion exchangers. However, ion exchange resins containing selective functional groups have been widely tested for noble metal-ions separation from various solutions (Pilśniak & Trochimczuk, 2007; Pilśniak et al., 2009). Woźniak et al. (2008) observed that the diamine Au(I) cationic complex from ammonia solution could be adsorbed onto alpha zirconium(IV) bismonohydrogen phosphate intercalated with butylamine. On testing a series of synthesised resins for gold adsorption from ammoniacal solutions, Pilśniak and Trochimczuk (2007) found that 1-methylimidazole resin shows the highest affinity towards gold with as high as 15.5 mg_{Au}/g_{resin} sorption from a 100 g/dm^3 NH_4OH, 50 g/dm^3 $(NH_4)_2SO_4$ solution in the presence of copper.

2.5.3 Challenges of Ammonia Leaching

Despite ammoniacal leaching medium having the advantage of selectivity leaching of copper, it has many technical, operational and environmental challenges. Some of these challenges include its volatility, its noxious odour detected even at low concentrations, its toxicity to aquatic organisms, and its adverse health effects such as corrosiveness to the respiratory track and burning of the skin. The conventional suite of alkaline lixiviants, such as ammonia and its derivatives, is very limited particularly when reagent consumption is significant as obtained with oxidised base metal ores. Ammonia also has problems, volatility, high lixiviant to base metal stoichiometric requirements, recovery and recycle, and ease of oxidation.

These challenges have limited the application of the ammoniacal system, especially in the heap leaching of low grade ores and other open systems (vat leach and in-situ leach). Ammonia is not well received by nearby communities and the use thereof may face significant legislative hurdles. These reagents are particularly unsuitable for base metal extraction through heap leaching, which is often seen as the only viable alternative to treat low grade oxide and transition ore deposits.

To improve copper recovery from ammoniacal solutions, there is a continuous search for

extractants that can efficiently load high concentrations of copper from solutions while rejecting ammonia.

As a result of the aforementioned limitations of ammonia leaching, and with the acceptance that alkaline leaching is the way forward for processing low grade ores (which are rather becoming a norm in the mineral industry), the motivation of this research which proposes glycine as an alkaline lixiviant for leaching low-grade copper gold ores is further justified. The following section discusses the properties and the aqueous copper/gold- glycine chemistry.

2.6 Glycine as Copper and Gold Lixiviant

2.6.1 Structure, Physical and Chemical Properties

Glycine or aminoacetic acid is the simplest amino acid. As indicated by their name, amino acids are organic compounds containing both a carboxyl group (-COOH) and an amino group ($-NH_2$) bonded to the same carbon atom in α position. The distinguishing factor for different amino acids is the side chain denoted as R, which in turn governs the properties of the amino acid. The general structure of an amino acid is given by Figure 2.5.

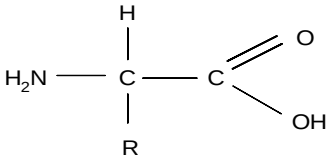

Figure 2.5 General structure of amino acid

Glycine (2- aminoacetic acid) is the simplest amino acid having a hydrogen atom as a side chain, H_2N-CH_2-COOH(de Farias et al., 1999).

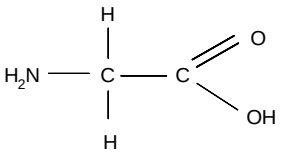

Figure 2.6 Structure of glycine

Glycine is characterised as follows (Wade, 2013):

- Colourless, odourless, sweet crystalline solid in pure form;
- Soluble in water (25 g/100mL at 25 °C), acids, alkalis but not soluble in organic solvents

(0.038 g/100mL) (Fleck & Petrosyan, 2014);

- High melting point of 262 °C and decomposition point 292 °C (Huang et al., 2013); and
- Optically inactive because of the two hydrogen atoms at the alpha carbon (Chan et al., 2006; Nelson & Cox, 2013).

2.6.2 Industrial Applications of Glycine

The applications of glycine can be found in pharmaceuticals, medicine, agronomy, nutrition and some metal processing applications (Drauz et al., 2000; United States International Trade Commission, 2008). The following points summarize the uses and applications of glycine in different industrial fields:

- Taste enhancer and sweetener in food production industries;
- Buffering agent in cosmetics, most deodorants and antiperspirants;
- Dietary supplement as restorative iron supplements for humans are produced from an Fe-glycine complex;
- Chelating agent in crop production for cationic micronutrients and also as a fertilizer source of nitrogen;
- Pharmaceuticals and medicine in intravenous injections, for treatment of schizophrenia (Tsai et al., 1998), stroke, benign prostatic hyperplasia. Glycine in combination with other amino acids used to heal wounds and treat ulcers.
- Main ingredient in the production of Glyphosate (N-phosphonomethyl-glycine which is the most widely used herbicide worldwide (Nicolia et al., 2014), and is manufactured by Monsanto sold as “Roundup”; and
- Levelling agent in acidic electroplating of Cu(Aksu & Doyle, 2001) and Zn-Fe (Karahan, 2013) to produce smoother deposits by modifying the structure and topography .

2.6.3 Glycine Production

Glycine can be produced through chemical synthesis or from the hydrolysis of natural compounds that have high levels of protein (Couriol et al., 1999). Chemical synthesis is the main method of producing glycine industrially as it is more economical. Common chemical synthesis methods for glycine are: Bucher method, the Strecker method and the ammonolysis of monochloroacetic acid (MCA). The most widely used pathways for producing glycine industrially are the Strecker and MCA-ammonia methods.

The Strecker method involves the reaction of formaldehyde with ammonia and hydrogen cyanide to form aminoacetonitrile (Equation 2.11) which is then hydrolysed to produce glycine (Fujiwara et al., 1993; Koch et al., 2008). This is one of the simplest and most economical methods of producing glycine both in the laboratory and on an industrial scale (Cai & Xie, 2014).

$$RCHO + NH_3 + HCN \rightarrow NH_2RHCCN + H_2O \rightarrow NH_2RCOOH \quad (2.11)$$

Ammonolysis of monochloroacetic (MCA) acid proceeds with the neutralization of MCA by ammonia to produce an ammonium salt of MCA. This salt is then reacted with hexamethylenetetramine to produce a quaternary ammonium salt and ammonium chloride as co-product. The quaternary ammonium salt is further ammonolysed leading to the production of glycine and hexamethylenetetramine. These reactions are illustrated by Equations 2.12, 2.13 and 2.14:

$$ClCH_2COOH + NH_3 \rightarrow ClCH_2COO^- + NH_4^+ \quad (2.12)$$

$$C_6H_{12}N_4 + ClCH_2COO^- + NH_4^+ \rightarrow [C_6H_{11}N_4^+ - CH_2\text{-}COO^-] + NH_4Cl \quad (2.13)$$

$$[C_6H_{11}N_4^+ - CH_2COO^-] + NH_3 \rightarrow C_6H_{12}N_4 + H_3N^+CH_2COO^- \quad (2.14)$$

The ammonolysis of MCA produces a higher quality product and does not require hazardous reagents like the Strecker method.

2.6.4 Aqueous Chemistry of Glycine

Glycine occurs as an amphoteric agent in aqueous solution acting as an acid (proton donor) and a base (proton acceptor) depending on the solution pH. Below the pH of 2.35; the glycinium cation $^+H_3NCH_2COOH$ (H_2L) is predominant. The zwitterion $^+H_3NCH_2COO^-$(HL) is stable between the pH of 2.35 to 9.78. When the pH is above 9.78 the glycinate anion $H_2NCH_2COO^-$(L) is predominant. Energetically, the zwitterion is more stable both in solid state and in solution (Rega et al., 1998; Smith & Martell, 1989; Tortonda et al., 1996; United States International Trade Commission, 2008). The association of these monomeric species results from the formation of hydrogen-bonds between them in concentrated solutions while their stability in dilute solutions is ensured by the formation of hydrogen bonds with water molecules. Apart from the monomeric proton complexes, polymeric associated forms like

$[HL_2]^-$, H_2L_2 and $[H_3L_2]^+$ might exist in highly concentrated solution (Kiss et al., 1991). During the titration of glycine, two equilibrium reactions occur with each having its own dissociation constant (pK_a) value (Equations 2.15 and. 2.16).

$$^+H_3NCH_2COOH_{(aq)} \leftrightarrows {}^+H_3NCH_2COO^-_{(aq)} + H^+_{(aq)} \quad pK_{a1} = 2.34 \tag{2.14}$$

$$^+H_3NCH_2COO^-_{(aq)} \leftrightarrows H_2NCH_2COO^-_{(aq)} + H^+_{(aq)} \quad pK_{a2} = 9.6 \tag{2.15}$$

The titration curve for glycine with NaOH shown in Figure 2.7, is unique to glycine and can be used to identify the presence of glycine in solution as each amino acid has its own distinctive titration curve

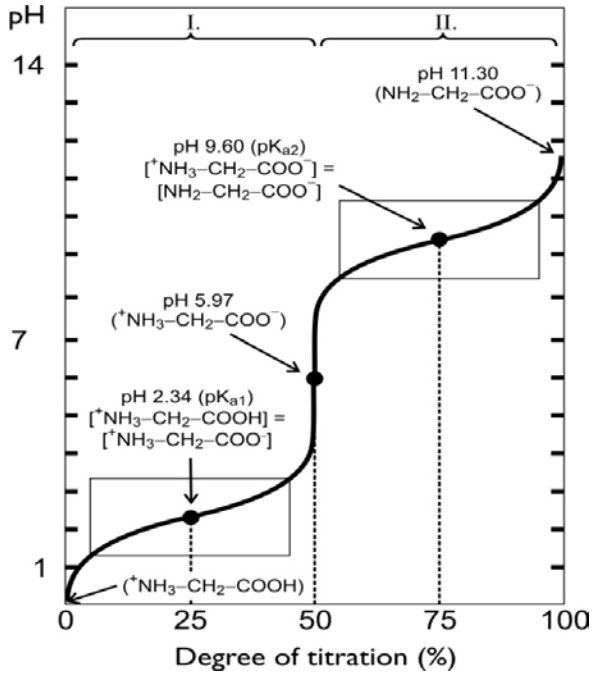

Figure 2.7 Titration curve of a 0.1 M glycine solution with NaOH. Frames indicate pH plateaus (Hegyi et al., 2013)

In the presence of strong oxidizing agents, the amino group is attacked and converted into an iminocarboxylic acid. This iminocarboxylic is unstable and can be further hydrolysed to an oxocarboxylic acid which then undergoes decarboxlylation to produce ammonia and aldehyde (Drauz et al., 2000).

The oxidation of glycine by both one-electron oxidants (e.g., Mn^{3+}, $Fe(CN)_6^{3-}$, two-electron oxidants (e.g., $K_2S_2O_8$) and multi-electron oxidants (e.g., $KBrO_3$, $Mn(H_2O)_3^{2+}$, $KMnO_4$) have been reported to generally produce formaldehyde, carbon dioxide and ammonia although minor products are formed from different oxidizing agents (Insausti et al., 1992; Sarathi et al., 2005). Ozone and hydroxyl radicals (•OH) were reported by Berger et al. (1999) to oxidize

glycine where the hydroxyal radical is unchanged, derived from the breakdown of hydrogen proxide, and should not be confused with the hyroxyl anion). The products formed from molecular ozonation of glycine were ammonia, nitrites and nitrates while ammonium ions, oxalic acid and formic acid were produced from hydroxyl radical decomposition of glycine.

It is important to point out that no research to date has shown oxidative degradation of glycine with dissolved oxygen. However, the studies above clearly indicate that, in the presence of sufficiently strong oxidants, glycine can be degraded and destroyed.

In the presence of bacteria such as cell suspensions of Proteus and Pseudomonas aeruginosa, glycine can be aerobically oxidised to ammonia, carbon dioxide, cyanide and water (Campbell, 1955; Wissing, 1974). However, this oxidation process could be inhibited by pyrrolnitrin (Wissing, 1974).

Glycine has also been observed to undergo oxidation on platinum and gold electrodes in acidic, neutral and basic solutions (Chia et al., 2013; Marangoni et al., 1989). Cyclic voltammetry analysis of glycine adsorption on Au electrode in 0.1 M phosphate buffer at room temperature indicated irreversible oxidation of glycine at $E > 0.6$ V. The main products of the electrolytic oxidation of glycine include: ammonia, formaldehyde, formic acid, carbon dioxide, cyanide, carbon monoxide, and methyl, dimethyl, and trimethyl amines. According to Marangoni et al., (1988), the main product of electro-oxidation of glycine under both acidic and basic conditions is formaldehyde. In basic glycine solutions, they calculated the thermodynamic potential for which glycine oxidation occurs to be 1.33 V, $E_{SCE.}$ They noted that the potential corresponds to that at oxygen evolution. Thus, the electrochemical oxidation of glycine in alkaline medium occurs when the solution potential is higher than that for H_2O/O_2 decomposition.

If free amino acids are heated above 200°C, especially in the presence of soda lime or metal ions, they readily decarboxylate to form amines (Drauz et al., 2007).

Glycine has the ability to form complexes (acting as chelating ligand) with metals through the oxygen atom of the carboxylic group and the nitrogen atom of the amine group. These groups can simultaneously form two bonds with metals by donating a pair of electrons. Glycine has been observed to form complexes with copper, gold, silver, arsenic, cobalt, vanadium (Kajala & Gupta, 2009; Khorrami et al., 1996; Remko & Rode, 2006; Uvdal et al., 1990).

2.6.4.1 Aqueous Chemistry of Copper and Glycine

In the semiconducting industry, copper is increasingly being used as an interconnect metal in integrated circuit boards due to its high electrical conductivity. Chemical-mechanical planarization (CMP) is a method which proceeds by the mechanical removal of surface layers and the dissolution of the abraded particles in CMP solution. The chemical composition of the CMP fluid is important as it needs to facilitate oxidation and removal of excess copper (Deshpande et al., 2004). The new model of using peroxide and glycine as CMP solution has led many researchers to investigate the fundamental interaction between the different chemical constituents in the solution (Aksu & Doyle, 2001, 2002; Chen et al., 2013; Green & Jeffrey J. Mueller, 1999; Du et al., 2004; Seal et al., 2003; Tianbao et al., 2004; Tripathi et al., 2010; Zhang & Shankar, 2001). The proposed mechanism is that the peroxide oxidizes the copper and the oxidized copper ions form a stable, water soluble Cu-glycinate complex (Tianbao et al., 2004). It was observed that, in either acidic or basic medium, the dissolution of copper increased as the glycine concentration was increased while an increase in hydrogen peroxide concentration beyond 0.25 wt % H_2O_2 led to a decrease in copper dissolution (Aksu & Doyle, 2003). As it can be seen in Figure 2.8, the copper glycinate complex is stable over a wide pH range (2.6 – 12). The major copper(II) glycinate complexes are: $Cu(H_3NCH_2COO)^{2+}$ ($CuHL^{2+}$), $Cu(H_2NCH_2COO)^{+}$ (CuL^{+}) and $Cu(H_2NCH_2COO)_2$ (CuL_2), while the predominant copper(I) complex is $Cu(H_2NCH_2COO)_2^{-}$ (CuL_2^{-}).

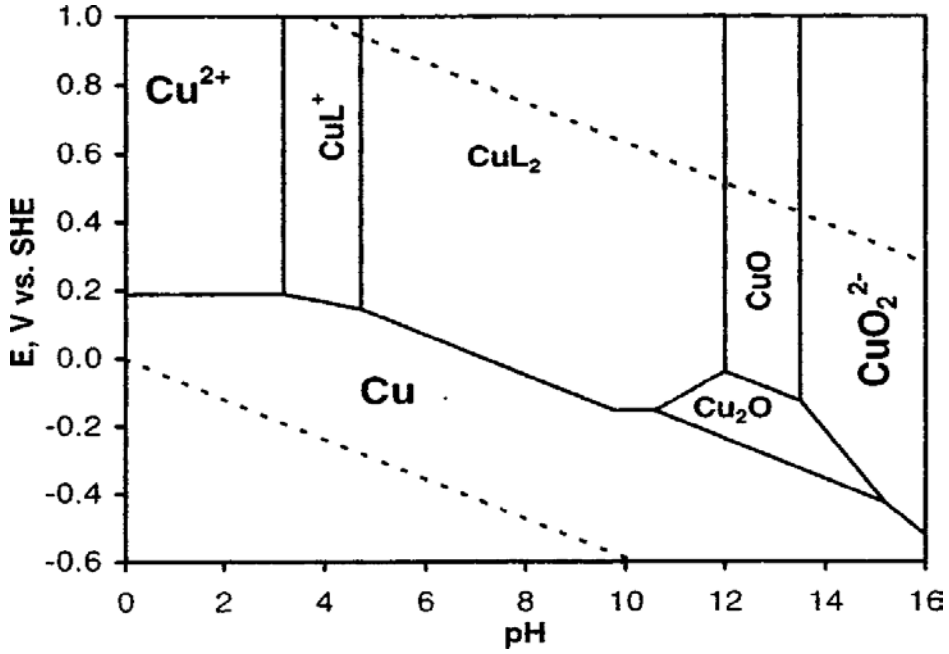

Figure 2.8 Eh-pH diagram for copper-water-glycine system at a total dissolved copper activity of 10^{-5} and total glycine activity of 10^{-2} at 25℃ and 1 atm (Aksu et al., 2003).

Table 2.7 indicates the stability constants of Cu (I) and Cu(II) glycinate complexes.

Table 2.7 Copper glycine complexes and their stability constants (Aksu & Doyle, 2001)

Copper ion	Copper-glycine complex	log*K*
Cu^{2+}	$Cu(H_2NCH_2COO)_2$	15.6
Cu^{+}	$Cu(H_2NCH_2COO)_2^{-}$	10.1
Cu^{2+}	$Cu(H_2NCH_2COO)^{+}$	8.6

The copper glycinate complex has been identified in biological systems, especially in enzymes where it occurs in active sites. This has led to a huge research to understand the mechanisms of interaction between the cupric ions and amino acids which act as the medium for transporting copper in living organisms (Bukharov et al., 2014). In an earlier investigation, Bukharov et al. (2012) determined the mechanisms and effectiveness of chemical reactions and studied the rotational dynamics of copper(II) amino complexes by electron paramagnetic resonance (EPR) and nuclear magnetic resonance (NMR) relaxation methods and observed that the trans isomer of $Cu(Gly)_2$ is the dominant species in solution.

The solubility of copper glycinate in alkaline solutions, however, depends on temperature, concentration of components and pH (Gyliné, 2001). Experiments conducted by Gyliné, (2001) showed that both cis-$Cu(Gly)_2$ and trans-$Cu(Gly)_2$ form precipitates after several hours or days when NaOH or KOH is used as pH modifier.

2.6.4.2 Aqueous Chemistry of Gold and Glycine

Liedberg et al. (1985) performed investigations to understand and explain the interaction between biological molecules and metals occuring in many biological processes. They studied the adsorption of glycine on hydrophilic gold and noted that glycine forms thin films on the surface of gold with the nitrogen end directed towards the gold surface. To further elucidate the interactions between gold/silver and glycine, Pakiari and Jamshidi (2007) used the density functional theory (DFT) to postulate that the interaction between gold and silver clusters with glycine is governed by two principal bonding factors: the anchoring N-Au and O-Au bonds and the nonconventional N-H----Au hydrogen bonds. This observation has been confirmed by Xie et al. (2012) who used the same DFT to report that complexes having the Au-NH_2 anchoring bond are more energetically stable with sole pair of electrons being transferred to the antibonding orbitals of gold.

It has been reported that bacteria secrete complexing chemicals like amino acids which in

the presence of oxidizing agents such as oxygen and potassium permanganate or peroxide can solubilize gold from ores (Groudev et al., 1995). Glycine, amongst a range of amino acids, secreted by bacteria, reacts with gold in the presence of permanganate to form a gold(I) glycine complex through the formation carboxyl ions and the amino acid group nitrogen (donor-acceptor) bonds (Mineev & Syrtlanova, 1984). The solubility of gold in different amino acids has originally been studied by (Brown et al., 1982; Jingrong et al., 1996) e.g. in studies looking at the interaction of jewellery with body fluids. The interaction between gold and glycine was also reported in the adsorption of glycine on a gold electrode in alkaline solutions (Bogdanovskaya et al., 1986). Gold extractions in thiosulfate solutions have been reported to be improved by the addition of amino acids (L-valine, glycine, DL-a-alanine and L-histidine)(Feng & Van Deventer, 2011).

Recently, extensive research in the use of amino acids as leaching agent for copper and/or precious metals by Eksteen and Oraby (2015b) of the Gold Technology Group-Curtin University has led to the development of a patent for the recovery of these metals from their resources. They reported that, although amino acids can act in synergy to dissolve gold, glycine shows the highest gold dissolution as a single amino acid (Eksteen & Oraby, 2015a). The leaching rate of gold in solutions containing 0.5 M glycine, 1 % peroxide at pH 11 and 60 °C for 48 hours was found to be 0.322 µm/m^2. This is comparable to the gold leaching rate of 0.22-0.25 µm/m^2 in thiosulfate-oxalate systems in the presence of thiourea for six days (Oraby & Eksteen, 2014a). The general reaction between gold and glycine is illustrated by Equation 2.16

$$4Au + 8NH_2CH_2COOH + 4NaOH + O_2 \rightarrow 4Na[Au(NH_2CH_2COO)_2] + 6H_2O \qquad (2.16)$$

2.6.5 Glycine Analysis

A lot of research has been undertaken to develop on-the-spot sensitive methods for the determination of both the presence and concentration of free glycine.

As amino acids, including glycine, do not have wavelengths in regions of interests, colorimetric indicators with different UV spectra in acidic and basic medium have been developed to study the dissociation of amino acids (Ryan et al., 1997; Xiang & Johnston, 1994). Moore & Stein (1954) introduced the ninhydrin method for the photometric quantitative determination of amino acids in the 1940s and this has undergone several modifications to make it safer and reliable (Sun et al., 2006). The method is based on the

reaction of amino acids with reduced ninhydrin (triketihydrindenhydrate) at a pH of 5. Stannous chloride is employed as the reducing agent (Rosen, 1957). This reaction yields a "Ruhemann's purple" colour as an end product and the resulting mixture is assayed colorimetrically to determine the content of amino acid (Yokoyama & Hiramatsu, 2003). The ninhydrin method has been used in the determination of the concentration of glycine in antiperspirant (Chin & Achari, 1982).

The most acceptable and widely applied method for quantitative analyses of amino acids is the reverse-phase-high performance liquid chromatography (RP-HPLC) which is preceeded by the precolumn derivation of the amino acids. The precolumn derivation presents covalently bound chromophores vital for interactions with apolar stationary phase for high resolution and also for photometric detection (Kochhar et al., 2002). The HPLC method has also been reportedly used for glycine analysis in antiperspirant.

2.7 Leaching Methods Applicable to Low Grade Ores

The leaching technique employed for any extraction project depends most importantly on the mineralogical composition of the ore, head grade, and the expected value of metal in solution. Any leaching technique should produce as much wanted metals in solution as possible, in the shortest possible time, using as little as possible energy and reagents. It is also well known that there is the continuous growth in the inventory of low grade copper resources falling below the cut-off grade for conventional concentrate production method. As can be seen in Figure 2.9, head grades for most copper deposits will fall below 1% by 2022.

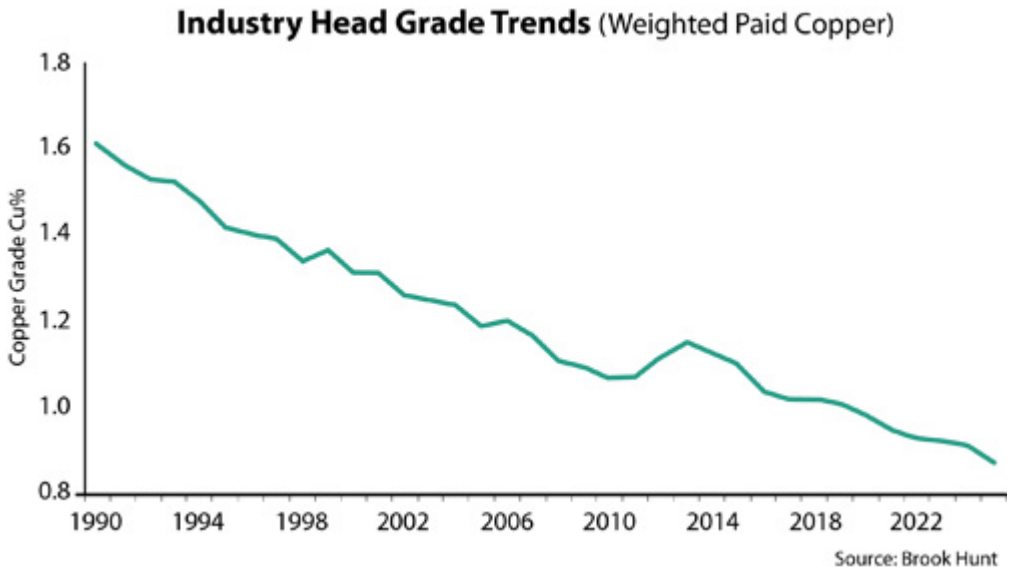

Figure 2.9 Falling industrial copper ores head grade trends (Brook Hunt)

For most conventional processing methods, decreasing ore grades results in an exponential increase in the operating cost with mining and milling incurring the highest proportion as shown in Figure 2.10 (Tiang et al., 2012).

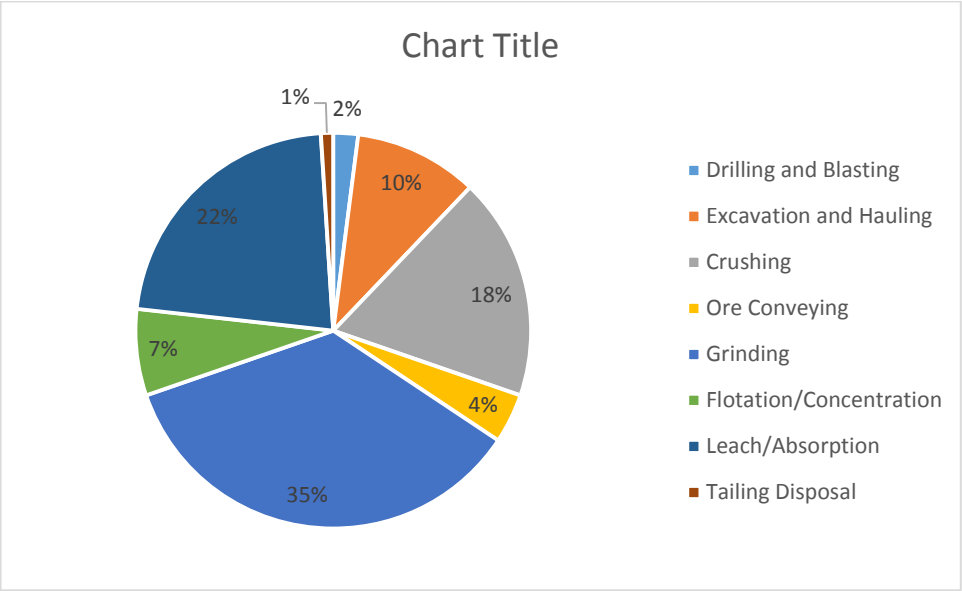

Figure 2.10 Energy consumption in mineral processing (Stadler, 2015)

Copper ore grades of <0.8 % and <0.5 % as obtained in Greenfield and Brownfield applications respectively are uneconomical by conventional processing paradigms (AMIRA International, 2014). With grinding taking up to 35% of the energy consumption of most mine sites, declining ore grades is an indication that most mining operations should be moving from conventional methods to energy efficient strategies for low grade ores (Stadler, 2015). Investigations on the total energy consumption for mineral processing routes by Marsden

(2008) demonstrated that hydrometallurgy consumed less energy as compared to alternative grinding, floating and refining routes. It was also shown that lower grade ores demand more energy for their processing as obtained in Figure 2.11

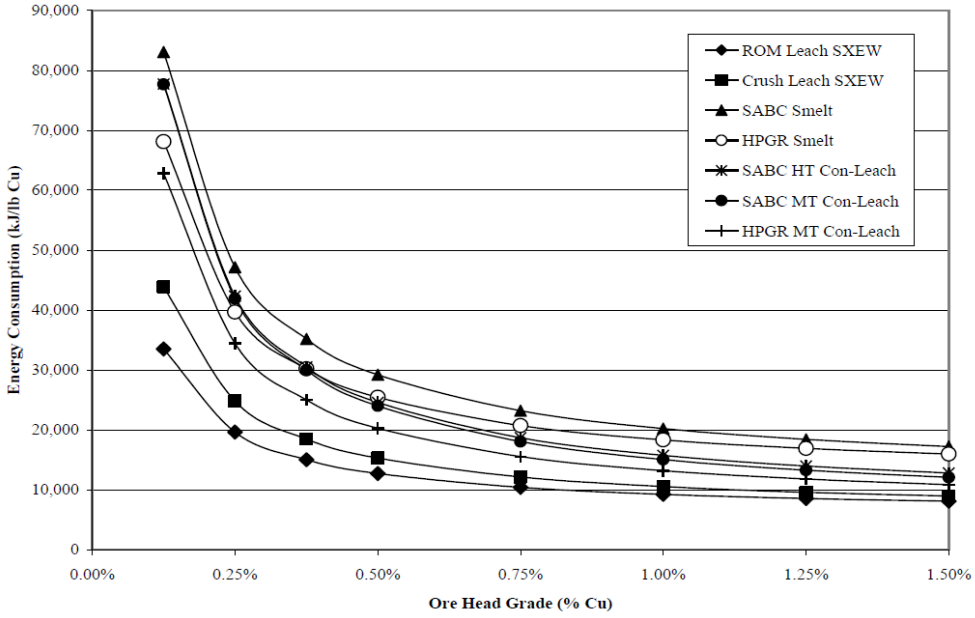

Figure 2.11 Total energy consumption as a function of head grade for various process routes (Marsden, 2008)

Hydrometallurgical methods are therefore mostly optimum for the recovery of low grade ores because of the low capital and operational costs, short construction time, simplicity of operation, proven technologies and environmental advantages. The main techniques that are preferable for the processing of low grade ores are dump, heap and vat leaching (Watling, 2013).

2.7.1 Dump Leaching

Historically, the application of this method dates back to the sixteenth century in the Harz Mountains in Germany (Habashi, 1980). Dump leaching is generally applied to run-of-mine (without any significant crushing) which contains very small amounts of valuable metal that is uneconomical (i.e., below cutoff grade) to treat by any traditional leaching method. The dumps, which can be as high as 200m, 250m wide, containing 50,000 to 300,000 tons, are placed on impervious ground close to the mine site using the natural terrain which can be steep-sided valleys or hillside to enhance drainage. Processing is done by sprinkling the leaching solution on top and, as the solvent trickles down, the metal passes into solution and the pregnant leach solution (PLS) is collected at the bottom for recovery (Habashi, 1989).

Figure 2.12 shows a dump leaching technique on a slope to facilitate drainage.

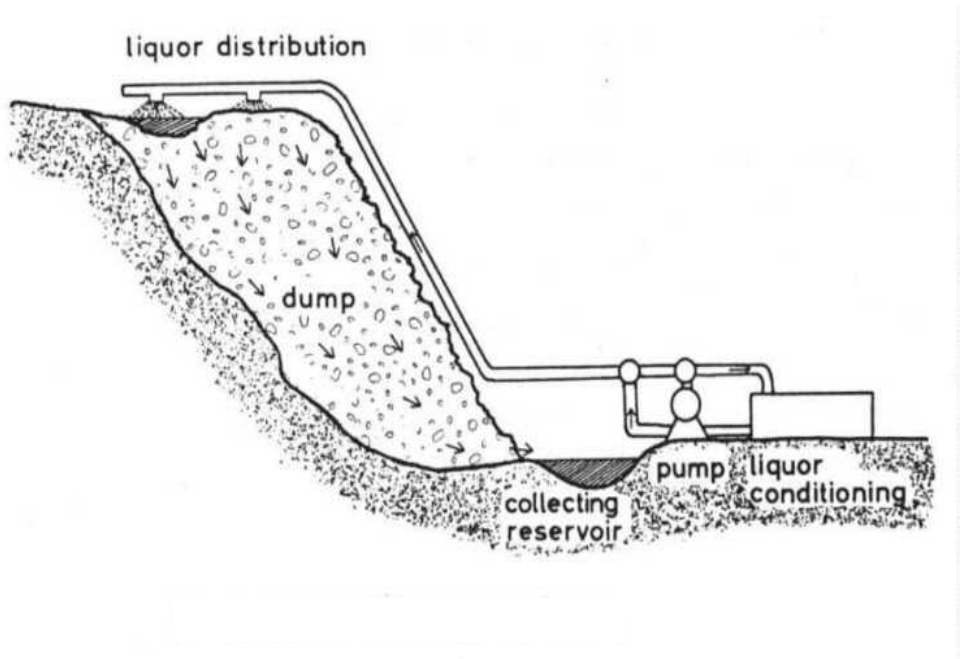

Figure 2.12 Dump leaching (Näveke, 1986)

2.7.2 Heap Leaching

Heap leaching is applied for valuable metals recovery from low-grade ore (i.e., at ir above cutoff grade) that has been deposited on a prepared lined pad (impermeable) constructed using synthetic material, asphalt or compacted clay. In heap leaching, the ore is frequently beneficiated by some type of size reduction (usually crushing and sometimes agglomeration) prior to placement on the pad. The lixiviant solution sprayed on top of the heap permeates and transverses the heap by gravity implying that the process is slow and might last for several days and up to 600 days for some sulfide ores (Mellado et al., 2009; Zanbak, 2012). Just as in dump leaching; most leach sites are selected to take advantage of existing natural slope of ridges and valleys for the collection of PLS. Heap leaching has found world applications in the processing of low grade gold, silver, uranium, and copper ores. There are several parameters that have been identified to influence this process, e.g. pH of the lixiviants, height of the heap, ore particle size distribution, spraying flow rate, irrigation technique, permeability, porosity, aeration, impurities, valuable metals, accompanying metals, temperature of the PLS, solid-to-liquid ratio, etc. (Lwambiyi et al., 2009). Heap leaching can be performed using both oxygenated acidic solutions or solutions containing bacteria as is the case in Talvivara–Finland. A schematic presentation of heap leaching is shown in Figure 2.13. Heap leaching finds application in the recovery of low grade ores

because of its low cost, short construction time, operational simplicity, and environmental advantages (Watling, 2006).

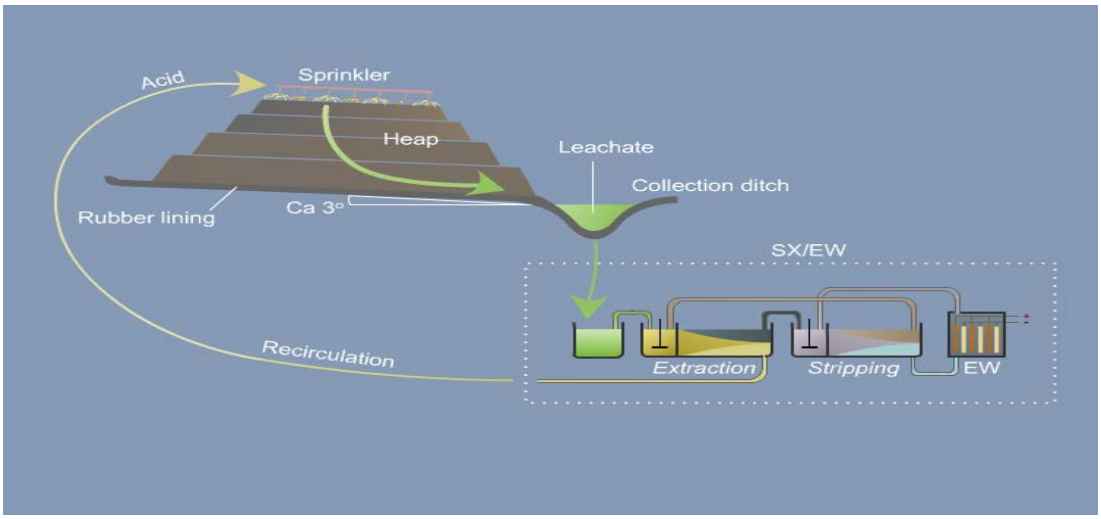

Figure 2.13 Heap leaching (Biomine, 2014)

2.7.3 Vat Leaching

In vat leaching, the leaching agent is added onto the ore that has been placed in a tank fitted with a false bottom covered with a filtering medium. These tanks are usually placed in series and arranged in counter current system in which the ores remains in the tank and is successively leached with leaching reagent of increasing strength. The particle size and porosity of the material are of absolute importance, making impossible the application of this method to slimy materials which will block the efficient flow of the leaching reagents. The major advantages of this method are the low consumption of leaching reagents, production of high concentration PLS, and the elimination of the use of expensive thickeners and filters. Figure 2.14 shows vat leaching of copper at Mantos Blancos, Chile, 1995.

Figure 2.14 Vat leaching of copper at Mantos Blancos, Chile, 1995 (Source: INNOVAT Limited)

2.7.4 Bioleaching

Bioleaching refers to the leaching of sulfide ores involving a variety of microorganisms including not only bacteria, but also archaea (group of single-celled microorganisms) at various temperatures and pH ranges (Suzuki, 2001). The involvement of bacteria in the leaching of metals in natural environments has been practised for many years although the bacteria (*Thiobacillus Ferrooxidans*) that plays a major role in dump leaching was only identified in the 1940s (Trivedi & Tsuchiya, 1975). Sand et al. (2001) indicated that bacterial solubilisation of minerals containing iron is achieved both by direct (contact) leaching by bacteria and by indirect leaching with ferric irons. For indirect leaching, the microorganisms derive their energy by oxidising ferrous ion to ferric ion and, by so doing, generate solutions with relatively high redox potential that leach the sulfide minerals. In direct leaching, the bacteria attaches to the mineral sulfide and oxidises the mineral to sulfate and metal cations by an enzyme-oxygen system.

Bioleaching is mostly suitable for dump and heap or possibly vat (large tanks) operations. A full scale example is the BacTech and Mintech process in Monterrey, Mexico and Talvivara, Finland (Habashi, 2009).

2.8 Summary

A literature review has revealed that there is a huge reserve of discovered and undiscovered copper-gold resources in the form of porphyry copper deposits that are distributed all over the world. Out of the 2100 million metric tonnes of identified copper deposits porphyry copper deposits account for 60 %. It is postulated that twice the amount of identified copper reserves is yet to be identified. The literature has also established that the current technologies for the processing of copper-gold ores are inefficient or not environmentally benign and the need for further research on ways to effectively extract the metals of interest from these resources in a benign manner is necessitated. Attributes of good lixiviants have also been investigated. Glycine, which is the simplest amino acid, is physically and chemically stable over a wide pH-Eh range, forms stable complexes with metals, has shown great capabilities for the selective leaching of copper, gold and other metals. With ore grades on a continuous decline, different processing techniques such as dump, heap and vat leaching applicable to such ores have been explored and may see increasing use in the future.

Chapter 3 Materials and Methods

3.1 Chapter Objectives

A variety of materials and research methods have been used to meet the goals of this thesis as outlined in Chapter 1. The main objective of this chapter is therefore to give a detailed description of the materials, procedures and analytical techniques that were employed in this research.

With the primary aim of investigating the leachability of low grade copper-gold ores and copper minerals in a new leach process, ores and minerals samples used for all experimentation are described, along with the methods for sample characterization and preparation for experiments. These minerals and ores underwent a variety of batch leach tests including leaching, solvent extraction and sulfide precipitation. The equipment and conditions used for these experiments are detailed in this chapter. Glycine as the main lixiviant in this study and other reagents used for the various experiments are listed in this chapter as well.

Lastly, this chapter explains the fundamentals of different techniques that were used to collect the data needed in the subsequent chapters. The experimental conditions, parameters and different procedures for samples preparation, copper minerals leaching, copper speciation, leaching kinetics, copper-gold ores leaching, column leaching, solvent extraction and metals precipitation are described in the following sections.

3.2 Materials and Reagents

All reagents were of analytical grade. De-ionized water was used for preparing all solutions. A list of different copper minerals and gold-copper ore samples used for different experiments are given in Table 3.1. Table 3.2 also shows a list of the analytical grade reagents and gases used in different experiments described in the thesis.

Table 3.1 List of different copper minerals and gold-copper ores used in this study

Mineral/ore sample	Experiment
Azurite	Leaching behaviour
Malachite A	Leaching behaviour
Malachite B	Leaching kinetics
Cuprite	Leaching behaviour
Chrysocolla	Leaching behaviour
Chalcocite A	Leaching behaviour
Chalcocite B	Leaching kinetics
Chalcopyrite A	Leaching behaviour
Chalcopyrite B	Leaching kinetics
Copper-gold ore A	Copper and gold leaching
Copper-gold ore B	Copper and gold leaching
Copper-gold ore C	Copper and gold leaching
Copper-gold ore D	Copper and gold leaching

Table 3.2 List of different analytical grade reagents and gases used in this study

Reagent	Formulae	Purpose	Purity
Glycine	H_2NCH_2COOH	Main lixiviant	AR
Sodium hydroxide	NaOH	pH modifier	AR
Lime	$Ca(OH)_2$	pH modifier	Industrial grade
Hydrogen peroxide	H_2O_2	Oxidizing agent	AR
Oxygen	O_2	Oxidizing agent	Industrial grade
Air		Oxidizing agent	Atmospheric
Sodium persulfate	$Na_2S_2O_8$	Oxidizing agent	AR
Sodium nitrate	$NaNO_3$	Effect on Cu_2S leaching	AR
Sodium chloride	NaCl	Effect on Cu_2S leaching	AR
Sodium sulfite	Na_2SO_3	Effect on Cu_2S leaching	AR
Sodium hydrosulfide	NaHS	Precipitation reagent	AR
Mextral 84H	2-hydroxy-5-nonylacetophenone oxime	Copper extractant	AR
Mextral 54-100	1-benzoyl-2-nonyl ketone	Copper extractant	AR
DT-100		Diluent for extractant	AR
Sulfuric acid	H_2SO_4	Stripping agent	AR

3.3 Procedures

3.3.1 Mineral and Ore Specimens Preparation

3.3.1.1 Minerals

Copper mineral specimens were to study their dissolution behaviour in alkaline glycine solutions after crushing and grinding to 100 % passing 75 µm. Each sample was representatively split and a portion of the sample was analysed by XRD to ensure that the mineral sample contained only the copper mineral phase of interest (with or without other metal phases). Upon confirmation of the copper mineral phase in the sample, another portion from the sample was analysed by XRF to determine the elemental composition of the mineral sample. Oxidation of the finely ground sulfide minerals was minimized by storing the samples in a freezer.

Once the mineral phases were confirmed, samples were crushed and screened at different size fractions for leaching kinetics studies. The sulfide samples were then stored in the freezer to minimize oxidation.

3.3.1.2 Ores

Copper-gold ore specimens were also crushed and ground to 100 % passing 75µm and sub-samples were analysed for mineralogical and elemental composition by XRD and XRF, respectively. Samples with phase concentrations less than 1 %, which are generally not detected by XRD, were analysed by Tescan Integrated Mineral Analysis (TIMA) technique to detect any copper mineral phases at low concentrations.

Column leaching experiments were performed with two different copper-gold ore types. One of the samples was a flotation tail and was used as received since more than half of it was already agglomerated from drying. A representative sample was analysed for its mineralogy and elemental compositions. The second sample was crushed and sieved to obtain a +1/-8 mm size fraction. Mineralogical and elemental analysis were also performed on a sub-sample of this ore.

3.3.2 Leaching Behaviour of Copper Minerals

All solutions used in these experiments were prepared from reagent grade glycine, obtained from Sigma Aldrich, and de-ionised water. Sodium hydroxide was used for solution pH adjustments. The redox potential (E_h) of the leach solution was measured and reported according to Ag/AgCl reference electrode and pH measurements were performed using a TPS 90FLMV field meter. Unless specified, all experiments were conducted in a 2.5 L Winchester bottle (OD 44 cm and L 30 cm) using a bottle roller (The major advantage of bottle rolling is that one can rapidly determine the effect of conditions (e.g. reagent concentration, pH, and solid/liquid) by running simultaneous experiments (up to 15). The required mass of mineral specimen was weighed to give the equivalent of 2.0 g total copper in the solid. The weighed sample was then placed in the bottle and the leaching solution was added. The percentage solids used for each mineral specimen is given in Table 3.3. Slurry agitation was provided by immediately placing the bottle (sample and leaching solution) onto a bottle roller rotating at 100 rpm. To ensure that enough oxygen was available for the leaching reaction, the bottles were capped with lids having a centered 5 mm in diameter hole. During the leaching experiments, several intermediate samples were collected. This involved removing the bottles from the roller, allowing to stand for one minute to allow the solids to partially settle, and then withdrawing 3 mL of slurry and filtering by means of a syringe-membrane filter (pore size 0.45 µm). An Atomic Absorption Spectrometer (AAS), Agilent 55B model was used to determine the concentration of copper in the filtrate. For experiments showing a low copper recovery, the leached residues were rinsed with deionised water, dried and observed under a Scanning Electron Microscope (SEM) to understand the change in surface morphology of the samples during leaching.

Table 3.3 Solid percentage used for the dissolution behaviour of copper mineral specimens

Ore	Cu in ore,%	Mass Cu, g	Mass ore, g	Solution, mL	% w/v solids
Azurite	42.12	2.00	4.75	500	0.95
Chrysocolla	24.70	2.00	8.09	500	1.62
Cuprite	20.09	2.00	9.96	500	1.99
Malachite	41.55	2.00	4.81	500	0.96
Metallic copper	99.99	2.00	2.00	500	0.40
Chalcocite	78.8	2.00	2.54	500	0.51
Chalcopyrite	14.81	2.00	13.50	500	2.70

3.3.3 Copper Speciation

Copper speciation experiments were performed to determine if Cu(I) and/or Cu(II) ions are dominant in the alkaline copper-glycine leach system. An Ultraviolet- Visible (UV-Vis) spectrometer was employed to detect and determine the concentration of copper (II)-glycinate species in solution. Cupric sulfate pentahydrate ($CuSO_4 \cdot 5H_2O$) was used to prepare synthetic solutions containing copper-glycinate complex. The influence of pH, glycine and sulfate concentrations on the absorbance and wavelength position were also investigated by varying their values in the solutions. Copper (I) chloride was also dissolved in the alkaline glycine solution and samples collected immediately after addition to determine the presence of any other peak apart from the Cu(II) peak.

Cupric sulfate pentahydrate was then used at different concentrations in alkaline glycine solution to generate a calibration curve at different Cu(II) concentrations. The final solution from leaching different copper minerals was analysed for total copper using AAS and for Cu (II)-glycinate using UV-Vis spectrometer.

3.3.4 Leaching Kinetics Experiments

All kinetic experiments were conducted in a 500 mL jacketed glass reactor fitted with a condenser, a mercury thermometer, an overhead teflon stirrer, and rubber stopper for the sampling inlet. The reactor was filled with a 500 mL solution of the desired reagent concentration and pH. For the leaching kinetics of chalcocite and chalcopyrite, the effect of dissolved oxygen (DO) on copper extraction was investigated. In order to do that, a DO controller system was set to measure the DO in solution and maintain a desired DO value by controlling the oxygen flow through an automatic valve controller. The required solution temperature was achieved and maintained with a digitally controlled heated circulating water bath. On attaining the desired temperature, the required mass of copper mineral sample was added to the solution and the stirring was started. After a specific leaching time, the stirring was stopped, a one minute interval was allowed for the particles to settle and 3mL solution was extracted for copper concentration determination by atomic absorption spectrometry. The percentage of copper extraction was calculated based on the copper released into the solution per total expected. Figure 3.1 and Figure 3.2 illustrate the apparatus setup for leaching kinetics.

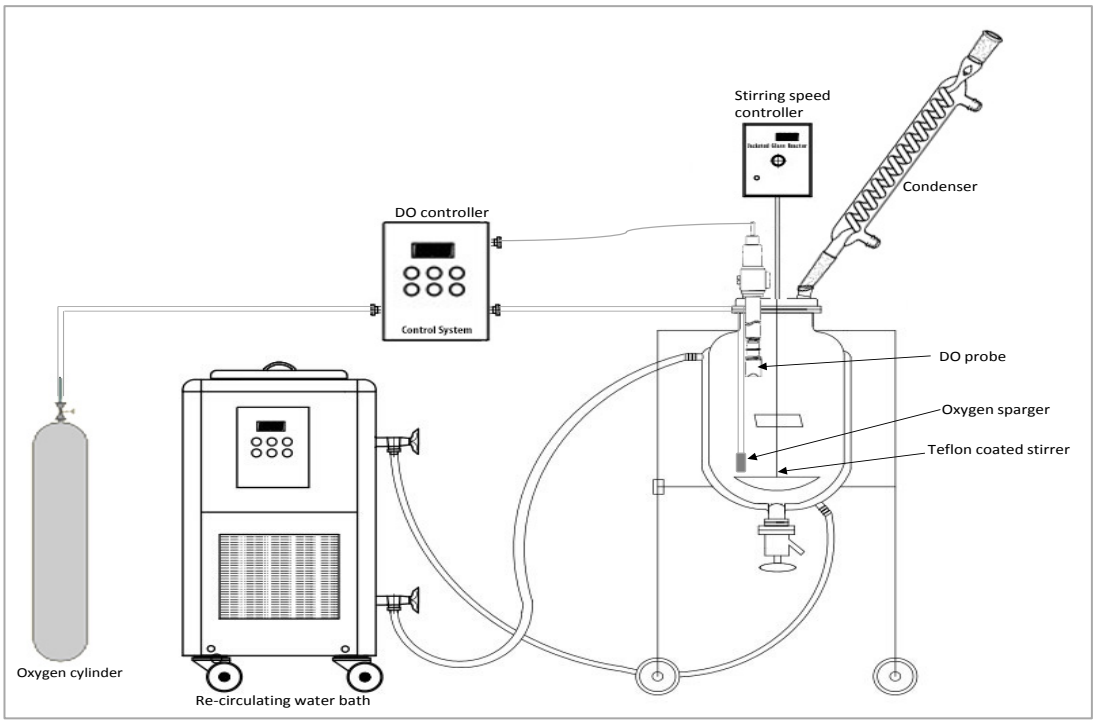

Figure 3.1 Diagram of leaching kinetics apparatus setup

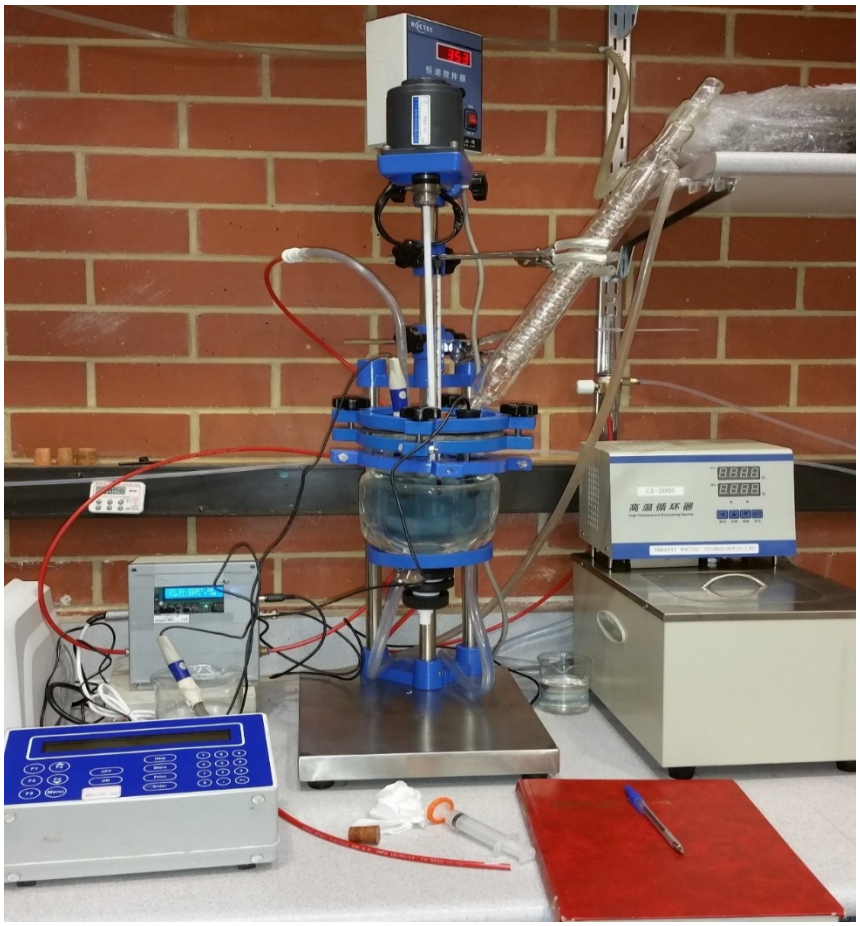

Figure 3.2 Laboratory leaching apparatus setup

3.3.5 Leaching of Copper-Gold Ores

Experiments were conducted to investigated the effect of glycine and solution pH on the leaching of copper from copper-gold ores in 2.5 L Winchester bottles opened to air, bottle rolled at 100 rpm and room temperature. The required mass of the copper-gold ore sample (Table 3.4) was placed in the bottle/reactor of leaching solution along with the required amount of reagents at a predetermined initial pH. Afterwards, the bottles were immediately placed on the bottle roller.

Table 3.4 Leaching vessel, ore type, solution volume and ore mass for leaching Cu-Au ores

Leaching vessel	ore	solution vol , mL	sample mass, g
Bottle roller	A	500	100
	B	500	100
	C	500	500
1 L reactor	B	500	100
	C	500	500

Effects of temperature, oxygen and pyrite addition were conducted in a 1000 mL jacketed glass reactor. The reactor was equipped with a condenser, a thermometer, an overhead stirrer, a fine oxygen sparger, and a sampling inlet with a rubber stopper. The solution temperature was maintained by connecting a digitally controlled heated circulating water bath to the reactor. Before the leaching was started, the solution (0.5 M gly, pH 11.5) was oxygenated at the desired oxygen flow rate for 10 minutes at the selected temperature. The ore sample was then added and the leaching time started.

At given leaching time intervals, sub samples were withdrawn from the leaching vessel and filtered using a 0.45 µm filter paper. The solids were returned to the leaching vessel while the filtrates were analysed for copper and gold by ICP-OES or ICP-MS. At the end of each experiment, leach residues were thoroughly washed with distilled water, dried and analysed by fire assay for gold and by XRF for base metals. Extraction percentages for both copper and gold were determined from re-calculated head grades.

3.3.6 Column Leaching

Laboratory heap leach experiments are generally performed using columns. Column leaching in the laboratory, with or without recirculation of leaching solution, simulates percolation

leaching operations because conditions are similar to those in the heap. The column may be considered as the centre of the heap with same conditions for air and access to leaching solution (Mousavi et al., 2008). Column experiments can provide useful information about different process variables (particle size, mineral type, chemical reactant, leach conditions, etc.).

Heap simulation experiments were performed in columns fabricated from 5 mm thick plexiglass. The column height was 1000 mm while the internal diameter was 90 mm. The bottom of the column had a support flat base with multiple holes for solution discharge while holding the solids. The support base also contains an air inlet which distributes air through 0.5 mm holes inserted along the diameter of the column base. The column is equipped with a lid to minimize solution loss. The lid contains 2 holes, one for solution inlet and the other for air escape.

Crushed, washed and dried quartz was placed at the bottom of the column for support and air distribution. The ore was then added to the column and quartz was again placed on top of the ore to assist in the homogeneous distribution of the leaching solution. The leaching solution was delivered to the top of the column by a peristaltic pump. Solution percolated through the ore by gravity and into a collection container from where it was re-circulated through a side loop by the pump. The solution re-circulation and aeration rates for different columns are given in Table 3.5.

Table 3.5 Solution and aeration rates for leaching columns

Column	Ore mass, g	Solution flow rate, L/h	Air flow, L/min
Cu-Au ore C (Column 1 & 2)	5000	0.21	0.1
Cu-Au ore D	2697.7	0.864	0.1

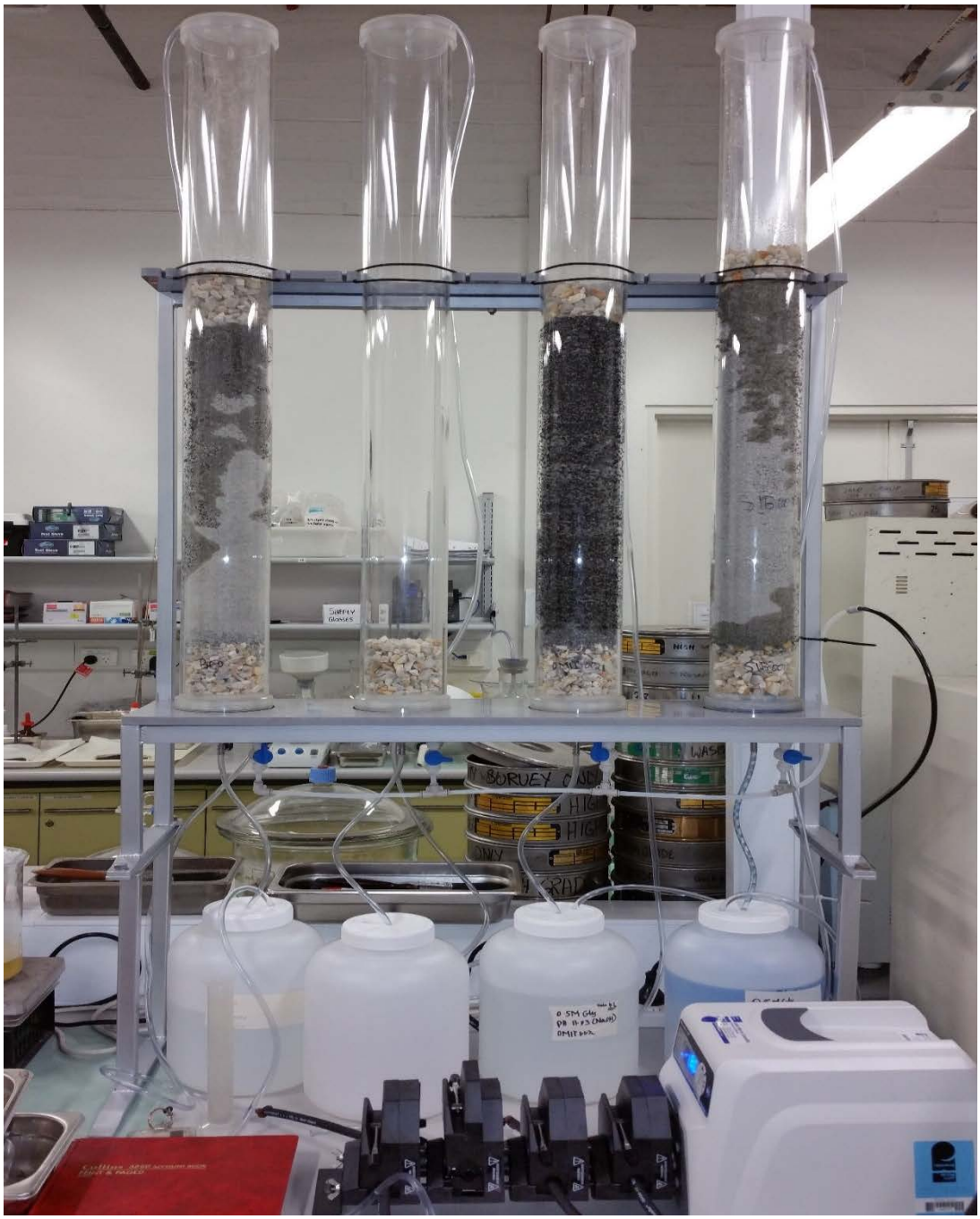

Table 3.6 Column leaching experimental setup

3.3.7 Solvent Extraction

Copper extraction and stripping experiments were carried out by mixing the required volumes of organic and aqueous phases in a volumetric flask, and then equilibrating by shaking in a thermostatic water bath shaker for the required time and at the established temperature. The mixture was transferred to a separating funnel and, after phase disengagement, the raffinate was separated and the equilibrium pH was measured with a TPS 90FLMV field meter. The aqueous solutions were analysed by AAS using a Varian

SpectraAA. The concentration of copper in the organic phase was calculated from the difference between the initial copper concentration in the PLS and its concentration in the raffinate at fixed organic to aqueous (O:A) phase ratios. Figure 3.4 shows the phase separation setup after solvent extraction.

To determine the fate of glycine after extraction, an aqueous solution was obtained by dissolving a known mass of glycine in deionised water to which copper sulfate was added to complex with the glycine at 1:3 molar ratio in a 100 mL volumetric flask. A sample of this solution was taken for glycine determination. Solvent extraction with both extractants was then performed. Glycine concentration was again determined after extraction. Determination of free glycine concentration before and after extraction was performed with a high pressure liquid chromatography UV-Vis after hydrolysis with HCl, neutralization with NaOH, and then pre-column derivatisation to form adjunct compounds with high UV-Vis absorption range(Llames & Fontaine, 1994; Rowan et al., 1992).

Stripping of the copper from loaded organic was carried out with different concentrations of sulfuric acid solutions. Aqueous solutions containing the main elements at concentrations to that of a typical return (30 g/L Cu and 180 g/L H_2SO_4) electrolyte associated with a conventional electrowinning tank house operation were then used to simulate a stripping circuit as obtained in the industry.

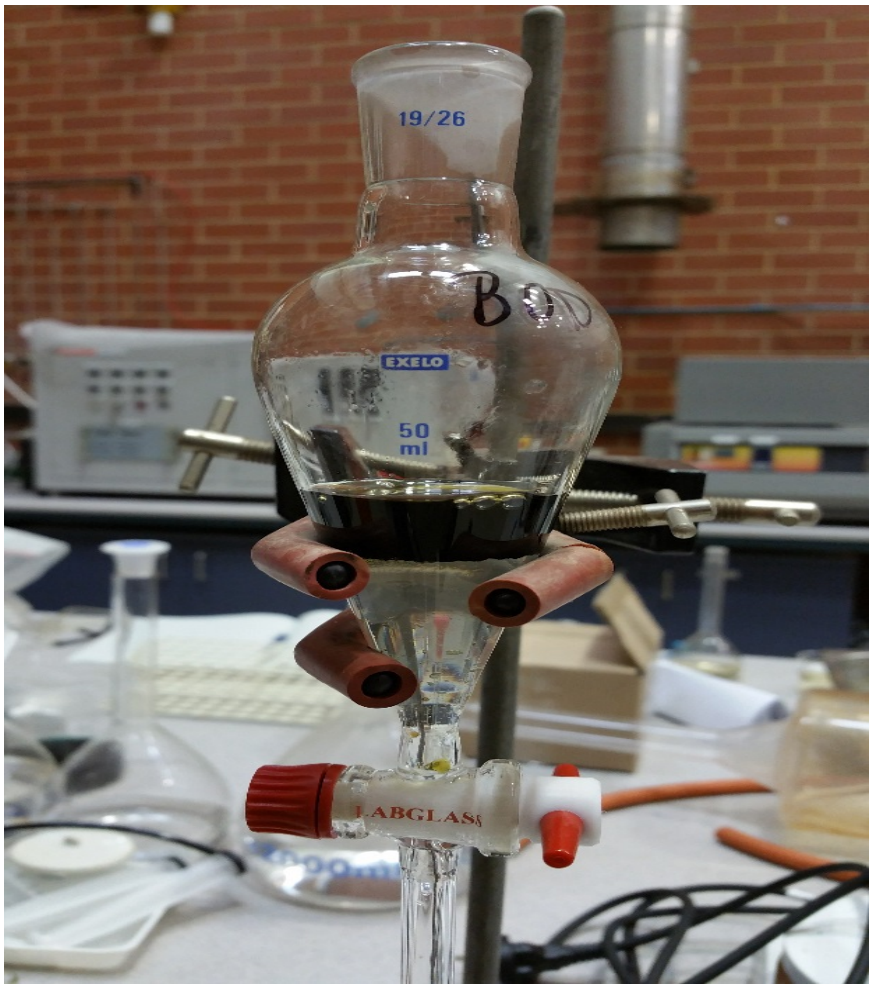

Table 3.7 Phase separation after solvent extraction

3.3.8 Precipitation

Copper precipitation as sulfide from the alkaline glycine solution was investigated by the addition of NaHS. During the precipitation tests, the required stoichiometric mass of dry NaHS powder was weighed and added to the copper glycinate solution. Copper concentration in solution before and after precipitation was measured using AAS. The particle size distribution of the precipitated solids was determined by means of laser diffraction. The precipitate was dried and analysed by XRD to determine its mineralogy.

3.4 Instrumental Analysis

A variety of analytical methods were used for both solid and solution analysis. These methods are well established in both academia and industry. A brief overview of the different analytical methods and instrumentation used in this study are given and described below.

3.4.1 X-Ray Diffraction (XRD)

XRD is a rapid analytical technique used for the identification and quantification of phases in a crystalline material (Böttger et al., 2000; Jenkins, 2000). The copper minerals used in this project were analysed by XRD to identify the interested copper mineral and impurities phases in each mineral specimen. The samples were finely ground (micronised) and homogenized to get representative results.

The XRD technique is based on the principle that crystalline substance can behave as a three dimensional diffraction grating for X-ray wavelengths similar to the spacing of the atomic-scale crystal lattice planes. Monochromatic radiation interacts constructively with the sample to produce diffracted x-rays according to Bragg's law (relates the wavelength of the electromagnetic radiation to the diffraction angle and the lattice spacing in a crystalline sample) as expressed in Equation 3.1

$$n\lambda = 2\mathrm{d}\sin\theta \tag{3.1}$$

where n is the order of diffraction, λ is the wavelength of the incident X-ray, d is the interplanar spacing of the crystal, and θ is the angle of incidence.

As each mineral has a unique (fingerprint) d-spacing, scanning a sample through a range of 2θ angles and comparing the processed data with standard reference patterns, the mineralogical phases present in the sample can be identified.

Mineral phase determination for samples used in this project were performed using a D8 Advance Bruker X-ray spectrometer at the John de Laeter Centre for Isotope Research of Curtin University. X-ray data obtained from the spectrometer was analysed with TOPAS software. Quantitative analysis results are given in Chapters 4 and 5 and spectrograms are given in Appendix A. Although XRD is a widely used analytical technique in the mineral industry, it however has some limitations. Only about a tenth of a gram of sample specimen that must be ground into a powder is required; implying that the sample must be a homogenous representation of the bulk. In multiphase specimens, not only a confusion in pattern similarities may arise but also, some observed phases may not be found on International Centre for Diffraction data (ICDD) powder diffraction files (Jenkins, 2000). XRD also has difficulties in identifying phases that are less than several tenths of one percent depending on the crystalline material being examined.

3.4.2 X-Ray Fluorescence (XRF)

XRF is a technique for analysing the elemental composition of materials (solid, liquid and thin-film samples). The principle of XRF is based on the fact that, when an external energy source is shone on atoms, they become excited and emit x-ray photons of a characteristic energy or wavelength. Identification and quantification of the elements present in the sample is achieved by counting the number of photons of each energy level emitted by the sample. As any other analytical technique, XRF has limitations and detection limits (Kadachia & Al-Eshaikhb, 2012). The ability of most commercially available XRF instruments is limited in the precise and accurate determination of the abundance of elements with atomic number less than 11. XRF is limited in differentiating disparity between isotopes of an element, and ions of the same element in different valence states (Gill, 1997).

The XRF technique on feed and residue mineral/ore samples for this project was conducted at Bureau Veritas analytical laboratories in Perth, Western Australia.

3.4.3 TESCAN Integrated Mineral Analyser (TIMA)

TIMA is high performance analytical scanning electron microscope that is capable of automatically measuring modal abundance, size-by-size liberation, grain size and minerals associations on multiple samples of polished sections, and thin sections or grain mounts. The instrument is based on the MIRA Schottky field emission or thermal emission microscope that has been integrated with an energy dispersive spectroscopy (EDS) system for full spectrum, ultra-fast data acquisition. The acquired data is analysed and presented using the TIMA software.

TIMA analysis for different samples was done using the Tescan TIMA GM model at the John de Laeter Centre (JDLC) of Curtin University. The main limitation of TIMA would be the size of the grains being analysed versus the step size that is used. Ideally, 8-10 pixels per grain is needed to ensure grains or inclusions are not missed and also that enough EDS is collected to accurately match the mineral definition files.

3.4.4 UV-Visible (UV-Vis) Spectrophotometry

This technique is based on the absorption of radiation in the visible or ultraviolet region. Transition metals such as copper have partially filled d-orbitals with electrons relatively free to absorb energy and be promoted to a higher energy level. The degree of absorption by a

sample at different wavelengths is recorded by a spectrometer and displayed as a plot of absorbance against the wavelength. Each element has a characteristic wavelength at which maximum absorption occurs. According to Beer Lambert's law, the intensity of a beam of monochromatic light passing via an absorbing substance linearly decreases as the concentration of the absorbing substance increases.

The visible absorption spectra of the copper (II)-glycinate solutions were detected with a Varian, Carry 50 UV-Visible spectrometer interfaced with a compatible PC. This technique has been used in Chapter 5 for copper speciation.

3.4.5 Particle Size Analysis (PSA)

For experiments in which the sample particle size was assumed to be less than 20μm, the Malvern laser diffraction particle size analyzer (at CSIRO Perth) was used to determine the particle size distribution of the sample. The instrument is based on the principle that every particle size has its own characteristic scattering pattern (as predicted by the Fraunhofel model) when it passes through a laser beam. The major components of this equipment are: the transmitter for production of laser beam, the sample area, and the receiver which collects and stores the information received from the scattering of the analyser beam as it passes through the sample. The collected data is then sent to a computer system for analysis and interpretation by the Malvern software.

3.4.6 Atomic Absorption Spectrometry (AAS)

Atomic absorption spectrometry (AAS) is a very reliable and common method for determining the concentration of metals and metalloids in liquid phase. The principle of AAS is based on the fact that electrons of atomized elements can absorb light of specific wavelengths and get promoted to higher orbitals (Platte, 1968). The amount of light absorbed is proportional to the number of atoms of the particular metal ions present in the sample.

Generally, the apparatus consists of a light source, a sample atomizer, a spectroscope, a photometer, and a recording system. There is also a background compensation system. Metal ions in solution are atomised by means of a flame. The flame source is a mixture of acetylene (1.5 dm^3/h) and air (3 dm^3/h) which is then ignited to burn together with an aspirated liquid sample. A light beam from a lamp whose cathode is of the element being

determined goes through the spectroscope where the wavelength slit is adjusted per particular element. The monochrome light passing through the flame falls on a photomultiplier that records the light intensity. The amount of radiation absorbed by the sample is compared to a calibration curve constructed by running standard solutions of the metal under similar conditions and this enables the computer unit attached to the AAS to calculate the concentration of the element of interest in the sample (Levison). In this project, an Agilent 55B AAS spectrometer has been used to determine most of the copper and gold concentrations in solutions.

3.4.7 Inductively Coupled Plasma Optical Emission Spectrometry (ICP-OES) and Inductively Couple Plasma Mass Spectrometry (ICP-MS)

Both ICP-OES and ICP-MS were used for determining the concentration of elements in solutions in this project. In both techniques, a very high temperature plasma 6000~ 10000K is produced by the interaction of an intense magnetic field passing on a tangential flow of argon through a concentric quartz tube. Initially, the argon gas is partially ionised by a high-voltage spark generating electrons and cations which are accelerated by the magnetic field resulting in elastic ions-neutral collisions and thus forming a stable, high temperature plasma. The sample being analysed is converted to an aerosol and sprayed into the centre of the plasma (Batsala et al., 2012; Olesik, 1996). ICP-OES and ICP-MS differ from this point forward. (Tyler).

ICP-OES, uses a diffraction grating to separate the light emitted by the plasma and, as each element has its own distinct wavelength, elements in the sample can be determined and quantified comparing the amount of emitted light to a calibrated range in the instrument.

In ICP-MS, the ions generated by the plasma are directed through a quadrupole mass spectrometer which identifies and quantifies elements based on their mass-to-charge ratio. ICP-OES is useful for measuring higher concentrations of elements while ICP-MS provides lower detection limits (Sakata et al., 2001; Stankova et al., 2011; Thompson et al., 2008). The detection capabilities of ICP depends on the technique of sample introduction which allows different quantities of sample to reach the ICP plasma. Detection limits can also depend on the sample matrix which can be affected by the extent of ionization in the chamber (Batsala et al., 2012)

ICP-MS was used to determine gold concentrations (ppb) from leached solutions resulting from the leaching of low grade copper-gold ores. Concentration of metals during solvent extraction experiments was determined exclusively by ICP as AAS efficiency is affected by organic reagents. ICP was also used in the determination of dissolved total sulfur and other impurities in the final leach solution. ICP analysis were performed at CSIRO AMRC, WA and Bureau Veritas Laboratories of WA.

3.4.8 High Performance Liquid Chromatography (HPLC)

HPLC is generally used to separate, purify, identify and quantify components of a complex mixture (McMaster, 2006). The separation is based on molecular structure and molecular composition of the mixed substances. The liquid mixture to be separated is injected under pressure through a stationary phase in the column in which mixture components having stronger interactions with the stationary move more slowly through the column as compared to components with weaker interactions. As the analytes elute the chromatographic column, detectors (UV-Vis, fluorescence, mass spectroscopy, electrochemical) located at the end of the column detect the component and send a signal to a computer which integrates the signal and presents it in a chromatogram for easy interpretation. The accuracy of HPLC depends on the efficiency of the column and the sensitivity and selectivity of the detection system (Lawrence, 1987).

In this project, HPLC was used to determine the concentration of free glycine before and after solvent extraction and sulfur speciation for sulfide containing ore leach solutions. The HPLC was outsourced to the ChemCentre of Western Australia. The HPLC instrument used for the analysis was an Agilent, 1100 series model.

3.4.9 Scanning Electron Microscopy (SEM)

In SEM, high energy electrons impinged as a beam on the surface of a sample interact with particles on the surface to produce signals that are used to generate information about composition and topography of the surface. The major components of SEM are the electron beam generator, column with electromagnetic lenses for electron travel, sample chamber under vacuum, electron detector and computer display for image viewing (Egerton, 2005).

Surface qualitative and quantitative analysis were performed by the use of an Energy

Dispersive X-ray Spectrometer (EDS). As the sample is being bombarded with the electron beam, vacancies created by ejected electrons are filled by electrons from a higher state. This process emits an X-ray to balance the energy between the different electron states. The X-ray energy is characteristic of the element from which it is emitted. The emitted X-ray is detected by the EDS detector and the relative abundance of the X-rays versus their energy is measured to evaluate elemental composition of the sample.

Most SEM instruments are limited in that samples must be analysed under a stable vacuum of 10^{-5} to 10^{-6} torr. Also, many SEM instruments cannot detect elements whose atomic numbers are less than 11. Electrically non-conductive samples being analysed in conventional SEMs must be coated with a conductive coating to avoid electron build-up on sample surface otherwise poor resolution results.

Scanning electron microscopy analysis was used to study the changes in the surface morphology of some minerals during and after leaching. These analyses were performed at The John de Laeter Centre of Curtin University using the NEON FIB-SEM, Zeiss manufactured Neon 40ESM model. It was operated at 5.0 kV with a beam aperture size of 30.0 µm.

3.4.10 X-Ray Photoelectron Spectroscopy

X-ray photoelectron (XPS) spectroscopy is a surface sensitive analysis technique that uses the photoelectric effect to identify and quantify elements on the surface of materials. This analysis is sensitive to the first 2-5 nanometres of the sample. The instrument focuses an X-ray beam at the target material; photoelectrons are ejected from the atoms of the material with a specific kinetic energy depending on their atom of origin. By measuring this kinetic energy, the identity of the origin atom is found and the number of electrons measured at that energy provides information about how much of this element is present.

Two spectral regimes can be produced by XPS: survey spectra and high resolution spectra. The survey spectra allow the identification and quantification of the elements on the surface; whereas, the high resolution spectra allow the identification and quantification of the bonding associated with an element.

XPS analysis in this project were performed using a Kratos AXIS Ultra DLD model at the John de Laeter Centre (JDLC) of Curtin University. The electron take off angle was normal to the sample surface. Spectra were interpreted using the software package CasaXSP.

3.4.11 Miscellaneous Analysis

Fire assay for gold content determination in the feed and residue of different gold-copper samples was conducted by Bureau Veritas laboratories of Western Australia.

3.4.12 Auxiliary Equipment

One of the most important equipment used through out the research was the TPS 90FL-T meter used for measuring both pH and the oxidation reduction potential of solutions. A mercury thermomter was also important in measuring solution temperatures

Chapter 4 Differential Leaching Behaviour of Copper Minerals: Towards a Geometallurgical Indicator

4.1 Chapter Objectives and Background

In Chapter 1, it was indicated that copper grades in common ore bodies are gradually dwindling with copper content of less than 1.0 % no longer being the exception but the rule. Moreover, the low copper grade is constituted of a multitude of copper minerals such as chalcocite, covellite and chalcopyrite in the hypogene and supergene layers and many oxides in the leached oxide cap. Processing of such complex ores challenges plant operators because each mineral is likely to respond differently to comminution, flotation or leaching. It is well known that copper minerals have different solubility in different leaching systems as was obtained by Hedley and Tabachnick (1968) for cyanide solutions. Oraby and Eksteen (2014b), using an alkaline glycine solution, reported that copper could be selectively leached from gold in a copper-gold gravity concentrate. In both cases, it was established that the oxide minerals were completely leached, while sulfide minerals were only partially leached. Oraby and Eksteen (2014b), rather, used a bulk sample in which the phase concentrations of the copper minerals was identified before and after the leaching process without further research on the behaviour of individual mineral.

The main objective of this chapter is to investigate and understand the leaching behaviour of individual copper minerals in alkaline glycine solutions at ambient temperature and atmospheric pressure. The effects of reagent concentration and initial solution pH were also investigated. To do this, it was imperative that each mineral specimen contained only a single copper mineral phase (although other non-copper-bearing gangue minerals were acceptable). The dissolution behaviour of azurite, malachite, cuprite, chrysocolla, metallic copper, chalcocite and chalcopyrite in alkaline glycine solutions have been studied and reported in order to discriminate amongst the leach behaviours of the different minerals rather than study the detailed kinetics of each mineral. As such, it is a study of the geometallurgical response of copper minerals in alkaline glycine solutions.

The dissolution procedure outlined in Chapter 3 indicates that all experiments in this chapter

were performed with a conventional bottle roll. Bottle rolls had the limitation that oxidation (only air through neck of bottle) and temperature could not be controlled. The batch nature experiments are generally limited as reactants get consumed to form products and equilibrium concentrations may be reached whereas continuous product withdrawal and reagent addition in real systems forces dissolution/leaching reactions. Bottle rolls are thus inadequate for process set point determination or optimization. The following sections cover the mineralogy and chemistry, the effect of glycine concentration, the effect of pH, and the effect of oxidants on the leaching of each copper mineral in alkaline glycine solutions.

4.2 Azurite

Azurite is a secondary copper mineral often found in the oxidized zones of copper bearing ore deposits. It is a copper-carbonate-hydroxide mineral with a chemical composition $2CuCO_3 \cdot Cu(OH)_2$. Single crystals of azurite are dark, royal blue and the mineral exhibits a brilliant azure blue colour when it is of dull or earthy luster.

4.2.1 Mineralogy and Elemental Composition

The azurite specimen obtained from a mineral collector in Australia was analysed for its mineralogical and elemental composition. The XRD analysis of this mineral specimen indicates that the specimen contains 65.0 % azurite which is the only copper mineral phase present in the specimen. The elemental analysis of the azurite sample was done by XRF and the results are shown in Table 4.1. It can be seen that the specimen has 42.1% copper and the rest represents the impurities in the sample.

Table 4.1 Mineralogical and chemical composition of azurite

Mineralogy	Phase	Azurite	Kaolinite-1A	Muscovite-2M1	Quartz	Amorphous Content
	wt %	65	3.4	6.2	7.4	18
Chemical composition	Metal	Cu (%)	Al (%)	Si (%)	Zn (ppm)	K (%)
	Value	42.1	1.9	6.4	50	0.6

4.2.2 Effect of Initial Glycine Concentration

To evaluate the effect of glycine concentration on the dissolution of copper from azurite mineral specimen, the initial solution pH was kept constant at 11.0 while glycine concentration was varied based on a glycine to copper (Gly: Cu) molar ratio. Ratios were chosen over molar concentration because the stable copper-glycine complex between pH 4 and 12 is $Cu(H_2NCH_2COO)_2$, implying that a minimum of two moles of glycine are needed for each mole of copper for the complex formation. The Gly:Cu ratios investigated were 2:1, 3:1, 4:1 and 8:1. This approach will be followed throughout this chapter. The grind for the azurite specimen was 100 % passing 75 µm and the % solids was 0.95 w/v (Table 3.3). The influence of the glycine concentration on copper extraction from azurite is shown in Figure 4.1. The percentage of copper extraction is observed to increase as the Gly:Cu increases. When the Gly:Cu is 2:1, the highest copper extraction is just 73.0 % over 48 hours, and when the ratio is 8:1, 98.0 % copper is extracted in just over 2 hours (the copper concentrations at which the stated extraction percentages are calculated from are given in Appendix H). From these results, a Gly: Cu ratio of 4:1 was then chosen as for further investigations.

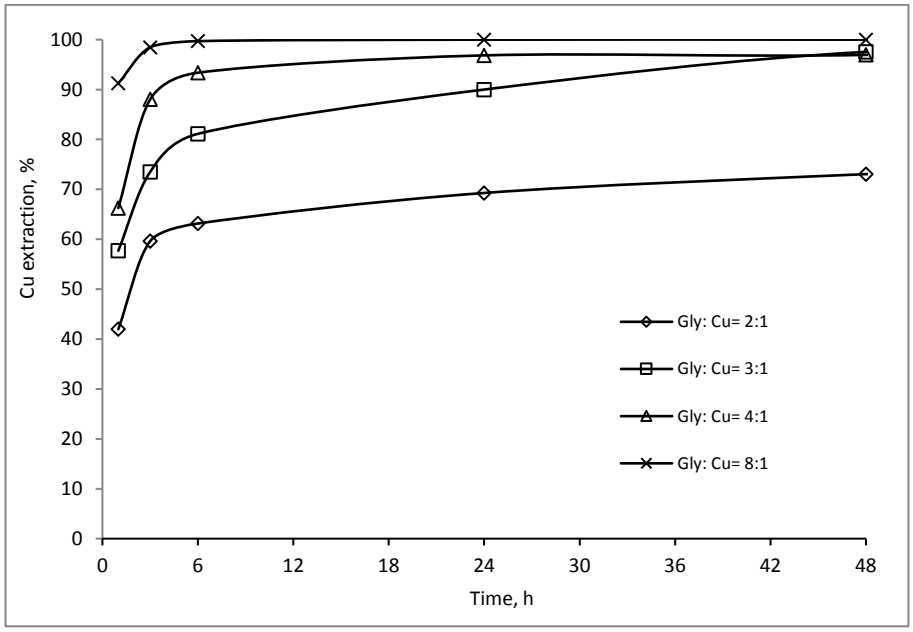

Figure 4.1 Effect of initial glycine concentration on the dissolution of copper from azurite: pH 11, P_{100} 75 µm and % solids 0.95 % w/v

4.2.3 Effect of Initial Solution pH

To study the relationship between copper dissolution from azurite and the initial leach solution pH, the initial pH was varied from 8.0 to 11.0 using sodium hydroxide. During the

duration of the experiments, the pH was monitored but uncontrolled. Initial Gly:Cu molar ratio was kept constant at 4:1. Figure 4.2 shows that, after 1 hour, leaching at pH 10 has a higher copper dissolution of 77.7 % compared to 66.3% at pH 11. However, after 3 hours of leaching, copper extraction at pH 11 exceeded that of solution pH 10. It can actually be seen that dissolved copper at pH 10 started to decrease as this was associated to a light blue precipitate formation. The observed drop out of copper from solution could be attributed to both the solution pH and the copper concentration in solution as shown in Figure 4.3. It is supposed that the precipitate is a copper glycinate complex as it redissolved when the solution was heated at 50 °C while mixing. The precipitation of $Cu(Gly)_2$ has also been reported by (Gyliene, 2001) when investigating the removal of heavy metals in solutions by complexing them with glycine and EDTA. The metal complex was then reported to precipitate after several hours or days. She also reported that the precipitation is influenced by temperature, pH and concentration of components. The production of Cu-glycinate powdered has been described to occur through the formation of a Cu-glycinate complex and then causing it to precipitate by adding ethnol (Imamura et al., 1978). Thus, depending on the temperature, pH and copper concentration, the Cu-glycinate complex has an upper limit of solubility in alkaline solutions. It could thus be concluded that, for azurite, under the given conditions: a copper concentration of more than 3.1 g/L, at pH 10.2 and at 25 °C, copper precipitates as $Cu(Gly)_2$.

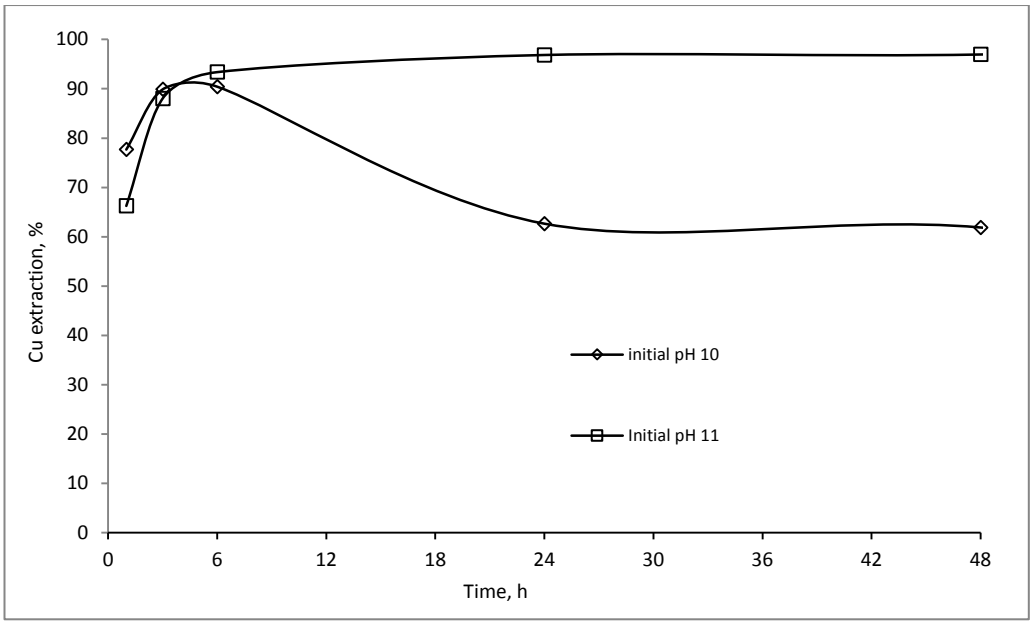

Figure 4.2 Effect of initial leach solution pH on copper dissolution from azurite: Gly:Cu 4:1, P_{100} 75 µm and % solids 1.95 % w/v

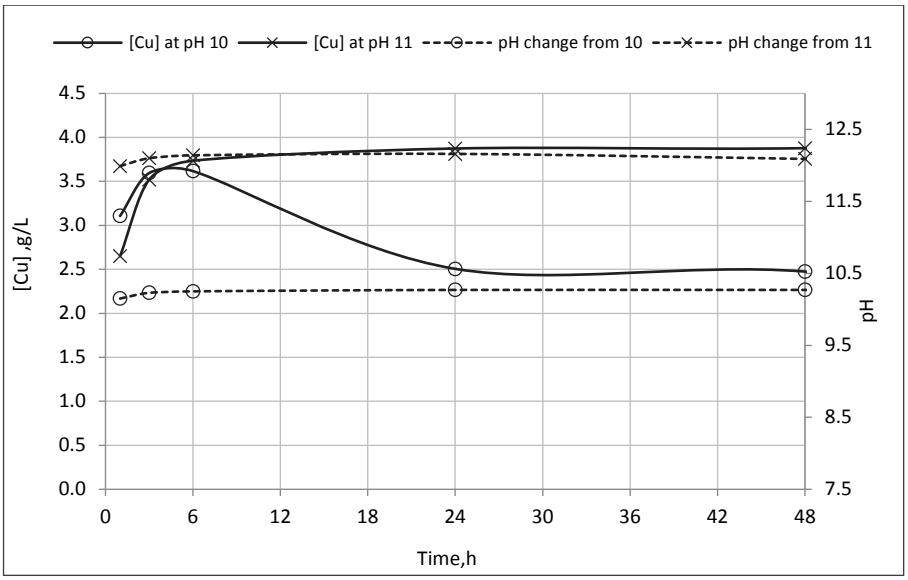

Figure 4.3 Correlation between the change in copper concentration and pH change during leaching of azurite: Cu:Gly 1:4, P_{100} 75 µm and % solids is 0.95 % w/v

The general leaching reaction of azurite can be written as in Equation 4.1:

$$2(CuCO_3)\cdot Cu(OH)_2 + 6(NH_2CH_2COO^-) \rightarrow 3[Cu(NH_2CH_2COO)_2] + 4OH^- + 2CO_3^{2-} \qquad (4.1)$$

4.3 Malachite A

Malachite is a copper carbonate hydroxide mineral with the formula $CuCO_3.Cu(OH)_2$. It is green, has a monoclinic crystalline structure and generally results from the weathering of copper ores and often occurs together with azurite. It is a very common secondary copper mineral in the oxidation zone of copper ore deposits and can also be associated with limestone copper deposits (Henn & Milisenda, 2004).

4.3.1 Mineralogy and Elemental Composition

The XRD of the malachite specimen A shows malachite as the only copper mineral present in the tested specimen. Quantitative mineralogy of other mineral phases present and the chemical composition of the sample is given in Table 4.2.

Table 4.2 Mineralogy and chemical composition of Malachite A

Mineralogy		**Chemical composition**	
Phase	weight %	Element	%
Goethite	1.7	Cu	41.6
Hematite	3.3	Al	0.1
Malachite	66.0	K	0.1
Quartz	16.7	Mg	0.4
Amorphous Content	12.0	Fe	3.5
		Ca	0.8

4.3.2 Effect of Initial Glycine Concentration

The effect of glycine on the dissolution of copper from Malachite A was investigated by varying the Gly:Cu molar ratio from 2:1 to 8:1 while keeping the initial leach solution pH at 11. The mineral specimen was ground to a P_{100} of 75 µm and the solids content during leaching was 1.62 % w/v. The results as illustrated by Figure 4.4 show that copper dissolution increases as the Gly:Cu ratio increases. In the first hour of leaching, copper extraction at Gly:Cu molar ratio of 2:1, 3:1, 4:1, and 8:1 was 52.0, 72.0, 81.0 and 87.0 %, respectively. This is not surprisingly, as increasing the glycine concentration means more glycinate anions were available on minerals surface to leach copper.

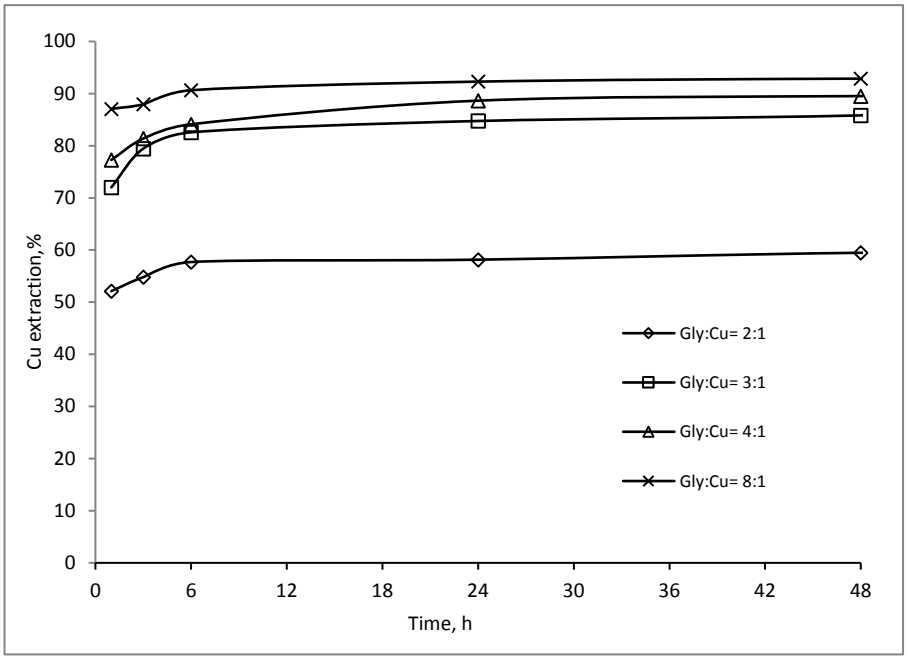

Figure 4.4 Effect of initial glycine concentration on the dissolution of copper from malachite A: pH 11, P_{100} 75 µm and % solids is 1.62 % w/v

4.3.3 Effect of Initial Solution pH

The influence of initial leach solution pH was studied by varying the pH from 9.5 to 11 while keeping the Gly:Cu molar ratio constant at 4:1. Higher copper dissolution was noted at higher pH as shown in Figure 4.5. It was also observed that, at the lower pH of 9.5, copper concentration begins to decrease after three hours of leaching as copper glycinate precipitate is produced. As can be noticed in Figure 4.6, the precipitation of crystalline copper glycinate from the leach solution at initial pH of 9.5 starts to occur at a copper concentration of 2.5 g/L and at a pH of 9.26.

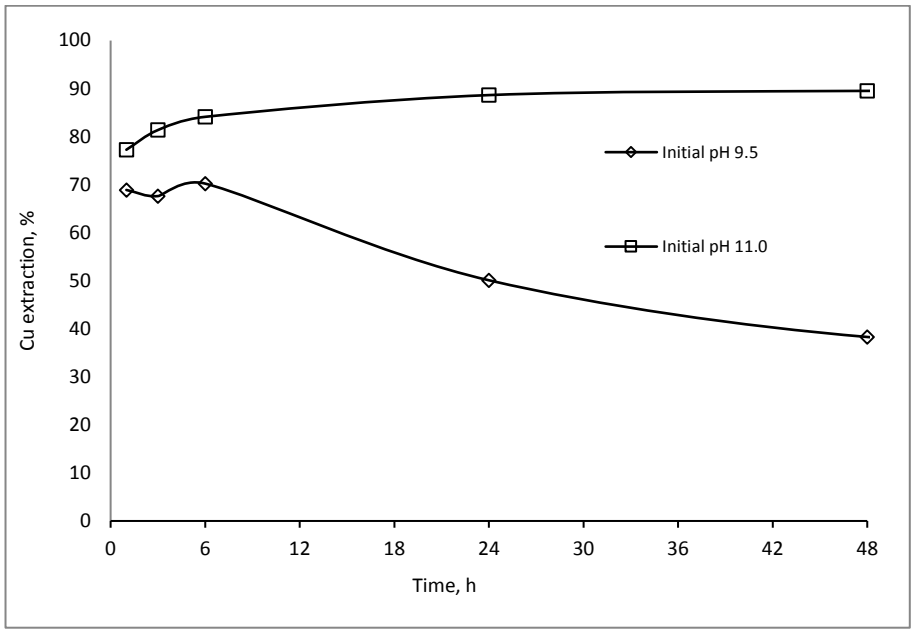

Figure 4.5 Effect of initial solution pH on the dissolution of copper from malachite A: Gly:Cu 4:1, P_{100} 75 µm and % solids 0.96 % w/v

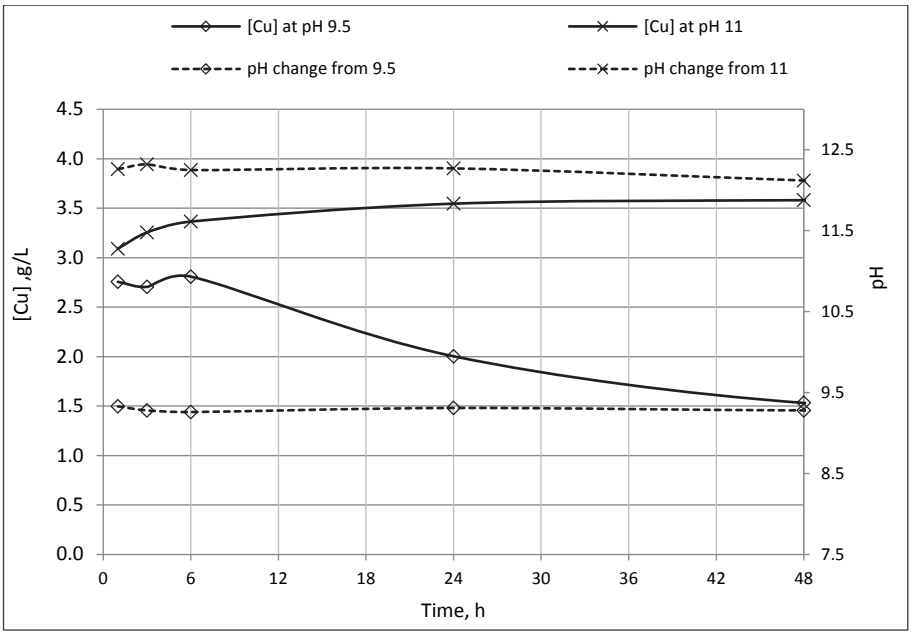

Figure 4.6 Correlation between the change in copper concentration and pH change during the leaching of malachite with glycine

The general leaching reaction of malachite can be written as in Equation 4.2

$$2(CuCO_3).Cu(OH)_2 + 6NH_2CH_2COO^- \rightarrow 2[Cu(NH_2CH_2COO)_2] + 2OH^- + 2CO_3^{2-} \quad (4.2)$$

4.4 Cuprite

Cuprite is an oxide mineral of copper with the formula Cu_2O. It occurs in the oxidized zone of copper deposits in association with tenorite, malachite, azurite, calcite, brochantite, antlerite, atacamite, chrysocolla, iron oxides and clay minerals. Optically, it is transparent to translucent with colors from cochineal-red, purplish red to nearly black. It is obtainable in cubic, octahedral and dodecahedral crystals with an interrupted cleavage and conchoidal to uneven fracture (Anthony et al., 1995). Cuprite notably occurs in USA, Africa, Chile, Australia and Europe.

4.4.1 Mineralogy and Elemental Composition

The mineralogy of the cuprite mineral specimen including other phases and the chemical composition of the cuprite sample are presented in Table 4.3 as determined by XRD and XRF

Table 4.3 Mineralogy and chemical composition of cuprite

Mineralogy	Phase	Cuprite	Dolomite	Goethite	Quartz	Amorphous Content
	weight %	23.4	62.1	0.5	1.0	27.0
Chemical composition	Element	Cu	Si	Mg	Fe	Ca
	%	20.1	0.5	9.6	1.9	16

4.4.2 Effect of Initial Glycine Concentration

The effect of glycine concentration on copper dissolution was investigated by varying the Gly:Cu molar ratio from 2:1 to 8:1 while keeping the initial leach solution pH constant at pH 11. Figure 4.7 shows that, as the Gly:Cu molar ratio increases, the percentage of copper extracted increased. After 24 hours of leaching, it was found that there is no significant difference between the amount of copper extracted at Gly:Cu ratios of 8:1 and 4:1 (85.6 % and 84.2 %, respectively). The copper extraction was only 68.1 % and 75.9 % at Gly:Cu molar ratios of 2:1 and 3:1, respectively.

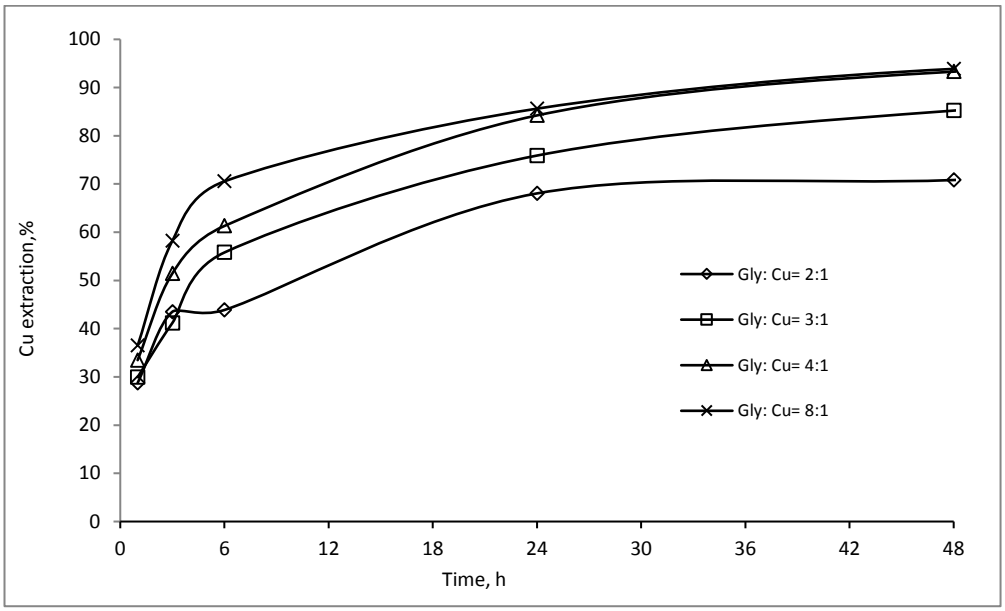

Figure 4.7 Effect of initial glycine concentration on copper dissolution from cuprite mineral specimen: pH 11, P_{100} 75 µm and % solids 1.99 % w/v

4.4.3 Effect of Initial Solution pH

The effect of initial leach solution pH on copper dissolution was investigated at pHs 9.0, 10.0 and 11.0. The Gly:Cu molar ratio was at 4:1 for all experiments. The results, as shown in Figure 4.8, indicate that the highest copper dissolution is obtained at pH 10, yieling 48.0 % after one hour of leaching and 97.0 % after 48 hours. During the same period at pH 11, 33.1

% Cu dissolution was obtained in the first one hour and increased to 93.0 % after 48 hours. A copper extraction of 40.0 % was obtained at pH 9.0 in the first hour of leaching and increased to 72.0 % after 6 hours. After this point, the copper content in solution decreased to 45.0 % after 48 hours presumably due to the precipitation of cupric glycinate. This is the same observation noted for the azurite and malachite at lower pHs. Figure 4.9 continues to suggest that copper precipitation at different pHs only occurs at a higher copper concentration (3.0 g/L for cuprite at pH 9).

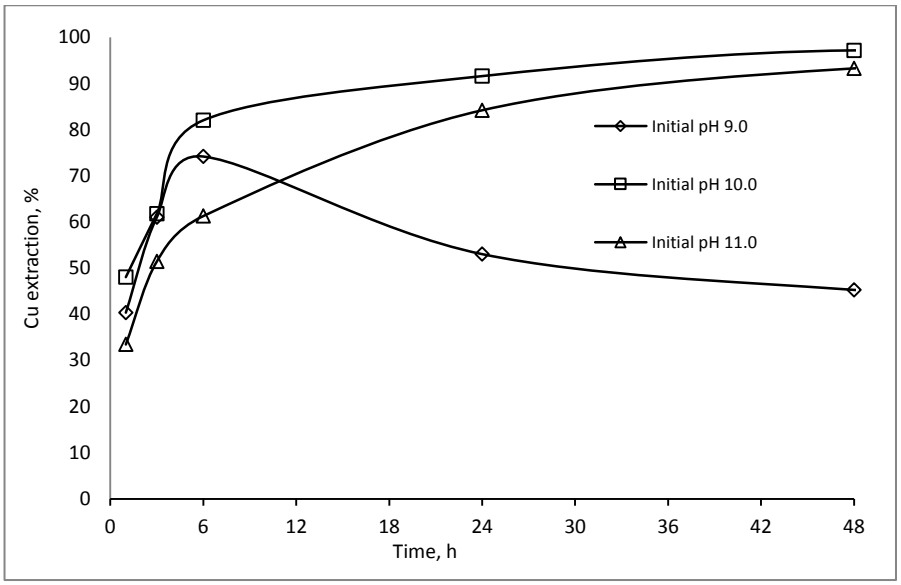

Figure 4.8 Effect of initial pH on copper dissolution from cuprite: Gly:Cu 4:1, P_{100} 75 µm and % solids 1.95 % w/v

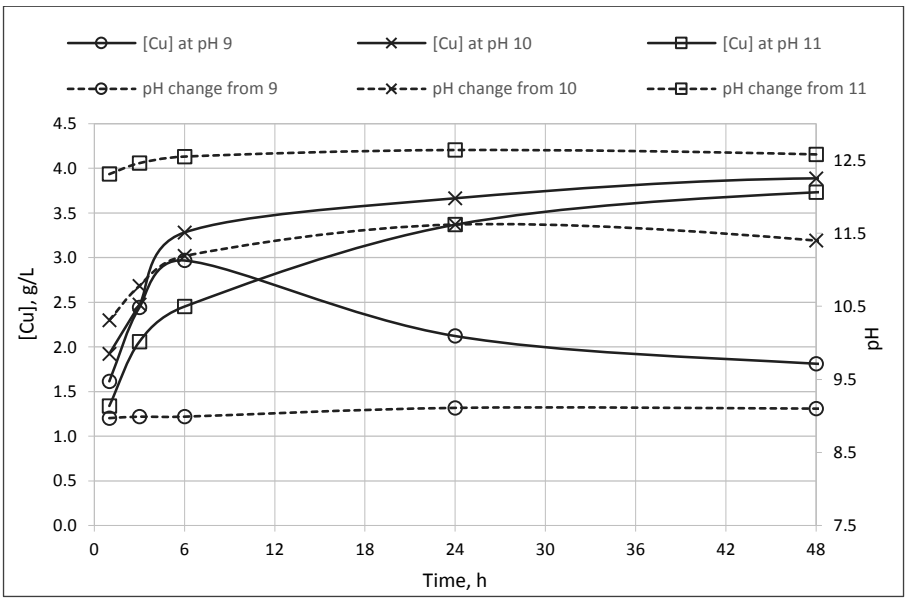

Figure 4.9 Correlation between copper concentration and leach solution pH during the leaching of cuprite with glycine

The general leaching reaction of cuprite can be written as in Equation (4.3)

$$Cu_2O + 4NH_2CH_2COO^- + 2H_2O + 1/2O_2 \longrightarrow 2[Cu(NH_2CH_2COO)_2] + 4OH^- \quad (4.3)$$

4.5 Chrysocolla

Chrysocolla is a hydrous silicate copper mineral having the formula $CuO{\cdot}SiO{\cdot}2H_2O$. It has a green to sky-blue, non-crystalline structure and amorphous silica gel or a gelatinous precipitate. Chrysocolla is relatively soft with a hardness of 2-4 on Mohs scale. It has no cleavage and shows an uneven or conchoidal fracture which is typical of glassy, amorphous materials. As with other oxidized copper minerals, it is found in the oxidized zones of copper veins and occurs in association with azurite and malachite (Anthony et al., 2001).

4.5.1 Mineralogy and Elemental Composition

XRD identified chrysocolla as the only copper phase. Rietveld refinement software could not be used for the quantitative weight % analysis of the identified chrysocolla phase as its inorganic crystal structure database (ICSD) file was not available. However, from the percentage copper obtained from an XRF analysis and considering the chemical formula of chrysocolla to be $CuO{\cdot}SiO_2{\cdot}2H_2O$, the percentage of chrysocolla in the sample was calculated to be the whole 59.0 % of the amorphous phase. The mineralogical and chemical composition of the chrysocolla sample is shown in Table 4.4

Table 4.4 Mineralogical and chemical composition of chrysocolla specimen

Mineralogy		Elemental composition	
Phase	weight %	Element	%
Kaolinite-1A	6.0	Cu	24.7
Muscovite -1M	13.5	Si	21.6
Muscovite -2M	12.8	Al	3.0
Quartz	6.7	k	1.4
Rutile	1.8	Ti	0.1
Chrysocolla	59.0	Mg	0.4

4.5.2 Effect of Initial Glycine Concentration

Figure 4.1 shows the insignificant effect of glycine concentration on the dissolution of copper from chrysocolla. P_{100} is 57 µm and % solids is 1.62 % w/v. An increase in Gly:Cu molar ratio from 2:1 to 4:1 results in only 12.0 and 19.0 % of copper extraction respectively. The leaching of chrysocolla has been reported to be generally slow requiring extended leaching times (Davenport et al., 2002a)

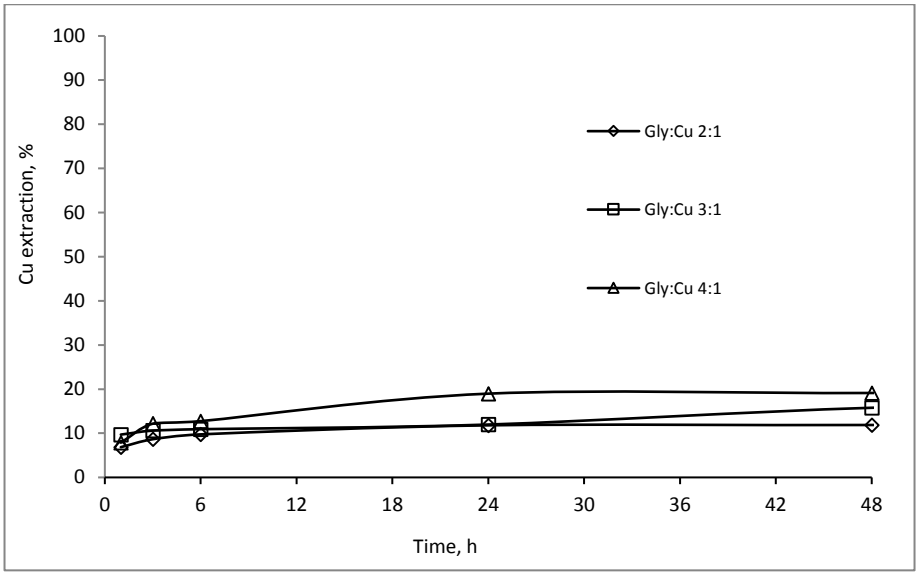

Figure 4.10 Effect initial glycine concentration on chrysocolla leaching; pH 11, P_{100} 75 µm and % solids is 1.62 % w/v

4.5.3 Effect of Initial solution pH

The effect of initial leach solution pH was studied by varying the pH from 8.0 to 11.0 while Gly:Cu molar ratio was maintained at 4:1. The results in Figure 4.1 show that lower pH favors copper dissolution with 26.0 % of copper dissolution at pH 8.0 as compared with 19.0 % at pH 11. It was observed that the leaching of azurite, malachite and cuprite at lower pHs resulted in copper precipitation. With these oxides, copper precipitation was noted to start occurring at about 2.8 g/L copper in solution. Figure 4.12 shows that as the maximum copper concentration in solution is 1.07 g/L at pH 8, there is no precipitation. This observation confirms the proposition that copper precipitation is not only a function of pH alone but that it would only occur when the concentration in solution is above a certain level (2.7 to 3 g/L as previously observed).

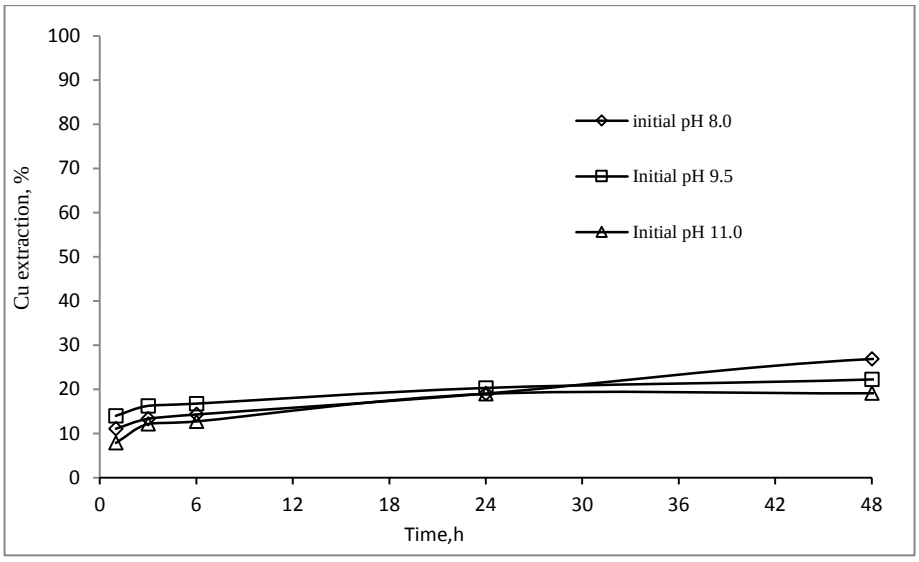

Figure 4.11Effect of initial leach solution pH on chrysocolla leaching: Gly:Cu 4:1, P_{100} 75 µm and % solids 1.62 % w/v

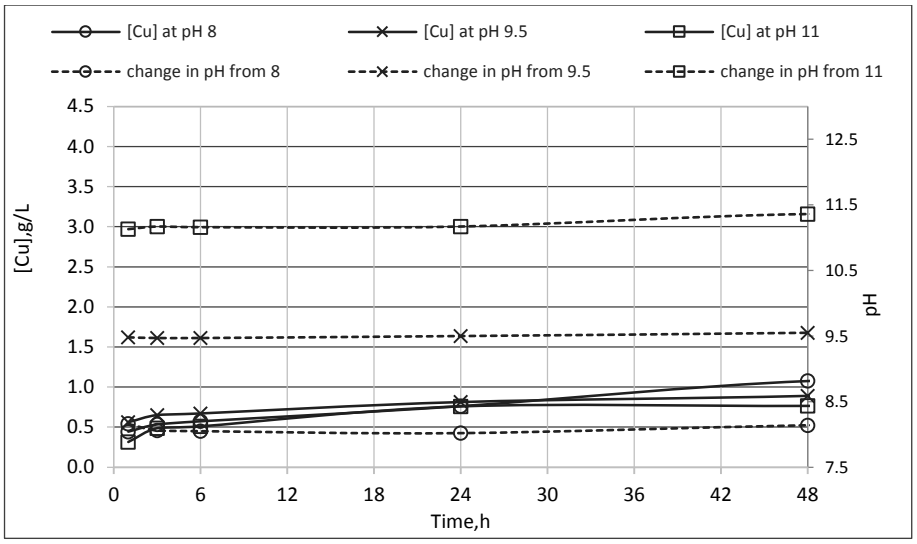

Figure 4.12 Correlation between [Cu] in solution and change in solution pH during glycine leaching of chrysocolla

The very low dissolution of chrysocolla is not uncommon in alkaline lixiviants. Leaching of chrysocolla in ammoniacal carbonate solutions reported only a 50.0 % of the total copper content (Warren & Devuyst, 1973). Wei et al. (2010) noted that, of all the copper minerals leached in ammonia-ammonium chloride solutions, copper silicates exhibited the poorest propensity to be leached. SEM results of the unleached and leached chrysocolla specimen in alkaline glycine solution (Figure 4.13) showed that the leach residue developed a spike-like surface morphology. This can be attributed to the concept that as the copper from chrysocolla is leached, an impervious layer of hydrated silica is left behind which restricts further copper leaching (Tanda et al., 2017).

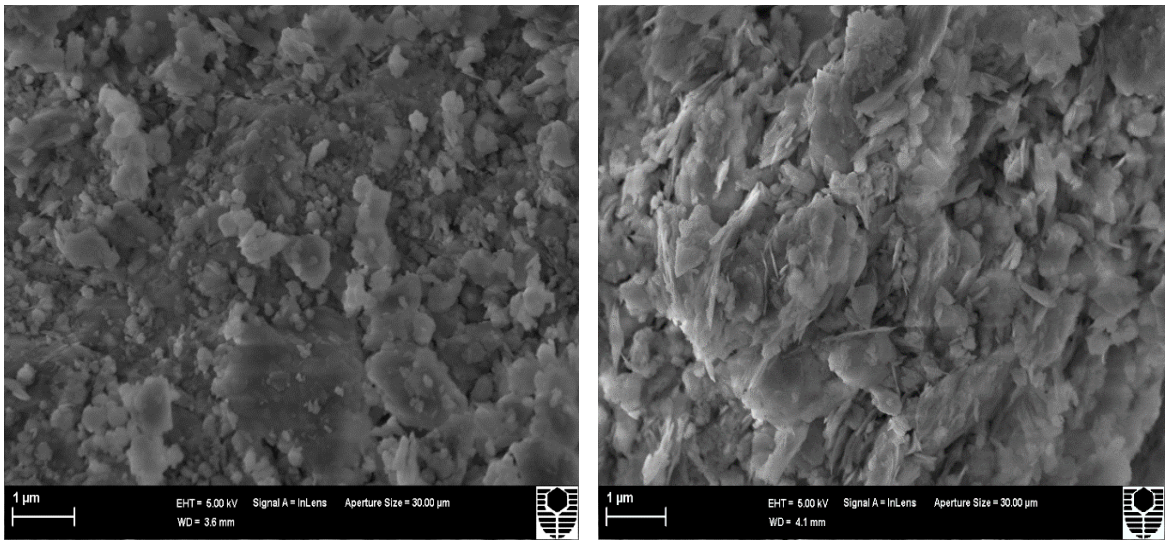

(a) (b)

Figure 4.13 SEM photographs of unleached (a) and partially leached (b) chrysocolla

The general leaching reaction of cuprite can be written as in Equation 4.4:

$$CuO{\cdot}SiO_2{\cdot}2H_2O + 2(NH_2CH_2COO^-) \rightarrow Cu(NH_2CH_2COO)_2 + H_2O + 2OH^- + SiO_2 \quad (4.4)$$

4.6 Metallic Copper

Metallic (native) copper can be found in association with copper minerals such as cuprite. In addition, an important source of metallic copper is from urban mining through the recycling of electrical and electronic equipment waste, demolished buildings, manufacturing offcuts as they contain substantial amounts of iron, lead, copper and other metals (Ping et al., 2009). Hydrometallurgy has been indicated as one of the best options for copper recovery and precious metals from electronic waste as the metal occurs with impurity elements requiring a selective leaching approach (Koyama et al., 2006).

4.6.1 Effect of Initial Glycine Concentration

Experiments to determine the influence of glycine concentration on the dissolution of metallic copper were conducted by leaching 2 g of 100 % passing 75 µm pure copper in solutions containing different initial concentrations of glycine at pH 11 for 48 hours. Hydrogen peroxide at a concentration of 0.5 % was added to the leach solution to enhance

the oxidation process. Figure 4.14 shows that, as the Gly:Cu ratio increases from 2:1 to 4:1, the copper concentration in solution over time also increases. After 48 hours of leaching, a copper dissolution of 91.7, 89.2, and 82.8 % was recorded for Gly:Cu ratios of 4:1, 3:1 and 2:1, respectively.

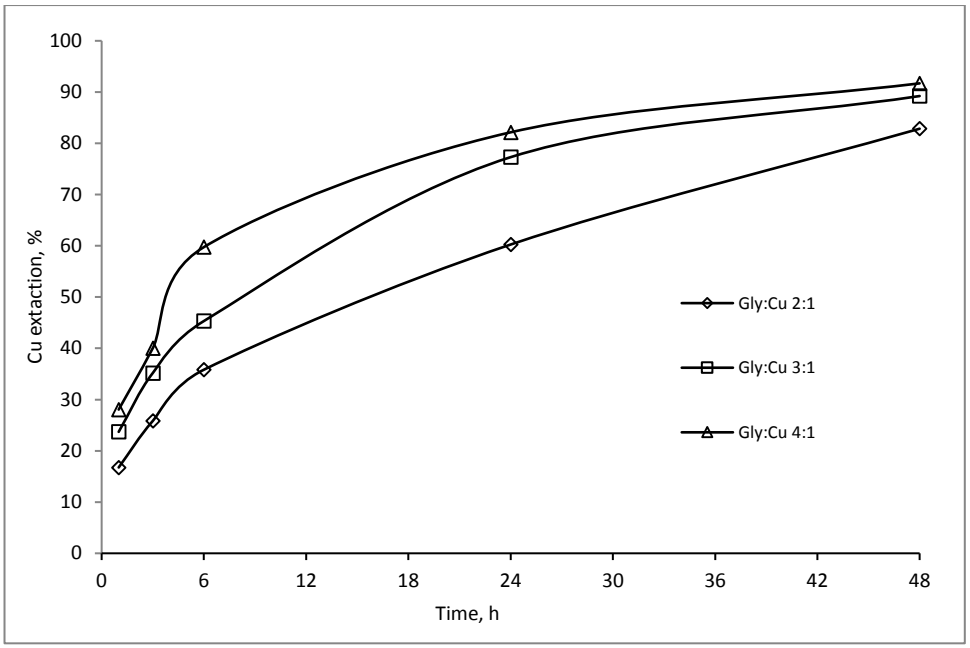

Figure 4.14 Effect of initial glycine concentration on metallic copper dissolution: pH 11, 0.5 % H_2O_2, P_{100} 75 µm and % solids 0.40 % w/v

4.6.2 Effect of Initial Solution pH

The effect of initial leach solution pH was investigated by varying the initial pH from natural glycine pH (5.8), pH 8 and pH 11 with NaOH as a pH modifier. A Gly:Cu molar ratio of 4:1 and 0.5 % H_2O_2 concentration was maintained for all experiments. The results shown in Figure 4.15 illustrate that higher solution pHs favour the dissolution of metallic copper. At the natural pH of 5.8, the percentage of copper dissolved gradually increases to a maximum of 51.4 % after 24 hours and then declines to 29.7 % at the end. For pHs 8 and 11, there is a fast dissolution with 57.1 % and 59.8 % copper dissolution respectively in 6 hours. Copper content in solution at pH 8.0 then decreased to 33.7 % and 26.4 % after 24 and 48 hours, respectively. At pH 11, copper precipitation did not occur over the same period and the copper dissolution reached 91.7% after 48 hours.

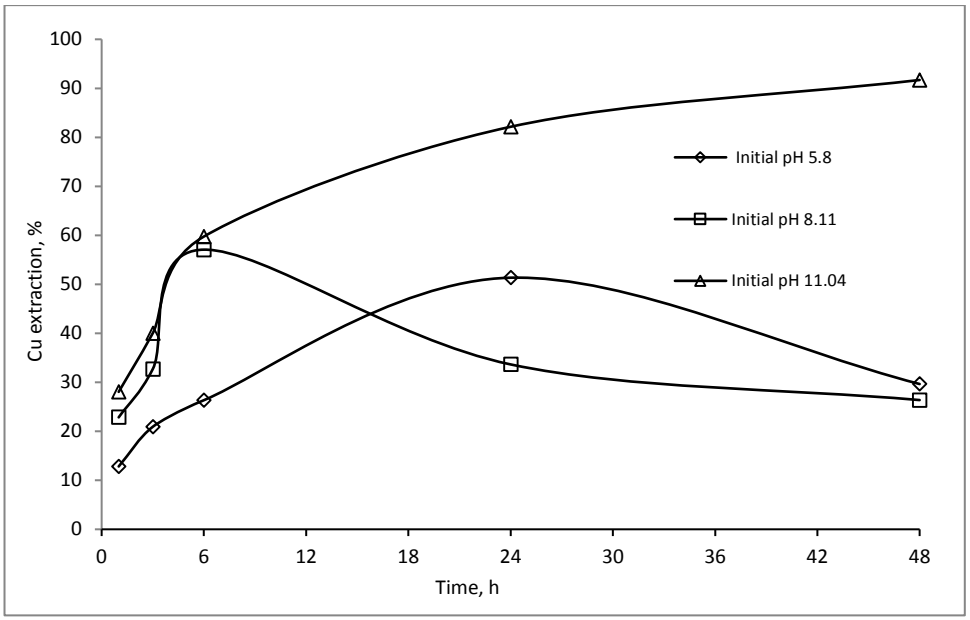

Figure 4.15 Effect of initial solution pH on metallic Cu dissolution; Gly:Cu 4:1, 0.5 % H_2O_2, , P_{100} 75 µm and % solids 0.40 % w/v

4.6.3 Effect of Hydrogen Peroxide

The effect of hydrogen peroxide as an oxidising agent on the metallic copper dissolution was studied by varying the initial peroxide concentration from 0 %, 0.1 %, 0.5 % and to 1.0 %. For all experiments, Gly:Cu ratio was kept at 4:1 and the leach pH was kept at 11. Although a very small improvement in copper dissolution was noted as H_2O_2 concentration increased in the first hour of leaching, H_2O_2 had no significant overall effect on metallic copper dissolution as shown in Figure 4.16. Initial hydrogen peroxide concentrations of 0, 0.1, 0.5 and 1.0 resulted in 88.3, 92.2, 91.7 and 91.2 % copper leaching respectively. This observation implies that oxygen from air entering the bottle provides sufficient oxidant for copper oxidation. It should however be noted that hydrogen peroxide rapidly converts to ·OH radicals which have been reported to oxidise glycine (Berger et al., 1999). The use of hydrogen peroxide should be avoided since it has no significant effect on copper leaching but can rather degrade the lixiviant.

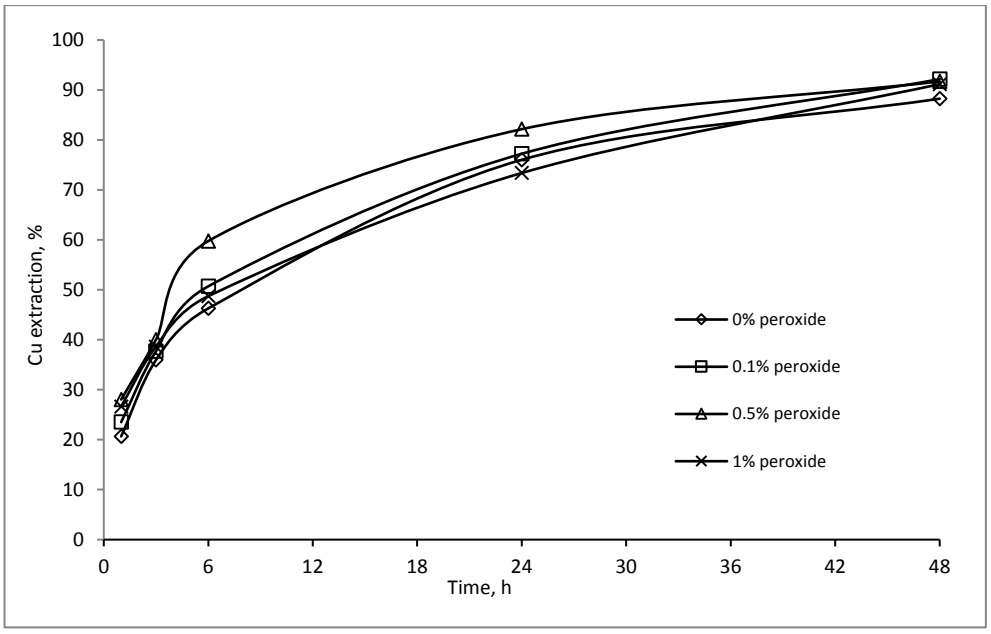

Figure 4.16 Effect of peroxide on metallic Cu dissolution: Gly:Cu 4:1, pH 11, , P_{100} 75 µm and % solids 0.40 % w/v

The general leaching reaction of metallic copper can be written as in Equation 4.5:

$$Cu + 2(NH_2CH_2COO^-) + 1/2O_2 + H_2O \rightarrow Cu(NH_2CH_2COO)_2 + 2OH^- \quad (4.5)$$

4.7 Chalcocite A

Chalcocite, copper(I) sulfide is a dark grey copper mineral which is commonly found in the supergene enriched environment beneath the oxidized zone of porphyry copper deposits due to copper leaching from the oxidized zone. Due to its high copper content and the relative ease to separate sulfur, it is a very profitable copper mineral to mine (Frost et al., 2007; Howard T. Evans, 1979). Most rich chalcocite deposits have generally been mined but valuable deposits of chalcocite are found in Ely-Nevada, Morenci-Arizona, Butte-Montana and Tsumeb-Namibia (Encyclopædia Britannica, 2016). A modern example of a chalcocite deposit that is currently being mined is Las Cruces in Sevilla-Spain where open pit mining is practiced. The ore is crushed and atmospherically leached in agitated reactors. This is followed by solvent extraction and then electrowinning to produce copper cathode (First Quantum Minerals; Tornos et al., 2017).

4.7.1 Mineralogy and Elemental Composition

Table 4.5 shows the mineralogical and elemental composition of the chalcocite specimen used for investigating the dissolution of chalcocite in alkaline glycine solution. The chalcocite mineral specimen contains 98.2 % chalcocite as the only copper mineral peak indicated by the Q-XRD analysis. Elemental composition of the specimen confirmed its high purity with a percentage copper being 78.8 % and 20.2 % sulfur.

Table 4.5 Mineralogy and elemental composition of chalcocite A

Mineralogy	Phase	Chalcocite	Quartz	Amorphous content
	weight %	98.2	0.6	0.2
Elemental composition	Element	Cu	S	Si
	%	78.8	20.2	0.2

4.7.2 Effect of Initial Glycine Concentration

The influence of glycine concentration on the chalcocite dissolution was studied by varying the Gly:Cu molar ratio from 2:1 to 8:1 in a solution containing 0.5 % H_2O_2 at pH 11. Figure 4.17 shows that, at higher Gly:Cu molar ratio, the copper dissolution from chalcocite sample was enhanced. After 48 hours of leaching, the maximum copper dissolution was 46.5 % at a Gly:Cu ratio of 8:1. The observed results indicate that the initial leaching rate of chalcocite (6 hours) in the alkaline glycine solution is very fast after which the rate is significantly slow. Such leaching trends have also been reported during chalcocite leaching in both acidic and alkaline solutions (Cheng & Lawson, 1991; Naderi et al., 2011; Salvador, 1978). It is generally accepted that the first step involves the conversion of chalcocite at the surface to copper ions and a covellite residue which leaches rather slowly as indicated in Equations 4.6 and 4.7.

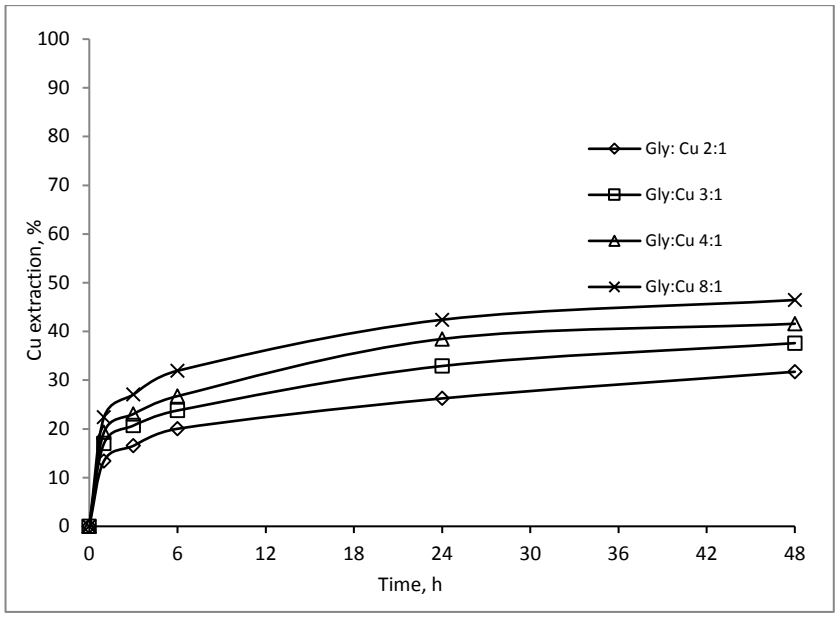

Figure 4.17 Effect of initial glycine concentration on the dissolution of chalcocite A: pH 11, 0.5 % H_2O_2, P_{100} 75 µm and % solids 0.51 % w/v

$$Cu_2S + 2(NH_2CH_2COO^-) + 1/2O_2 + H_2O \rightarrow Cu(NH_2CH_2COO)_2 + CuS + 2OH^- \quad (4.6)$$

$$CuS + 2(NH_2CH_2COO^-) + 2O_2 + H_2O \rightarrow Cu(NH_2CH_2COO)_2 + SO_4 + 2OH^- \quad (4.7)$$

4.7.3 Effect of Initial Solution pH

Figure 4.18 illustrates the dissolution behaviour of chalcocite under varied initial leach solution pHs. Copper dissolution at pH 9 and 10 is 38.0 and 41.0 % after 1 hour of leaching and does not change even after 48 hours of leaching. At pH 11, initial copper dissolution is rather slow with just 19.0 % obtained after 1 hour. However, copper extraction gradually increases over time up to 24 hours (38.0 %) at which it plateaus to 41.0 % at 48 hours. This observation continues to indicate that surface chalcocite rapidly converts to copper ions and residual covellite which leaches very slowly. At low solution pH, no copper precipitation is observed as was observed with metallic copper and oxide ores. The absence of precipitation during chalcocite leaching further confirms that copper precipitation would only occur at pH lower than 9.5 when copper content in solution increases above ~ 3 g/L as seen in Figure 4.19.

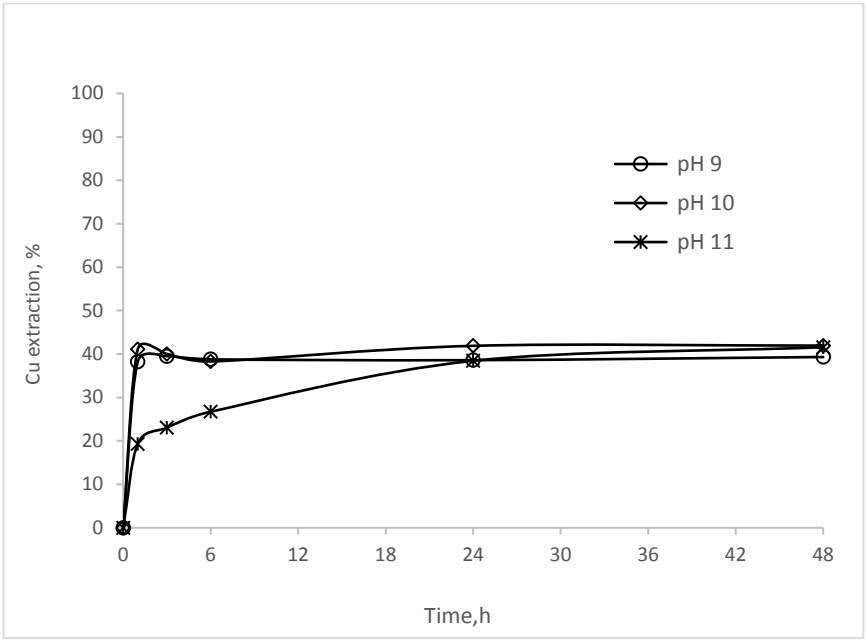

Figure 4.18 Effect of initial solution pH on the dissolution of chalcocite A: Gly:Cu 4:1, 0 % H_2O_2, P_{100} 75 µm and % solids 0.51 % w/v

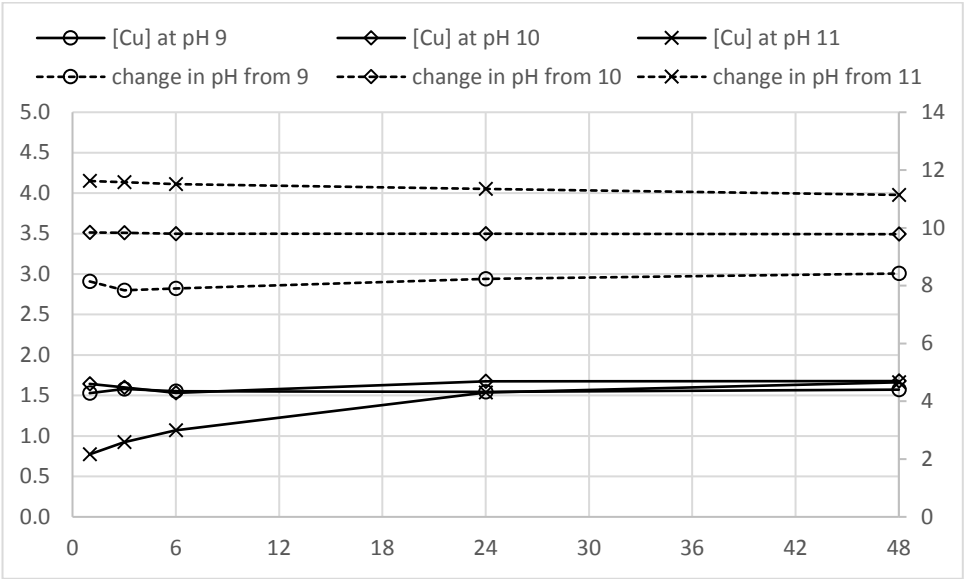

Figure 4.19 Correlation between [Cu] in solution and change in solution pH during glycine leaching of chalcocite

4.7.4 Effect of Hydrogen Peroxide

The influence of hydrogen peroxide as an oxidising agent during chalcocite dissolution was investigated by varying the initial peroxide concentration in the leaching solution. Figure 4.20 shows that, although the initial copper dissolution was higher with 0.5 % and 1.0 % peroxide, i.e. 19.0 % compared to 7.0 % Cu at 0 % peroxide, copper dissolution was found to be independent of peroxide concentration after 6 hours with all solutions resulting in 26.0 %

extraction. The final copper extraction for all solutions after 48 hours was between 42.0 % and 43.0 %. The percentage copper extraction in the absence of hydrogen peroxide being equal to that extracted in the presence of hydrogen peroxide after 6 hours of leaching could be attributed to the hydrogen peroxide being used up or decomposed in the first few hours of leaching. Rapid decomposition of hydrogen peroxide has been reported in the presence of Cu^{2+} ions (Antonijević et al., 1997; Turan & Altundoğan, 2013). Further chalcocite oxidation was accomplished by dissolved oxygen from air.

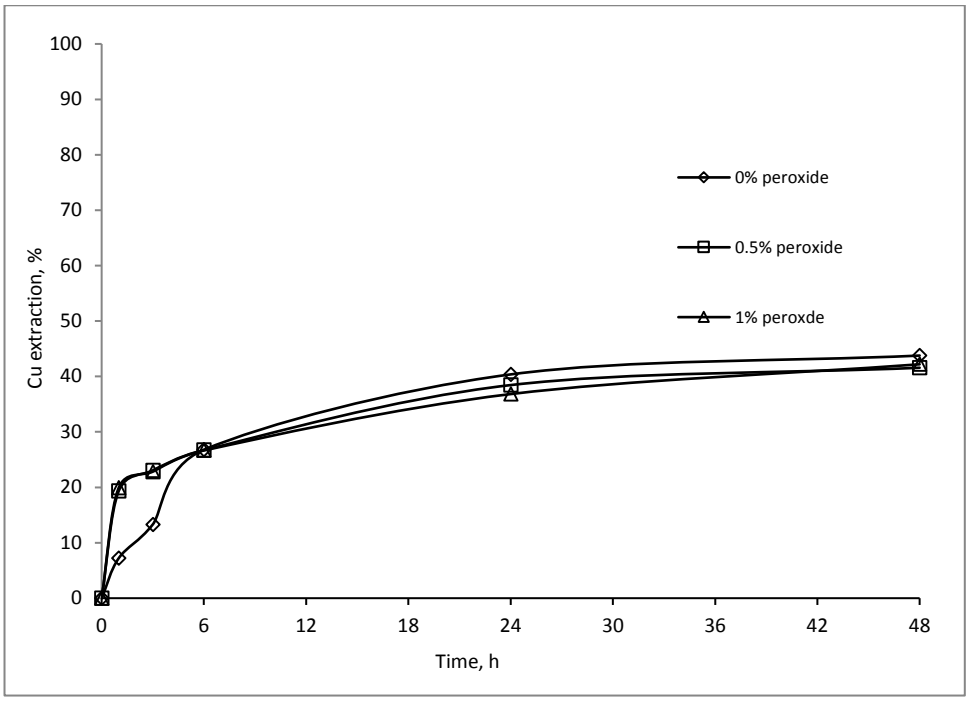

Figure 4.20 Effect of peroxide on chalcocite A dissolution: Gly:Cu 4:1, pH 11, , P_{100} 75 µm and % solids 0.51 % w/v

4.7.5 Effect of Additives

Various additives such as sodium chloride, sodium nitrate, sodium sulfite and persulfate have been reported to enhance the dissolution of copper from chalcocite in acidic or alkaline environments.

A review of the beneficial effect of chloride on the leaching of copper from sulfides in oxygenated sulfuric acid (Senanayake, 2009) indicated that the presence of chloride leads to the formation of a porous crystalline sulfur layer instead of a non-porous sulfur. Vračar et al. (2003) investigated the influence of sodium nitrate on chalcocite leaching in sulfuric acid and noted that the leaching rate increases as $NaNO_3$ increases.

Persulfate has been used as a strong oxidant for the recovery of metals in alkaline solutions

(Liu et al., 2012c; W. Reed, 2004). The addition of persulfate during ammoniacal leaching of copper from spent lithium batteries greatly enhances the leaching rate (Dun-Fang et al., 2009).

The effect of all these additives on the dissolution of chalcocite in alkaline glycine was studied at high and low values and the results are presented in Figure 4.21. As observed from the results, none of the additives had a significant positive effect on copper dissolution from chalcocite in alkaline glycine solutions. This observation suggests that the limited copper dissolution when 40.0 % Cu has been extracted is not a consequence of surface precipitation. It was, however, noted that $Pb(NO_3)_2$ had a large negative effect on copper leached into solution. Oishi et al. (2008) remarked that metallic lead can be easily oxidised by Cu (II) ions to Pb species in ammoniacal solutions. Also, with glycine having been reported to form complexes with Pb (Maeda et al., 1979), some of the glycine that could have been available to form $Cu(Gly)_2$ or drive the forward reaction was used up to form the $Pb(Gly)_2$ complex while Cu (II) ions acting as oxidising agent were being reduced.

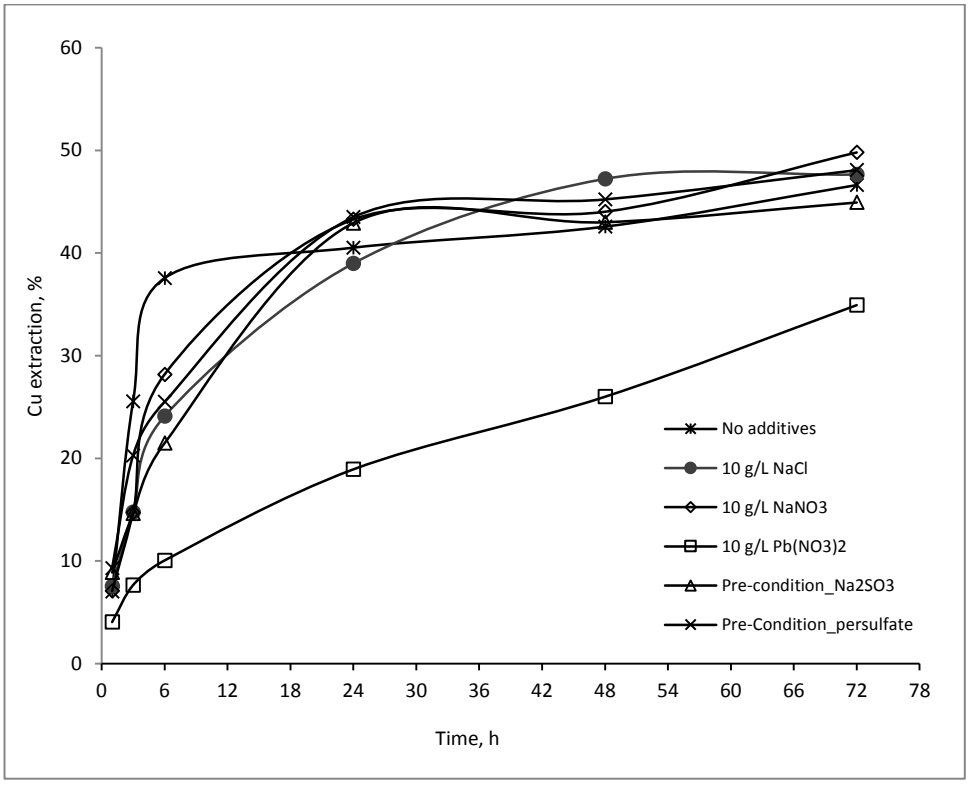

Figure 4.21 Effect of additives on copper dissolution from chalcocite A: Gly:Cu 4:1, pH 11, 0 % H_2O_2, P_{100} 75 µm and % solids 0.40 % w/v

4.8 Chalcopyrite A

Chalcopyrite with a general chemical formula of $CuFeS_2$ is the most abundant copper bearing mineral but it is also the most recalcitrant to leach (Parker et al., 2003). Chalcopyrite is a golden yellow metallic mineral. It is the principal mineral of porphyry-copper deposits occurring in hydrothermal veins and disseminations.

4.8.1 Mineralogy and Elemental Composition

The mineralogical and elemental composition of the chalcopyrite sample was analysed by XRD and XRF spectrometry with the results shown in Table 4.6. Chalcopyrite is the only copper mineral as indicated by the spectrograph (appendix) composing 35.0 % by weight. The percentage copper in the sample is 14.8 % and the presence of 30.8 % Fe mostly as pyrite.

Table 4.6 Mineralogical and elemental composition of chalcopyrite A

Mineralogy		Elemental composition	
Phase	Wt %	Element	%
Chabazite	0.8	As	0.709
Chalcopyrite	35	Ca	0.307
Clinochlore	1.5	Cu	14.810
Pyrite	29.4	Fe	30.870
Quartz	0.9	Mg	1.079
Rutile	0.4	Pb	0.289
Amorphous Content	32	Si	3.641
		S	32.400
		Zn	4.950

4.8.2 Effect of Initial Glycine Concentration

The effect of glycine concentration was studied by varying the Gly:Cu ratio from 2:1, 3:1, 4:1 to 8:1. Initial solution pH and peroxide concentration were 11 and 0.5 % for all experiments and the samples were leached extensively for over 800 hours on a bottle roller. The trend as illustrated in Figure 4.22 shows that increasing the glycine concentrations results in higher copper dissolution. A significant increase in copper extraction was observed after 266 hours of leaching at which 38.0 % and 43.0 % of copper was dissolved at 4:1 and 8:1 Gly:Cu molar ratio, while only 28.0 % and 22.0 % was obtained at 3:1 and 2:1, respectively. At the end of 864 hours of leaching, the highest copper dissolved was 71.0 % at Gly:Cu ratio of 8:1 while at 2:1 and 3:1 ratios copper extraction was 42.7 and 45.8 %, respectively. Over 55.1 % of copper

was extracted from the chalcopyrite sample at Gly:Cu ratio of 4:1.

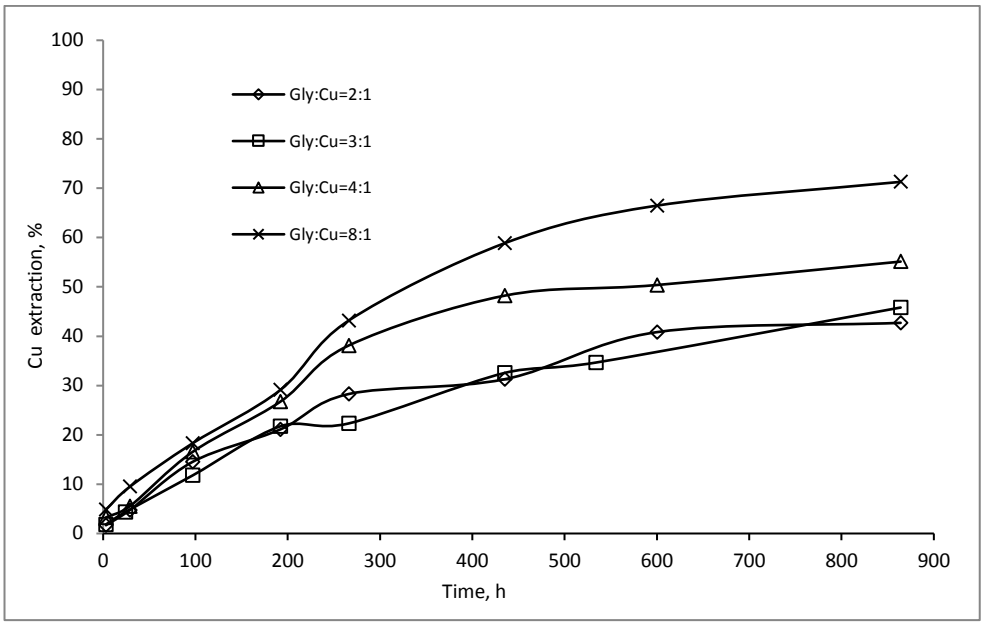

Figure 4.22 Effect of glycine concentration on copper dissolution from chalcopyrite A: peroxide 0.5 %, pH 11, P_{100} 75 µm and % solids 0.51 % w/v

4.8.3 Effect of Hydrogen Peroxide

It is well known that the leaching of chalcopyrite occurs in an oxidative environment (Koleini et al., 2011; McDonald & Muir, 2007; Qiu et al., 2007). Although the bottles were opened to air that will dissolve in solution and act as an oxidising agent, the effect of stronger oxidising agent (hydrogen peroxide) was investigated by varying its concentration from 0 %, 0.1 %, 0.5 % and to 1.0 %. The results in Figure 4.23 show that peroxide does not have any valuable influence on the dissolution of copper from chalcopyrite. As has been mentioned earlier in Section 4.6.3, hydrogen peroxide could be used up or decomposed so fast that its effect will become invisible after 12-24 hours. This then implies that, under the given conditions, dissolved oxygen from the atmosphere provides the necessary oxidative environment. The extent to which dissolved oxygen influences the dissolution behaviour of chalcopyrite has been studied and reported in Chapter 5.

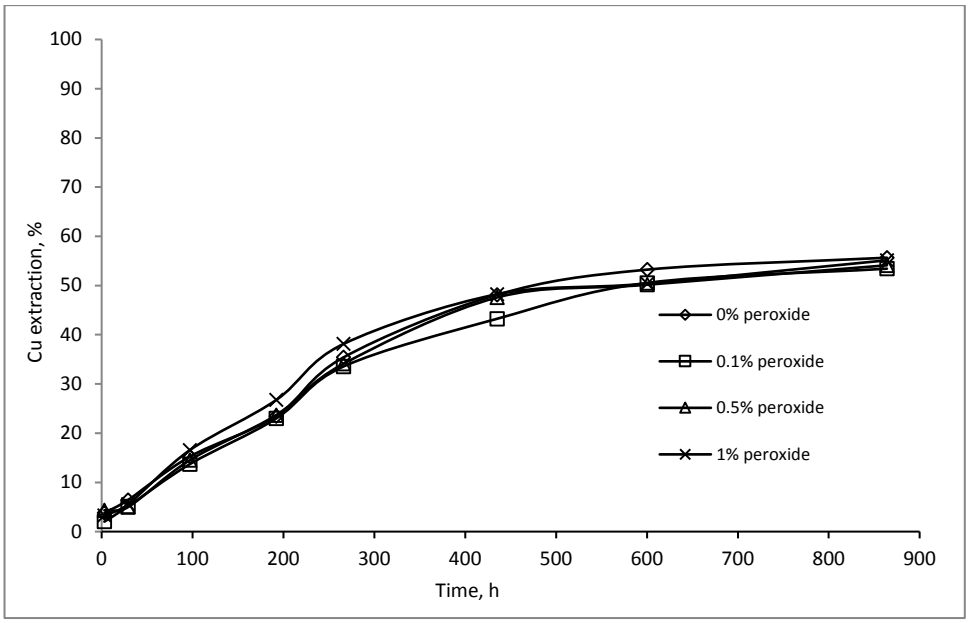

Figure 4.23 Effect of initial peroxide concentration on chalcopyrite A leaching: Gly:Cu 4:1, pH 11, P_{100} 75 µm and % solids 2.7 % w/v

4.8.4 Effect of Initial Solution pH

The effect of initial solution pH was studied at pH values of 9, 10 and 11. It is clearly illustrated in Figure 4.24 that more copper is leached from chalcopyrite as the pH is increased. The percentage of copper dissolved after 864 hours of leaching is 55.0, 44.0 and 20.0 % at pH 11, 10 and 9, respectively. Although the pH was not controlled during these experiments, it was monitored and noted to decrease during the leaching process as shown in Figure 4.25. As was the case with chalcocite leaching, no precipitation is noted when chalcopyrite is leached at pH 11. What is common with the two systems in which copper precipitation does not occur is that the copper concentration in solution is less than 2 g/L.

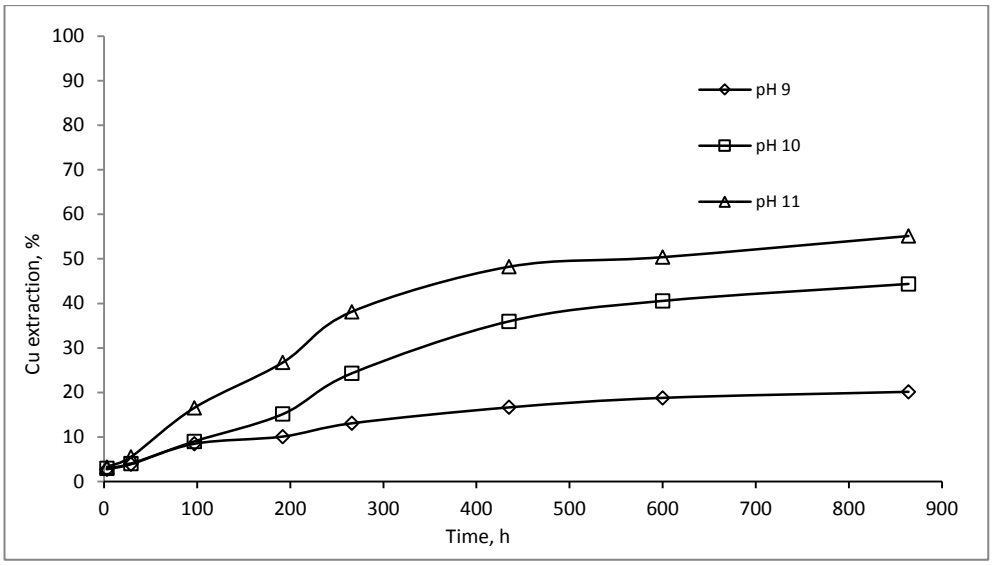

Figure 4.24 Effect of initial leach solution pH on chalcopyrite A leaching: Gly:Cu 4:1, peroxide 0.5 %, P_{100} 75 µm and % solids 0.27 % w/v

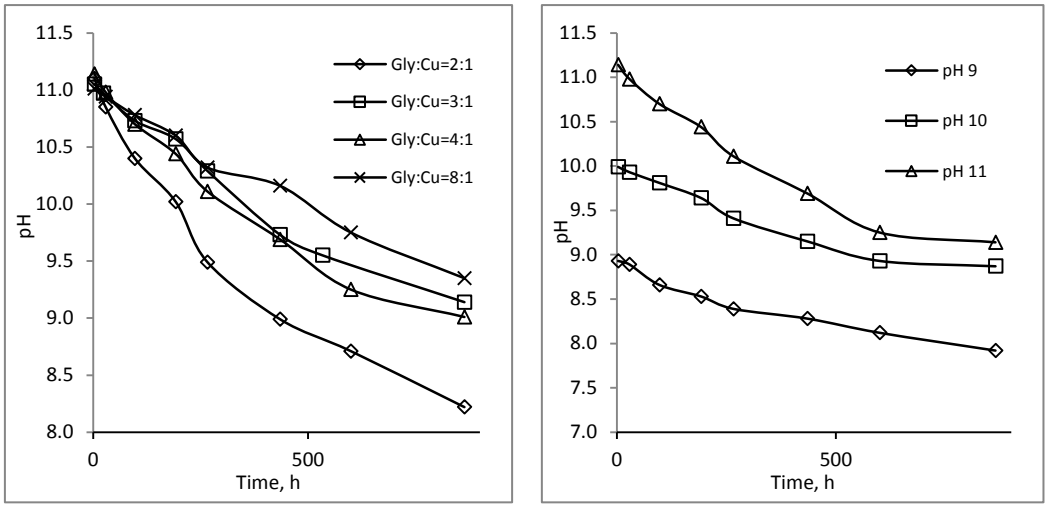

Figure 4.25 Change in solution pH during the leaching of chalcopyrite A: (a) different glycine concentrations, (b) different initial solution pH

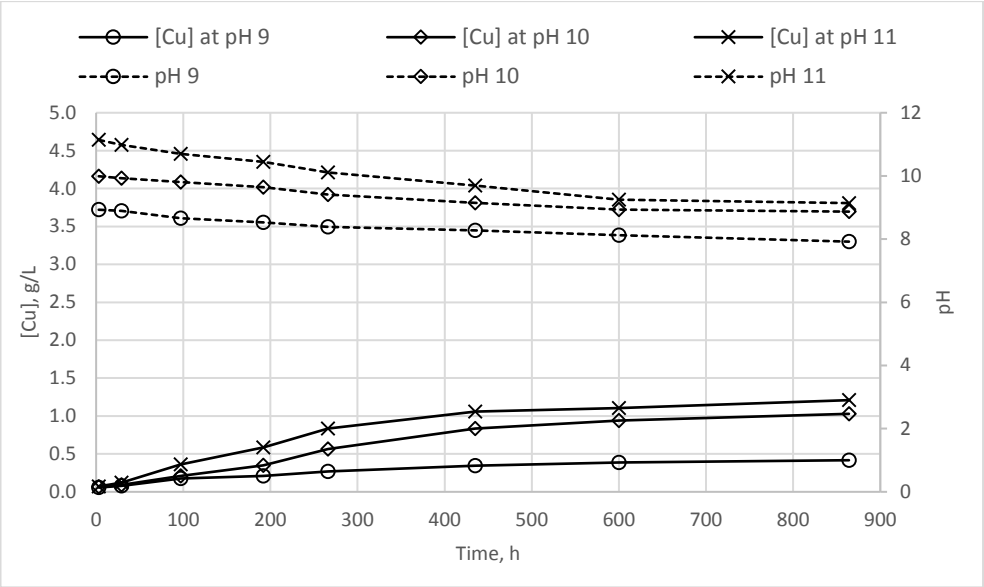

Figure 4.26 Correlation between [Cu] in solution and change in solution pH during glycine leaching of chalcopyrite A

Chalcopyrite leaching in alkaline glycine can be illustrated by Equation 4.8:

$$CuFeS + 2NH_2CH_2COO^- + 4.5O_2 + 2OH^- \rightarrow Cu(NH_2CH_2COO)_2 + H_2O + FeO(OH) + 2SO_4^{2-} \quad (4.8)$$

4.9 Dissolution of Impurities

As mentioned in Chapter 1, the traditional use of acids for the leaching of copper oxides leads to the dissolution of a wide range of impurities (silicon, iron, magnesium, calcium, aluminium, etc.) that may form precipitates and hamper solution flow in heaps and negatively influence downstream processes such as solvent extraction (Ekmekyapar et al., 2015). The final leach solutions from leaching the copper oxides and chalcopyrite mineral specimens were analysed by ICP to establish the leachability of major impurity elements in the alkaline glycine system. Although 247 mg/L Si was detected in solution during chrysocolla leaching, it only represents 7 % of total Si in the sample. If the sample was to be leached in acid medium, Si concentration in solution would have been 3456 mg/L. Such a concentration would lead to the formation of silica gel which is extremely difficult to separate from solution and thus creating processing challenges (Cooper et al., 2000). Table 4.7 shows that most impurity elements from copper oxides leaching dissolve to a very limited extent relative to copper. In the case of cuprite, in particular, the high dolomite content (62.1%) remained unaffected by the alkaline glycine solution. According to the data shown in Table 2.6, International Atomic Energy Agency (2001) report, if acid was used to leach such a deposit, about 582 kg/ton acid would be

consumed, making the process uneconomical. This gives the alkaline glycine leach system a further advantage over the acidic leaching of such copper oxide deposits.

Table 4.7 Concentration of copper and impurities in the final leach solutions and the calculated degree of extraction from leaching copper oxides: Gly:Cu 4:1, pH 11, P_{100} 75 µm

Mineral	Item/metal	Cu	Al	Si	K	Zn	Mg	Fe	Ca
Azurite	In soln, mg/L	3936.0	2.8	4.8	3.4	0.5	0.3		3.3
	Extracted, %	98.4	1.5	0.8	5.9	99.8	1.8		34.8
Chrysocolla	In soln, mg/L	769.0	0.2	247.0	12.2		0.2		4.1
	Extracted, %	19.2	0.0	7.1	5.4		0.3		12.7
Cuprite	In soln, mg/L	3766.0		0.1			4.4	2.7	27.3
	Extracted, %	94.2		0.1			0.2	0.7	0.9
Malachite A	In soln, mg/L	3884.0	0.4	11.2	3.1		0.7	0.7	3.0
	Extracted, %	97.1	3.4	1.4	31.8		1.9	0.2	3.9

The dissolution of impurity elements from chalcopyrite A specimen as shown in Figure 4.27 indicates the extent to which the dissolution of elements can be controlled by the leaching conditions. Arsenic and lead are observed to dissolve more at pH 9 and 10. Zinc leaching follows the same trend as that of copper with higher extraction noted as the pH increased. A zinc extraction of 60.0 % occurred at pH 11 while only 20.0 % zinc was obtained at pH 9. Zinc dissolution from poorly soluble salt was reported to be significantly enhance by the addition of glycine (Sobel et al., 2008). Under all conditions, less than 1.0 % Si and Mg were leached. Except for when pH is 9, less than 6 % Fe was leached under the other investigated conditions.

It can then be concluded that, from a polymetallic chalcopyrite specimen, alkaline glycine solution with pH above 11 favours copper leaching (and Zn, if present) while rejecting most impurity metals in the leach residue.

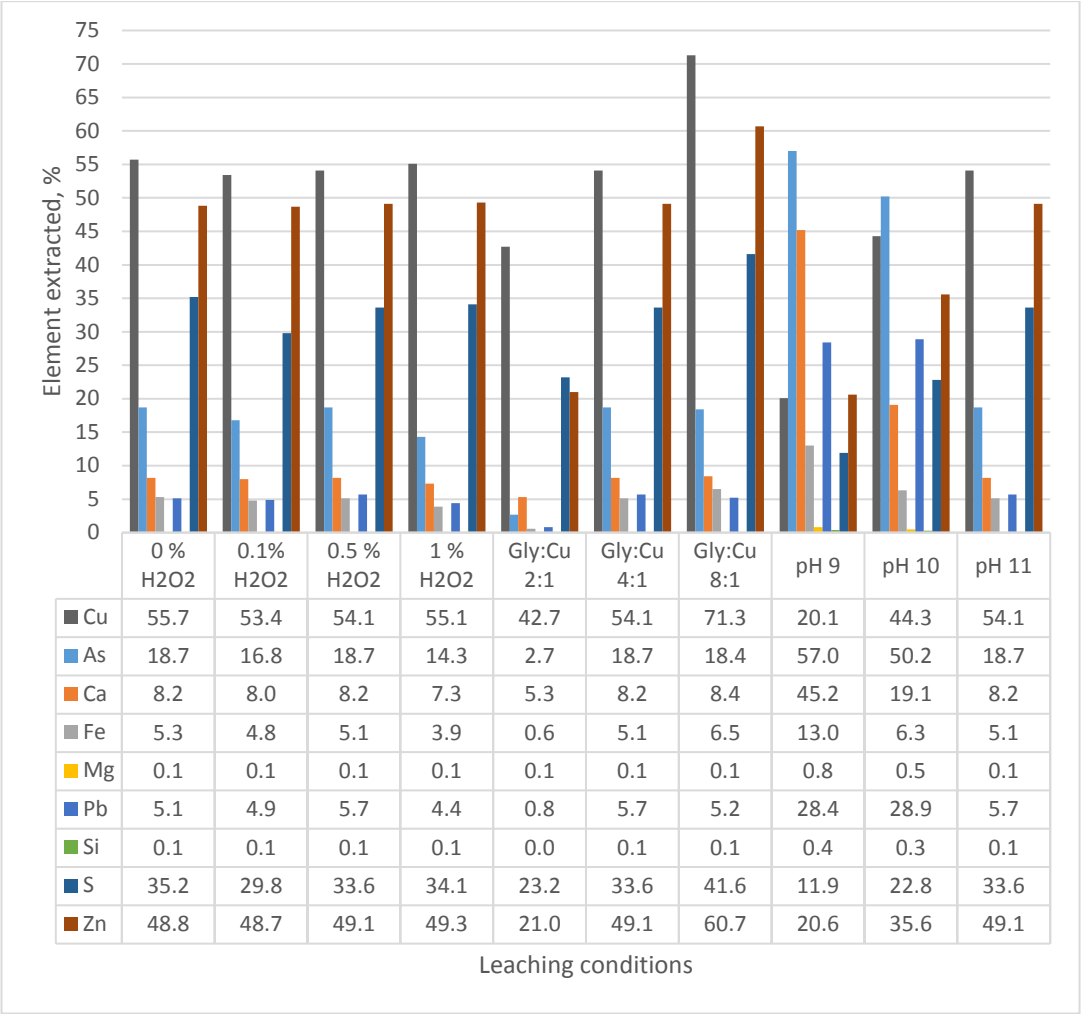

	0 % H2O2	0.1% H2O2	0.5 % H2O2	1 % H2O2	Gly:Cu 2:1	Gly:Cu 4:1	Gly:Cu 8:1	pH 9	pH 10	pH 11
Cu	55.7	53.4	54.1	55.1	42.7	54.1	71.3	20.1	44.3	54.1
As	18.7	16.8	18.7	14.3	2.7	18.7	18.4	57.0	50.2	18.7
Ca	8.2	8.0	8.2	7.3	5.3	8.2	8.4	45.2	19.1	8.2
Fe	5.3	4.8	5.1	3.9	0.6	5.1	6.5	13.0	6.3	5.1
Mg	0.1	0.1	0.1	0.1	0.1	0.1	0.1	0.8	0.5	0.1
Pb	5.1	4.9	5.7	4.4	0.8	5.7	5.2	28.4	28.9	5.7
Si	0.1	0.1	0.1	0.1	0.0	0.1	0.1	0.4	0.3	0.1
S	35.2	29.8	33.6	34.1	23.2	33.6	41.6	11.9	22.8	33.6
Zn	48.8	48.7	49.1	49.3	21.0	49.1	60.7	20.6	35.6	49.1

Figure 4.27 Comparative degree of extraction of Cu and impurity elements in final leach solutions of chalcopyrite A

4.10 Summary

The dissolution behaviour of azurite, malachite, cuprite, chrysocolla, metallic copper, chalcocite and chalcopyrite have been investigated at different Gly-Cu molar ratios, initial solution pH, and peroxide concentration (in case of metallic copper and sulfide minerals). It was observed that higher Gly-Cu ratios favor copper dissolution in all the minerals. Initial solution pH of 11.0 was noted to be the optimum for the dissolution of the all tested copper minerals specimens.

Leaching solution pHs lower than 9.5 could lead to the precipitation of copper-glycinate when the copper concentration in solution approached or exceeded 3 g/L. With copper oxides and metallic copper, the pH of the leaching solution increases during the first part of the leaching afterwhich it starts to decline. On the other hand, the solution pH continuously decreased

with sulfide mineral leaching.

Peroxide that was speculated to act as a strong oxidising agent during the leaching of metallic copper and the copper sulfide minerals had no significant influence. Dissolved oxygen from air acted as a good enough oxidising agent under the given leaching conditions.

Figure 4.28 compares behaviour of the different copper minerals, i.e., an indication of the geometallurgical response of copper minerals to alkaline glycine solutions at ambient pressure and temperature. It can be seen that with the exception of chrysocolla, azurite and malachite are easily leached in the alkaline glycine solution. Metallic copper has the same dissolution behaviour as cuprite which both show moderate initial dissolution rates. Chalcocite dissolution is higher than that of chalcopyrite but lower than that of cuprite. Copper dissolution from malachite plateaus between 40.0 and 50.0 % due to the supposed formation of slow leaching covellite on the mineral. Copper dissolution from chalcopyrite is the lowest but increases steadily with up to 71.0 % copper being dissolved after 800 hours of leaching at 8:1 Gly:Cu molar ratio and initial solution pH of 11.

Alkaline glycine leaching was found to leach copper selectively over gangue minerals such as Fe, Ca, Mg and Si as these impurities dissolved to a very limited extent relative to copper.

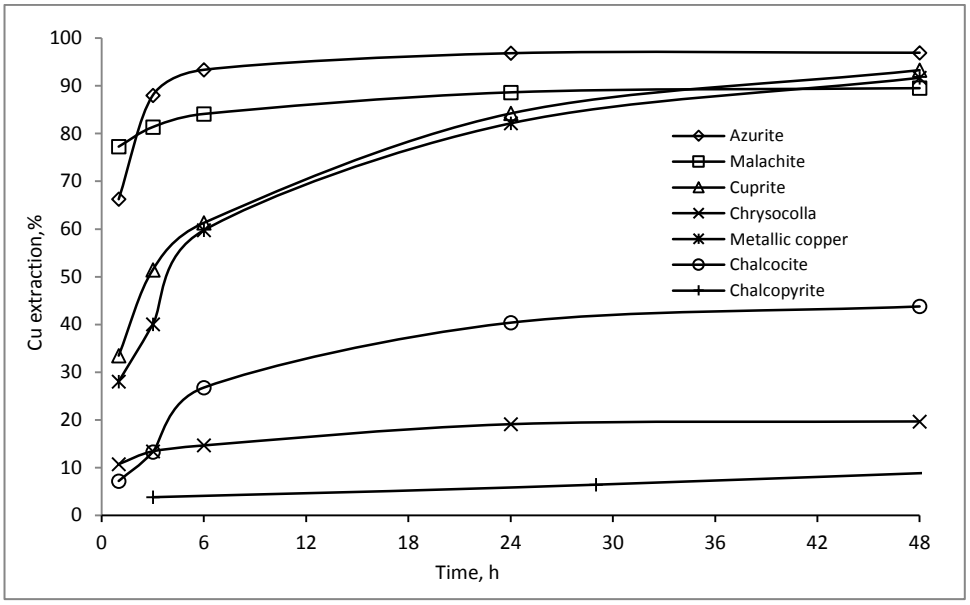

Figure 4.28 Comparative dissolution behaviour of copper minerals in the alkaline glycine solutions: Cu:Gly 1:4, pH 11, room temperature.

Finally, from the results and general observations in this chapter, a procedure for rapid evaluation of the response of any copper ore in alkaline glycine solution can be proposed. The equipment for the proposed procedure, reagents and their concentrations, and

experimental conditions are outlined below:

- Bottle Roll leaching experiments are to be conducted at room temperature at a revolution of 100 rpm. The leaching solution should be opened to air via an inlet on the cap of the bottle;
- Glycine molar concentrations, must be twice that of the total copper in the ore specimen. to ensure that there is enough glycine to complex all of the copper due to theformation of $Cu(gly)_2$;
- Deionised water should be used to ensure that no unwanted ions are introduced into the system;
- Ore specimens should be ground to 100 % passing 75 µm to make sure that the copper minerals present in the ore are sufficiently in contact with the leaching agent;
- Percentage solids in the leaching solution should be chosen such that, if complete copper leaching occurs, the copper content in solution does not exceed 3 g/Lin order to avoid that copper precipitatig as copper-glycinate; and
- Sodium hydroxide should be used to modify solution pH. An initial solution pH of 11 should be used during the investigation of other variables. The solution pH is not to be controlled during leaching but monitored to determine the ore's influence on solution pH.

With all the above conditions met, the required mass of ore is added to the leaching solution in the bottle which is then immediately placed on the bottle roller. Timely (30 minutes in first 2 hours) sub-samples should be taken to determine the extent of copper leaching. Additionally, solution pH and potential should be monitored during sub-sampling.

This method only serves to characterise the leachability of the ore, or ore domain. It is accepted that, once leachability has been demonstrated, the next step would be to optimise leaching conditions to align with the proposed leaching method (e.g. heap leaching, concentrate leaching, etc.) by changing the % solids and temperature and by seeking to maintain DO, pH levels and control reagent conditions throughout. This would normally require a well-controlled agitated reactor where mass transfer conditions can be improved and oxygen micro-bubbles can be sparged under controlled conditions. A system which removed the copper continuously (e.g. through precipitation) would prevent copper accumulation and potential reprecipitation.

Chapter 5 Mechanisms and Kinetics of Leaching Malachite, Chalcocite, and Chalcopyrite in Glycine Solutions

5.1 Chapter Objectives and Background

The main objective of this chapter is to study the leaching mechanisms and kinetics of the dissolution of malachite, chalcocite and chalcopyrite minerals in alkaline glycine solutions. These minerals are the most predominant minerals in the oxide cap, supergene and hypogene zones as one progresses deeper into a conventional copper deposit (porphyry).

Leaching, as indicated in Chapter 2, is a key unit operation in the hydrometallurgical processing of minerals as its' efficiency has a pivotal influence on the economics of the metal extraction business (Crundwell et al., 2011). Optimising the efficiency of the leaching process and the overall hydrometallurgical operation requires an accurate understanding of the dissolution mechanisms and particularly the kinetics of dissolution (Crundwell, 2013). Leaching kinetics are of prime concern to hydrometallurgists beacause they seek to determine what controls the rate of leaching reactions in order to be able to manipulate and improve the hydrometallurgical process with confidence.

Leaching reactions are generally heterogeneous in that reactions occur at the interface of a solid phase and a solute in an aqueous solution. Some processes such as gold cyanidation and pressure oxidation of sulfides involve a gaseous third phase. A simplified representation of such reactions is shown in Equation 5.1:

$$A(\text{fluid}) + bB(\text{solid}) \rightarrow \text{Products (fluid or solid or fluid and solid)} \qquad (5.1)$$

While the general expression for the reaction rate can be defined by Equation 5.2:

$$\frac{dN_B}{dt} = -Sbk_0k'[A]^m \quad (5.2)$$

Where dN_B/dt is the reaction rate in moles per unit time, S is the solid surface area, b is the stoichiometric number of moles of the solid reacting with one mole of the solute, [A] represents the concentration of the solute in solution, k' is the rate constant, k_o is the concentration of reactive surface sites (in moles per unit area), and m is the reaction order with respect to [A].

Based on the general rate expression, several models including the shrinking core model (SCM), shrinking particle model, and progressive-conversion model have been developed to study the reaction kinetics of such heterogeneous leaching processes. The shrinking core model is seen to reasonably represent reality in a broad variety of leaching situations (Levenspiel, 1999) and has been used extensively to describe leaching kinetics of most minerals (Li et al., 2013a). The model was first developed by Yagi and Kunii in 1955 who visualized that the leaching process progresses in five successive steps for particles of unchanging size (Park & Levenspiel, 1975):

- Diffusion of reactant "A" through the film surrounding the particle to the surface of the solid
- Penetration and diffusion of reactant "A" through the blanket of ash to the surface of the unreacted core
- Reaction of reactant "A" with solid at the reaction surface
- Diffusion of products through the ash back to the exterior surface of the solid
- Diffusion of products through the gas film back into the main body of fluid

These five main steps are illustrated in Figure 5.1.

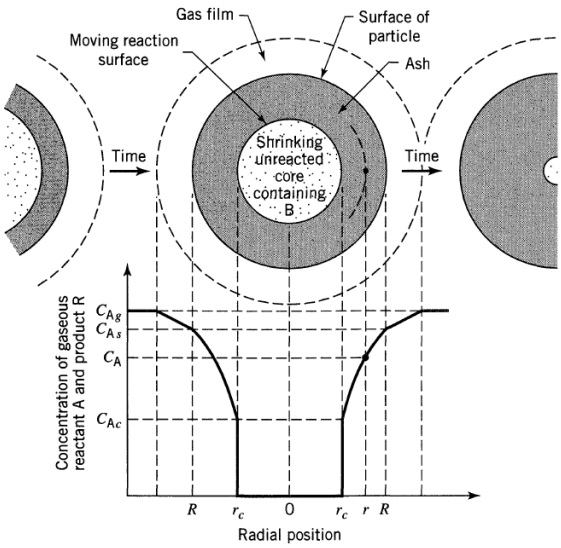

Figure 5.1 Representation of concentrations of reactants and products for a particle of unchanging size (Levenspiel, 1999).

In some processes, some of the steps do not occur and thus have no contribution to the resistance of the reaction. The resistance of different steps to reaction vary; however,that with the highest resistance (slowest step) becomes the rate-controlling step. A reaction is said to be diffusion controlled if the slowest step is diffusion (steps 1 and 2). If the reaction at the surface of the solid is the slowest step, then the reaction is said to be chemically controlled. Finally, a reaction is said to be "product-layer diffusion controlled" if resulting aqueous products increase concentrations at the surface due to resistance of their diffusion from the surface. The rate controlling step for a given reaction may change if conditions change. For example, if the concentration of a reactant is increased, the reaction may change from mass transfer to chemically controlled as more reagent is available to diffuse to the reaction surface (Marsden & House, 1992). It is worth noting that some anomalous reactions, such as precipitation and passivation of particle surfaces, may also control the overall reaction rates (Free, 2013). In such leaching processes in which passivation is observed to occur on the reacting mineral surface, models such as initial reaction theory are applied rather than simple kinetic models (Zhang, 2004).

Levenspiel (1999) used the shrinking core model to develop mathematical expressions where the various steps are rate controlling. In the case of spherical particles, the integrated expressions are shown in the following Equations:

$$\text{Film diffusion controlled: } k_l t = x \tag{5.3}$$

$$\text{Product layer diffusion controlled: } k_d t = 1 - 3(1-x)^{2/3} + 2(1-x) \quad (5.4)$$

$$\text{Reaction controlled: } k_r t = 1 - (1-x)^{1/3} \quad (5.5)$$

where x is the conversion fraction of the solid particles, k_l, k_d and k_r are the apparent rate constants for the different controlling steps, and t is the reaction time.

In reactions in which no product layer is formed (such as burning of pure charcoal), only the following three steps are assumed to occur: diffusion of reactant "A" through the liquid film to the solid surface, the reaction at the surface between solid and reactant "A" and thirdly the diffusion of the reactant products from the solid surface through the liquid film into the main body solution. If the process is surface chemical reaction controlled, the behaviour is like that of the unchanging size implying Equation 5.5 is applicable. Liquid film resistance at the particle surface depends on factors such as relative velocity between particle and fluid, size of particle, and fluid properties. When the liquid film diffusion controls, the integrated rate expression is as shown in Equation 5.6:

$$k_l t = 1 - (1-x)^{2/3} \quad (5.6)$$

where k_l is the apparent rate constant for liquid film diffusion controlled when product layer is not formed.

In order to determine which step is controlling for a given leaching reaction, experimental data is used to plot a graph of the right hand side of the rate expressions against time. A correlation of the kinetic data with the models is then assessed by using a correlation coefficient (R^2). A correlation value of reasonably closest one indicates that the actual leaching process is in agreement with the proposed model. The slopes of the plots are the respective apparent rate constants.

Many researchers have, however, noted that diffusion controlled or chemical reaction controlled models fail to represent the rate-controlling step of some leaching reactions (Ekmekyapar et al., 2003; Feng et al., 2015; Liu et al., 2012a). This is generally the case when leaching rates depend on temperature and concentration of reagents (Saxena & Mandre, 1992). Levenspiel (1999) stated that, in a scenario whereby not only a single step controls the reaction rate throughout, the individual rate equations could be combined in order to determine the extent to which individual steps contribute to limiting the leaching rate at any

given stage. This approach has been used by Sultana et al. (2014) to show that the leaching of iron oxide in oxalic acid is controlled by both diffusion through the product layer and chemical reaction models with the diffusion controlled process being the more dominating reaction. Another approach that simultaneously considers all three possible rate controlling mechanisms to determine the rate controlling stage is by applying a constrained multi-linear regression using the least square techniques (Nazemi et al., 2011). The advantage of this technique is not having to test individual rate controlling step formulas against the experimental data to establish the best fit data and then predict the rate controlling step. This new approach is also advantageous in that it avoids the scenario whereby close correlation coefficients (for fitted data) values make it difficult to determine the rate controlling process. Equation 5.7 is a combination of individual rate controlling model equations:

$$t = k_l x + k_d[1-3(1-x)^{2/3} + 2(1-x)] + k_r[1-(1-x)^{1/3} \quad (5.7)$$

The constants k_l, k_d, and k_r can be determined by a multi-linear regression analysis using the least square method. To avoid negative values for the constants, a constrained least square technique as expressed in Equation 5.8 is used:

$$\Phi = \sum_i [k_l x + k_d(1-3(1-x)^{2/3} + 2(1-x)) + k_r[1-(1-x)^{1/3} - t_i]^2 \quad (5.8)$$

$$\text{Min } \Phi \text{ subject to } k_l, k_d \text{ and } k_r > 0. \quad (5.9)$$

Equation 5.9 can then be solved by any optimization technique to determine the values of k_l, k_d and k_r. The results from the solve equation will estimate the time needed to complete a leaching process controlled by any limiting mechanism/step.

The two most important factors that influence the rate of leaching reactions are the concentration of reagents and temperature. These two factors are linked to the order of the reaction and the E_A as described Equation 5.10 (Crundwell, 2013):

$$rate = K[c]^n exp^{E_A/RT} \quad (5.10)$$

where K represents the rate constant, [c] is the concentration of reagent, n the order of the reaction, E_A the activation energy, R the gas constant, and T the temperature (Kelvin).

For reactions to occur, molecules must first collide with sufficient energy. This implies that reaction rates are related to collision frequency and collision energy. The Arrhenius equation

expresses the rate constant in terms of collision frequency factor and collision energy illustrated in Equation 5.11 (Free, 2013):

$$k_f = Ae^{E_A/RT} \quad (5.11)$$

It is generally accepted that systems with E_a more than 40 kJ/mol are controlled by chemical reaction while those with activation energy less than 40 kJ/mol are controlled by transport processes (Levenspiel, 1999). Also, for leaching processes that are chemically controlled, reaction kinetics are significantly improved by small increments in temperature (Dreisinger & Abed, 2002). However, some researchers have reported E_a's higher than 40 kJ/mol for diffusion controlled reactions (Baba et al., 2009; Vračar et al., 2000). Olanipekun (1999) suggested that the rate controlling mechanisms of heterogeneous dissolution reactions are sometimes better determined from kinetic equation plots rather than from E_a's.

Unfortunately activation energy does not give any more information on the reaction route. The order of the reaction on the other hand describes the dependency of the reaction rate on the reagent concentration.

The kinetics and the extent to which a leaching reaction proceeds are also influenced by particle characteristics, such as particle size, shape and porosity as these factors control the surface area available for reaction with a solution phase reactant (Li et al., 2014; Marsden & House, 1992). The influence of these parameters on the leaching kinetics of malachite, chalcocite, and chalcopyrite will be studied in this chapter.

5.2 Copper Speciation in Alkaline Glycine Solutions

Copper is known to form both Cu(I)-glycinate and Cu(II)-glycinate complexes (Section 2.6.1). To propose leaching mechanism/routes for copper minerals in the alkaline glycine solutions, it is necessary to determine if both Cu (I) and Cu (II) ions are present and stable in the leach system. Cu (II) sulfate was dissolved in an alkaline glycine solution at pH 11 and the complex solution was scanned at different wavelengths using a UV-Vis spectrometer. The maximum absorbance of the Cu (II) glycinate complex solution was observed at 635nm. This is in agreement with published data which reported Cu (II) in an aqueous alkaline glycine solution forms a deep blue complex which has a peak at a wavelength around 624-640 nm (Darj et al., 1996; Fernandes et al., 1997). Cu (I) chloride was also dissolved in alkaline glycine solution at

pH 11. As the dissolution of CuCl in the alkaline system is rather slow compared to that of $CuSO_4 \cdot 5H_2O$, solution samples were taken immediately after mixing at 2.5, 5, and 13 minutes for scanning with the UV-vis spectrometer at different wavelengths. The maximum absorbance for all the time interval samples also occurred at around the 635 nm wavelength as noted for the Cu (II) sulfate (Figure 5.2). This observation indicates that the Cu (I) ions are rapidly oxidized to Cu (II) ions which then form the stable Cu (II) glycinate complex. It should be recalled that according to Aksu and Doyle (2001) and, as shown in Table 2.7, the logK of the Cu^{2+} complex with glycine (CuL_2) is the most stable copper species in copper-glycine solutions.

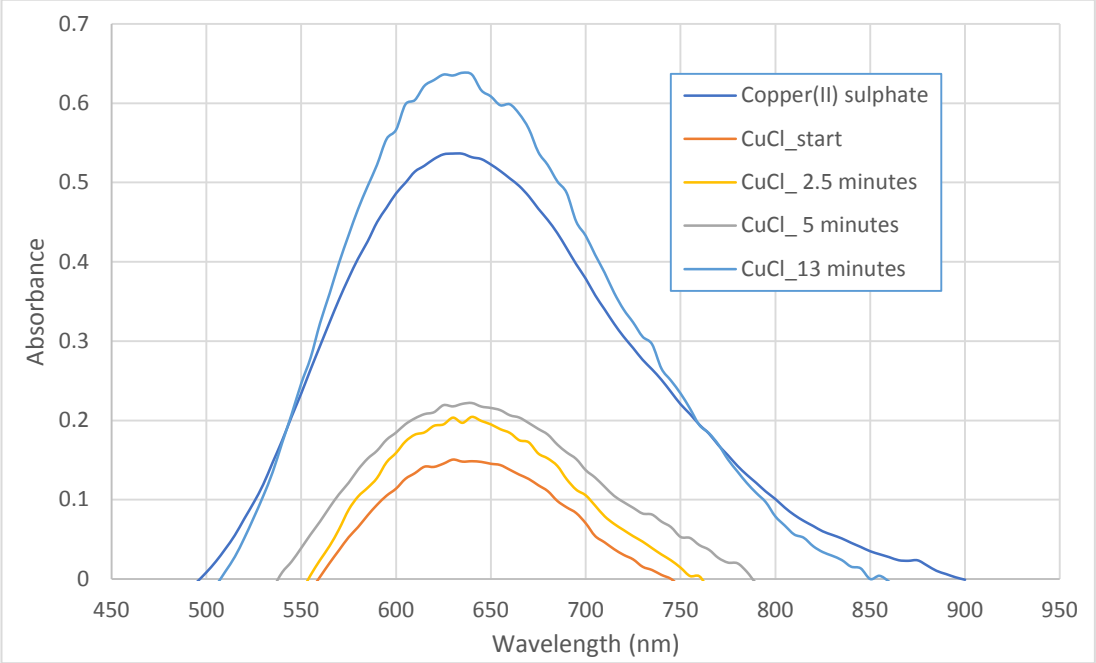

Figure 5.2 UV-Vis spectrum of Cu (II) sulfate and Cu (I) chloride dissolution in alkaline glycine at pH 11, Gly:Cu 3:1.

The final leach solutions for the different copper minerals were also scanned by using the UV-Vis spectrometer. Figure 5.3 shows the wavelength scan of the Cu (II) glycinate complex of leaching solutions of azurite, chrysocolla, cuprite, malachite, chalcocite and chalcopyrite. It can be seen that UV-Vis spectra from all minerals show a single peak at a wavelength of 635 nm which is the same position obtained for the standard Cu (II) glycinate complex.

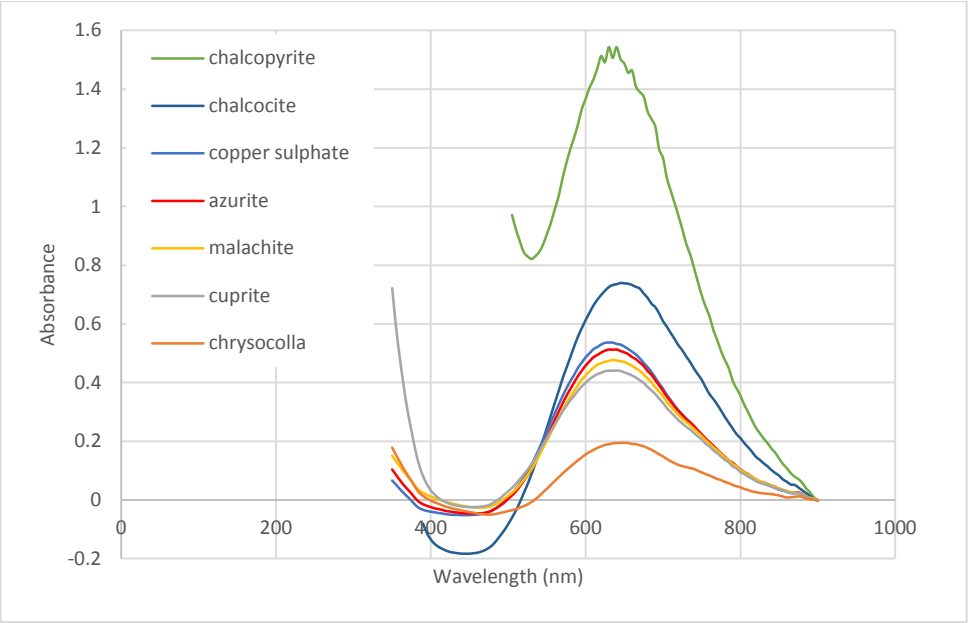

Figure 5.3 UV-Vis spectrum of Cu (II) sulfate (with alkaline glycine), azurite, chrysocolla, cuprite, chalcopyrite, and chalcocite in aqueous alkaline glycine of pH 11

To further confirm that only Cu(II) ions form the copper glycinate complex in alkaline glycine solutions, the concentration of Cu (II) ions determined by the UV-Vis spectrometer for copper sulfate, copper chloride and the different minerals was compared to the total copper in solution determined by AAS analysis. By comparing the Cu (II) concentration from the UV-Vis to the total copper concentration obtained from AAS analysis, a correlation line with R^2 of 0.9957 was obtained as illustrated in Figure 5.4. This confirms that the Cu (II) glycinate complex is the only copper species in the leach solution from all investigated copper minerals at alkaline medium. From these results, it can be concluded that Cu (I) minerals such as cuprite dissolve in an aqueous alkaline glycine system through the oxidation of Cu (I) to Cu (II) which then forms a stable Cu $(H_2NCH_2COO)_2$ complex.

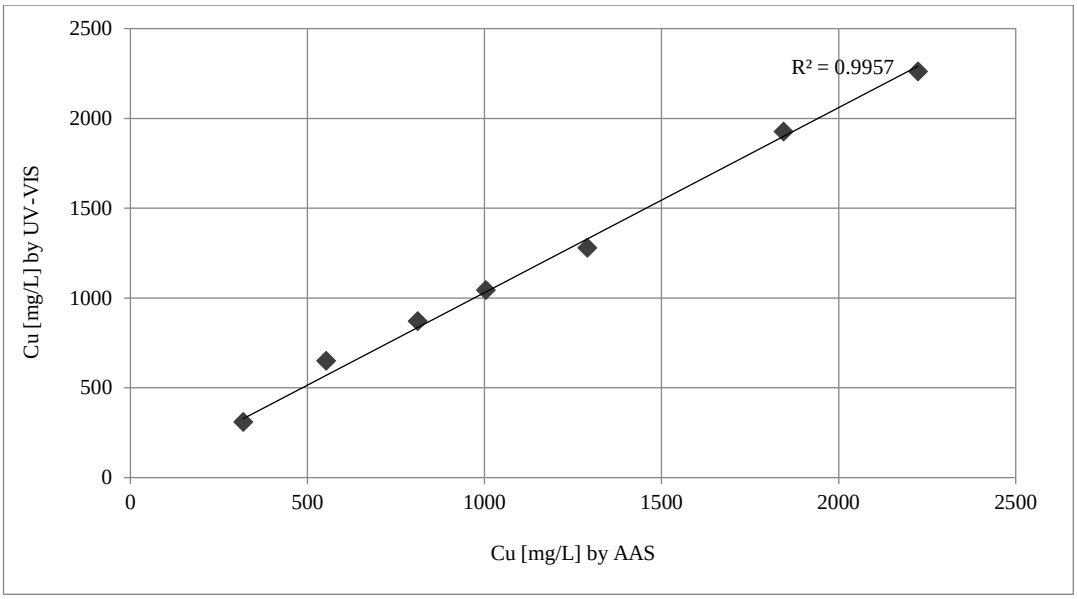

Figure 5.4 Correlation between Cu (II) concentration with UV-Vis and total copper by AAS

5.3 Sulfur Speciation from Copper Sulfides Leaching

Mineral sulfides are well known to form different sulfur species during their dissolution in common lixiviants (Breuer et al., 2008; Marsden & House, 1992). In order to predict and propose leaching reactions for sulfide minerals in the alkaline glycine solutions, a sulfur speciation on a chalcopyrite leachate was performed using an HPLC. The results presented in Table 5.1 show that up to 90.0 % of the sulfur in the solution is in the form of sulfate. From this observation, it can be concluded that sulfur in copper sulfide minerals is oxidised to the sulfate form during alkaline glycine leaching.

Table 5.1 Sulfur speciation for a copper sulfide (chalcopyrite) leached solution

Species name	Species formula	In solution, mg/L	% of total S
Sulfate	SO_4^{2-}	1142	89.8
Sulfite	SO_3^{2-}	74.0	7.2
Thiosulfate	$S_2O_3^{2-}$	22.2	3.0
Sulfide	S^{2-}	<0.1	-

5.4 Leach Residue Analysis

5.4.1 Chalcocite

It has been well established that chalcocite leaching in both acidic and alkaline mediums proceeds in two stages with the formation of covellite (CuS) as an intermediate product (Cheng & Lawson, 1991; Duda & Bartecki, 1982; Konishi et al., 1991). During the first stage, chalcocite is converted to Cu (II) ions leaving behind a copper deficient residue in the form of covellite. Senanayake (2007) suggested that as the covellite is formed on the outer surface, it begins to react and proceed in parallel with the first stage, but at a much lower rate and only becomes significant after 40.0 % dissolution of the initial copper.

Un-leached and leached chalcocite samples were then analysed by XPS and SEM-EDS in order to determine the type of product formed on the residue surface. The analysis involved the collection of a survey spectrum and a high resolution spectra for copper and sulfur. The survey spectrum was collected so that the elements on the surface of the mineral particles could be identified and quantified while the high resolution spectra collected for copper and sulfur allowed the determination of their oxidation states. The survey spectrum shows the major elements detected on the surface of the sample represented by a labelled peak. Additional unlabelled peaks correspond to minor photoelectron emission and auger peaks. Figure 5.5 shows the survey spectrum of un-leached and leached chalcocite samples. Figure 5.5 also shows a generated table of elements detected and their calculated atomic concentration (At%). The generated table shows that the At% ratio of Cu: S in the un-leached chalcocite is 22:4 while that in the leached chalcocite is 22: 29. The At% ratio of Cu:S in the leached sample is similar to that obtained in pure covellite (CuS) as reported in National Institute of Standards and Technology database. Also, the positions (binding energy) of Cu 2p3/2 and S 2p3/2 in the un-leached and leached chalcocite (Table 5.2) are comparable to those of pure chalcocite and covellite given in the XPS reference pages (Naumkin et al., 2012; X-ray Photoelectron Spectroscopy (XPS) Reference Pages, 2016). The results shown in Figure 5.5 and Table 5.2 clearly indicate that covellite is a product of chalcocite leaching in the alkaline glycine solution.

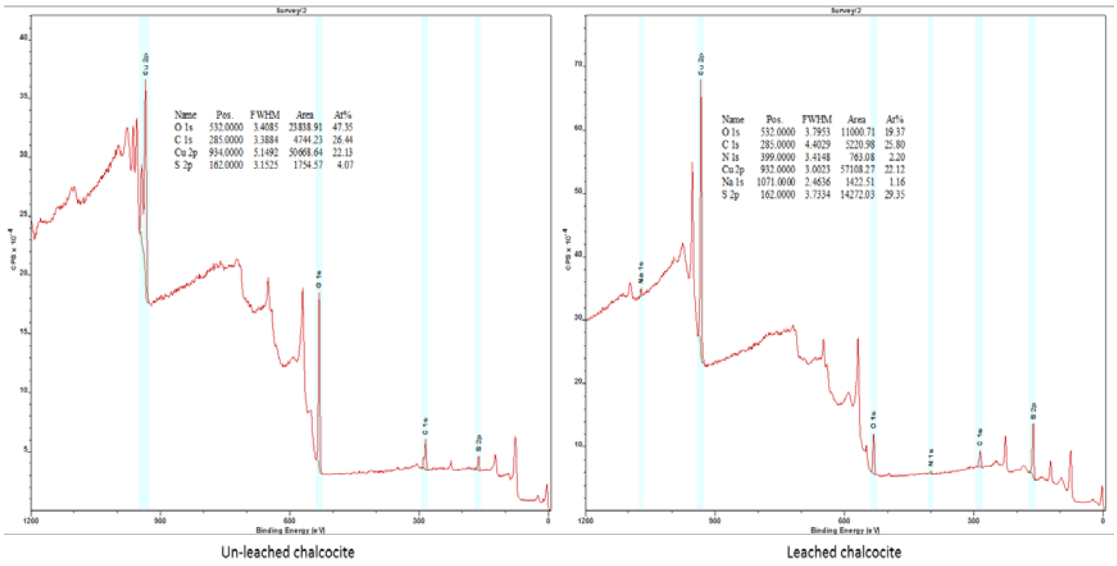

Figure 5.5 The survey spectrum of un-leached and leached chalcocite samples.

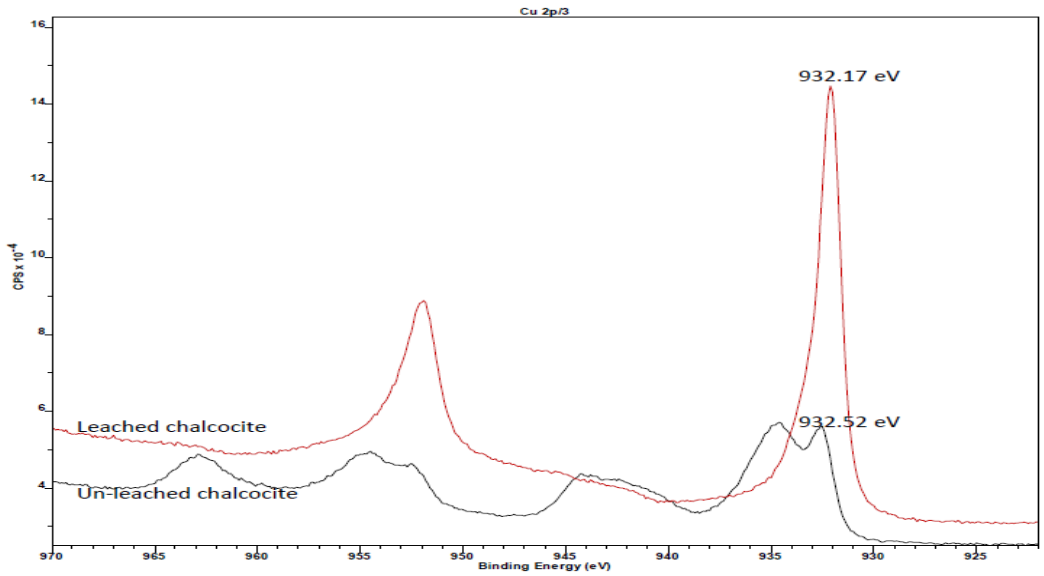

Figure 5.6 The high-resolution spectra for copper from un-leached and leached chalcocite samples

Table 5.2 Binding energies of chalcocite and covellite from NIST database and from un-leached and leached chalcocite

	Species	Cu 2p3/2 B.E.(eV)	S 2p3/2 B.E.(eV)
NIST database	Cu_2S	932.5	161.9
	CuS	932.3	162.1
Experimental	Un-leached chalcocite	932.52	161.8
	leached chalcocite	932.17	162.1

SEM-EDS analysis of un-leached and leached chalcocite (Figure 5.7) shows that the ratio of Cu:S in the leached sample is 1:1 as opposed to the 2:1 ratio noted for the un-leached chalcocite. With the atomic formula of chalcocite being Cu_2S and covellite CuS, the SEM-EDS analysis indicates the presence of covellite as an intermediate product in the alkaline glycine leaching system. This observation confirms the report by Konishi et al. (1991) that the leaching kinetics of natural chalcocite leaching in alkaline Na_4EDTA occurs in two consecutive stages with solid covellite being the product of the first stage and then reacting the second stage at a rate 10 times lower than the first stage.

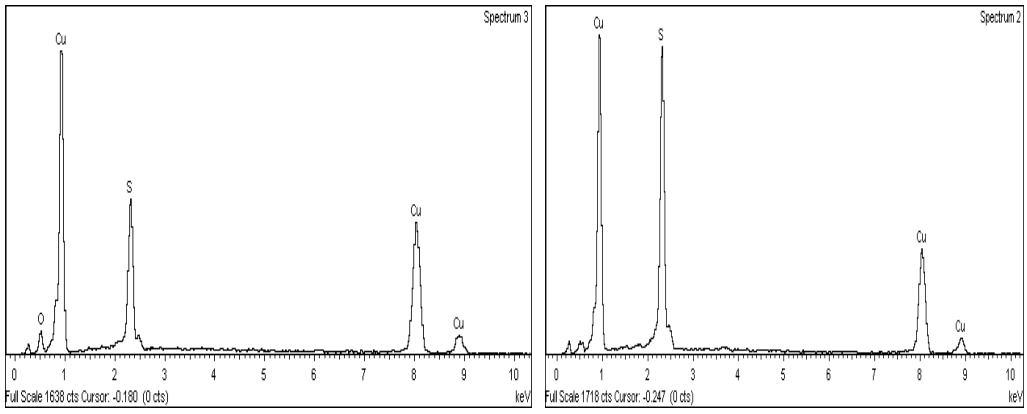

Unleached chalcocite Leached chalcocite

Figure 5.7 SEM-EDS spectra for unleached and leached chalcocite

5.4.2 Chalcopyrite

The surface analysis of chalcopyrite leached residues have shown that the presence of a range elemental species and compounds are precipitated on the surface (Harmer et al., 2006; Klauber, 2008; Klauber et al., 2001; Li et al., 2010; McIntyre & Zetaruk, 1977; Parker et al., 2003). Some of these species such as elemental sulfur and iron-hydroxide compounds have been suggested to passivate the chalcopyrite layer (Ghahremaninezhad, 2012). Generally, the nature of the species formed depends on the solution pH.

In order to determine the type of species formed during chalcopyrite leaching in alkaline glycine solution and thus predict reaction routes, un-leached and leached samples were analysed by XPS and SEM-EDS.

The surface atomic concentrations calculated from the XPS survey spectra (Appendix D2) indicated the absence of elemental sulfur on leached residue surface (Table 5.3). This is in agreement with results obtained on the sulfur speciation of a chalcopyrite leachate demonstrating that sulfur is completely oxidised to sulfate when leached in the alkaline

glycine solution (Section 5.3). The deconvolution of the high oxygen resolution spectra (Figure 5.8) identified that the percentage of lattice hydroxide significantly increased from 13.5 % in the un-leached sample to 79.9 % in the leached sample. With most copper being dissolved into solution as copper glycinate, the high lattice OH^- concentration is most likely to be associated with an Fe oxyhydroxide species (Fe(III)-O-OH) at 711 eV as shown in Figure 5.9. Iron oxyhydroxide surface species have also been observed on leached chalcopyrite surfaces (Li et al., 2010; McIntyre & Zetaruk, 1977).

Table 5.3 Elemental surface concentrations of un-leached and glycine leached chalcopyrite sample calculated from their relative XPS survey spectra.

Element	At %	
	Un-leached	Leached
O 1s	49	39.1
C 1s	11.29	38.43
Na 1 s	-	1.22
N 1s	-	10.48
Cu 2p	11.85	9.31
Fe 2p	4.69	1.55
S 2p	10.76	0.00
Si 2p	11.56	-

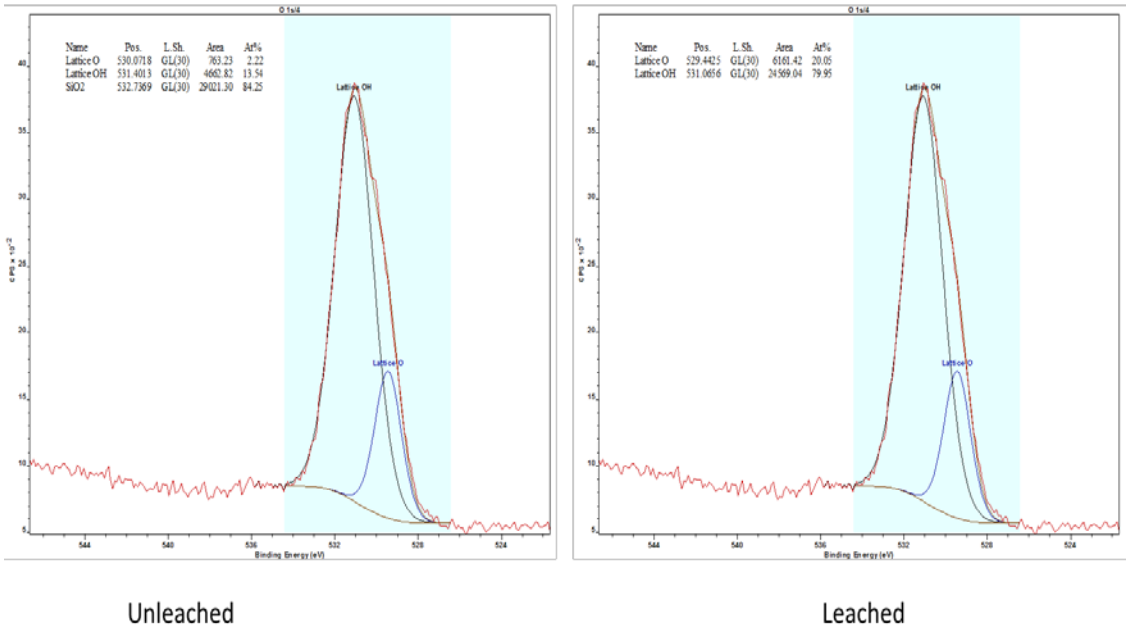

Figure 5.8 High-resolution spectra of oxygen from un-leached and glycine leached chalcopyrite specimen

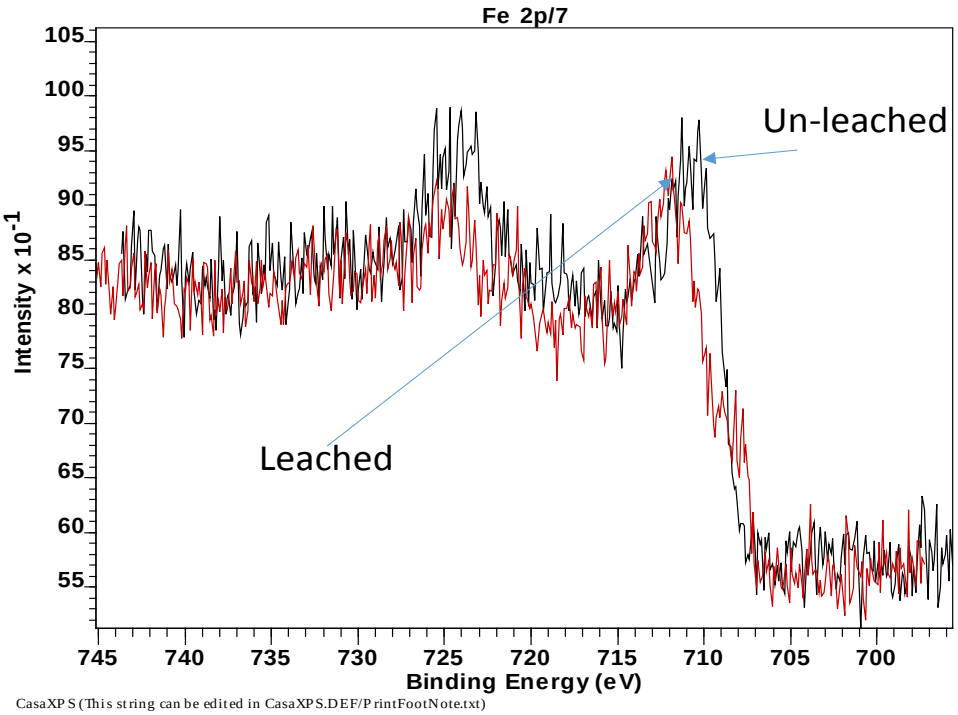

Figure 5.9 The high resolution spectra of un-leached and leached chalcopyrite specimen

By analysing both chalcopyrite samples by SEM-EDS analysis, the absence of oxygen atoms on the chalcopyrite surface as illustrated in Figure 5.10 suggests that the goethite product obtained during the leaching of chalcopyrite does not form a passivation layer on the chalcopyrite surface.

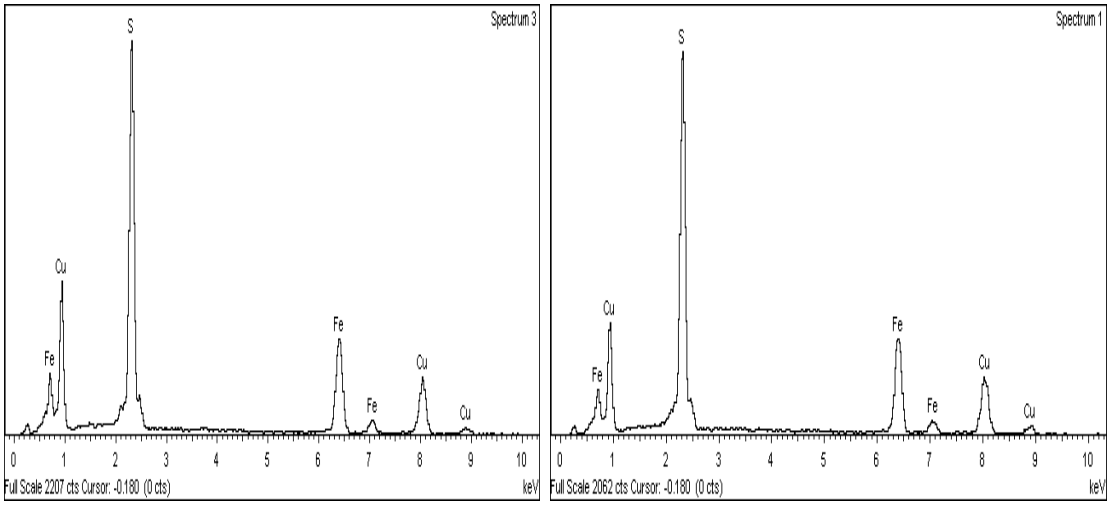

Figure 5.10 SEM-EDS spectra for un-leached and glycine leached chalcopyrite

5.5 Proposed Leaching Equations

From observations and predictions made from Sections 5.2, 5.3 and 5.4, the following overall leaching reactions for azurite, malachite, cuprite and chrysocolla can be presented as shown in Equations 5.12, 5.13, 5.14, and 5.15, respectively. Chalcocite leaching is illustrated by Equation 5.16 given that covellite is an intermediate product.

$$2(CuCO_3)\cdot Cu(OH)_2 + 6NH_2CH_2COO^- = 3[Cu(NH_2CH_2COO)_2] + 2OH^- + 2CO_3^{2-} \quad (5.12)$$

$$(CuCO_3)\cdot Cu(OH)_2 + 4NH_2CH_2COO^- = 2[Cu(NH_2CH_2COO)_2] + 2OH^- + CO_3^{2-} \quad (5.13)$$

$$Cu_2O + 4NH_2CH_2COO^- + 2H_2O + 1/2O_2 = 2[Cu(NH_2CH_2COO)_2] + 4OH^- \quad (5.14)$$

$$CuO.SiO_2\cdot 2H_2O + 2NH_2CH_2COO^- = Cu(NH_2CH_2COO)_2 + SiO_2 + H_2O + 2OH^- \quad (5.15)$$

$$Cu_2S + 2NH_2CH_2COO^- + 1/2O_2 + H_2O = Cu(NH_2CH_2COO)_2 + CuS + 2OH^- \quad (5.16)$$

With the confirmation of sulfate as the major sulfur species from sulfide minerals leaching and goethite formation during chalcopyrite leaching, Equation 5.17 could then be proposed to illustrate the chalcopyrite leaching in alkaline glycine solutions.

$$CuFeS_2 + 2NH_2CH_2COO^- + 4.5O_2 + 2OH^- = Cu(NH_2CH_2COO)_2 + FeO(OH) + 2SO_4^{2-} + H_2O \quad (5.17)$$

5.6 Leaching Kinetics of Malachite, Chalcocite and Chalcopyrite

5.6.1 Malachite B

Malachite is an abundant copper oxide mineral found in the Democratic Republic of the Congo, Gabon, Zambia, Namibia, Mexico, Australia (Broken Hill, New South Wales) , France (Lyon), Israel (Timna Valley), and the Southwestern United States, most notably in Arizona (Anthony et al., 2001; Mindat.org, 2016). The kinetic analysis of malachite is important since malachite is the most common copper oxide mineral.

5.6.1.1 Mineralogy and Elemental Composition

XRD analysis to determine the mineralogy of the specimen indicated that malachite makes 99.0 % of the sample while the remaining 1.0 % is cristobalite. Chemical composition of the sample was performed by XRF and the results showed a copper content of 56.0 %. The mineral sample was crushed, ground and then sieved using standard test sieves into four size fractions (+20-38, +38-53, +53-75 and +75-106 µm). With the exception of experiments investigating the effect of particle size, all other experiments were carried out with the +53-75 µm size fraction.

5.6.1.2 Effect of Initial Glycine Concentration

The effect of glycine concentration on the leaching kinetics of malachite was studied by varying the initial glycine concentration from 0.1, 0.2 and 0.4 to 0.8 M in 500 mL of solution at pH 10. Other process variables such as stirring speed (SS), temperature, and particle size (PS) were fixed at 350 rpm, 25°C, and 53-75 µm, respectively. Since the formation of the copper-glycine complex needs two moles of glycine for every one mole of copper (Aksu & Doyle, 2001; Eksteen et al., 2016), the minimum glycine concentration of 0.1 M ensured that the required glycine to copper ratio of 2:1 in solution is obtainable if complete mineral dissolution occurs. Figure 5.11 shows that copper dissolution increases with increasing glycine concentration. When glycine concentration is increased from 0.1 to 0.2 M, the percentage copper dissolved after three hours increased from 67.6 to 91.3%. At a glycine concentration of 0.4 M, 98.0 % Cu was dissolved under 2 hours of leaching. At 0.8 M glycine concentration copper extraction was similar to the copper extracted at 0.4 M. This indicates that glycine concentration has an upper limit at which further increments have no positive effect on the leaching rate.

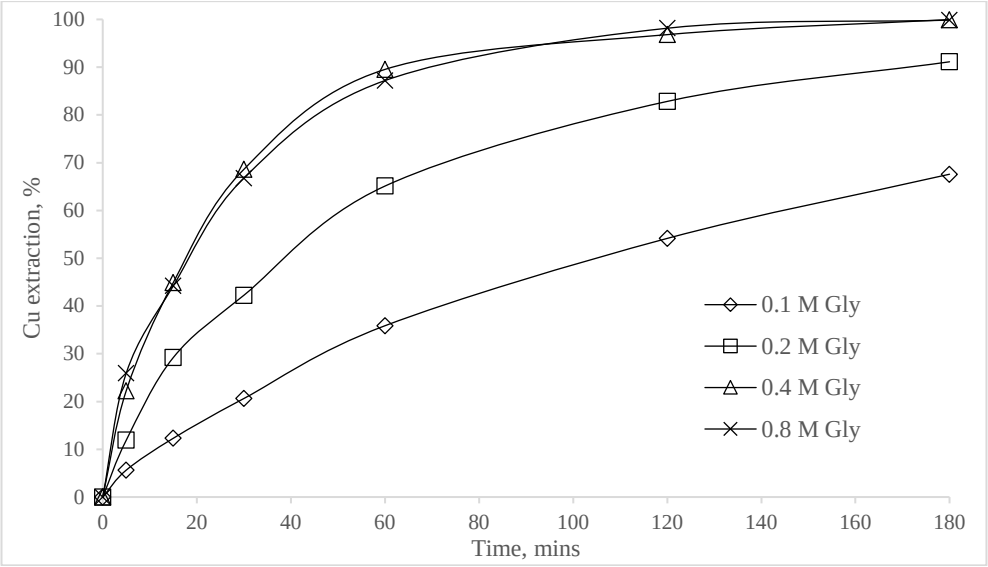

Figure 5.11 Effect of glycine concentration on copper dissolution from malachite B: 25 °C, +53-75 µm, 350 rpm and 0.36 %w/v solids

5.6.1.3 Effect of Temperature

The relationship between temperature and copper dissolution rate is shown in Figure 5.12. During the leaching process, the initial glycine concentration, stirring speed, particle size was maintained at 0.4 M, 350 rpm and 53-75 µm respectively while the solution temperature was varied from 25 to 50 °C. The results indicate that temperature has a profound effect on the copper dissolution rate. At 50 °C, 83.6 % copper dissolution occurs in 5 minutes while 22.3 % copper is dissolved at 25 °C, over the same time. Complete copper dissolution was noted in under 30 minutes of leaching at 50 °C, after 2 hours at 40 °C and only after 3 hours at 25 °C. Although higher temperatures significantly improve malachite leaching rates, raising the leaching temperature may be limited by increased capital and operating costs. Thus, 25 °C was maintained during the evaluation of the other parameters.

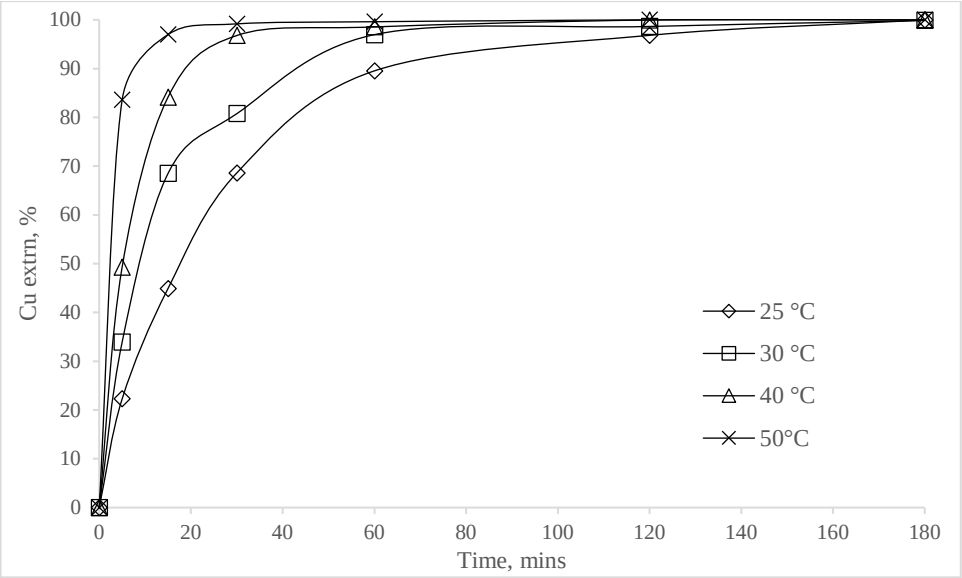

Figure 5.12 Effect of temperature on copper dissolution from malachite B: [Gly] 0.4 M, +53-75 µm, 350 rpm, and 0.36 %w/v solids.

5.6.1.4 Effect of Stirring Speed

In order to examine the influence of stirring speed on the leaching rate of malachite, experiments were carried out at various stirring speeds (150, 350, 550 and 800 rpm) at 25 °C in solutions containing 0.4 M Gly at an initial pH of 10. The results as shown in Figure 5.13 indicate that leaching rate increases as stirring speed is increased from 150 to 350 rpm. However, increasing the stirring speed from 350 to 800 rpm does not result in significant improvement in copper dissolution. This observation suggested that the leaching kinetics might not be controlled by diffusion through the liquid film. However, the result still indicates that fluid flow rate is important. This is particularly significant in vat, heap and in-situ leaching where an optimum leaching solution flow rate is required to carry reagents to and products from the mineral surface. The fluid flow should be optimum to ensure adequate reaction contact time between the reagent and the solids.

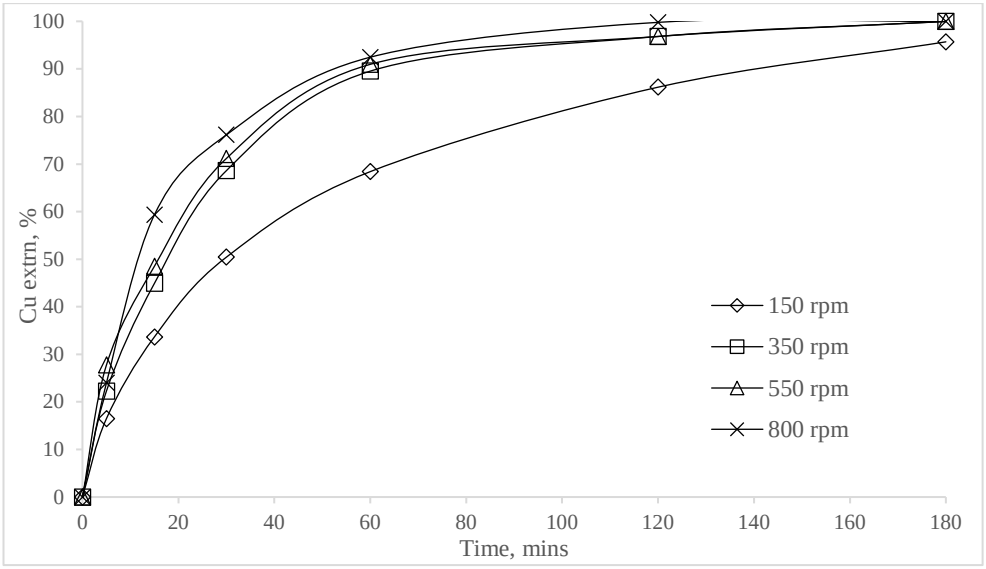

Figure 5.13 Effect of stirring speed on copper dissolution from malachite B: [Gly] 0.4 M, 25 °C, +53-75µm and 0.36 %w/v solids.

5.6.1.5 Effect of Particle Size

The influence of particle size on the leaching of malachite in 0.4 M glycine at pH 10 and 25 °C was investigated and the results are shown in Figure 5.14. The particle size ranges of +20-38 µm, +38-53 µm, +53-75 µm, +75-10 µm were leached for 180 minutes. Rapid dissolution rates were obtained at smaller particle sizes although no noticeable difference was obtained between +20-38 and +38-53. After 60 minutes of leaching, copper extraction for +75-106 and +53-75 µm was 82.8 and 89.5 %, respectively, while 99.0 % copper was extracted at +20-38 and +38-53 µm fractions. Leaching fine particles increases the leaching rate by providing larger contact surface areas for contact with the leaching solution. According to Li et al. (2014), if the leaching rate is significantly dependent on particle size, then it is an indication that the kinetics is controlled by diffusion through the product layer. Thus, the insignificant difference between the copper leaching rates from +20-38 and +38-53 µm size fractions even though the surface area was increased by finer grinding can be explained by assuming that below a particular particle size (-53 µm in this case), malachite leaching rate is predominantly influence/limited by chemical reaction rather than by diffusion models.

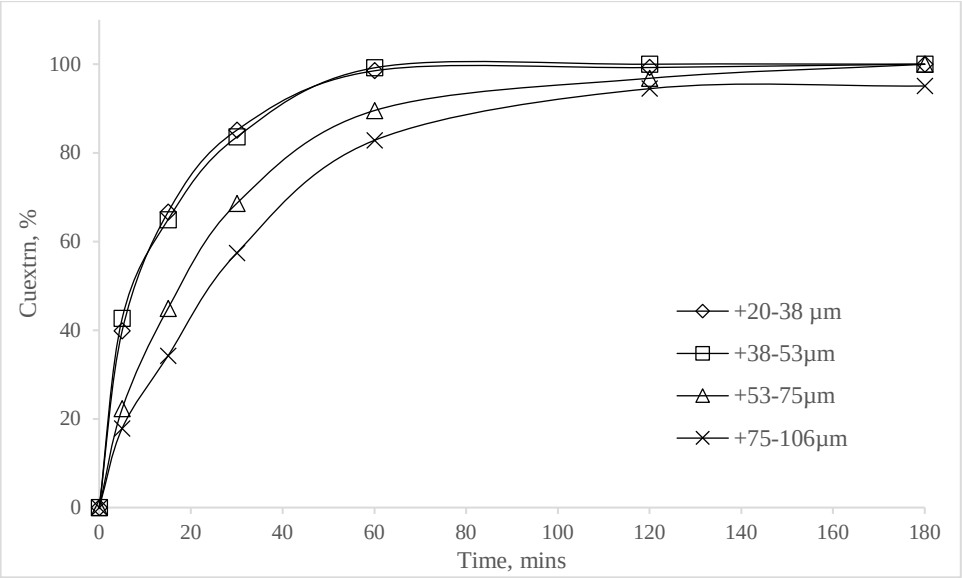

Figure 5.14 Effect of particle size on copper dissolution from malachite B: [Gly] 0.4 M, 25 °C, 350 rpm and 0.36 %w/v solids

5.6.1.6 Kinetic Analysis

As malachite leaching at 50 °C is completed within 30 minutes, the leaching kinetics have been investigated for the initial 30 minutes. According to the shrinking model equations (Equations 5.3, 5.4, 5.5 and 5.6) given in Section 5.1, if the leaching is controlled by any of the kinetic models, plotting the right hand side of the equation against time should give a straight line with the regression correlation coefficient values close to 1. The slope of the straight line represents the apparent rate constant. The regression correlation coefficient values from the plotted kinetic models have been determined and shown in Table 5.4.

Table 5.4 Correlation coefficient values of shrinking core kinetic models for malachite B

Variables	Correlation coefficient for evaluated models: R^2			
	Diffusion through liqiuid film controls	Diffusion through product layer controls	Chemical reaction controls	No product layer formation- Film diffusion at particle surface controls
	x	$1-3(1-x)^{2/3}+2(1-x)$	$1-(1-x)^{1/3}$	$1-(1-x)^{2/3}$
Gly concentration				
0.1	0.9824	0.9710	0.9878	0.9852
0.2	0.9553	0.9898	0.9731	0.9647
0.4	0.9581	0.9753	0.9906	0.9774
0.8	0.9336	0.9803	0.9766	0.9579
Temperature				
25	0.9581	0.9753	0.9906	0.9774
30	0.8476	0.9754	0.9245	0.8880
40	0.7970	0.9909	0.9592	0.8833
50	0.5218	0.8161	0.7659	0.6200
Stirring speed				
150	0.9539	0.9868	0.9782	0.9671
350	0.9581	0.9753	0.9766	0.9766
550	0.9282	0.9847	0.9906	0.9564
800	0.9166	0.9887	0.9633	0.9395
Particle size, µm				
20-38	0.857	0.9995	0.9878	0.9821
38-53	0.8351	0.9996	0.9422	0.9770
53-75	0.9581	0.9753	0.9906	0.8931
75-106	0.9737	0.9576	0.9915	0.9119

On comparing the correlation coefficients values for the fitted rate controlling models, it can be noted that it is difficult to predict which model controls the leaching rate of malachite given that the R^2 values for all models under different process conditions are very similar. The new approach of a constrained multi-linear regression analysis using the least square technique as proposed by Nazemi et al. (2011) was then applied to determine the rate controlling step in order to determine the contribution of each rate model at any stage of the process.

Table 5.5 shows the calculated results of fitted experimental data to Equation 5.8 and solving Equation 5.9 by the constraint least square technique. It can be deduced from the results that the leaching rate (first 3 hours) of malachite is controlled only by diffusion through the product layer.

Table 5.5 Data showing the rate-controlling model of malachite B at different temperatures using the least square technique of constrained multi-linear analysis

Temperature °C	K_l (min)	K_d (min)	K_r (min)	R^2
25	0	162.15	0	0.9777
30	0	137.18	0	0.9115
40	0	38.27	0	0.9954
50	0	25.73	0	0.9035

The apparent rate constant, k, at various leaching temperatures were obtained from linearised plots. The apparent rate constant values were then plotted against temperature according to the Arrhenius equation (Equation 5.11). The plot of lnK vs. 1/T shown in Figure 5.15 was a straight line with its gradient being $-E_a/R$ from which the apparent E_a could be estimated. The apparent E_a was determined to be 48.26 kJ/mol. The high E_a is unexpected for a diffusion controlled reaction.

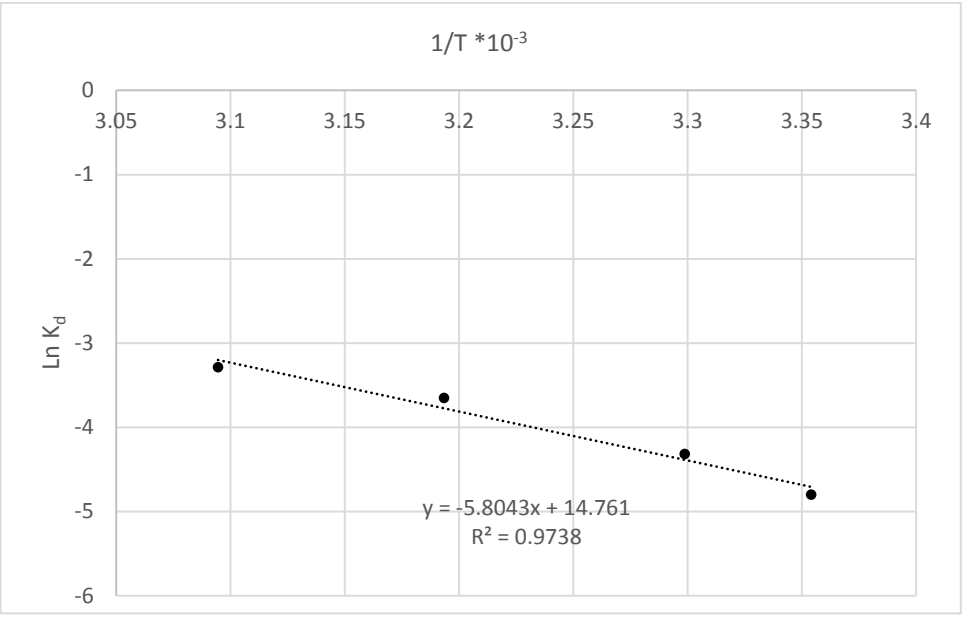

Figure 5.15 Arrhenius plot for product layer diffusion controlled malachite leaching

Using K_d values obtained for each investigated process variable, plots of K_d versus *ln[Gly], ln[SS], ln[PS]* were obtained. The slope of the straight line in each plot shows the calculated order of the reaction with respect to glycine, stirring speed and particle size. The order of the reaction with respect to glycine concentration, stirring speed, particle size were found to be 1.36, 0.64, and -0.96, respectively.

5.6.2 Chalcocite B

Chalcocite, as earlier mentioned in Section 4.7, is a secondary copper sulfide mineral and very profitable to mine due to its high copper content. This necessitates investigations to understand its leaching kinetics in this project.

5.6.2.1 Mineralogy and Chemical Composition of chalcocite B

The chalcocite specimen used in this study was obtained from GeoDiscoveries, a bulk minerals supplier in Australia. The mineral was ground and sieved to obtain five different size fractions: less than 20 µm, +20-38 µm, +38-53 µm, +53-75 µm and +75-106 µm. Q-XRD diffraction of the ground sample showed that the sample contains 82.0 % chalcocite (Cu_2S) and 18.0 % djurleite ($Cu_{1.938}S$). The copper concentration of the various size fraction was determined by XRF analysis. Results are as shown in Table 5.6.

Table 5.6 Copper content in each particle size fraction of chalcocite B

Size fraction, µm	P80 18.92	20-38	38-53	53-75	75-106
Cu, %	78.4	79.2	78.5	78.6	77.6

5.6.2.2 Effect of Initial Glycine Concentration

Figure 5.16 shows the influence of glycine concentration on the leaching kinetics of chalcocite. It can be seen that copper extraction increases as glycine concentration increases. It is, however, clear that there is an upper limit above which any further glycine addition does not lead to higher copper extraction. Under the given experimental conditions (25°C, 400 rpm, DO 8 ppm), 0.5 M was selected as an optimum glycine concentration as similar copper extraction (43.0 %) was extracted at 1.0 M Gly in 48 hours.

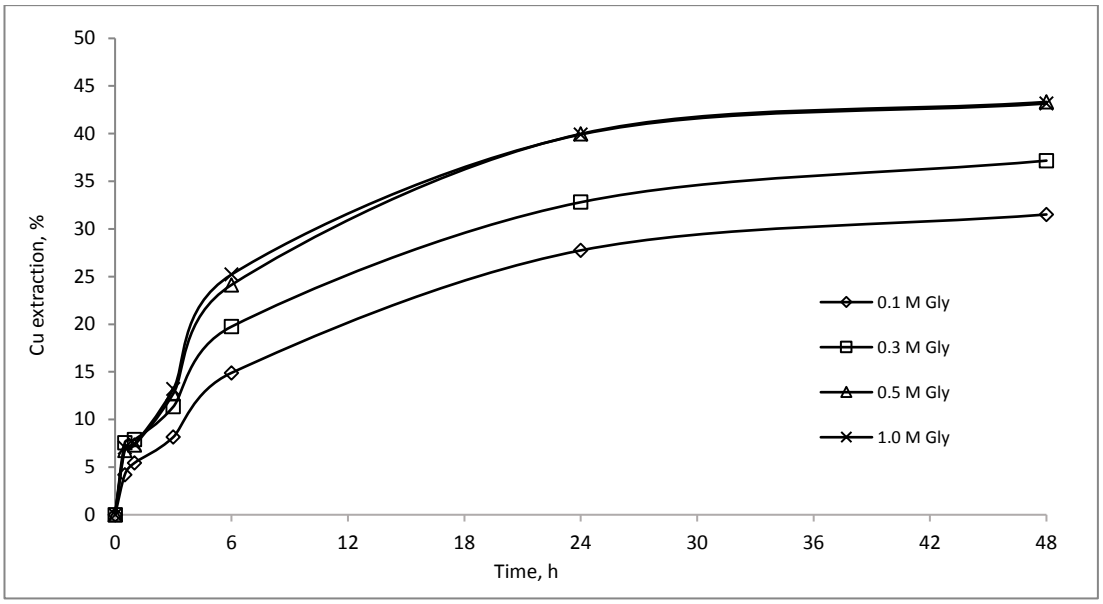

Figure 5.16 Effect of glycine concentration on chalcocite B leaching kinetics: 25°C, 400 rpm, DO 8 ppm, PS 38-53 µm, 0.25 %w/v solids.

5.6.2.3 Effect of Stirring Speed

The effect of stirring speed was studied by varying the speed from 200 to 800 rpm. It can be clearly seen from the results shown in Figure 5.17 that, as the stirring speed is increased from 200, 400 and 600 rpm, copper extracted after 48 hours also increased from 23.8, 43.3 and 52.4 % respectively. The results also show that copper extraction at 800 rpm was lower than at 600 rpm (44.1 % Cu after 48 hours). This observation indicates that agitation at 800 rpm is too high to establish an optimum contact between the chalcocite particles and the leach solution.

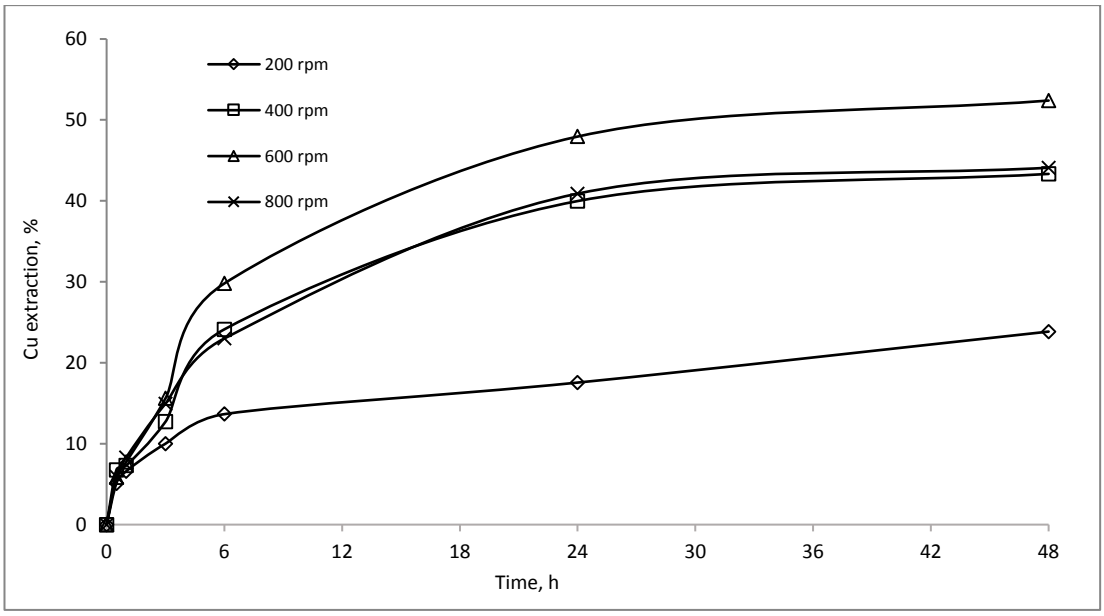

Figure 5.17 Effect of stirring speed on chalcocite B leaching kinetics: 0.5 M Gly, 25°C, DO 8 ppm, PS 38-53 µm, 0.25 %w/v solids.

5.6.2.4 Effect of Particle Size

The effect of particle size on chalcocite leaching rate was studied using five different particle size fractions: P80: 18.88 µm [d(0.5): 8.4 µm], +20-38, +38-53, +53-75, and +75-106 µm. P80: 18.88 µm [d(0.5): 8.4 µm] indicates a size fraction of 80 % passing 18.88 µm and 50 % of particles less than 8.4 µm. As shown in Figure 5.18, the effect of particle size is quite evident after 6 hours. It can be expectantly noted that copper extraction increases as the particle size decreases. Leaching for 48 hours resulted in 78.2 % Cu extraction from P80 18.88 µm size fraction while particle size fractions of +20-38 and +38-53 both resulted in 43.0 % Cu extraction and the size fractions of +53-75 and +75-106 both resulted in only 31.0 % Cu extraction. The significant improvement in Cu extraction with fine grinding is an indication that product layer diffusion might be the rate limiting step during chalcocite leaching in alkaline glycine solutions.

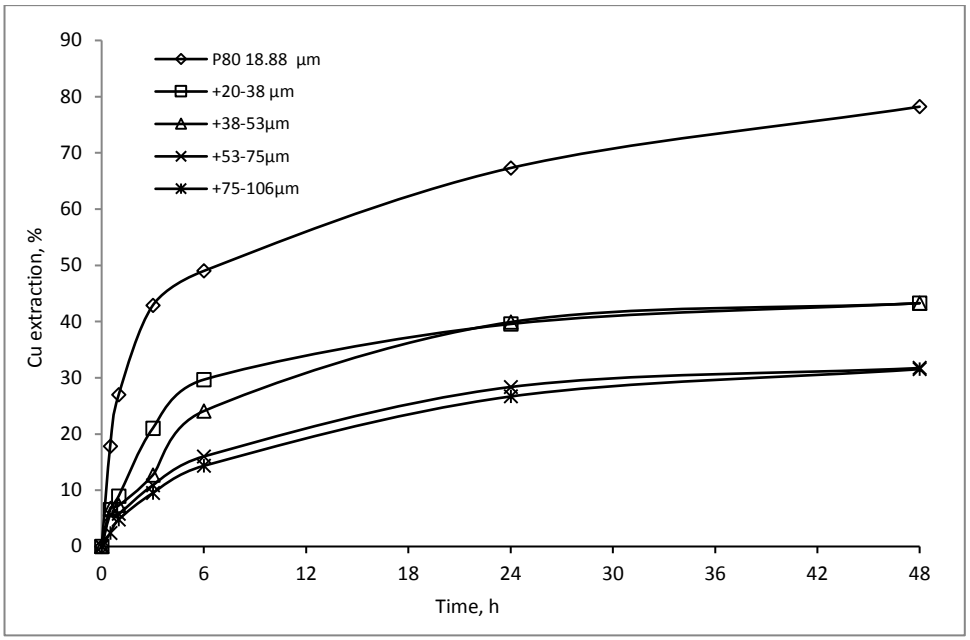

Figure 5.18 Effect of particle size on chalcocite B leaching kinetics: 0.5 M Gly, 25 °C, 400 rpm, DO 8 ppm, 0.25 %w/v solids.

5.6.2.5 Effect of Dissolved Oxygen (DO) Concentration

The effect of DO on the leaching rate of chalcocite was studied at 8, 15, 20 and 25 ppm. The results are plotted in Figure 5.18. As shown in Figure 5.19, increasing the DO concentration generally leads to increases in copper extraction. After 6 hours of leaching, at 25 ppm DO, copper extraction plateaued at 44.5 % while copper extraction at 15 and 20 ppm DO increased to 49.8 and 54.0 %, respectively, after 48 hours. The reason for this is not well understood, but could be attributed to some form of copper alteration products on the mineral surface under such high DO conditions or glycine degradation. As it was indicated in Section 5.4.1, covellite, which is an intermediate product during chalcocite leaching, might quickly form on the surface under high DO and this consequently slows down the leaching rate.

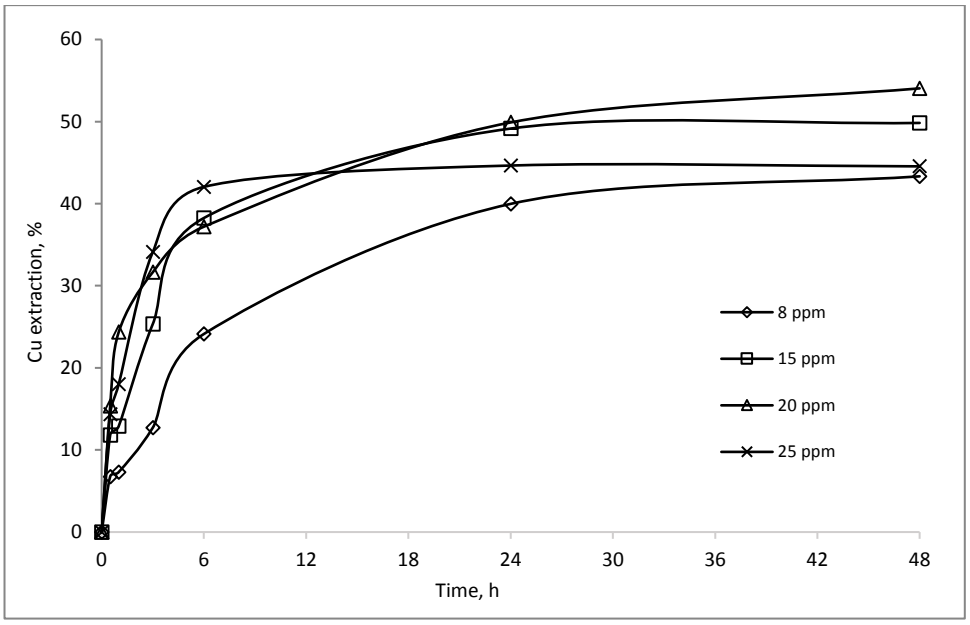

Figure 5.19 Effect of dissolved oxygen on chalcocite B leaching kinetics: 0.5 M Gly, 25 °C, 400 rpm, and +38-53 µm, 0.25 %w/v solids.

5.6.2.6 Effect of Temperature

The effect of temperature on chalcocite leaching is presented in Figure 5.20. The results show that the leaching rate generally increases as temperature increases. This observation is clear in Figure 5.20 where leaching for 6 hours at 25, 35, 45, and 55 °C resulted in copper extractions of 24.1, 31.8, 32.1, and 39.0 %, respectively. After 24 hours of leaching at 45 and 55 °C, copper extraction rate continued to increase steadily while extractions at 25 and 35 °C showed a decrease in the copper extraction rate. As it has been shown earlier that chalcocite leaching occurs in two stages with the second dominated by covellite leaching formed from the first stage (Section 5.4.1), the observed steady increase in Cu extraction rates at 45 and 55 °C after 24 hours suggest that covellite leaching may be improved at higher temperature.

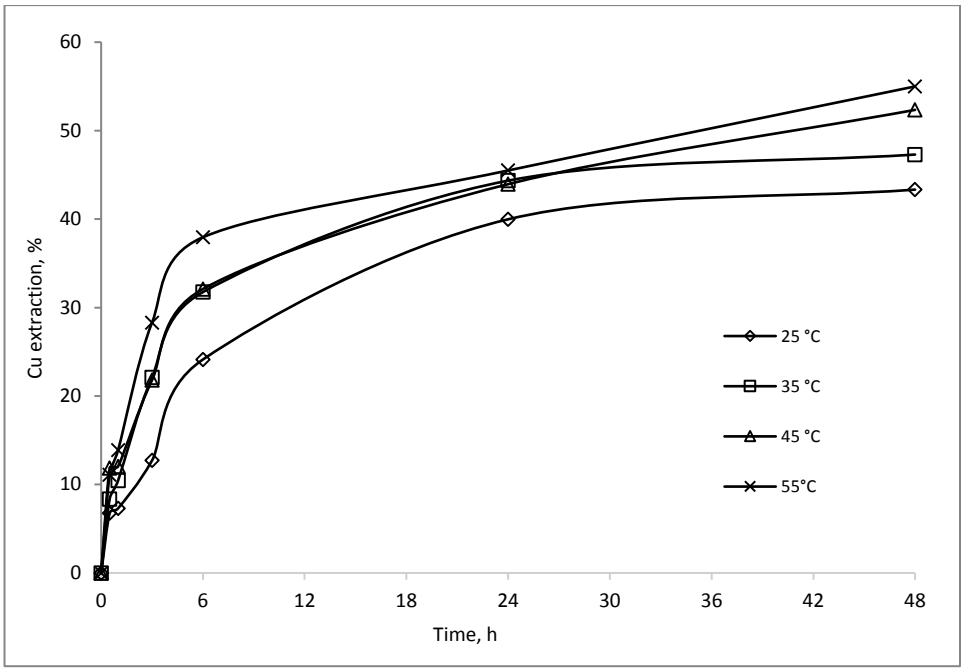

Figure 5.20 Effect of temperature on the leaching kinetics of chalcocite B: 0.5 M Gly, 400 rpm, DO 8 ppm, 38-53 µm, 0.25 %w/v solids.

5.6.2.7 Kinetic Analysis

Assuming that the chalcocite particles are spherical, the shrinking core model and its rate controlling equations as previously outlined in Section 5.1 can be applied to determine the rate limiting steps during leaching. Using the experimental data, the right hand side of each rate controlling equation was plotted against reaction time for each variable. The kinetic model that gives the best fit results for the experimental data would then be the rate limiting step. Table 5.7 shows the correlation coefficients, R^2-values of the fitted data for the first 6 hours of leaching. By comparing all of the R^2-values for the different experimental variables in Table 5.7 , it could then be predicted that the initial leaching rate (0-6 hours) of chalcocite in aqueous alkaline glycine solutions is controlled by diffusion through the product layer since the R^2-values for this model are closest to 1.0.

Table 5.7 Correlation coefficient values of shrinking core kinetic models for chalcocite B

Variables	Correlation coefficients for evaluated models, R^2		
	Diffusion through film control	Diffusion through product layer control	Chemical reaction control
	x	$1-3(1-x)^{(2/3)}+2(1-x)$	$1-〖(1-x)〗^{\wedge(1/3)}$
Gly concentration			
0.1	0.9426	0.9518	0.9483
0.2	0.8911	0.9513	0.9034
0.4	0.9569	0.9393	0.9632
0.8	0.9579	0.9372	0.9641
Temperature			
25	0.9569	0.9393	0.9632
35	0.9419	0.9953	0.9576
45	0.9021	0.9905	0.9247
55	0.9133	0.9964	0.9367
Stirring speed, rpm			
200	0.8546	0.9961	0.8659
400	0.9569	0.9393	0.9632
600	0.9467	0.9405	0.9887
800	0.9855	0.9908	0.9575
Particle size, μm			
20-38	0.9493	0.9942	0.9617
38-53	0.9569	0.9393	0.9631
53-75	0.9138	0.9932	0.9237
75-106	0.9595	0.9936	0.9650
Dissolved oxygen, ppm			
8	0.7899	0.9393	0.8393
15	0.9361	0.9881	0.9079
20	0.7198	0.9289	0.7832
25	0.8621	0.9831	0.9345

Diffusion through the product layer as the rate controlling step during the leaching of chalcocite was also confirmed by applying the constrained multi-linear regression using the least square technique on experimental data as shown in Table 5.8. It could be noted that,

as one moves from the first leaching stage (0-6 hours) to the second leaching stage (24-48 hours), the resistance to leaching increases as demonstrated by the higher estimated time needed to complete the leaching process.

Table 5.8 Rate-controlling model of chalcocite leaching determined for 0-6, 6-48 hours and the overall leaching data at different temperatures using the least square technique of constrained multi-linear analysis

Temperature °C	K_l (min) *10^3	K_d (min) *10^3	K_r (min) *10^3	R^2
0-6 hours leaching				
25	0	8.3821	0	0.9855
35	0	7.0068	0	0.9993
45	0	6.3407	0	0.9958
55	0	5.5667	0	0.9982
6-48 hours leaching				
25	0	11.428	0	0.9086
35	0	10.296	0	0.9147
45	0	8.6874	0	0.9878
55	0	6.7736	0	0.97734
Whole leaching process				
25	0	29.892	0	0.9556
35	0	22.875	0	0.9331
45	0	20.619	0	0.9763
55	0	17.617	0	0.9554

Using the apparent rate constants derived by application of Equation 5.4, the Arrhenius plot (ln k_d vs 1/T(K) was obtained for the first and second leaching stages as shown in Figure 5.21. The calculated apparent activation energies are 25.36 kJ/mol and 108 kJ/mol for the first and second leaching processes respectively.

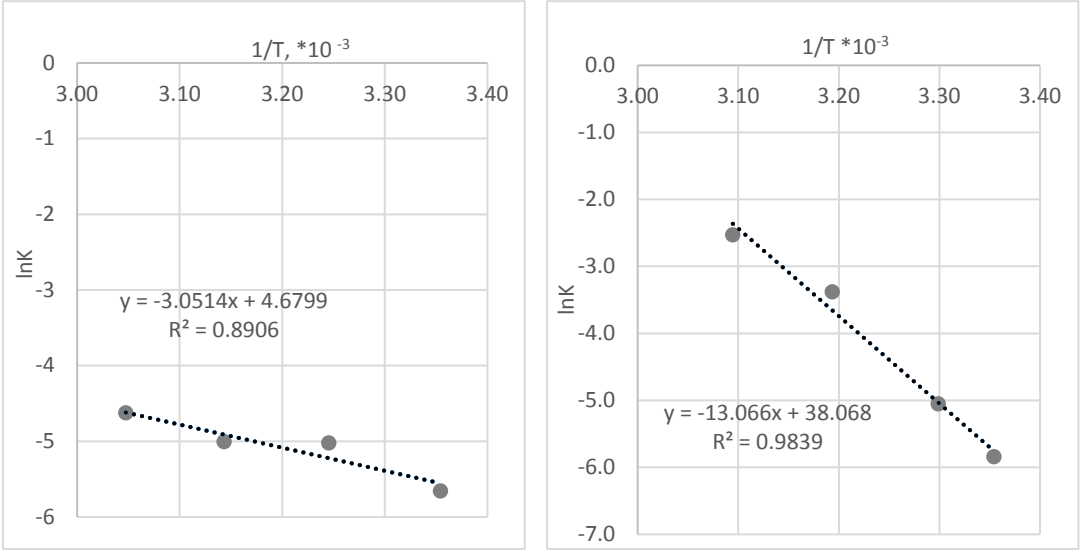

Figure 5.21 Arrhenius plot for product layer diffusion controlled chalcocite leaching

Using K_d values obtained for each investigated process variable, plots of K_d versus *ln[Gly], ln[O_2], ln[SS], ln[PS]* for the first leaching stage were obtained. The slope of the straight line in each plot shows the calculated order of the reaction with respect to glycine, oxygen, stirring speed and particle size. The order of the reaction with respect to glycine concentration, dissolved oxygen concentration, stirring speed, particle size were estimated to be 0.48, 1.11, 0.95 and -1.39, respectively.

5.6.3 Chalcopyrite B

Chalcopyrite mineral makes up about 70 % of the world's copper resources (Harmer et al., 2006). Determining the leaching kinetics of chalcopyrite is thus as important as the mineral in order to have full understanding of copper extraction in alkaline glycine solutions.

5.6.3.1 Mineralogy and Chemical Composition of Chalcopyrite B

The chalcopyrite specimen used in this study was obtained from a local mineral collector in Perth, Australia. The mineral was ground and then sieved to obtain five different size fractions, less than 20 µm, +20- 8 µm, +38-53 µm, +53-75 µm and +75-106 µm. The sample fraction below 20 µm was further pulverized with a ring mill and a P80 of 8.56 µm (laser particle size analyser) size fraction obtained. Q-XRD analysis of the ground sample showed that the bulk sample contains 67.0 % chalcopyrite, 10.0 % pyrite and 14.0 % ankerite as major

phases (Table 5.9). The elemental composition of the different size fractions was determined by XRF analysis and the results are as shown in Table 5.10.

Table 5.9 Mineralogical composition of chalcopyrite B

Phase	Pyrite	Chalcopyrite	Ankerite	Siderite	Pyrrhotite	Sepiolite	Quartz
% mass	10	67	14	5	1	1	1

Table 5.10 Elemental composition of different size fractions of chalcopyrite B

Size fraction/ Element	75-106 µm	53-75 µm	38-53 µm	20-38 µm	-20 µm
Ag (ppm)	28.50	26.00	23.50	21.00	30.00
Fe (%)	31.40	31.51	31.16	30.97	30.48
SiO_2 (%)	2.09	1.64	1.63	1.75	2.98
MnO (%)	0.10	0.10	0.10	0.11	0.10
CaO (%)	2.20	2.16	2.00	1.79	1.72
S XRF (%)	33.10	33.30	32.60	32.30	31.40
MgO (%)	1.59	1.54	1.53	1.54	1.84
Zn (%)	0.17	0.17	0.15	0.15	0.19
Pb (%)	0.07	0.07	0.05	0.04	0.06
Cu (%)	26.60	27.20	27.20	27.20	26.20
As (%)	0.03	0.03	0.02	0.02	0.03
LOI1000	16.27	16.04	15.87	16.19	17.10

5.6.3.2 Effect of Initial Glycine Concentration

The effect of glycine concentration on the leaching kinetics of chalcopyrite was studied by varying the glycine concentration in the range of 0.1 to 1.0 M. The particle size range of +20-38 µm was used for the investigation of the effects of other process variables unless particle size was being investigated. Stirring speed of 400 rpm, temperature at 50 °C, dissolved oxygen concentration (DO) at 15 ppm were kept fixed. The initial solution pH used for all experiments was 11.5. The results shown in Figure 5.22 indicate that an increase in glycine concentration results in an increase in copper extraction over time. This observation can be clearly noted after 96 hours at which 0.1, 0.3, 0.5 and 1.0 M glycine resulted in 17.4, 24.6, 28.2 and 28.5 % Cu extraction, respectively.

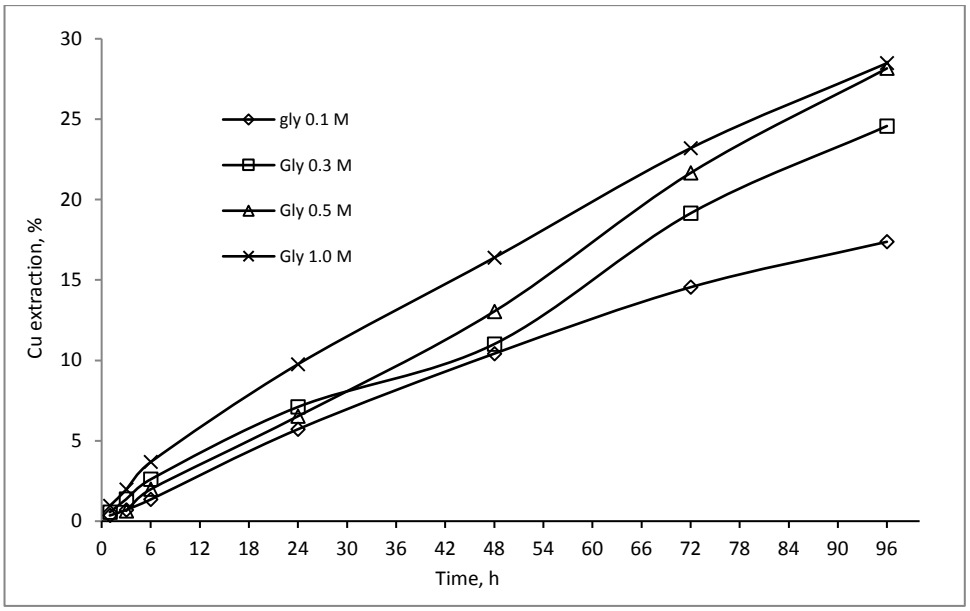

Figure 5.22 Effect of glycine concentration on the leaching kinetics of chalcopyrite B: pH 11.5, [O_2] 15 ppm, PS 20-38 µm, 50 °C, SS 400 rpm, and 0.76 %w/v solids

5.6.3.3 Effect of Stirring Speed

Some researchers have reported that chalcopyrite oxidation is independent of stirring speed (Antonijević & Bogdanović, 2004; Dutrizac, 1981). During the leaching of chalcopyrite in peroxide-glycol system, increasing stirring speeds to above 100 rpm led to a decrease in copper dissolution (Mahajan et al., 2007). Similarly, Sokić et al. (2009) also reported a slight decrease in chalcopyrite leach rate with increasing stirring speed which has been attributed to reduced contact between the particles and the oxidant. To investigate the effect of stirring speed on chalcopyrite leaching in the alkaline glycine system, the speed was varied from 200 to 800 rpm while glycine concentration was 0.5 M. Figure 5.23 shows that the dissolution rate of chalcopyrite increases with stirring speed. The highest copper dissolution after 96 hours of 39.25 % occurred at 800 rpm. This observation is an indication that diffusion is significant in the leaching kinetics of chalcopyrite.

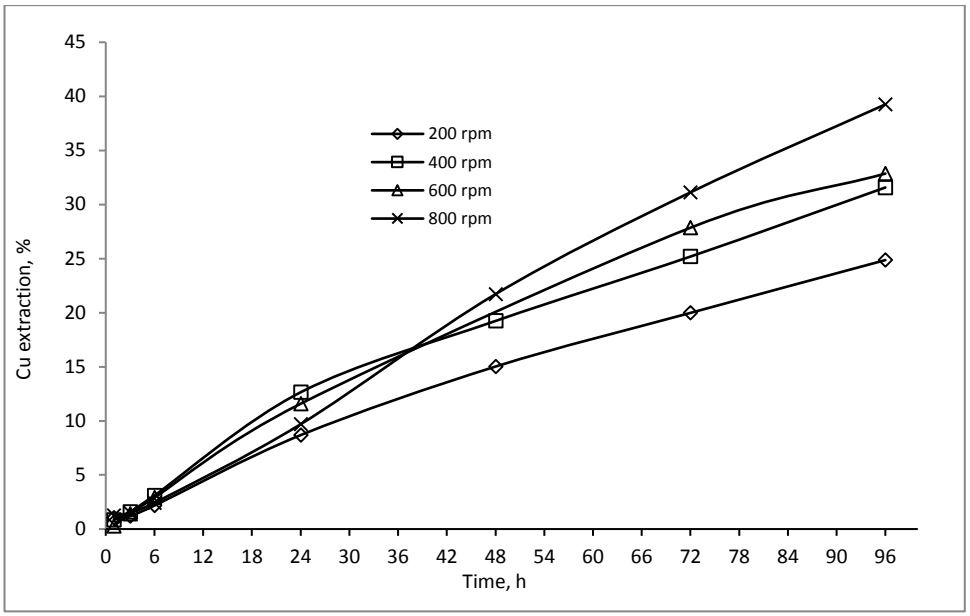

Figure 5.23 Effect of stirring speed on the leaching kinetics of chalcopyrite B: [Gly] 0.5 M, pH 11.5, [O_2] 15 ppm, PS 20-38 µm, 50 °C and 0.76 %w/v solids

5.6.3.4 Effect of Particle Size

In industrial leaching operations, reactor design and power consumption significantly depend on the particle size range being leached (Dreisinger & Abed, 2002). The shrinking core kinetic model and its application depend on the type and size of particle being leached (Li et al., 2014). If the leaching rate is significantly dependent on particle size, then it is an indication that the kinetics is controlled by diffusion through a product layer.

Figure 5.24 shows the effect of various size fractions (-10, +20-38, +38-53, +53-75 and +75-106 µm) on chalcopyrite leaching rate. The results illustrate that varying the particle size has no significant influence on chalcopyrite dissolution rate. The results show that, after 96 hours leaching, copper extraction of 32.0 % was achieved for all size fractions ranging from +20-38 to +75-106 µm. Surprisingly, over the same period, about 90.0 % of Cu was extracted from the 100 % passing 10 µm size fraction. It was also observed that the initial copper dissolution rate from the -10 µm fraction was remarkably high with up to 46.8 % copper extracted in just 6 hours as compared to 1.7 % for all other size fractions. This significant difference in the dissolution rates as a result of particle size reduction is an indication that diffusion plays a role in limiting the leaching process since fine grinding increases particle surface layer and reduces the diffusion barrier. Another main reason for the significant improvement in leaching rate of the -10 µm size could be attributed to the mechano-chemical activation of

the mineral caused by extended grinding. Mechano-chemical activation according to Juhász and Opoczky (1990,) comprises the structural and physiochemical changes (as well as chemical reactions) which are induced in solids by deformation, disintegration and dispersion due to the application of mechanical energy. These activations induce defects on the crystalline structure of the mineral. Leaching kinetics have been reported to be greatly enhanced by mechano-chemical activation (Balaž, 2000).

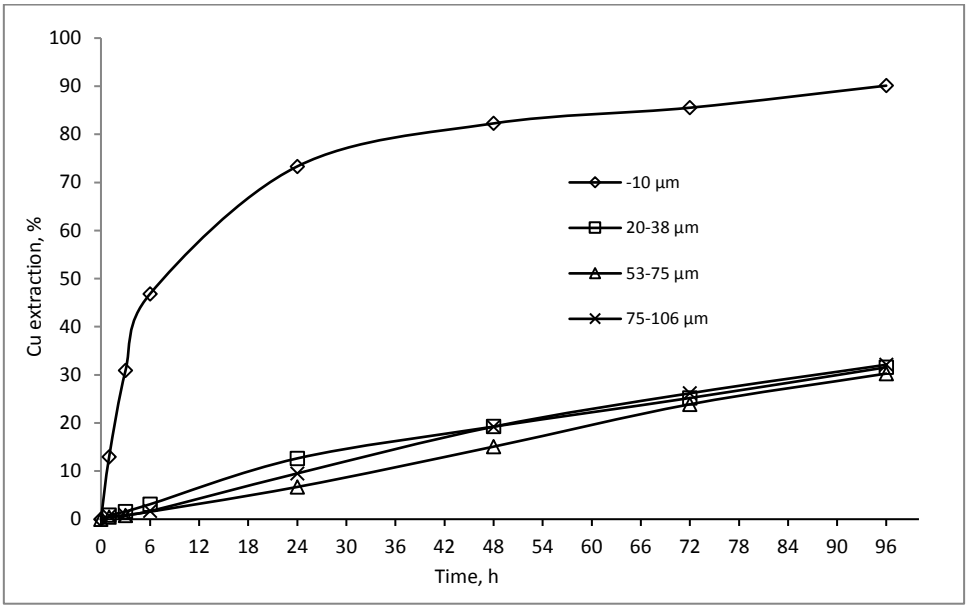

Figure 5.24 Effect of particle size on the leaching kinetics of chalcopyrite B: [Gly] 0.5 M, 50 °C, pH 11.5, [O_2] 15 ppm, SS 400 rpm, and 0.76 %w/v solids.

5.6.3.5 Effect of Dissolved Oxygen (DO) Concentration

The effect of different DO concentrations on copper dissolution from chalcopyrite B is shown in Figure 5.25. Copper dissolution generally increases with increased DO concentration up to 48 hours at which copper dissolution at 25 ppm levels off at 25.4 %. Copper dissolution at DO 8 and 15 ppm was observed to increase steadily with both eventually reaching 31.50 % after 96 hours of leaching. The flattening of the extraction curve after 48 hours of leaching with 25 ppm DO could be attributed to the rapid depletion of surface copper, and by so doing, increasing the diffusion barrier for further reagent and product diffusion. This may also be attributed to glycine degradation which has been reported to occur at such high oxidation conditions (Berger et al., 1999). Other amino acids have also been reported to be oxidised by oxygen based radicals (Chen et al., 2012)

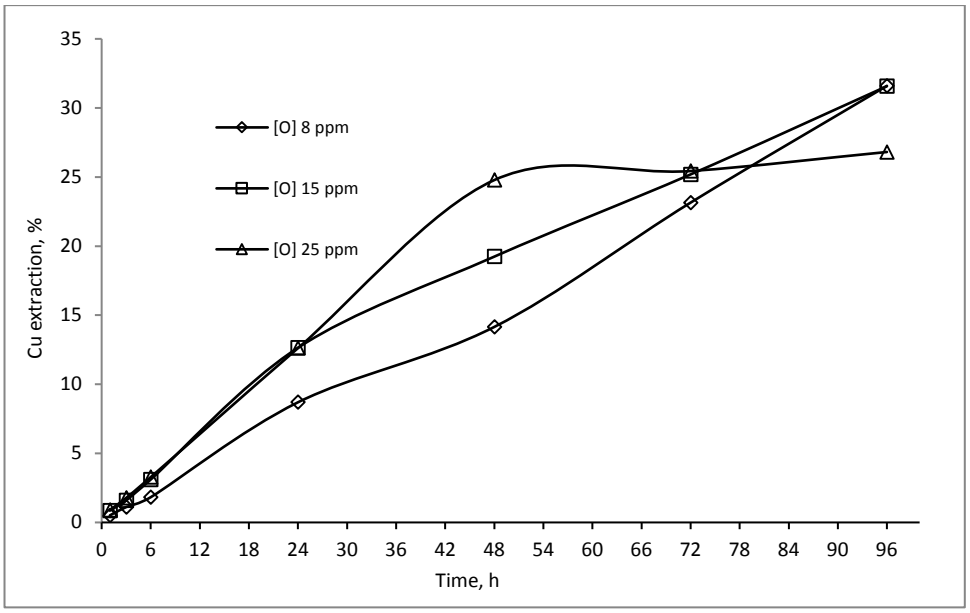

Figure 5.25 Effect of dissolved oxygen on the leaching kinetics of chalcopyrite B: [Gly] 0.5 M, pH 11.5, 40 °C, PS 20-38 µm, SS 400 rpm, and 0.76 %w/v solids

5.6.3.6 Effect of Temperature

With temperature being the key process variable used to determine the leaching rate controlling step, and given that two types of curves are noted when the effect of particle size was investigated (Figure 5.24), the effect of temperature on dissolution rate of copper from chalcopyrite B was investigated using the - 10 µm and +20-38 µm size fractions.

Leaching +20-38 µm Size Fraction

Temperature dependence experiments for chalcopyrite dissolution rate were carried out in range of 40 to 70 °C in solutions containing 0.5 M Gly and DO concentration of 15 ppm for 96 hours. The results shown in Figure 5.26 indicate that copper dissolution increases as the temperature increases with final extraction values of 14.1, 31.6, 39.1 and 42.1 %, at 40, 50, 60 and 70 °C, respectively. Although copper dissolution increases as temperature increases, it is quite noticeable that increasing the temperature from 40 to 50 °C doubles the copper extraction. However a temperature increase from 50 to 60 °C and from 60 to 70°C has less effect on copper extraction.

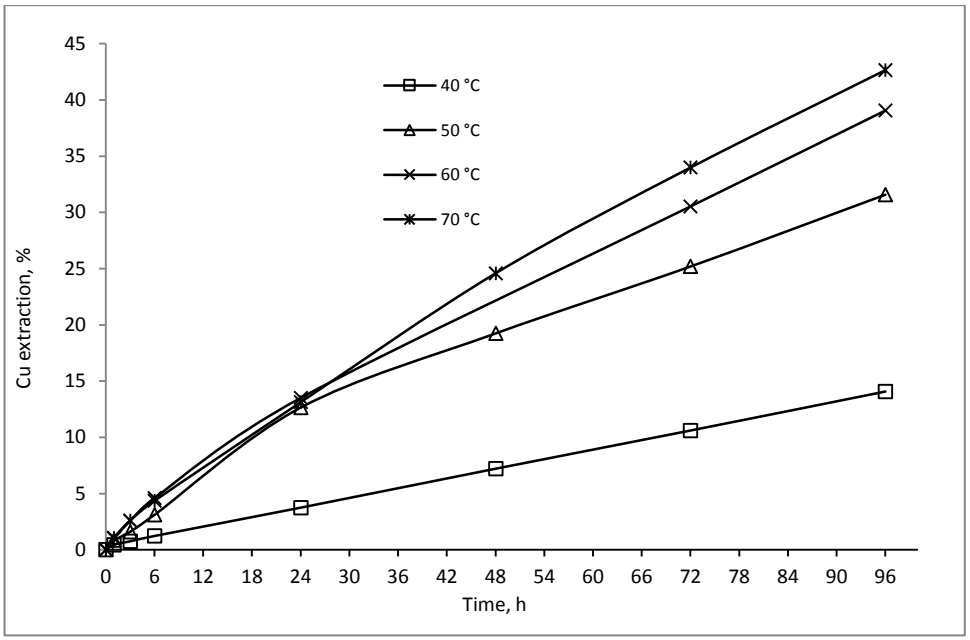

Figure 5.26 Effect of temperature on the leaching kinetics of 20-38 µm chalcopyrite B: [Gly] 0.5 M, DO 15 ppm, pH 11.5, PS 20-38 µm, SS 400 rpm and 0.76 %w/v solids

Leaching -10 µm size fraction

The kinetics of heterogeneous reactions such as leaching is not only determined by contact area but also by mineral structure which can be altered by intensive grinding (Baláž et al., 1992; Pourghahramani & Forssberg, 2006). Assuming that the ultrafine grinding of chalcopyrite (in order to obtain the -10 µm fraction) might have altered it leaching kinetics significantly by mechano-chemical activation as shown in Figure 5.24, investigating effect of temperature on the leaching of -10 µm was investigated to see if it influenced the rate controlling model. The temperature was varied from 30, 40, 50 to 60 °C under the following leaching conditions: 0.5M Gly, stirring speed 500 rpm, and DO 10 ppm. The results of the effect of temperature on copper extraction from the -10 µm are shown in Figure 5.26. Higher copper dissolution was clearly noted with an increase in the leaching temperature. However, the rate of copper dissolution from 10 µm was significantly higher (72.6 % Cu at 60 °C after 24 hours) when compared to that from +20-38 µm size fraction (Figure 5.25) at the same temperature (13.1 % Cu at 60 °C after 24 hours). The leaching curves in Figure 5.27 are rather parabolic as opposed to the straight lines obtained when leaching 20-38 µm. This difference and its effect on the rate controlling model will be determined in Section 5.6.3.7

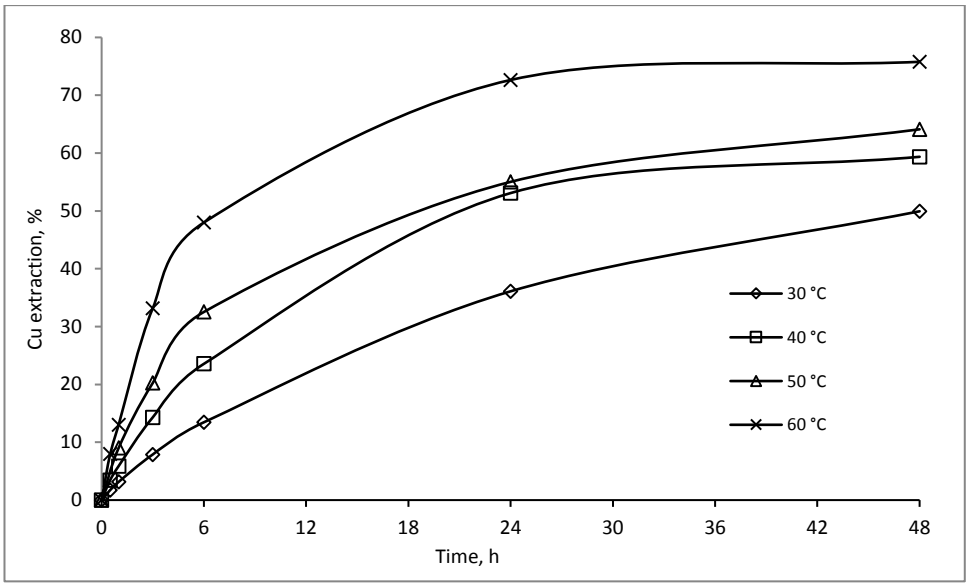

Figure 5.27 Effect of temperature on the leaching kinetics of < 10 µm chalcopyrite B size fraction: [Gly] 0.5 M, DO 10 ppm, pH 11.5, PS < 10µm, SS 500 rpm

5.6.3.7 Kinetic Analysis

The rate constants and their correlation coefficients for each process variable were determined from plots of the various shrinking core kinetic models. Table 5.11 shows the determined R^2-values for the different models and variables.

Table 5.11 Correlation coefficient values of shrinking core kinetic models for chalcopyrite B

Variables	Correlation coefficients for evaluated models, R^2		
	Diffusion through film control	Diffusion through product layer control	Chemical reaction control
	x	$1-3(1-x)^{2/3}+2(1-x)$	$1-(1-x)^{1/3}$
Gly concentration, M			
0.1	0.9898	0.9742	0.9924
0.3	0.9939	0.9136	0.9928
0.5	0.9979	0.9110	0.9959
1	0.9917	0.9646	0.9957
Temperature			
25	0.9896	0.9615	0.9906
40	0.9996	0.9310	0.9996
50	0.9858	0.9180	0.985
60	0.9932	0.9700	0.9971
70	0.9950	0.9530	0.9992
Stirring speed, rpm			
200	0.9890	0.9720	0.9932
400	0.9801	0.9749	0.9875
600	0.9888	0.9847	0.9934
800	0.9984	0.9295	0.9983
Particle size, µm			
20-38	0.7246	0.9293	0.8496
38-53	0.9806	0.9742	0.9878
53-75	0.9980	0.9207	0.997
75-106	0.9917	0.9652	0.9959
Dissolved oxygen, ppm			
8	0.9968	0.8691	0.9838
15	0.9806	0.9264	0.9878
25	0.8959	0.9742	0.9017

As was noted with the kinetic analysis of malachite, the regression coefficients obtained by fitting the experimental data to the shrinking core models are too close to deduce the rate controlling mechanism of copper dissolution from chalcopyrite. On applying the constrained multi-linear regression analysis using the least square technique, it was possible to identify

the rate controlling mechanism for both +20-38 µm and <10 µm particle size fractions.

The calculated results, as shown in Table 5.12, indicate that chalcopyrite leaching of +20-38 µm size fraction in alkaline glycine solution is controlled by both liquid film diffusion and diffusion through the product layer. However, diffusion through the product layer is the more dominant rate limiting step as estimated time contribution at different temperatures are far higher than those of fluid diffusion controlled model.

Table 5.12 Data showing rate-controlling model for 20-38 µm size fraction chalcopyrite B at different temperatures using the least square technique of constrained multi-linear analysis

Temperature °C	K_l (min)*10^4	K_d (min) *10^4	K_r (min) *10^4	R^2
40	3.77	6.97	0	0.9970
50	0.96	7.21	0	0.9989
60	0.96	3.37	0	0.9992
70	0.98	2.13	0	0.9998

On the other hand, when the constrained multi-linear regression analysis using the least square technique is applied on the leaching data of < 10 µm (Table 5.13), the leaching kinetics is controlled by the diffusion through the product layer for temperature values of 40 °C and above are considered. When leaching is conducted at 30 °C, both diffusion through the product layer and chemical reaction control the leaching process. However, chemical reaction's contribution was very limited and eliminated when temperature was elevated to 40 °C.

Table 5.13 Data showing rate-controlling model for < 10 µm size fraction chalcopyrite B at different temperatures using the least square technique of constrained multi-linear analysis

Temperature °C	K_l (min)*10^4	K_d (min) *10^4	K_r (min) *10^4	R^2
30	0	1.8708	0.3858	0.9993
40	0	1.5124	0	0.9736
50	0	1.2872	0	0.9841
60	0	0.7063	0	0.9408

The apparent rate constants obtained from the plots of $1-3(1-x)^{(2/3)}+2(1-x)$ versus time at investigated temperatures were used to construct an Arrhenius plots for both +20-38 µm

and < 10 µm size fractions. From the data shown in Figures 5.28 and 5.29, the apparent E_A's were calculated to be 36.25 kJ/mol for +20-38 µm and 29.62 kJ/mol for the < 10 µm size fraction. The lower activation value for the < 10 µm size fraction can be attributed to the mechano-chemical activation of the mineral surface when subjected to ultrafine grinding.

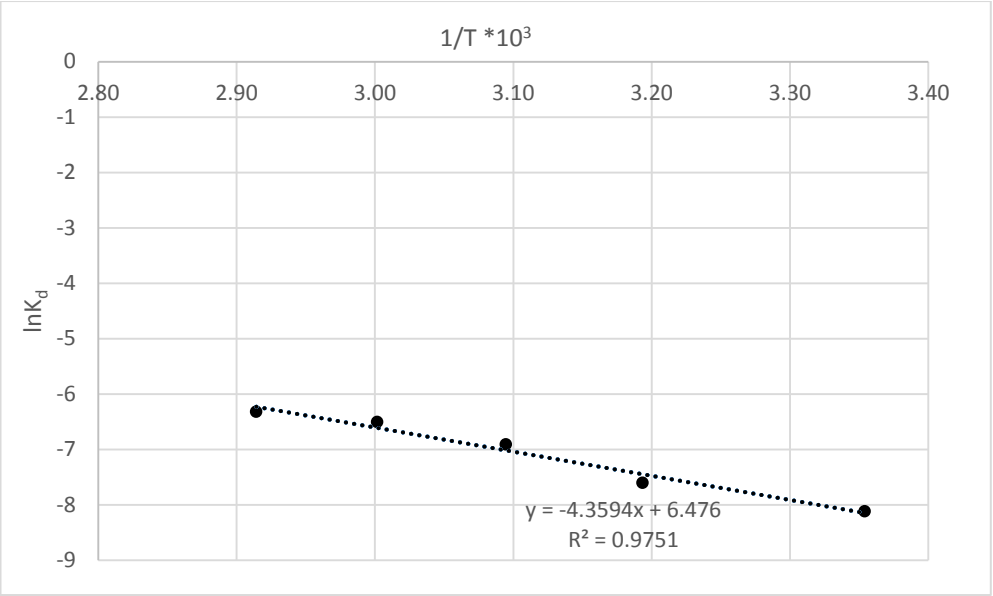

Figure 5.28 Arrhenius plot for product layer diffusion controlled leaching of chalcopyrite B

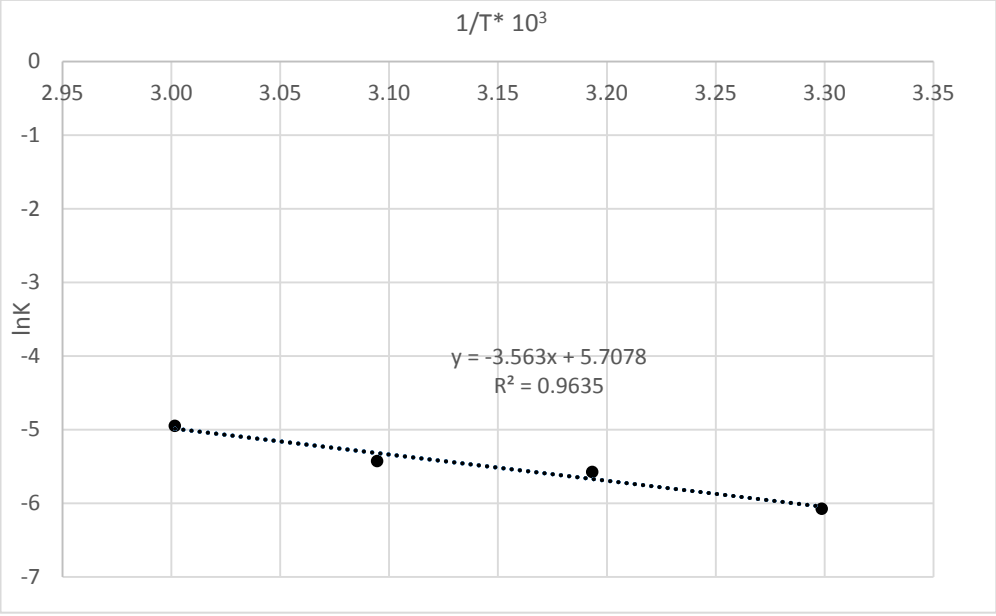

Figure 5.29 Arrhenius plot for product layer diffusion controlled leaching of <10 µm chalcopyrite B fraction

In order to obtain reaction orders with respect to process variables for chalcopyrite leaching, K_d values determined for each process variable were used to make plots of lnK_d versus *ln[Gly], ln[O_2], ln[SS], ln[PS]*. The slope of the straight line in each plot shows the calculated reaction

order with respect to the variable. The order of the reaction with respect to glycine concentration, dissolved oxygen concentration, stirring speed, particle size were 0.21, -0.87, 0.31, and -0.12, respectively.

5.7 Summary

Copper speciation from malachite, azurite, cuprite, chrysocolla, chalcocite and chalcopyrite leachates by UV-Vis and AAS established that only Cu(II) ions are available in the pregnant leach solutions to form the stable copper-glycinate complex $Cu(H_2NCH_2COO)_2$.

Sulfur speciation of the chalcocite and chalcopyrite leachate showed that sulfate species make up 90 % of the total sulfur in solution.

The dissolution of chalcocite occurs in two stages. The first stages involves the conversion of Cu_2S to covellite (CuS) and Cu ions. The CuS formed in the 1st stage is then leached in the second stage at a rather slower rate when compared to the fast conversion rate of Cu_2S in the first stage.

During chalcopyrite leaching, goethite was reported as one of the main by-products. However, SEM-EDS analysis of the leached residure indicated that the goethite does not form a passivation layer on the chalcopyrite surface given that no oxygen atoms were identified on the mineral surface after leaching.

Kinetic analysis of malachite and chalcocite showed that the leaching processes are both controlled by diffusion through product layer. Chalcopyrite leaching on the other hand is controlled by liquid film diffusion and diffusion through the product layer (dominant) when +20-30 µm size fraction was considered. For the < 10 µm chalcopyrite size fraction, the leaching is also controlled by diffusion through the product layer for temperatures above 30 °C.

Chapter 6 Leaching of Copper-Gold Ores

6.1 Chapter Objectives

The main objective of this chapter is to study the effect of process variables (reagent concentration, pH, temperature, oxygen concentration, galvanic effect) on the dissolution of copper and gold from different copper-gold ores.

Three copper-gold ore specimens (A, B, and C) were used to investigate the effect of process variables on the dissolution of copper and gold from these ores. All samples were crushed, milled and screened to achieve 100 % passing 75 µm.

Heap leaching simulation experiments were conducted with sample C and sample D (flotation tail). Sample C was crushed and screened to obtain a size fraction of 1-8 mm. The flotation tail specimen (dry) was leached as received (42.4 % of particles >2mm and 57.6 % <2mm).

6.2 Copper- Gold Ore A

6.2.1 Mineralogical and Elemental Composition

The XRD analysis of Cu-Au ore A showed chalcopyrite as the only copper mineral and pyrite as the major gangue phase (Table 6.1). Gold content determination by fire assay showed that the sample contains 1.96 ppm gold and XRF analysis showed a copper concentration of 3.56 %. According to literature, such an ore would normally not be processed by conventional cyanidation as huge amounts of cyanide would be consumed by copper dissolution. A more feasible approach would be to float and smelt. It is, however, important to understand the behaviour of such ores when leached in the alkaline glycine system.

Table 6.1 Mineralogy and elemental composition of Cu-Au ore A

Mineral phase	Mass %	Element	value
Clay mineral	6	Au (ppb)	1960
Kaolinite	2	Al (%)	1.74
Clinochlore	9	As (%)	0.048
Talc	2	Ca (%)	0.63
Annite - biotite - phlogopite	1	Co (%)	0.048
Muscovite - sericite	1	Cu (%)	3.56
Amphibole	1	Fe (%)	32.90
Alpha quartz	6	K XRF (%)	0.18
Calcite	2	Mg (%)	1.58
Dolomite - ankerite	4	Mn (%)	0.24
Siderite	1	Ni (%)	0.01
Chalcopyrite	9	Pb (%)	0.47
Covellite	11	Si (%)	5.96
Pyrite	38	Sn (%)	0.01
Pyrrhotite	4	S XRF (%)	30.20
Magnetite	5	Zn (%)	4.97
		U XRF (%)	0.03
		Cl (%)	0.01

6.2.2 Effect of Glycine

Experiments to study the effect of glycine on copper and gold leaching from Cu-Au ore A were conducted by varying the initial Gly:Cu molar ratios from 2:1, 4:1, and 8:1 and bottle rolled at 100 rpm. The Cu-Au sample was ground to 100 % passing 75 µm and 100 g was added to 500 ml of leaching solution making 20 % w/v solids. Figure 6.1 shows that copper leaching increases with increasing Gly:Cu ratio. After 168 hours of leaching, 50.4, 46.7 and 37.4 % Cu was leached at Gly:Cu ratios of 8:1, 4:1 and 2:1, respectively. The observed linear relationship between copper extraction and time indicates that there is no passivation on the ore surface.

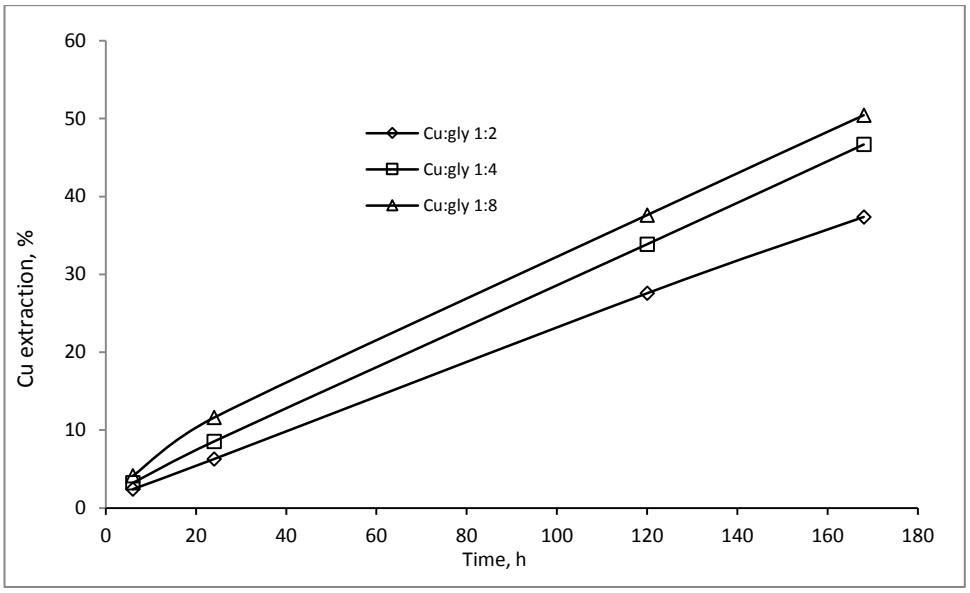

Figure 6.1 Effect of glycine concentration on Cu leaching from ore A: pH 11, 0 % H_2O_2, P_{100} 75 µm, 25°C, and 20 %w/v solids.

Gold leaching from the ore was not monitored during sub-sampling since, according to Oraby and Jacques (2014a, 2014b), copper should be selectively leached over gold under the given conditions (room temperature). Literature on dissolution of gold in alkaline ammonia (Meng & Han, 1996) also states that gold dissolution only becomes significant above 60 °C . At the end of the leaching experiment, 168 hours, gold concentration in the leach solution was determined to establish if gold leaching occurred. On discovering the presence of gold in solution, the percentage of gold leached was determined by comparing gold concentration in solution to the re-calculated head grade. Figure 6.2 indicates that gold leaching decreases as the Gly:Cu ratio increases. After 168 hours of leaching, 40.5, 42.3 and 50.3 % of Au was leached at Gly:Cu ratios of 8:1, 4:1 and 2:1, respectively. The reason for the observed gold leaching in the glycine solution at room temperature is yet to be understood but can be linked to galvanic interactions between gold and the sulfide minerals present in the ore. Such interactions have been noted to significantly improve gold leaching rates in different leaching solutions (Aghamirian & Yen, 2005; Jeffrey et al., 2006; Lorenzen et al., 1994). The influence of galvanic interactions on gold leaching in alkaline glycine solutions will be investigated in a subsequent section in this chapter.

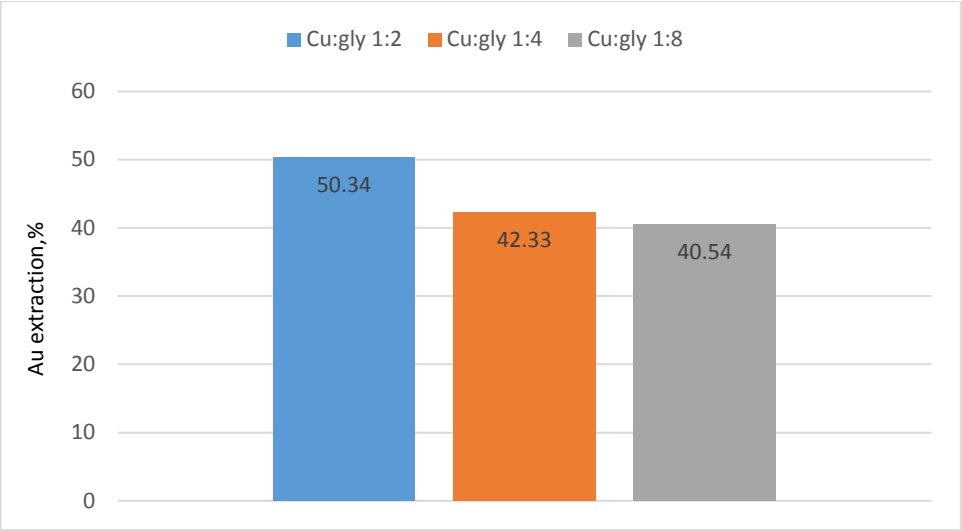

Figure 6.2 Effect of glycine concentration on Au leaching from Cu-Au ore A: pH 11, 25 °C, 0 % H_2O_2, 168 h, P_{100} 75 µm and 20 %w/v solids.

6.2.3 Effect of Initial Solution pH

Figure 6.3 shows the effects of initial leach solution pH on the copper extraction from Cu-Au ore A. It can be noted that there was no difference between the amount of copper leached at pH 11 and 12. However, at pH 10 the percentage of copper leached was reduced as a maximum of 31.4 % was obtained after 168 hours compared to 46.5 % at pH 11 and 12. In the case of gold, Figure 6.4 shows that an increase in the initial solution pH led to a slight decrease in gold leaching. The experiment with an initial pH of 10 resulted in 51.4 % gold leaching while leaching at pH 11 and 12 resulted in 42.3 % and 39.6 % gold extraction ,respectively. This observation is an indication that the Au-glycinate complex has a higher stability at low pH. Determination of the stability region (pH-Eh) of Au-Gly is beyond the scope of this project.

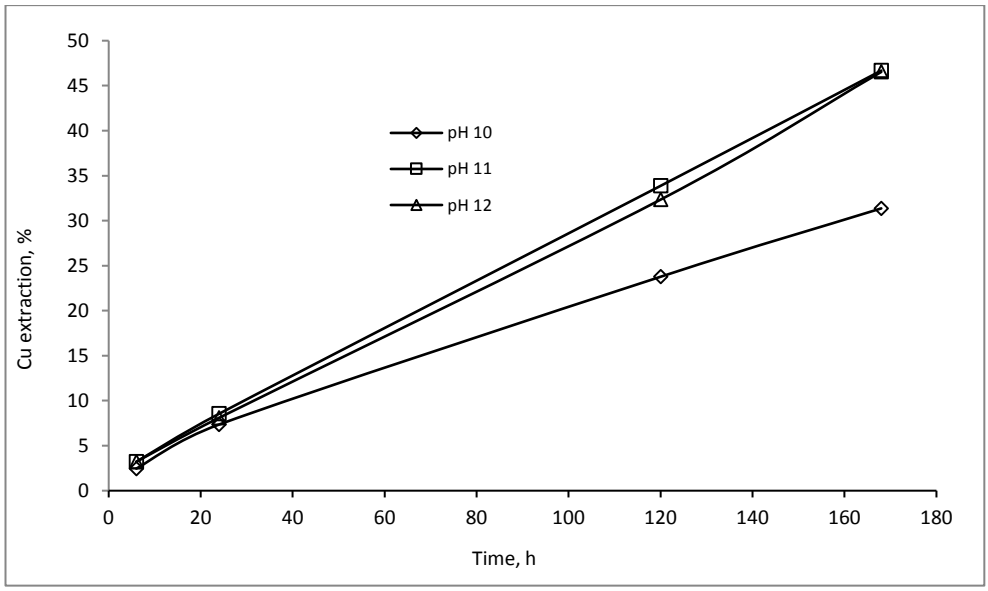

Figure 6.3 Effect of initial solution pH on Cu leaching from Cu-Au ore A: Gly:Cu 4:1, 0 % H_2O_2, P_{100} 75 µm and 20 %w/v solids.

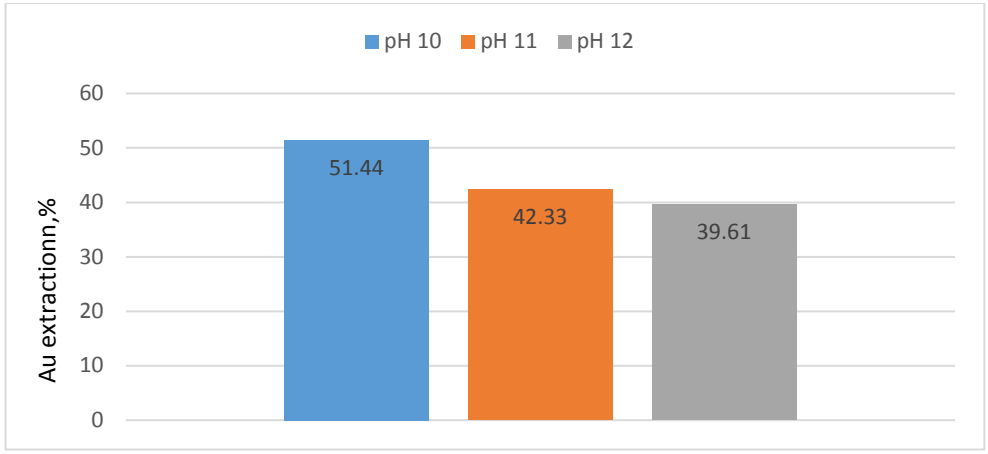

Figure 6.4 Effect of initial solution pH on Au leaching from Cu-Au ore A: Gly:Cu 4:1, 25 °C, 0 % H_2O_2, P_{100} 75 µm, 20 %w/v solids, 168 hours.

6.2.4 Effect of Hydrogen Peroxide

The effect of hydrogen peroxide on copper and gold leaching from Cu-Au ore A was studied at zero and 1 % peroxide in the leaching solution. Figures 6.5 and 6.6 show that the presence of peroxide has a slight positive effect on copper leaching but has a negative effect on gold leaching over the same period. In the absence of peroxide, 42.3 % Au was leached while just 4.7 % Au was obtained at 1 % peroxide. The reason for this is rather unclear as earlier investigations by Eksteen and Oraby (2015a) reported that peroxide enhanced gold in glycine from a pure gold foil. With the rate of peroxide decomposition being affected by its

concentration, temperature as well as impurities (Dougherty & Anslyn, 2005), the use of peroxide on a “dirty” ore such as Cu-Au ore A could lead to the oxidation of impurity metals and would be excluded in the next investigations.

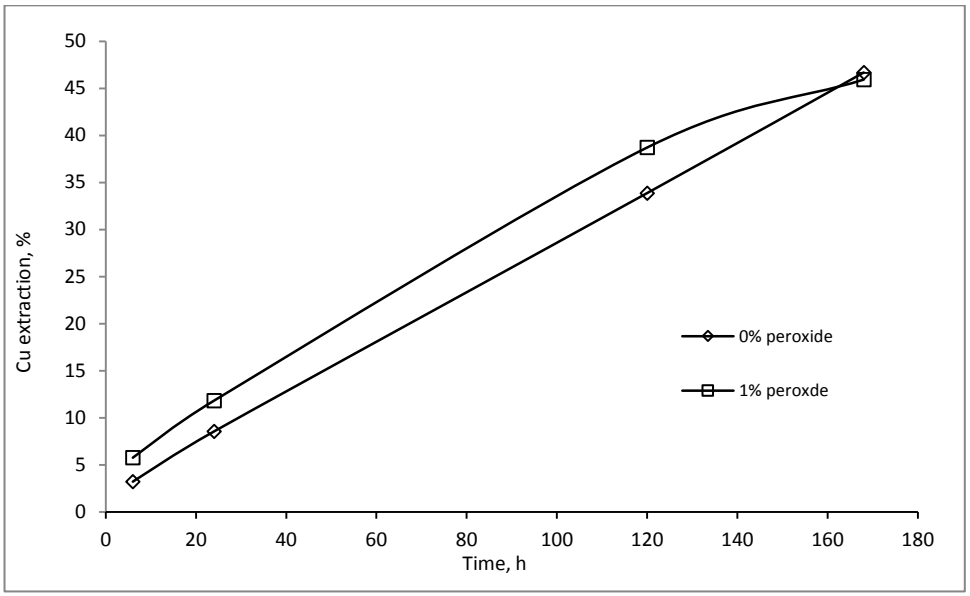

Figure 6.5 Effect of peroxide on Cu leaching from Cu-Au ore A: Gly:Cu 4:1, pH 11, 25 °C, P_{100} 75 µm and 20 %w/v solids.

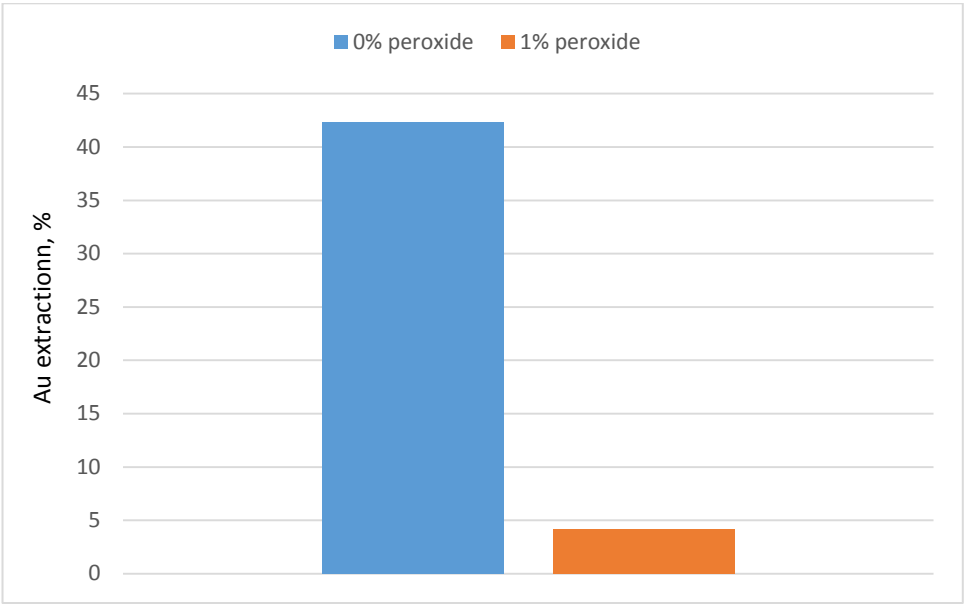

Figure 6.6 Effect of peroxide on Au leaching from ore A: pH 11, Cu:Gly 1:4, P_{100} 75 µm, 25 °C, 20 %w/v solids, 168 hours.

6.3 Copper - Gold Ore B

6.3.1 Mineralogy and Elemental Composition

Copper- gold ore B was analysed for its mineralogical and elemental composition by Q-XRD and XRF spectroscopy, respectively. Gold content in the ore was determined by fire assay. The copper phase in the ore could not be determined by XRD as it was assumed to be less than 1 % (Macchiarola et al., 2007). The ore sample was then further analysed by Tescan Integrated Mineral Analysis (TIMA) at the John de Leader Centre of Curtin University to identify and quantify mineral phases. Both the mineralogical and elemental composition of copper-gold ore B are shown in Table 6.2. The copper phase was determined to be <1 % cuprite. Elemental analysis showed that the ore contains 13.2 ppm gold and 0.04 % copper. The occurrence of copper in this ore is at a nuisance level to the cyanidation of gold, meaning that the presence of copper adds additional treatment costs without bringing any additional revenue (Sceresini, 2005).

Table 6.2 Mineralogical and elemental composition of Cu-Au ore B

Phase	%	Element	value	Element	value
Cuprite	<1	Au (ppm)	13.2	S XRF (%)	0.09
Quartz	86	Ag (ppm)	123	K XRF (%)	0.52
Mica	7	Al (%)	2	Na (%)	0.04
Rutile	<1	Fe (%)	0.54	Mn (%)	0.01
Kaolin	6	Pb (%)	0.07	Ti (%)	0.42
		Ca (%)	0.02	Zn (%)	0.03
		Mg (%)	0.06	P XRF (%)	0.02
		S XRF (%)	0.09	Cu (%)	0.04
		Ba (%)	0.01	S LECO	0.10

6.3.2 Effect of Glycine

Increasing the glycine concentration from 0.1 to 1.0 M has no effect on copper extraction from this ore as shown in Figure 6.7. This may be due to the high stiochimetry of glycine with respect to the low copper content (0.04 %). The Cu leaching curve shows that, at all glycine concentrations, about 75 % copper is leached after 3 hours with no further changes noted. This rapid dissolution of copper in the first hour of leaching confirms the presence of an oxide

ore which has been reported to quickly dissolve in alkaline glycine solutions (Tanda et al., 2017). Under these conditions, gold is barely leached as the highest extraction is 0.36 % (Figure 6.8). The reason for the insignificant gold dissolution from Cu-Au B as compared to that from Cu-Au A is the absence of galvanic interactions since Cu-Au B does not contain any sulfide minerals that can initiate such interactions. From the above observation, such an ore (Au-Cu oxide) could be processed in two stages. In the first stage, ambient conditions are maintained to selectively leach copper over gold. In the second stage conditions could be changed to optimise gold leaching. If selective recovery of copper or gold from the PLS containing both Cu and Au is possible, finely ground pyrite (for galvanic interactions) can be added to the ore before leaching. A single stage leaching would then be implemented.

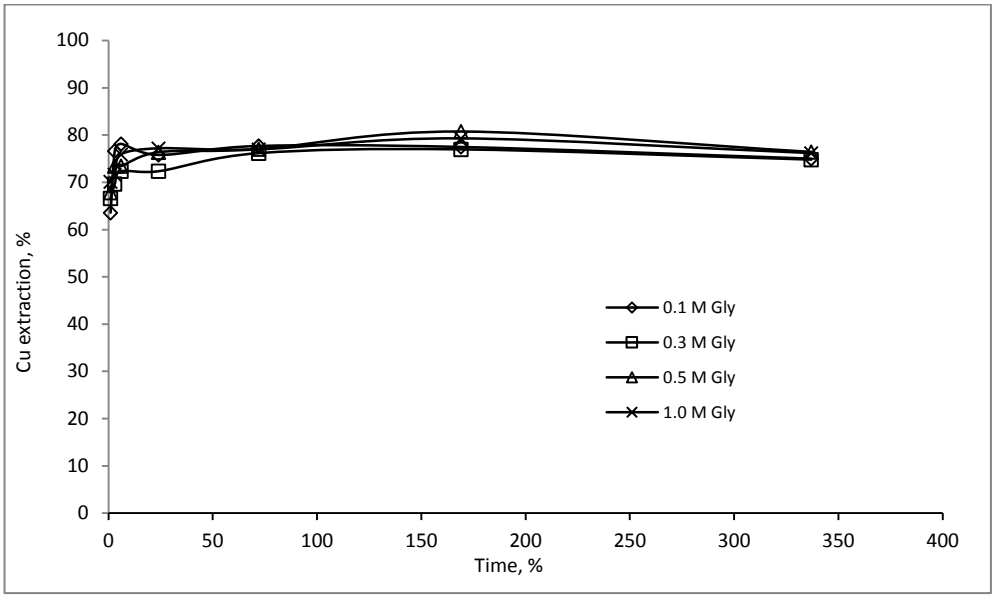

Figure 6.7 Effect of glycine on Cu leaching from Cu-Au ore B: pH 11.5, 25 °C, P_{100} 75 µm and 20 %w/v solids.

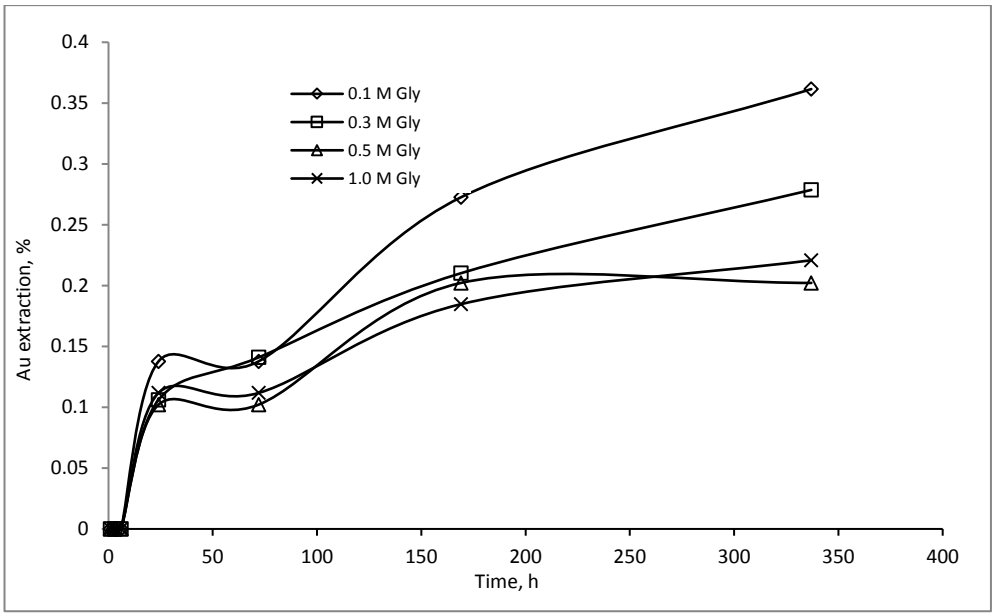

Figure 6.8 Effect of glycine on Au leaching from Cu-Au ore B: pH 11.5, 25 °C, P_{100} 75 µm and 50 %w/v solids.

6.3.3 Effect of Initial Solution pH

The effect of initial solution pH on the leaching of copper and gold from Cu-Au ore B was investigated by varying the pH from 8 to 11. Figure 6.9 shows that the initial solution pH has no effect on copper leaching from the ore as the percentage Cu extraction of 72-76 % for all pHs was obtained during the entire leaching time. In the case of gold, Figure 6.10 shows that gold leaching is insignificant at all pHs as less than 0.3 % Au was dissolved.

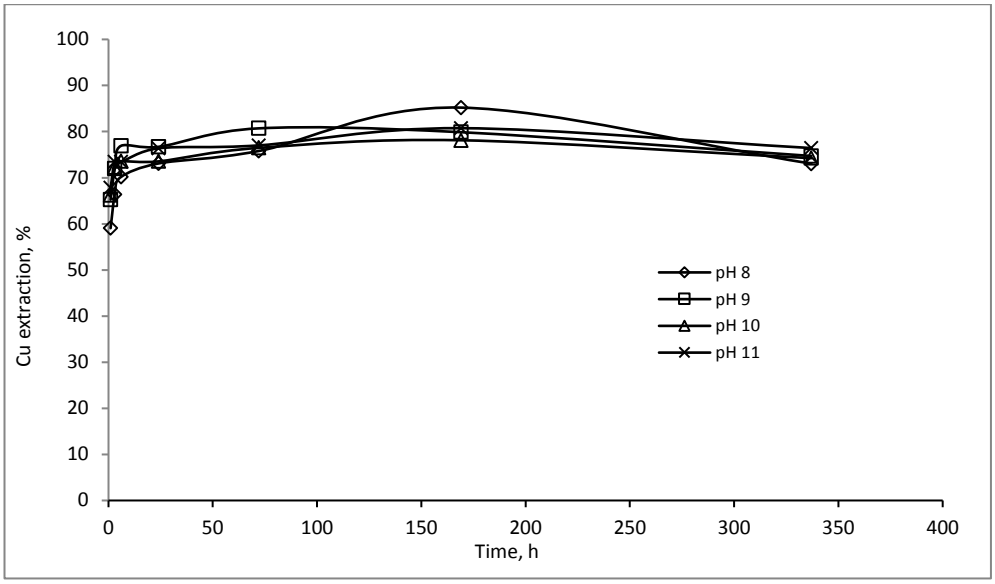

Figure 6.9 Effect of initial pH on Cu leaching from Cu-Au ore C: [Gly] 0.5 M, 25 °C, P_{100} 75 µm and 20 %w/v solids.

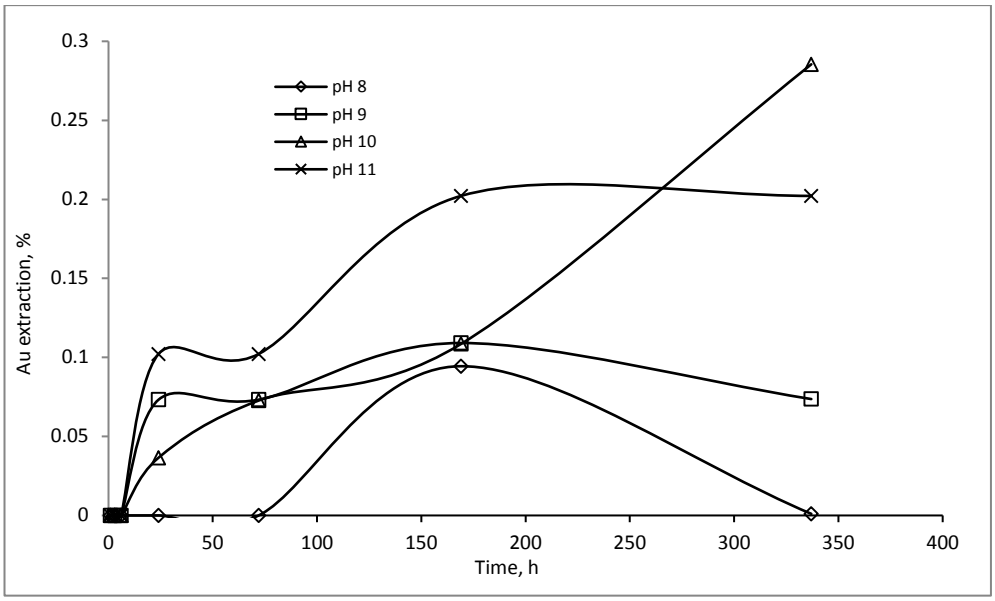

Figure 6.10 Effect of initial pH on Au leaching from Cu-Au ore B: [Gly] 0.5 M, P_{100} 75 µm and 20 %w/v solids.

6.3.4 Effect of Temperature

The effect of temperature on copper and gold dissolution from Cu-Au ore B was studied using a glass reactor and at the following leach conditions: 25 or 60 °C with solutions containing 0.5 M glycine, pH 11.5, stirring speed 250 rpm, and oxygen flow rate of 0.2 L/min. Figure 6.11 shows that initial copper extraction at 60 °C was higher than that at 25 °C but the extraction after 75 hours was 80 % for both systems. Au dissolution from the ore as shown in Figure 6.12 is strongly dependent on temperature with a 32.2 % extraction at 60 °C compared to only 0.45 % at 25 °C. It should also be noted that, at the higher temperature, the rate of Au dissolution starts to increase sharply after 24 hours. This confirms the results obtained by Oraby and Eksteen, (2014) stating that, even at elevated temperature, gold leaching in alkaline glycine solution only starts after 24 hours.

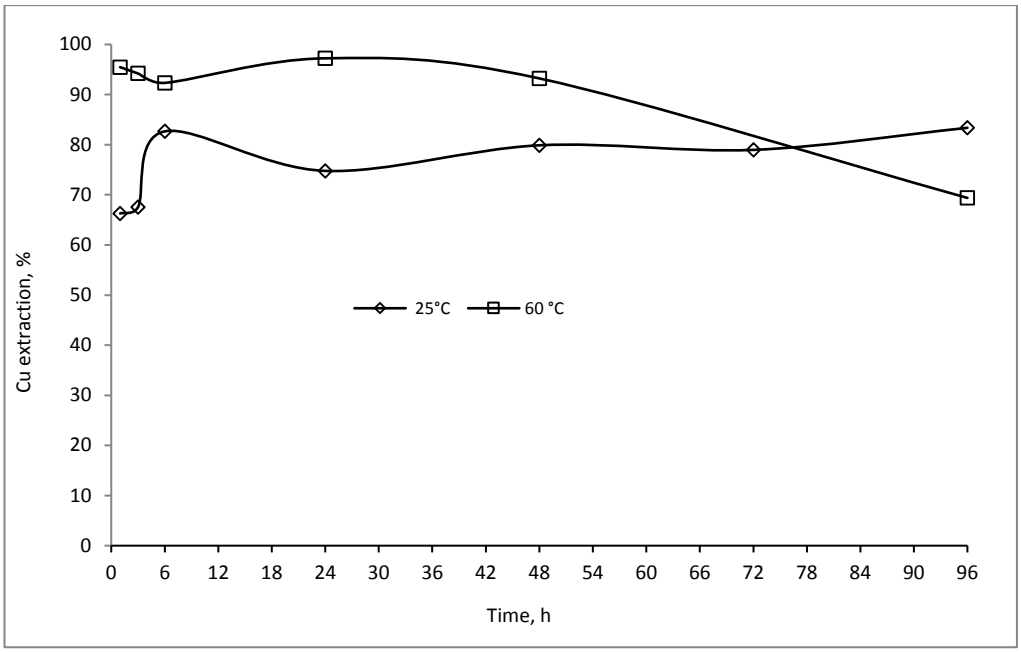

Figure 6.11 Effect of temperature on Cu leaching from Cu-Au ore B: [Gly] 0.5 M, pH 11.5, O_2 0.2 L/min, P_{100} 75 µm and 20 %w/v solids.

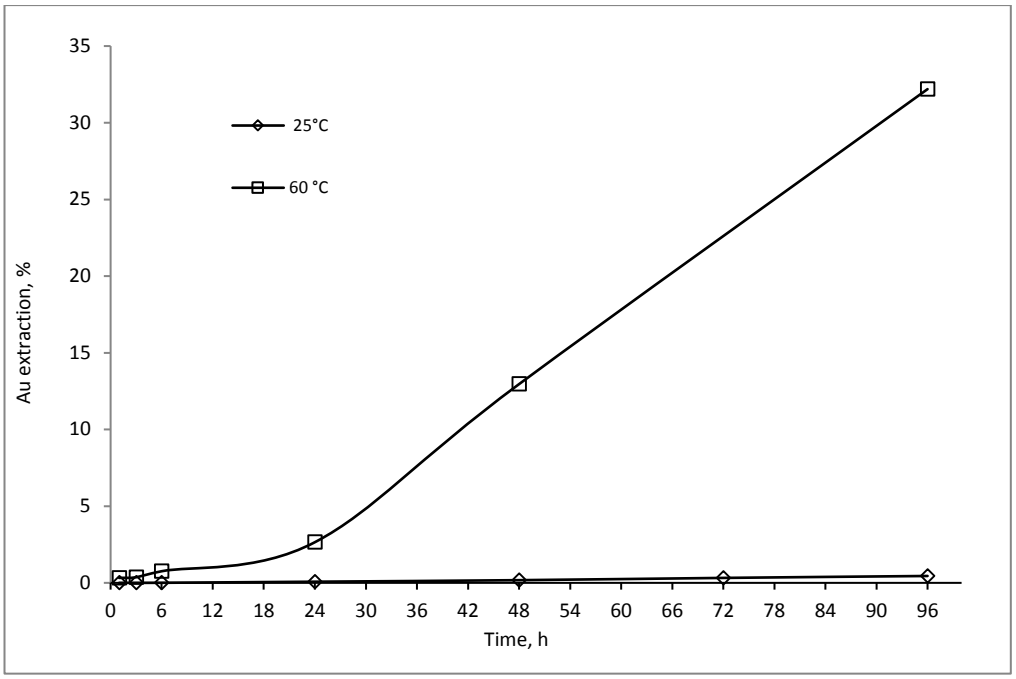

Figure 6.12 Effect of temperature on Au leaching from Cu-Au ore B: [Gly] 0.5 M, pH 11.5, O_2 0.2L/min, P_{100} 75 µm and 20 %w/v solids.

6.3.5 Effect of Oxygen

Figure 6.13 shows that the higher oxygen flow rate of 0.2 L/min had a slight positive effect on copper dissolution from Cu-Au ore B in the first 48 hours of leaching. After this point, both

oxygen flow rates had a Cu extraction of 77. 7 %. After 96 hours, the copper extraction from 0.05 L/min measures 80.3 % which is slightly higher than the 74.5 % from 0.3 L/min oxygen flowrate experiment. This difference can be attributed to glycine oxidation under the given conditions. This observation agrees with results in Chapter 4 indicating that copper oxide minerals easily dissolve in alkaline glycine solutions without addition of air or oxygen. However, Au dissolution, as can be noted in Figure 6.14 increases with increase in oxygen flow rate since gold in its natural state must be oxidised to gold ions in order to complex with glycine.

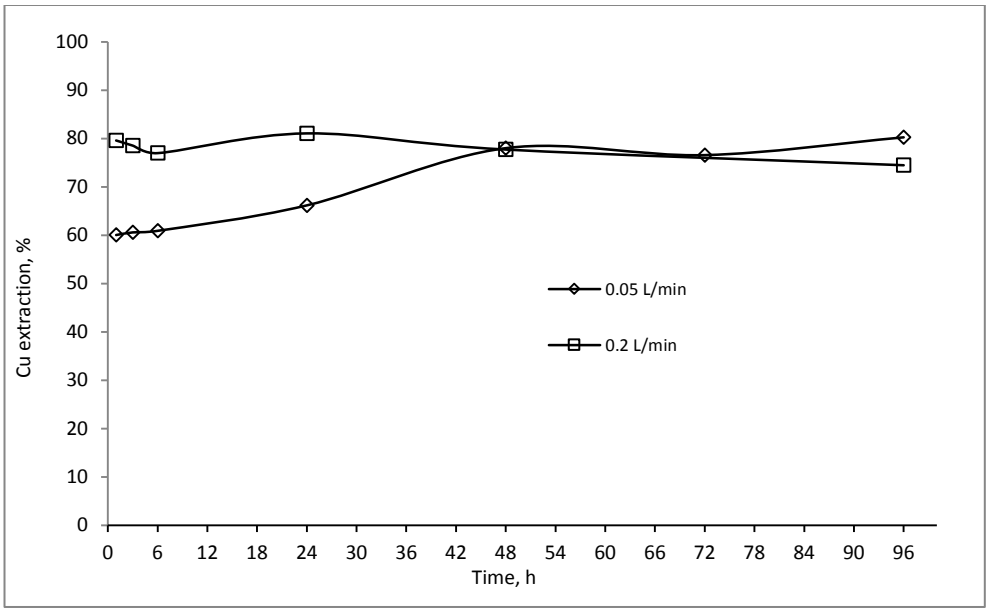

Figure 6.13 Effect of oxygen on Cu leaching from Cu-Au ore B: [Gly] 0.5 M, pH 11.5, 60 °C, P_{100} 75 µm and 20 %w/v solids.

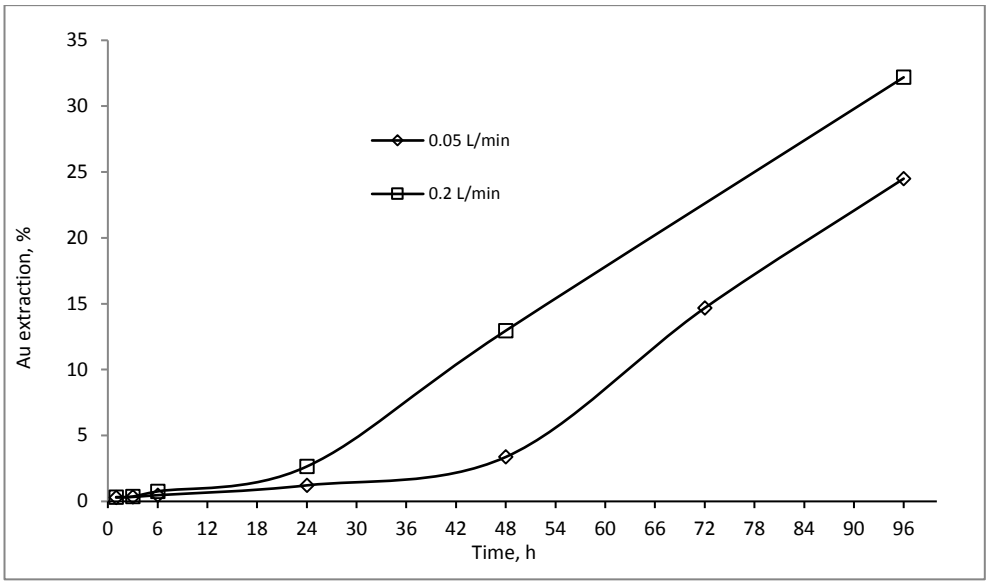

Figure 6.14 Effect of oxygen on Au leaching from Cu-Au ore B: [Gly] 0.5 M, pH 11.5, 60 °C, P_{100} 75 µm and 20 %w/v solids.

6.3.6 Effect of Galvanic Interactions

Galvanic interactions, which are caused by the difference between rest potentials of minerals that are in contact during electrochemical leaching, have been reported to improve the dissolution of metals from their ores (Li et al., 2013b). Sarveswara Rao et al. (1992) reported that galvanic interaction by means of pyrite addition during ammonia leaching of multimetal sulfides enhanced chalcopyrite dissolution. The effect of galvanic interactions on the dissolution of copper and gold from Cu-Au ore C was studied by adding different amounts of pure pyrite. The effect of galvanic interactions on the dissolution of copper and gold from Cu-Au ore B was investigated by comparing experiments with no pyrite to 5 kg/t and 20 kg/t pyrite additions. Figure 6.15 shows that, within the initial 48 hours of leaching, pyrite addition led to a slight improvement in copper dissolution. After this point, Cu extraction for all experiments remained at around 80 %. The influence of galvanic interactions is more significant during gold leaching as shown in Figure 6.16. The addition of 20 kg of pyrite per tonne of ore improved both the rate of gold dissolution (43.23 % Au extracted in 24 hours) and the extent of gold extraction with the highest gold extraction of 60.4 %. Final Au extraction in the presence of 5 kg/t pyrite and with no pyrite were 42.95 and 23.4 %, respectively.

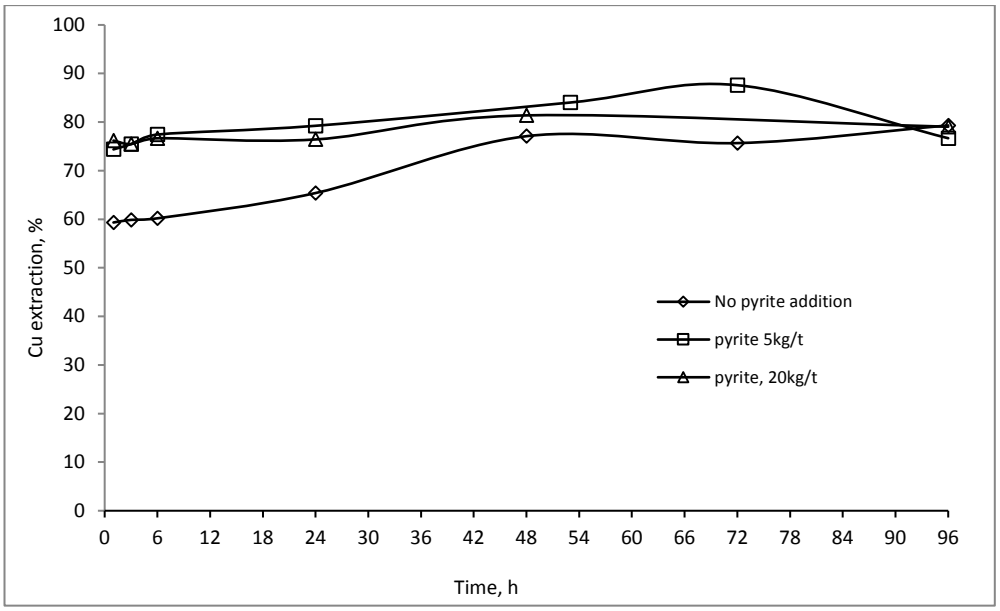

Figure 6.15 Effect of galvanic interactions on Cu leaching from Cu-Au ore B: [Gly] 0.5 M. pH 11.5, 60 °C, O_2 0.05 L/min, P_{100} 75 µm and 20 %w/v solids.

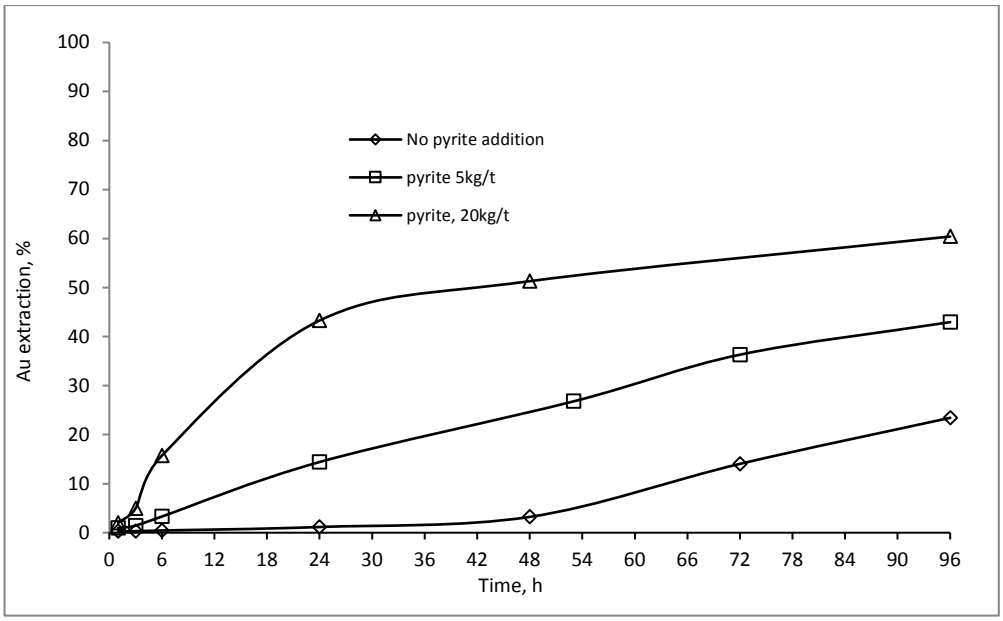

Figure 6.16 Effect of galvanic interactions on Au leaching from Cu-Au ore B: [Gly] 0.5 M. pH 11.5, 60 °C, O_2 0.05 L/min, P_{100} 75 µm and 20 %w/v solids.

6.4 Copper-Gold Ore C

6.4.1 Mineralogical and Elemental Composition

TIMA analysis of the Cu-Au ore C indicated the presence of chalcopyrite at 0.23 % as shown in Table 6.3. XRF analysis showed the copper concentration in the ore to be 0.136 %. The gold

content determined by fire assay is 510 ppb. Cu- Au ore C is thus a typical example of a low grade copper-gold ore with huge deposits relatively abundant as mentioned in Chapter 2.

Table 6.3 Mineralogical and Major Elemental composition of Cu-Au ore C

Minerals	Mass [%]	Minerals	Mass [%]
Actinolite	2.45	Ilmenite	0.05
Albite	0.01	Kaersutite	0.71
Ankerite+clay(Fe)	0.01	Magnesiogedrite	0.77
Anorthite	0.32	Muscovite	0.68
Apatite	0.22	Orthoclase	4.63
Biotite	4.64	Plagioclase	50.03
Calcite	0.02	Pyrite	0.21
Chalcopyrite	0.23	Pyrrhotite	0.27
Ferro-Actinolite	0.05	Quartz	32.12
Ferrosaponite	0.08	Rutile	0.02
Garnet - Pyrope	0.86	Scheelite	0.01
Hematite/Magnetite	0.14	Zircon	0.03
Titanite	0.71	The rest	0.04
Tschermakite	0.68	Total	100
Hornblende	0.01		

Element	Mass %
Au (ppb)	510
Cu (%)	0.15
As (%)	0.01
Fe (%)	3.64
Mg (%)	1.74
Al (%)	7.99
Si (%)	30.3
Ca (%)	3.22
S (%)	0.37
K (%)	1.39

6.4.2 Effect of Glycine

The effect of glycine on the leaching of copper and gold was investigated by varying the glycine concentration from 0.1 to 1.0 M. Figure 6.17 shows that copper leaching increases by increasing the glycine concentration. The highest copper extraction was 65.1 % after 528 hours at 1.0 M glycine. Glycine concentrations of 0.5 M, 0.3 M and 0.1 M resulted in 55.6 %, 46.0 % and 20.8 % copper extraction, respectively. Gold leaching, as shown in Figure 6.8, was also noted to be improved as the glycine concentration increased. A significant improvement in gold extraction occurs after 192 hours at 1.0 and 0.5 M glycine when the percentage of gold leached jumped from 13.5 to 40.5 %. After 361 hours of leaching, gold extraction was only 7.7 % at 0.1 M glycine and increased to 13.1 % at 0.5 M glycine at same leaching time. After 528 hours of leaching, gold extracted from 1.0 M Gly solution was 53.1 % while that from 0.1 M Gly solution was only 5.5 %.

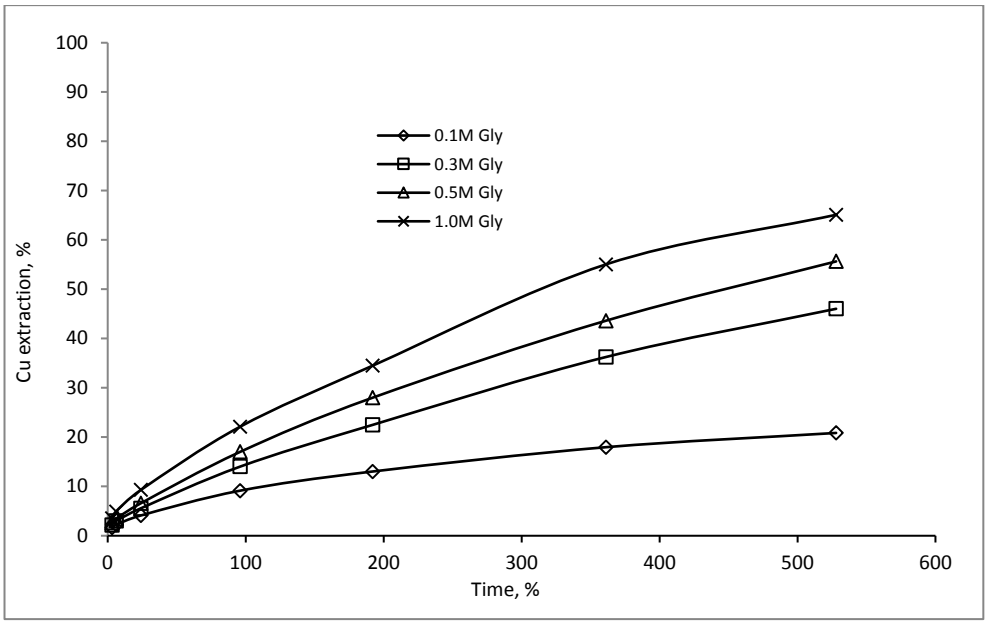

Figure 6.17 Effect of glycine on Cu leaching from Cu-Au ore C: pH 11.5, 25 °C, P_{100} 75 µm and 50 %w/v solids.

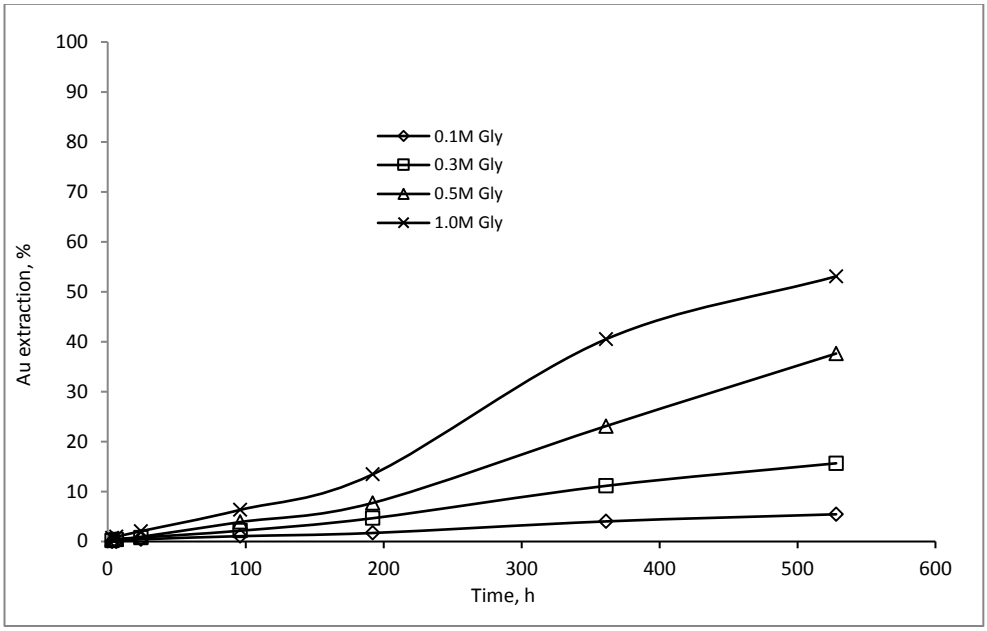

Figure 6.18 Effect of glycine concentration on Au leaching from Cu-Au ore C: pH 11.5, 25 °C, P_{100} 75 µm and 50 %w/v solids.

6.4.3 Effect of Initial Solution pH

Figure 6.19 shows that copper leaching from Cu-Au ore C is increased by the initial leaching solution pHbeing raised. After 528 hours of leaching, 55.6 % Cu was leached at pH 11 while

18.9 % was leached at pH 8. During the same time, 51.8 % and 41.8 % Cu was leached at pH 10 and 9, respectively. With regards to gold, Figure 6.20, shows that higher pH also favours its leaching. It was, however, noted that, after 192 hours, there was a significant jump in gold dissolution at pH 11 as opposed to very modest changes at the other pHs. After 528 hours of leaching, 37.6 % Au was leached at pH 11 while the closest was 7.8 % at pH 10. The response of gold to different initial solution pH in this ore is contrary to what was observed with Cu-Au ore A in which a lower pH of pH 10 led to higher gold leaching compared to pH 11 and 12. The mineralogy of individual ores could be the reason for the disparity in their response to process conditions.

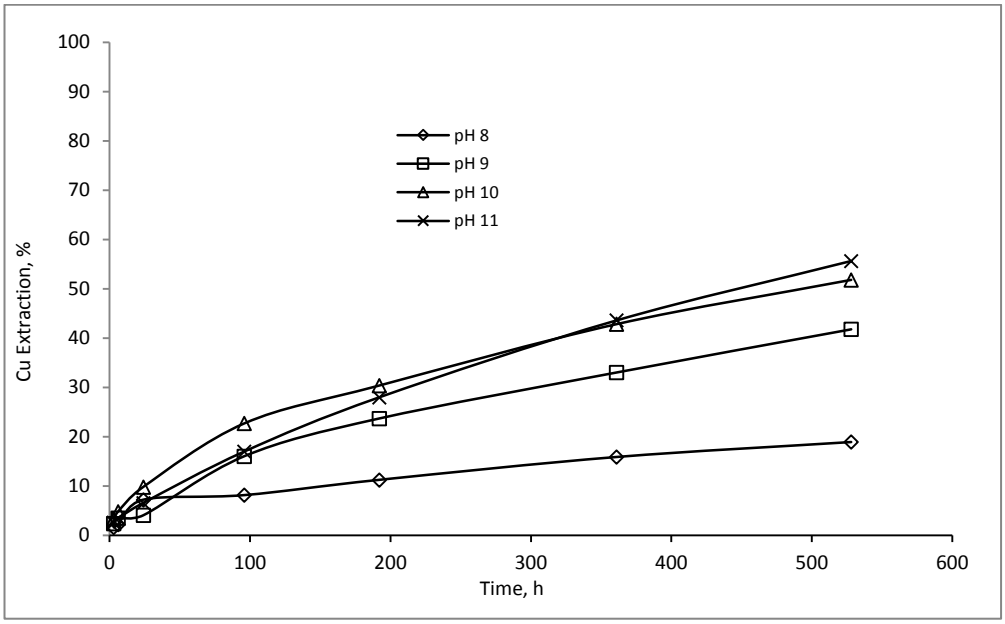

Figure 6.19 Effect of initial solution pH on Cu leaching from Cu-Au ore C: [Gly] 0.5 M, 25 °C, P_{100} 75 µm and 50 %w/v solids.

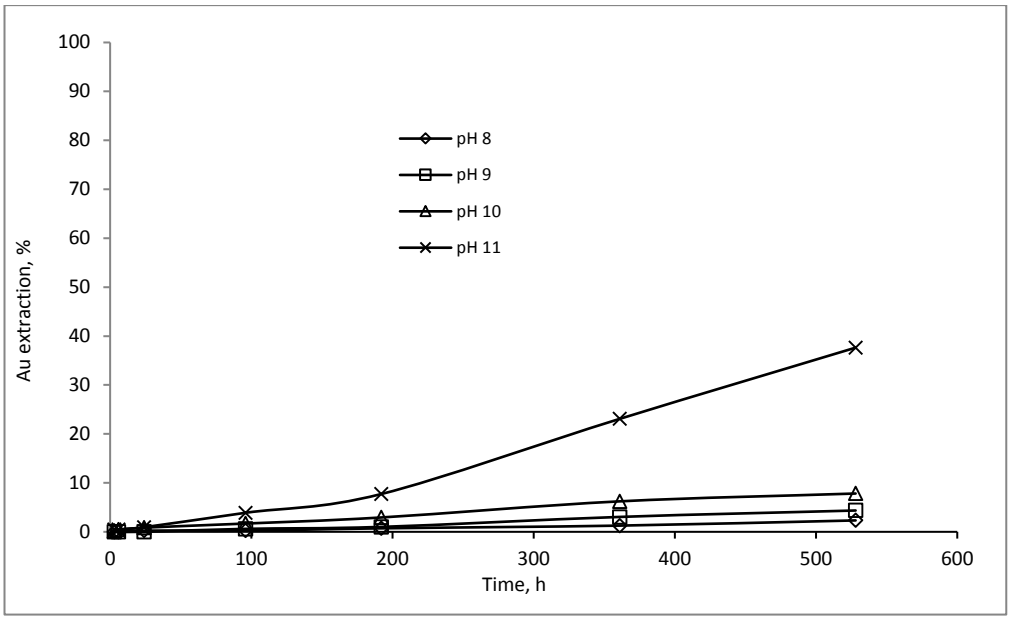

Figure 6.20 Effect of initial solution pH on Au leaching from Cu-Au ore C: [Gly] 0.5 M, 25 °C, P_{100} 75 µm and 50 %w/v solids.

6.4.4 Effect of Temperature

The effect of temperature on copper and gold dissolution from Cu-Au ore C was studied at 25 and 60 °C. The glycine concentration was kept at 0.5 M and oxygen flow rate was maintained at 0.3 L/min. Figure 6.21 shows that higher temperature favoured copper dissolution with a 65.96 % copper extraction at 60 °C while 40.67 % was dissolved at 25 °C. Gold dissolution was also noted (Figure 6.22) to be improved with the temperature increase: 15.39 % gold extraction was achieved at 60 °C and 8.52 % at 25 °C after 96 hours.

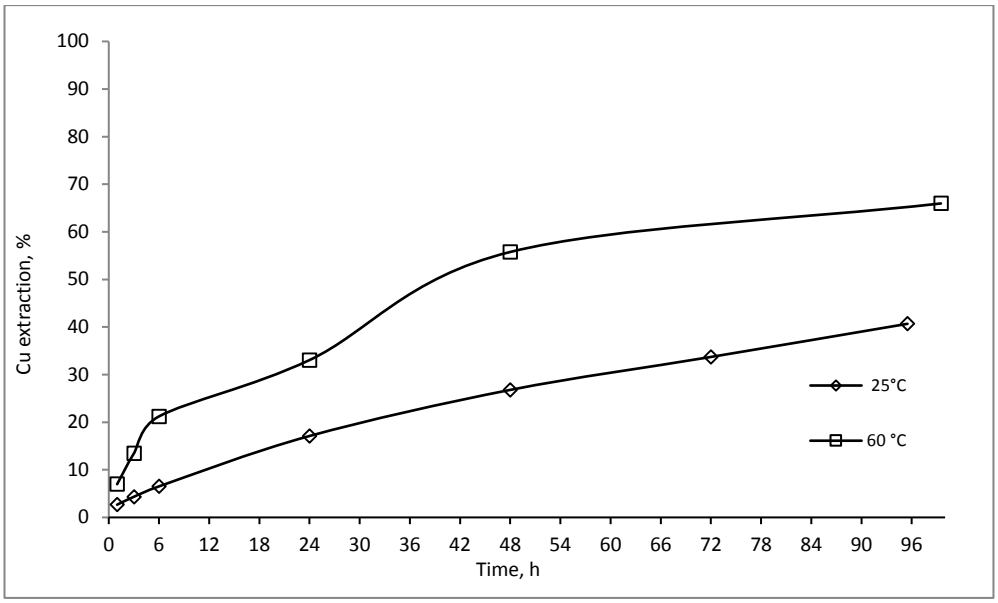

Figure 6.21 Effect of temperature on Cu leaching from Cu-Au ore C: [Gly] 0.5 M, pH 11.5, O_2 0.3 L/min, P_{100} 75 µm and 50 %w/v solids.

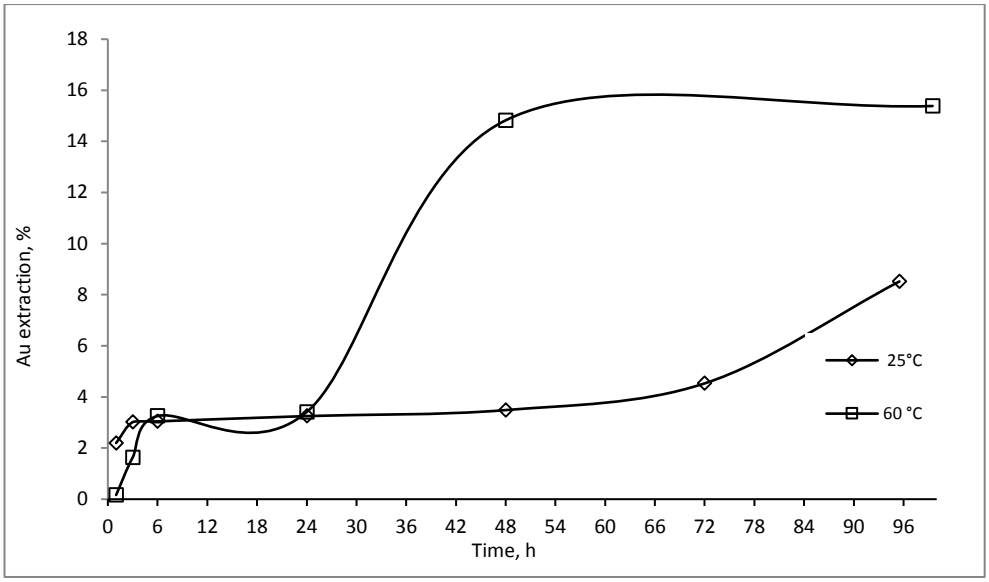

Figure 6.22 Effect of temperature on Au leaching from Cu-Au ore C: [Gly] 0.5 M, pH 11.5, O_2 0.3 L/min, P_{100} 75 µm and 50 %w/v solids.

6.4.5 Effect of Oxygen

The effect of oxygen on copper and gold dissolution from Cu- Au ore C was examined at 0.05 and 0.3 L/min. Figure 6.23 shows that a higher oxygen flow rate led to a higher copper extraction. By comparison, Figure 6.24 rather shows that the higher oxygen flow of 0.3 L/min resulted in a lower gold dissolution of 15.38 % as opposed to 24.91% obtained with a 0.05 L/min after 96 hours of leaching.

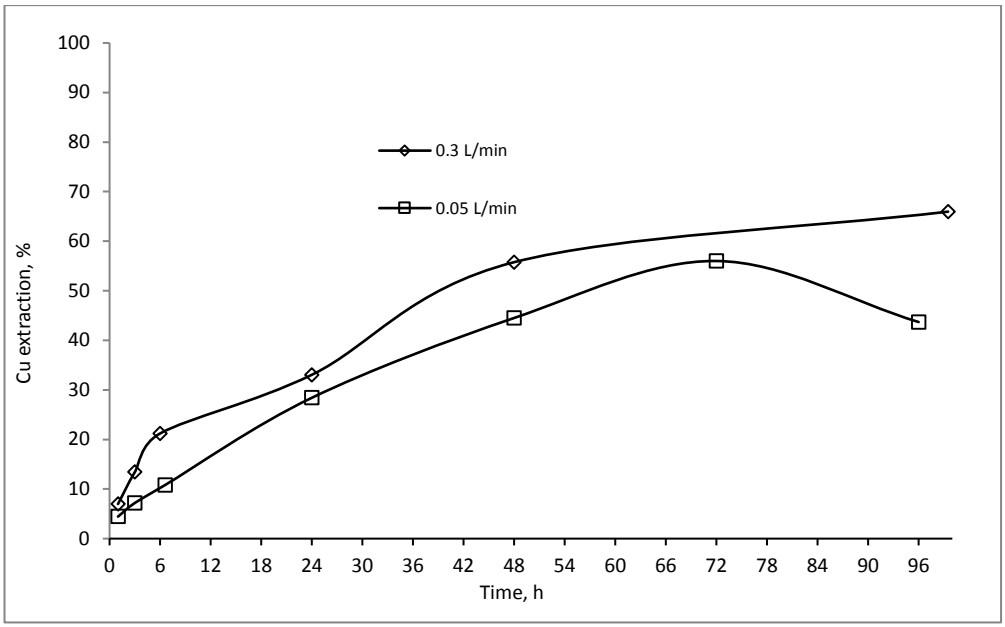

Figure 6.23 Effect of oxygen on Cu leaching from Cu-Au ore C: [Gly] 0.5 M. pH 11.5,60 °C, P_{100} 75 µm and 50 %w/v solids.

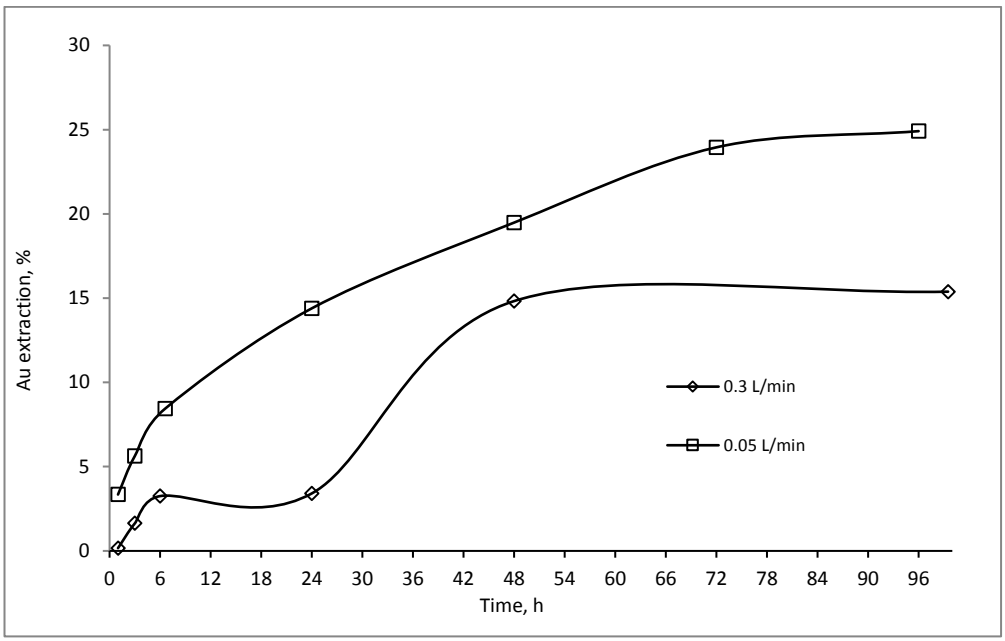

Figure 6.24 Effect of oxygen on Au leaching from Cu-Au ore C: [Gly] 0.5 M. pH 11.5, 60 °C

6.4.6 Effect of Galvanic Interaction

The results in Figure 6.25 indicate that galvanic interactions, which might be occurring between chalcopyrite and pyrite, resulted in about a 10 % improvement in copper dissolution. Figure 6.26 shows that the effect of galvanic interactions on gold dissolution is rather unclear as experiment with no pyrite addition had the highest gold dissolution of 44.93

%. Gold extraction in the presence of 8 kg/t and 4 kg/t pyrite was 29.70 and 21.35 %, respectively. The trendless results could be a consequence of the varying concentrations of pyrite in the sample as the ore initially contained about 0.2 % pyrite.

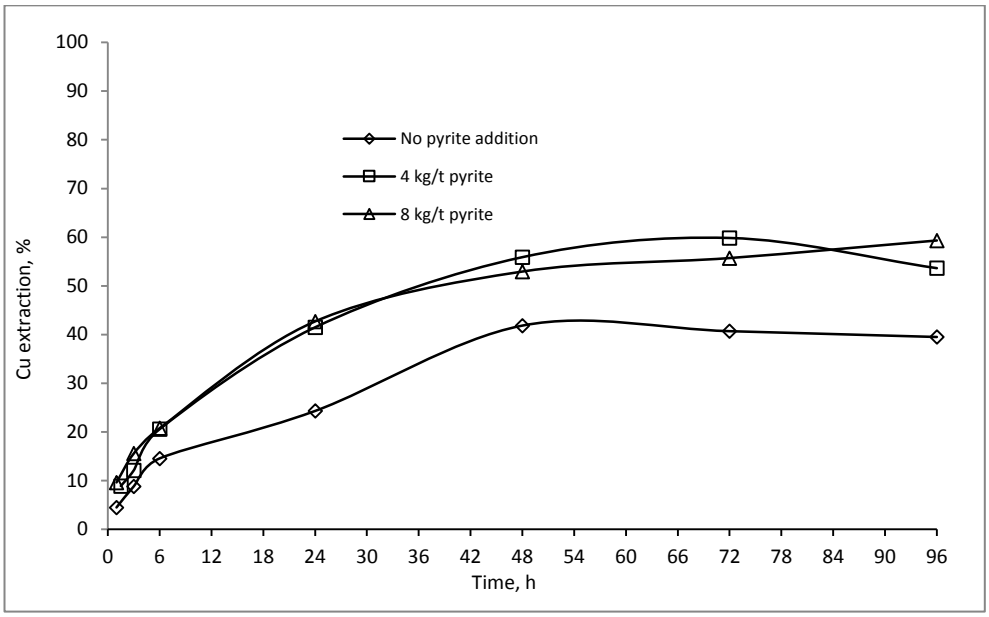

Figure 6.25 Effect of galvanic interactions on Cu leaching from Cu-Au ore B: [Gly] 0.5 M, pH 11.5, 60 °C, O_2 0.05 L/min, P_{100} 75 µm and 50 %w/v solids.

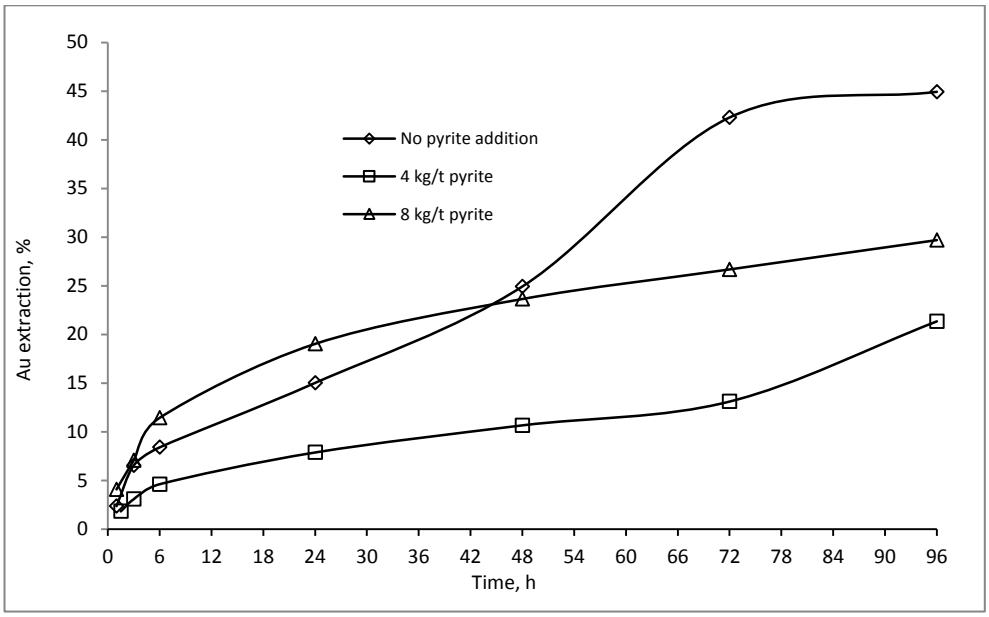

Figure 6.26 Effect of galvanic interactions on Au leaching from Cu-Au C: [Gly] 0.5 M, pH 11.5, 60 °C, O_2 0.05 L/min, P_{100} 75 µm and 50 %w/v solids.

6.5 Heap Leach Simulation

The heap leaching technique (discussed in Section 2.6) is the most economical method for processing low grade ores due to their high gangue content. The essence of the heap simulation experiments in this research was not to determine optimum conditions for heap application but to investigate the possibility of extracting copper and gold by heap leaching using alkaline glycine solutions from such low grade copper-gold ores. The leaching process was monitored by measuring the concentration of copper and gold in the PLS collected at the base of the columns.

6.5.1 Copper-Gold ore C

The mineralogical composition of the Cu-Au C ore used for the column test was given in Section 6.3.1. The ore is a low grade chalcopyrite containing gold. A particle size range of 1-8 mm was selected in order to avoid any clogging that reduces percolation which is critical in heap leach operations (Lwambiyi et al., 2009). The size distribution of the ore is given in Table 6.4. Elemental analysis of the ore used is shown in Table 6.5.

Table 6.4 Particle size distribution for column leaching of Cu-Au ore C

Size range, mm	mass, g	Percentage	Cumm. %
+1-1.40	79.5	13.73	13.73
+1.4-2.0	73.51	12.70	26.43
+2.0-2.8	83.36	14.40	40.83
+2.8-3.35	53.91	9.31	50.14
+3.35-40	62.21	10.75	60.88
+4-5.6.7	130.68	22.57	83.46
+5.6-6.7	62.2	10.74	94.20
+6.7-8.0	33.58	5.80	100.00

Table 6.5 Elemental composition of Cu-Au ore C used for heap simulation

Element	Value	Element	Value
Au (ppb)	782	Rb (%)	0.015
Al (%)	8.2	Si (%)	30.08
Ba (%)	0.022	S XRF (%)	0.23
Ca (%)	3.47	Sr (%)	0.02
Co (%)	0.002	Ti (%)	0.38
Cr (%)	0.02	V (%)	0.008
Cu (%)	0.095	Y (%)	0.008
Fe (%)	3.39	Zn (%)	0.008
GA_X (%)	0.002	Zr (%)	0.021
K XRF (%)	1.29	U XRF (%)	0.007
Mg (%)	1.73	Cl (%)	0.013
Mn (%)	0.05	W XRF (%)	0.007

6.5.1.1 Copper and Gold Dissolution

Two different glycine concentrations (0.1 M and 0.5 M) were used for leaching. A mass of 5 kg ore was loaded in each column and caustic was used to control the leach solution at pH 11. The solution was circulated from a 4.5 L container at a rate of 33 L/m^2/h. Copper and gold recoveries from the ore were determined based on solution assays and head grades. The corresponding copper recovery curves are plotted in Figure 6.27. As expected, copper dissolution was improved by higher glycine concentration with 6 % extracted after 36 days for 0.5 M and 3.5 % with 0.1 M glycine. Although copper dissolution is slow, the steady increase over time as shown by the curves indicate that the closed circuit leaching can be lengthened in order to get more extraction. Gold dissolution, as can be seen in Table 6.6, was rather slow with 1.61 % achieved after 159 days for 0.1 M glycine and 0.99 % gold after 103 days of leaching with 0.5 M glycine.

The slow Cu and Au dissolution could be attributed to insufficient contact between host minerals and lixiviant due to the relatively large particle size or poor permeability of ore (Zanbak, 2012)

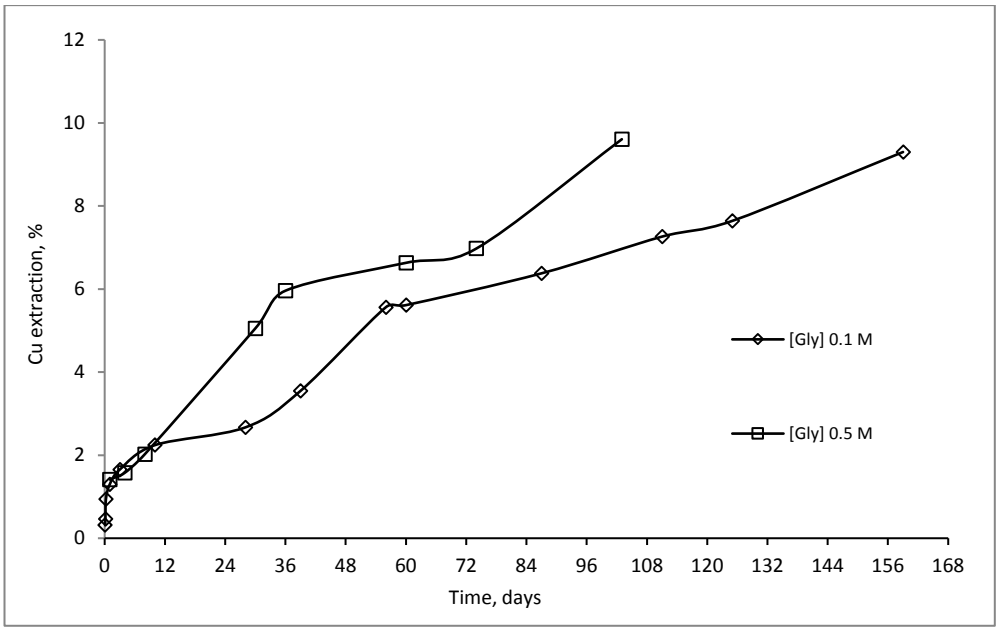

Figure 6.27 Column Cu leaching from Cu-Au ore C, pH 11, 25 °C, 33 L/m^2/h

Table 6.6 Column Au leaching from Cu-Au ore C, pH 11, 25 °C, 33 L/m^2/h

[Gly]	Time, days	Au extraction, %
0.1 M	87	0.54
	111	1.46
	159	1.61
0.5 M	36	0.31
	60	0.54
	103	0.99

6.5.2 Copper-Gold ore D

Copper-gold ore D was a flotation tail from a copper processing plant in Western Australia. The dry Cu-Au ore as received was partly and naturally agglomerated (during drying). It was screened at 2 mm screen size and found that about 57.56 % of the ore was below 2 mm while the remaining 42.4 % was made up of particles with diameters >2 mm.

6.5.2.1 Mineralogy

Mineralogical analysis of the ore by TIMA revealed that chalcopyrite is the only copper phase and makes up < 1 % by mass as shown in Table 6.7. The major gangue phases were pyrite and quartz at 43 % and 32 %, respectively. The gold content of the ore was 648 ppb as determined

by fire assay. XRF analysis showed that the ore contains 0.37 % copper. This is another typical example of a low grade copper-gold ore with heap leaching being the most economical technique for such ores. A column leaching experiment was thus conducted to simulate a heap leaching technique.

Table 6.7 Mineralogy and elemental composition of Cu-Au ore D

Phase	%
Chalcopyrite	<1
Pyrite	43
Spinel group	2
Quartz	32
Chlorite	10
Gypsum	10
Mica	2

Element	value	Element	value
Au (ppb)	648	K XRF (%)	0.11
Ag (ppm)	12	Na (%)	0.14
Al (%)	2.08	Mn (%)	0.16
Fe (%)	23.75	Ti (%)	0.09
Pb (%)	0.11	Zn (%)	1.13
Ca (%)	1.13	P XRF (%)	0.03
Mg (%)	1.46	Ba (%)	0.02
S XRF (%)	19.20	Cu (%)	0.37
Ni (%)	0.01	S LECO (%)	19.70

6.5.2.2 Copper and Gold Dissolution

The experiment was conducted according to the procedure outline in Chapter 3 and at ambient temperature. The leaching solution at pH 11 containing a glycine concentration of 0.5 M was circulated at a rate of 135 L/m^2/h. Air was injected at the bottom of the column at a rate of 0.1 L/min. The results as shown in Figure 6.28 indicate that copper dissolution increased steadily throughout the 48 days of leaching with 53.6 % Cu extracted. Gold dissolution was noted to be very slow with 7.6 % Au leached after 48 days (Table 6.8).

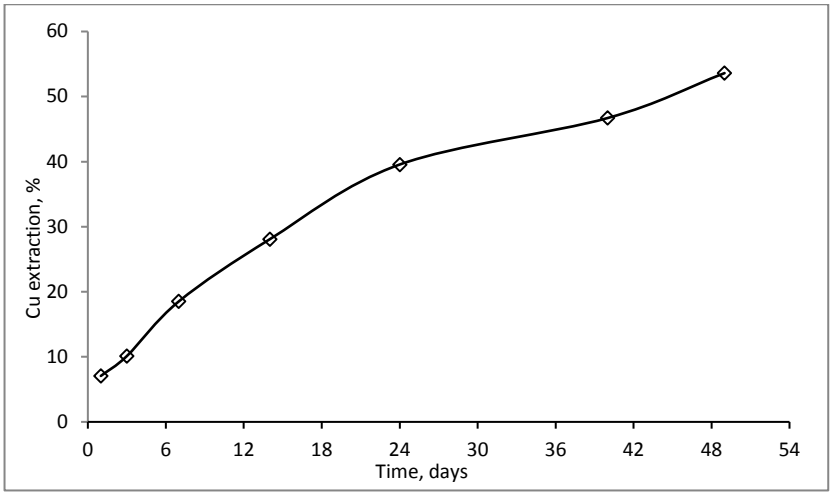

Figure 6.28 Column Cu leaching from Cu- Au ore D: pH 11, 25 °C, 135 L/m^2/h

Table 6.8 Column Au leaching from Cu-Au ore D: pH 11, 25 °C, 135 L/m^2/h

Time, days	[Au], mg/L	Au extraction, %
40	1.15	5.032
49	1.32	7.548

6.5.3 Improving heap leaching rates

Heap leaching, which is generally accepted as the most economical method for processing low grade ores has however, been hampered by low recoveries and long leaching times as much as 1-2 years, if not more (Ghorbani et al., 2013). As was noted with the heap leaching of Cu-Au B, copper recoveries were very low with only 9 % in over 156 days. The rock was observed to be quite competent (not friable and not porous), indicating that only the mineral grains on the surface were exposed to the lixiviant. It has been suggested that leaching rates are closely linked to the method by which the ore was crushed prior to leaching (Watling, 2006). Comminution by high pressure grinding rolls (HPGR) introduces cracks at grain boundaries (Unland & Szczelina, 2004) leading to mineral liberation and higher exposure of mineral grains to leach solutions (Ghorbani et al., 2013). The results of research conducted by (Daniel, 2007) on energy efficient mineral liberation using HPGR showed a higher gold leachability when the ore was crushed by HPGR compared to conventional crushing. Thus, for ores such as Cu-Au ore B with high competency, leaching rates could be significantly improved by crushing the ore with HPGR grinding before leaching.

In Sections 6.3.4 and 6.4.4, it was realised that elevated temperature of 60 °C significantly improved the extent of copper and gold extraction. In heap leaching, such temperatures could be achieved by the use of solar heating systems to heat leaching solutions and black piping for the transport of heated solutions to the top of the heap. Investigations on the potential for solar thermal energy in the heap bioleaching of chalcopyrite showed that copper extraction increased from 67 % to 85 % by heating the leach solution through the solar heating system. It was further reported that the net present values and internal rates of return of the project were positive (Murray et al., 2017).

Oxidation is an important part of chalcopyrite and gold leaching. It was noted in Sections 6.3.5 and 6.4.5 that higher oxygen flow rates significantly improve both copper and gold leaching as this increases the concentration of dissolve oxygen in the leach solution. In some

industrial applications, air is pumped into the heap from the bottom (Wu et al., 2009) and as illustrated by Figure 3.3. Tests conducted to explore ways of increasing heap leaching efficiency by the addition of oxygen to the leaching solution have shown major improvement in metal extraction rates (Kenney et al., 1987). Thus in the leaching of some sulfide minerals in which the need for high DO is critical, oxygen can be injected directly into the barren leach solutions.

6.6 Summary

Copper dissolution from the gold-copper oxide ore (Cu-Au ore B) was not influenced by glycine concentration, initial solution pH, temperature, oxygen flow rate and galvanic interactions as the overall percentage of copper dissolved under all conditions was around 75 %. However, gold dissolution from the gold-copper oxide ore (Cu-Au ore B) was influenced by temperature, oxygen and galvanic interactions. At 60 °C, gold dissolution reached 32.2 % mean while only 0.5 % Au was extracted at 25 °C. Galvanic interactions through the addition of finely ground natural pure pyrite resulted in a significant improvement in gold dissolution from the gold-copper oxide ore as 60.4 % was dissolved with the addition of 20 g/t pyrite. In the absence of these galvanic interactions (i.e., no pyrite addition), only 23.4 % gold was extracted.

The extent and rate of copper and gold dissolution from the gold-copper sulfide ores was more dependent on process variables than the oxide ore. Copper and gold dissolution from Cu-Au ore C increases as the glycine concentration increases. At 1.0 M glycine, copper and gold extraction were 65.1 % and 53.1 %, respectively, after 500 hours of leaching by a bottle roll technique. Higher temperature favoured copper dissolution with a 65.96 % obtained at 60 °C after 96 hours of leaching as opposed to 40.67 % at 25 °C. The oxygen flow rate of 0.3 L/min positively affected copper dissolution but unexpectedly affected gold dissolution negatively.

The major difference between the behaviour of gold-copper oxide ore and gold-copper sulfide ore is the simultaneous dissolution of gold and copper from the copper-gold sulfide ores at room temperature. The significant improvement in gold dissolution from the gold-copper oxide ore emanates from the addition of pyrite. Thus, gold dissolution from the copper-gold sulfide ores at room temperature could be attributed to the presence of galvanic interactions between the gold and the inherent pyrite in the ore.

Chapter 7 Recovery of Metals from Alkaline Glycine Pregnant Leach Solutions

7.1 Chapter Overview and Background

In order to consider the feasibility of any new leaching system, it is imperative to study both the leachability of valuable metals from their different resources and the recovery of these metals from the leach solutions (Awakura et al., 1991). Alkaline glycine solutions have been shown to be an effective lixiviant system for copper and precious metals from various mineralised sources including oxides, native and sulfide mineral forms (Oraby and Eksteen, 2014a and 2014b; Eksteen et al., 2016). The leaching behaviour of copper oxides in aqueous alkaline glycine solutions studied by Tanda et al. (2017) confirmed the selective dissolution of copper over impurity elements, in particular of iron, magnesium, aluminium and silicon. It has also been confirmed in Section 5.2 that, during the leaching of copper minerals with alkaline glycine/glycinate solutions, only cupric ions form the stable complex with glycine [$Cu(H_2NCH_2COO)_2$]. With leachability of copper having been studied and reported in the previous chapters, the next main objective of this work will be to investigate methods for recovering copper from the alkaline glycine PLS. Two methods, the versatile solvent extraction and metal sulfide precipitation will be investigated.

Solvent extraction (SX), since its introduction in the mineral industry in the 1940s, has become a major unit processing step in hydrometallurgy due to its versatility in the extraction, separation/purification and recovery of metals from aqueous solution (Cox, 2004; Junior et al., 2012). The continuous popularity of SX in hydrometallurgy the development of new extractants with improved selectivity, faster kinetics and phase disengagement times, and efficient equipment with less area and reagent inventory, means that the technique can be applied to lower value metals. Leaching/Solvent extraction/Electrowinning (L/SX/EW) process generally portray lower capital and operating cost compared to traditional floatation/smelting approaches. L/SX/EW can obtain copper at a low cost from low-grade overburden that needs to be mined but which would not be otherwise processed by float/smelt routes (Kordosky, 2002). For any extractant to be used commercially, it must meet the criteria of availability at low cost, low solubility in aqueous and high solubility in organic diluents, and high selectivity to form complexes with target metals and from which

the metal can easily be recovered while the extractant is recycled (Gupta & Mukherjee, 1990).

A variety of solvent extraction reagents have been investigated for the recovery of copper from pregnant leach solutions. Oximes and β-diketone extractants have been extensively studied and applied commercially in the extraction of copper from acidic and alkaline aqueous solutions (Ackerley et al., 1977; Alguacil, 1999; Mickler et al., 1992; Reddy et al., 2005; Sarangi et al., 2007; Tinkler et al., 2009). The oximes do have higher extraction strength that might lead to low stripping efficiencies. In acidic medium, the β-diketones are less effective than the oximes but pose an advantage in the alkaline medium such as ammonia solutions as they do not co-extract ammonia. Another advantage of β-diketones is their ability to transfer higher amounts of copper from the leached solutions which can then be easily stripped as compared to oxime extractants (Cox, 2004). To exploit the advantages presented by oxime and β-diketones, they are used together for the extraction of metals. Common commercially available oxime and β-diketone extractants are LIX 84I (2-hydroxy-5-nonylacetophenone oxime) and LIX 54-100 (1-phenyldecane-1, 3-dion), respectively (Kordosky, 2002). LIX 84 is a popular extractant for copper (Sengupta et al., 2007) and LIX 54-100, which was specifically developed for the recovery of copper from ammoniacal leaching solutions (Alguacil & Alonso, 1999; Fu et al., 2010), is being used in the industry for the recovery of copper from its leached solutions (Kordosky et al., 1999). Recently, Mextral 84H and Mextral 54-100, which were used as extractants in this research project, were synergistically used for the solvent extraction of zinc from an ammoniacal/ammonium sulfate solutions with sulfonated kerosene as diluent (Tang *et al.*, 2016). Mextral 84H has the same active component (2-hydroxy-5-nonylacetophenone oxime) as LIX 84I.

In the copper solvent extraction of Cu-glycinate solution, the extractant can extract the metal of interest from the solution by replacing the glycine ligands and, by so doing, form a copper-extractant complex. Alternatively, the whole Cu-glycinate complex can be picked up by the extractant as is the case with Cu- cyanide complex and LIX 7950 extractant (Xie & Dreisinger, 2010).

The general extraction process can be represented as in Equation 7.1 while that for stripping is given by Equation 7.2.

$$2RH_{(org)} + Cu(H_2NCH_2COO)_{2\,(aq)} = R_2Cu_{(org)} + 2H_2NCH_2COOH_{\,(aq)} \qquad (7.1)$$

$$R_2Cu_{(org)} + 2H^+(aq) = 2RH_{(org)} = Cu^{2+}_{(aq)} \quad (7.2)$$

The rich electrolyte solution from the stripping stage is fed into an electrowinning unit to produce high purity copper at the cathode as depicted by Equation 7.3.

$$Cu^{2+}_{(aq)} + 2e^- = Cu_{(s)} \quad (7.3)$$

Metal precipitation is also an essential unit process in the hydrometallurgical industry. It is based on the solubility or actually the lack of it in the precipitated product. In practice, precipitation can be done by hydroxide (CaO or $Ca(OH)_2$, $Mg(OH)_2$, NaOH and NH_4OH), sulfide (FeS, CaS, Na_2S, NaHS, $(NH_4)_2S$, H_2S, $Na_2S_2O_3$) or carbonate. Although hydroxide precipitation is commonly applied in the industry, metal sulfide precipitation presents advantages such as lower solubility of metal sulfides, fast precipitation rates, better settling properties and the stability of the metal sulfides formed (Lewis & van Hille, 2006; Lewis, 2010). Metal sulfide precipitation from synthetic copper alkaline glycine solutions and from actual leach solutions using NaHS as a precipitant will be explored in this chapter. H_2S and Na_2S may also be considered, but the chemistries are likely similar and was therfore considered to be beyond the scope of this work.

7.2 Solvent Extraction of Copper from Synthetic Copper Glycinate Solution

7.2.1 Effect of Aqueous pH

The effect of pH on copper extraction by Mextral 84H, a mixture of ketoxime (2-hydroxy-5-nonylacetophenone oxime) with a high flash point hydrocarbon diluent and Mextral 54-100, a β-diketone (1-benzoyl-2-nonyl ketone) in a mixture with high flash point hydrocarbon diluent) was determined using an aqueous solution containing 2 g/L Cu and 7.1 g/L glycine to yield a glycine-to-copper (Gly:Cu) molar ratio of 3:1. The initial aqueous pH was varied with sodium hydroxide from 9 to 12. The extractions were carried out by mixing the organic phase composed of 10 % extractant in DT 100 diluent at an A:O ratio of 1:1 for 15 minutes at 20 °C. The results shown in Table 7.1 indicate that initial pH of the aqueous phase does not significantly influence copper extraction by Mextral 84H as the percentage of copper extracted exceeds 99 % for all pH values evaluated. However, for Mextral 54-100, when the

pH is raised from 9 to 12, a slight increase in the copper extracted from 97.3 to 99.5 % is noted.

Table 7.1 Effect of pH on copper extraction. Experimental conditions: Gly:Cu 3:1, A:O 1:1, 20°C

Extractant/pH	pH 9	pH 10	pH 11	pH 12
Mextral 84H	99.49	99.47	99.66	99.68
Mextral 54-100	97.29	98.08	98.66	99.48

7.2.2 Effect of Temperature

Extraction experiments were carried out using an aqueous solution containing 2 g/L Cu at Gly:Cu molar ratio of 3:1 and pH 11. The different phases were allowed to attain the set temperature (15 to 55 °C) and then contacted at an A:O 1:1 for 15 minutes at the set temperatures. Results in Table 7.2 show that, within the studied temperature range, there is no significant influence on the copper extracted by either of the extractants as the percentage extracted stayed between 99.67 to 99.89 % and 97.36 to 97.89 % for Mextral 84H and Mextral 54-100, respectively.

Table 7.2 Effect of temperature on copper extraction. Gly:Cu 3:1, A:O 1:1, 20°C.

Extractant / Temperature (°C)	15	30	40	55
Mextral 84H	99.67	99.63	99.79	99.83
Mextral 54-100	97.36	97.67	97.89	97.32

7.2.3 Effect of Contact Time

The impact of contact time between the aqueous and organic phases was studied using an A:O ratio of 1:1, pH 11.0 and at 20 °C for different contact periods ranging from 2 to 30 minutes. The results shown in Table 7.3 indicate that copper extraction is very rapid as equilibrium is reached within 2 minutes. A mixing time of 10 minutes was then selected for the rest of the extraction experiments to ensure equilibrium is attained.

Table 7.3 Effect of mixing time on copper extraction. Gly:Cu 3:1, pH 11, A:O 1:1, 20°C.

Extractant/ Time(mins)	2	5	10	30
Mextral 84H	99.88	99.88	99.88	99.89
Mextral 54-100	97.53	97.56	97.58	97.60

7.2.4 Effect of Glycine Concentration

The influence of glycine, which is the main leaching agent for this system, was investigated by varying the Gly:Cu ratio in the aqueous phase from 2:1 to 16:1 while the aqueous copper content was kept at 2g/L and pH 11. The organic phases from either extractant (10 % v/v extractant) were then contacted with the aqueous phases at an A:O ratio of 1:1 at 20°C for 10 minutes. The results presented in Table 7.4 show that increasing the Gly:Cu ratio from 2:1 to 16:1 has no significant effect on the copper extractability by Mextral 84H as percentages stay above 99.9 % at all ratios. With Mextral 54-100, a drop in copper extraction from 97.86 to 93.02 % was noted as the Gly:Cu ratio is increased from 2:1 to 16:1.

Table 7.4 Effect of glycine concentration on copper extraction: pH 11, A:O 1:1, 20°C

Extractant/Gly:Cu	2:1	3:1	8:1	16:1
Mextral 84H	99.97	99.93	99.94	99.94
Mextral 54-100	97.86	97.05	96.35	93.02

7.2.5 Effect of Extractant Concentration

The effect of the extractant concentration was studied by varying the content of extractant in the diluent (2.5 to 30 % v/v). The aqueous phase composed of 2 g/L Cu at a molar ratio of 3:1 Gly:Cu at pH 11 was mixed with the organic phases at an A:O ratio of 1:1 for 10 minutes at 20 °C. After phase separation, the equilibrium pH values were within 9.38-10.12 for Mextral 84H and 9.34 to 9.55 for Mextral 54-100. The raffinates were analysed and the percentage copper extracted was plotted against extractant concentration as shown in Figure 7.1. For Mextral 84H, when the extractant concentration was increased from 2.5 % to 5 %, the percentage copper extracted increased from 57 to 99 % with no change with further increments of extractant concentration up to 30 %. Although 2.5 % Mextral 54-100 led to a 78.44 % copper extraction, the percentage copper extracted plateaued at 97 % with 10 % extractant and above.

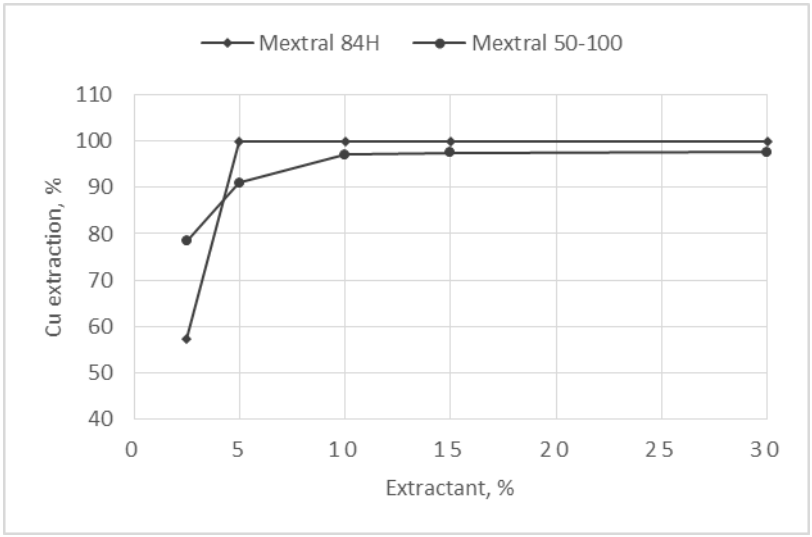

Figure 7.1 The effect of extractant concentration on copper extraction: Gly:Cu 3:1 A:O 1:1, 20 °C, 10 minutes

7.2.6 Loading Capacity of Mextral 84H and Mextral 54- 100

The loading capacity of an extractant is an important factor in its commercial application as it indicates the maximum metal concentration that the extractant can contain under specific conditions (Srivastava et al., 2015). The loading capacities can either be determined by varying the organic to aqueous phase ratios or by recontacting the organic phase with fresh aqueous phase until saturation is reached (Ritcey, 2004). The recontacting method has been used for these studies.

An aqueous phase containing 2 g/L Cu complexing at a 1:3 mole ratio with glycine at pH 11 was contacted with the organic phases (10 % v/v of either extractants in DT100) at a 1:1 phase ratio, 20 °C and mixed for 10 minutes. The organic phases were repeatedly contacted with a fresh aqueous phase and after 5 cycles, Mextral 54-100 contained 10.16 g/L copper while Mextral 84H contained 5.43 g/L. The extractants concentrations were raised to 30 % and the copper content on loaded Mextral 54-100 was noted to be 29.65 g/L as opposed to just 15.33 g/L obtained in Mextral 84H. These results indicate that, for the same concentration of extractant, the amount of copper loaded on Mextral 54-100 doubles that on Mextral 84H. This observation supports the reported potential of betadiketones having higher copper net transfer than their oxime counterparts (Hu et al., 2010; Kordosky et al., 1999).

7.2.7 Extraction Distribution Isotherm

In solvent extraction, an extraction isotherm is generally constructed to determine the number of stages needed to efficiently extract the metal of interest at a given phase ratio. The organic phases of 5 % Mextral 84H and 10 % Mextral 54-100 were mixed with the aqueous phase at different A:O ratios within 10:1 to 1:4 and pH 11 at 20 °C for 10 minutes. The copper content of the aqueous and organic phases after phase disengagement was determined. The results showed that at an A:O ratio of 2:1, 99.90 % Cu was extracted by 5 % Mextral 84 while 95.87 % copper extraction was attained with 10 % Mextral 54-100.

The McCabe-Thiele plot as shown in Figure 7.2 has been constructed at an operating A:O phase ratio of 2:1 indicated that copper can be completely extracted in one stage with 5 % Mextral 84H and two stages with and 10 % Mextral 54-100.

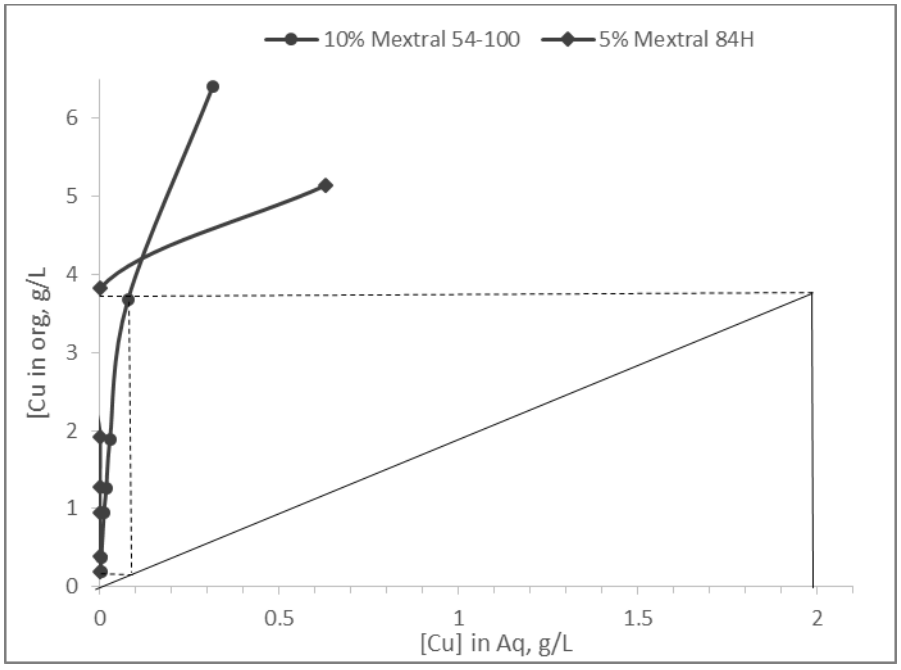

Figure 7.2 Extraction isotherm of copper with 5% Mextral 84H and 10% Mextral 54-100. Conditions operating A:O 2:1, 20 °C, for 10 minutes.

7.2.8 The Fate of Glycine during Solvent Extraction

It is well known that some extractants co-extract lixiviants together with the metals of interest during the extraction process. LIX 64N (an oxime extractant), studied for the extraction of copper and nickel from an ammoniacal-ammonium carbonate solution, has been noted to transfer ammonia; requiring a scrubbing step to remove the transfered

ammonia (Sandhibigraha & Bhaskara Sarma, 1997). Similarly, LIX 7950 extracts the complete copper cyanide complex (Xie & Dreisinger, 2010) implying that acidic stripping cannot be done for Cu-CN systems since it would lead to the production of toxic HCN gas. Thus in this study, there is the need to establish if Mextral 84H or Mextral 54-100 transfers glycine from the leached solution to the organic phase. 10 % Mextral 84H and 10 % Mextral 54-100 were used to recover copper from the aqueous solution at an A:O of 1:1 and 20 °C. HPLC-UV/Vis analysis for free glycine/glycinate in the aqueous phase after extraction showed that neither extractants transferred glycine/glycinate into the organic phases.

7.2.9 Sulfuric Acid Stripping of Copper Loaded Organics

The copper loaded organic phases of 5 % Mextral 84H and 10 % Mextral 54-100 were stripped with different concentrations of sulfuric acid solutions (10-200 g/L) at an A:O ratio of 1:1 and 20 °C for 10 minutes of mixing time. From Table 7.5, Mextral 84H copper stripping increased from 54.0 to 97.7 % with increasing acid concentration from 10 to 120 g/L. However, copper was readily stripped with sulfuric acid solution from Mextral 54-100 with > 97 % stripping using 10 g/L sulfuric acid solution. This is an indication that copper tends to form stronger complexes with Mextral 84H, a ketoxime, than with Mextral 54-100, a di-ketone.

The stripping of copper from an oxime type extractant, Acorga M5397, has also been reported to be completed at high sulfuric acid concentrations of 2.0 M (Amari et al., 2013). During the stripping of copper from loaded LIX 54, a ketone extractant, Qi-wen et al. (2011) reported that copper can be efficiently stripped at low acid concentration (96.70 % Cu at 100 g/L H_2SO_4).

Table 7.5 Stripping of copper loaded 5% Mextral 84H and 10% Mextral 54-100 with various H_2SO_4 concentrations. Conditions: A:O ratio 1, 20°C.

$[H_2SO_4]$, g/L	% Cu stripped	
	Mextral 84H	Mextral 54-100
10	54.02	97.34
30	86.00	99.95
50	96.57	100.00
80	59.14	100.00
120	97.62	100.00
150	97.32	100.00
180	97.27	100.00

7.2.10 Stripping Isotherm and Counter Current Stripping Simulation

To determine the number of stripping stages and the operating A/O ratio, a stripping isotherm for each extractant was constructed with the stripping solution bearing similar conditions to that of a spent electrolyte (SE) exiting an electrowinning operation of 30 g/L Cu and 180 g/L H_2SO_4 (Sarangi et al., 2007). The loaded organic phases containing 2g/L Cu were contacted with the SE at various A:O ratios (2:1 to 1:10) at 40 ° C for 10 minutes. At an A:O ratio of 1:10, 99.59 % copper is stripped from loaded Mextral 54-100. Under the same conditions, only 79.95 % copper was stripped from Mextral 84H.

The McCabe-Thiele plot in Figure 7.3 illustrates that that three stages will be needed to effectively strip copper from the loaded Mextral 84H at the A:O ratio of 1:10 while just one stage is needed for Mextral 54-100.

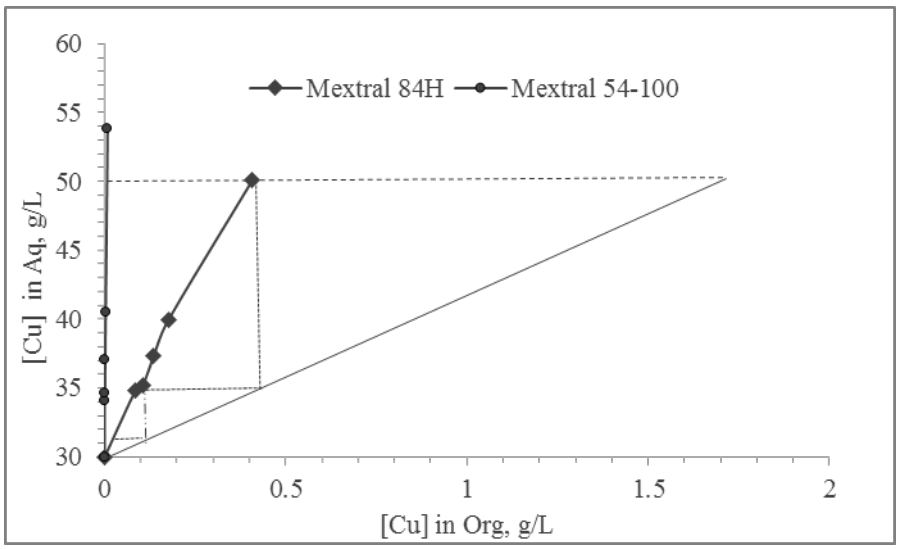

Figure 7.3 Stripping isotherm of copper loaded organic. Conditions: 30 g/L Cu and 180 g/L H_2SO_4, A:O= 10:1, at 40°C

7.3 Solvent extraction from Malachite leachate and stripping of Cu from Extractant

The mineralogical and elemental analysis of the malachite ore specimen, leached to provide a feed solution for the SX study, is shown in Table 7.6. Malachite is the only copper mineral in the ore specimen.

Table 7.6 Mineralogical and elemental composition of copper oxide (malachite) specimen

Phase	Goethite	Hematite	Malachite	Quartz	Amorphous Content		
Wt %	1.7	3.3	66	16.7	12		
Element	Cu	Al	Si	K	Mg	Fe	Ca
%	41.55	0.13	8.49	0.11	0.38	3.53	0.81

The malachite sample was bottle rolled for 24 hours at pH 11 at a Cu-Gly molar ratio of 1:4. The leachate had a copper concentration of 2.620 g/L and a final pH of 12. Copper extractions were carried out using 5 % Mextral 84H and 10 % Mextral 54-100 at different organic to aqueous ratios.

Table 7.7 shows the percentage copper extracted at different organic to aqueous ratios. For both extractants, 99 % copper was extracted at an O:A ratio of 2:1. Any increments in aqueous volume resulted in lower copper extractions for both reagents. The fate of impurities was determined by ICP analysis of the aqueous raffinate derived from the O:A ratio 1:1 extraction.

Table 7.7 Percentage copper extractions from malachite by 10 % Mextral 54-100 and Mextral 84H at different O:A ratios

Organic: Aqueous Ratio	Mextral 54-100	Mextral 84H
	% Cu extraction	% Cu extraction
2:1	99.39	99.93
3:2	99.27	99.82
1:1	98.90	99.14
1:2	95.64	44.53
1:4	76.13	13.53

The results shown in Table 7.8 indicate that both extractants selectively extract copper from the leached solutions. The results also confirm the selectivity of leaching copper with alkaline glycine solutions (Tanda et al., 2017).

Table 7.8 Elemental analysis of malachite leachate and raffinate before and after solvent extraction respectively with 10 % Mextral 54-100 and Mextral 84H at an O:A ratio of 1:1

Leachate before and after SX	Concentration, mg/L						
	Cu	Fe	Mg	Ca	Si	Al	pH
Leachate before SX	2620	<0.2	<0.2	0.85	3.65	0.237	12.00
Raffinate after SX with Mextral 54-100	24.9	<0.2	<0.2	0.88	3.64	0.240	9.76
Raffinate after SX with Mextral 84H	19.4	<0.2	<0.2	1.22	3.58	<0.2	10.00

The results of the stripping test are presented in Table 7.9. The loaded organic phases derived from the malachite leachates were contacted with the spent electrolyte solution (30 g/L Cu, 180 g/L H_2SO_4) at various O:A ratios (2:1 to 1:10) at 40 ° C, for 10 minutes. At an O:A ratio of 10:1, about 99.3 % of the copper was stripped from loaded Mextral 54-100 extractant. Under the same conditions, only 78.3 % copper was stripped from the loaded Mextral 84H extractant. At an O:A stripping ratio of 1:1, the spent electrolyte proxy solution could strip the loaded Mextral 54-100 extractant from 99.96 % of its copper, while it only strips 90.01 % copper from the loaded Mextral 84H organic phase.

Table 7.9 Stripping of copper from loaded Mextral 54-100 and Mextral 84 H (Cu loaded from malachite leachate) using a proxy spent electrolyte solution (30 g/L Cu, 180 g/L H_2SO_4) at various organic to aqueous ratios: 40 °C, 10 mins.

Organic:Aqueous Ratio	Cu stripped from loaded Mextral 54-100, %	Cu stripped from Mextral loaded 84H, %
10:1	99.32	78.30
4:1	99.82	86.29
2:1	99.98	88.77
1:1	99.96	90.01
1:2	99.99	90.64

7.4 Solvent Extraction of Copper from Chalcopyrite B Leachate and Cu Stripping from Extractant

The mineralogy and elemental composition of the chalcopyrite specimen is given in Table 7.10. A “dirty” concentrate consisting of low grade chalcopyrite with significant impurities was used to obtain the proxy pregnant leach solution.

Table 7.10 Mineralogical and elemental composition chalcopyrite B specimen

Mineral Phase	Chaba-zite	Chalco-pyrite	Clino-chlore	Pyrite	Quartz	Rutile	Amor-phous		
Wt %	0.8	35.0	1.5	29.4	0.9	0.4	32.0		
Element	As	Ca	Cu	Fe	Mg	Pb	Si	S	Zn
Wt %	0.709	0.31	14.8	30.9	1.08	0.29	3.64	32.4	4.95

The chalcopyrite specimen was leached in a glass reactor at 60 °C and DO concentration of 20 ppm at pH 11.8 for 24 hours. The final leach solution contained 2.288 g/L Cu at pH of 10.5. Copper extraction experiments using 5 % Mextral 84H and 10 % Mextral 54-100 were carried out at different organic to aqueous ratios. Copper extractions of 93.20 % and 95.57 %, for 10 % Mextral 54-100 and 5 % Mextral 84H, respectively, were obtained at an O:A ratio of 2:1 (Table 7.11). The lower copper extraction obtained for chalcopyrite leachate as compared to that from synthetic solutions could be attributed to the partial co-extraction of other base metals. The influence of the leached impurities on the copper SX process was monitored by analysing the concentration of copper and impurities in leachate before and after SX.

Table 7.11 Percentage copper extractions from chalcopyrite B leachate by 10 % Mextral 54-100 and Mextral 84H at different O/A ratios

Organic/Aqueous ratio	Mextral 54-100	Mextral 84H
	% Cu extraction	% Cu extraction
2:1	93.20	95.57
3:2	92.66	92.70
1:1	91.01	86.66
1:2	87.92	83.01
1:4	78.45	55.12

Table 7.12 shows that, although some impurity elements are leached along with copper (though to lower extent), the extractants selectively extracted copper from the leached solution.

Table 7.12 Elemental analysis of chalcopyrite B leachate and raffinate before and after solvent extraction respectively with 10 % Mextral 54-100 and Mextral 84H at an O:A ratio of 1:1

Leachate before and after SX		Leachate before SX	Raffinate after SX with Mextral 54-100	Raffinate after SX with Mextral 84H
Concentration , mg/L	Cu	2288	205	304
	Zn	699	584	709
	Fe	3.5	14	14.2
	Mg	1.66	2.12	2.05
	As	1.17	2.07	1.76
	Ca	5.5	5.33	6.05
	Pb	<0.2	<0.2	<0.2
	Si	0.49	1.47	1.12
	Co	15	17.4	16.8
	Ni	8.15	8.39	8.96
Raffinate pH before and after SX		10.55	9.87	9.91

Cu from the loaded organics was stripped using a spent electrolyte solution (30 g/L Cu, 180 g/L H_2SO_4) at different O:A ratios (10:1 to 1:2) at 40 °C for 10 minutes. Table 7.13 gives the strip recovery of Cu from loaded Mextral organic at various O:A ratios. About 99.4 % Cu was stripped from loaded Mextral 54-100 at an O:A ratio of 10:1 while 81 % Cu was obtained from Mextral 84H at the same O:A ratio. At a 1:1 O:A stripping ratio, the spent electrolyte proxy solution could strip 99.99 % copper from the loaded Mextral 54-100 extractant while it could only remove 89.45 % of the copper from the loaded Mextral 84H extractant.

Table 7.13 Stripping of copper from loaded Mextral 54-100 and Mextral 84H (Cu loaded from chalcopyrite leachate) using a proxy spent electrolyte solution (30g/L Cu, 180g/L H_2SO_4) at various organic to aqueous ratios: 40 ° C, 10 mins.

Org/Aq ratio	Cu stripped from loaded Mextral 54-100, %	Cu stripped from Mextral loaded 84H, %
10:1	99.37	81.43
4:1	99.93	85.38
2:1	99.98	89.15
1:1	99.99	89.45
1:2	99.99	90.69

The fate of impurity elements during copper stripping from the loaded organics was investigated at an O:A ratio of 2:1. On stripping from loaded Mextral 54-100, the

concentrations of Cu, Zn, Co and Ni in the rich aqueous phase were 35.0 g/L, 101 mg/L, 1.45 mg/L, and 1.15 mg/L respectively. For Mextral 84H, the concentrations of Cu, Zn, Co and Ni were 34.4 g/L, 2.86 mg/L, 1.31 mg/L, and 2.01 mg/L respectively. Therefore the concentration increase of copper in the aqueous electrolyte strip solution, from the 30 g/L baseline, was the order of 4.4 g/L (from Mextral 54-100 strip) to 5.0 g/L (from Mextral 84H strip).

The main objective of the extraction and stripping evaluation from actual leachates is to provide a measure of the deportment of typical impurity elements. The two leachates were chosen as examples of leachates derived from a copper oxide and a copper sulfide mineral source..

7.5 Solvent Extraction of Copper from a Copper-Gold leachate

The concurrent dissolution of copper and gold from their ores as noted in Chapter 6 makes it paramount to investigate the fate of Au-glycinate during the solvent extraction of copper from the leachate. The feed solution for this investigation was obtained by leaching 500 g copper-gold ore C (mineralogy of the ore was reported in Section 6.3.1) in a 1 L glass reactor for 96 hours under the following conditions: 100 % passing 75 µm, 60 °C, 0.5 M Gly and 0.05 L/min oxygen at an initial solution pH of 11.85 . The leachate at pH 10.32 contained 784 mg/L Cu and 0.241 mg/L Au. Copper extraction by 10 % Mextral 54-100 and 5% Mextral 84H at an A:O ratio of 2:1 was carried out and the results are shown in Table 7.14. Copper extraction was 80.2 % and 99.8 % for Mextral 54-100 and Mextral 84H, respectively. Although the results indicate that gold concentration in solution after copper extraction with Mextral 54-100 and Mextral 84H, respectively, reduced by 1.7 and 2.1 %. The values are within an accepted analytical error range. It can thus be concluded that the Au ions/Au-glycinate complex is not picked up by either extractant. It has been reported by Eksteen and Oraby (2015a) that gold from alkaline glycine solutions can be loaded onto activated carbon. Hence, a flowsheet can be proposed in which Cu-Au ores are leached in alkaline glycine solutions, Cu can be recovered by solvent extraction and then Au by activated carbon. Au recovery from alkaline glycine solutions has already been studied by Oraby and Jacques, 2015. They found out that, Au could be adsorbed onto carbon at a rate of 13.2 Kg_{Au}/t_{carbon}.

Table 7.14 Copper extraction from Cu-Au ore C leachate using Mextral 54-100 and Mextral 84H: A:O 2:1, pH 10.32, 25 °C

Extractant	Cu extraction, %	Au extraction, %
10 % Mextral 54-100	80.22	1.66
5 % Mextral 84H	99.79	2.07

7.6 Qualitative Comparison of Cost Drivers of the Alkaline Glycine Leach-SX and Conventional Sulfuric Acid Leach-SX Processes for Copper Ores.

The production capacity of installed conventional sulfuric acid based Leach-SX-EW as of 2001 was 2.8 million tonnes of copper accounting for about 20% of primary copper production (Kordosky, 2002). Generally, several variables account for the operating costs of copper acid leaching processing plants, and the cost of acid consumption forms a significant portion of the operating cost. This is especially significant for treating carbonaceous ores whereby 1 ton of carbonate mineral requires about a ton of sulfuric acid (International Atomic Energy Agency, 2001). With alkaline glycine leach system having been proven to selectively leach copper over carbonates and other impurity elements (Eksteen et al., 2016; Oraby & Eksteen, 2014; Tanda et al., 2017), lower operating costs due to low reagent inventory could be realised. In addition, almost all of the glycine can be recovered and recycled to the leach circuit, especially when CCD do not follow agitated leaching in which water (containing glycine) is lost with solids.

Remote users of sulfuric acid incur high logistical and transportation costs due to safety concerns. The capital cost of a site sulfur burning sulfuric acid plant could be very high as well. With glycine being environmental friendly and supplied in a granular form, transportation costs are low as safety concerns are insignificant.

Crud formation causes loss of reagent with entrainment (Rydberg et al., 2005). Crud is common to most acidic solvent extraction operations and hampers the interaction of organic and aqueous solutions. Crud is made up of organics, aqueous, air and solid particles. The presence of cations such as Fe, Si, Ca, Mg and Al with sufficient agitation can produce stable cruds (Aminian & Bazin, 1999; Rydberg et al., 2005). Major components of crud from a copper

SX plant in China were found to be SiO_2, Al_2O_3, Fe_2O_3, CaO, MgO and MnO (Chengyan, 2005). The nature of solvent extraction feed has been shown to influence crud formation during SX (Mukutuma et al., 2008). Alkaline glycine leaching could significantly reduce crud formation during SX by preventing the dissolution of crud forming metals and particles that would otherwise be dissolved in sulfuric acid medium. As a comparison, whereas acidic heap leach systems (of oxide ores) often lead to contaminant levels of Fe, Mn, Si, Al, Ca and Mg between 0.5 and 18 g/L in heap leach pregnant leach solutions (Zarate & Torres, 2016) in Chilean heap leach operations, the alkaline nature (at 9<pH<12) of the glycine leach suppresses the dissolution of these elements to below 20 ppm (Tanda et al. 2017; Oraby and Eksteen, 2014), whilst Cu tenors of between 1 and 5 g/L can be achieved, giving a selectivity of around between 100:1 to 1000:1 relative to the concentration of lithophile elements in solution.

In most SX operations from sulfuric acid leach, extraction occurs in two stages (Davenport et al., 2002b) but the results in this research indicate that a 1-stage SX is probably sufficient for glycine L/SX.

Capital costs related to construction material for glycine L/SX could be relatively lower as compared to H_2SO_4 L/SX due to the less corrosive nature of alkaline glycine solution. In sulfuric acid heap leach for example, HDPE is used as pads and 316 stainless steel used for the construction of most mixer-settler equipment (Davenport et al., 2002b). However, in the alkaline glycine leach process, painted mild steel can be easily used, similar to cyanide leahing operations. In addition, the use of low cost portland cement binders/agglomeration agents can be considered in the heap leach without the risk of dissolution.

Given that the alkaline glycine system has been shown to be able to dissolve copper oxide minerals (Tanda et al., 2017) and native copper and copper sulfides including chalcopyrite (Oraby and Eksteen, 2014, Oraby et al., 2016), it provides for a highly versatile leach system across the geometallurgical spectrum of typical copper deposits, whilst minimising lithophile element dissolution (e.g. Fe, Cr, Mn, Al, Mg, Ca and Si), thereby giving a significantly cleaner pregnant leach solutions feeding into the solvent extraction circuit.

An important similarity between glycine L-SX of copper and that of conventional acid L-SX is that copper can be stripped by a spent electrowinning electrolyte from both systems. Thus the glycine system can replace a conventional acid leaching system without any change in plant equipment.

7.7 Copper Precipitation from a Synthetic Copper Glycinate Solution

The feed solution used to study the effect of Cu:S molar ratio and pH was obtained from the dissolution of $CuSO_4 \cdot 5H_2O$ in an aqueous alkaline glycine solution to obtain a copper concentration of 2 g/L and a Gly:Cu ratio of 3:1. Sodium hydrogen sulfide, which is commonly used in the industry (Lewis, 2010) was used as a precipitant. Precipitation experiments were performed in a magnetically stirred open beaker and at room temperature (22-25 °C) by adding a stoichiometric mass of NaHS powder into the copper glycinate solution. Copper concentration in solution before and after precipitation was measured using AAS to determine the extent of precipitation.

7.7.1 Effect of Copper to Sulfide Ratio (Cu:S)

The effect of Cu:S molar ratio was studied by varying the molar ratio of Cu^{2+} to S^{2-} ions. Results in Table 7.15 show that copper precipitation increases as the Cu:S ratio increases. At Cu:S ratio of 1:1.2, 98.8 % of copper was precipitated in less than 10 minutes. This higher S:Cu ratio needed for 98.8 % precipitation as opposed to the theoretically expected 1:1 could be attributed to waters of hydration of NaSH (hydroscopic) that could be up to 20 % (O'Brien, 2012) which increases the mass of NaSH needed. This explains why a 1:1.2 gave the best results. However, it is noted that 100 % copper precipitation is not desired since low concentrations of Cu^{2+} ions in the recycle solution will act as oxidising agents in the leaching of copper from its ore.

Table 7.15 Effect of Cu:S ratio on copper precipitation from alkaline glycine solution

Cu:S ratio	1:0.5	1:0.8	1:0.9	1:1	1:1.2
Cu precipitated, %	58.83	74.46	85.61	94.27	98.84

7.7.2 Effect of pH

The effect of solution pH on copper precipitation was studied by varying the solution pH from 8 to 11. Results in Table 7.16 indicate that the extent of copper precipitation from an alkaline glycine solution is not influenced by the pH values considered.

Table 7.16 Effect of pH on copper precipitation from alkaline glycine solution: Cu:S 1:1.

pH	8	9	10	11
Cu precipitated, %	93.76	92.99	93.81	94.27

7.7.3 Precipitate Analysis

To determine the type of precipitate produced from NaSH precipitation, the precipitate was dried and analysed by XRD. Figure 7.4 indicates that 100 % of the precipitate is covellite (CuS). This result is further confirmed by the information given in Section 5.2 that only Cu^{2+} ions are involved in the formation of the stable copper glycinate complex in alkaline solutions.

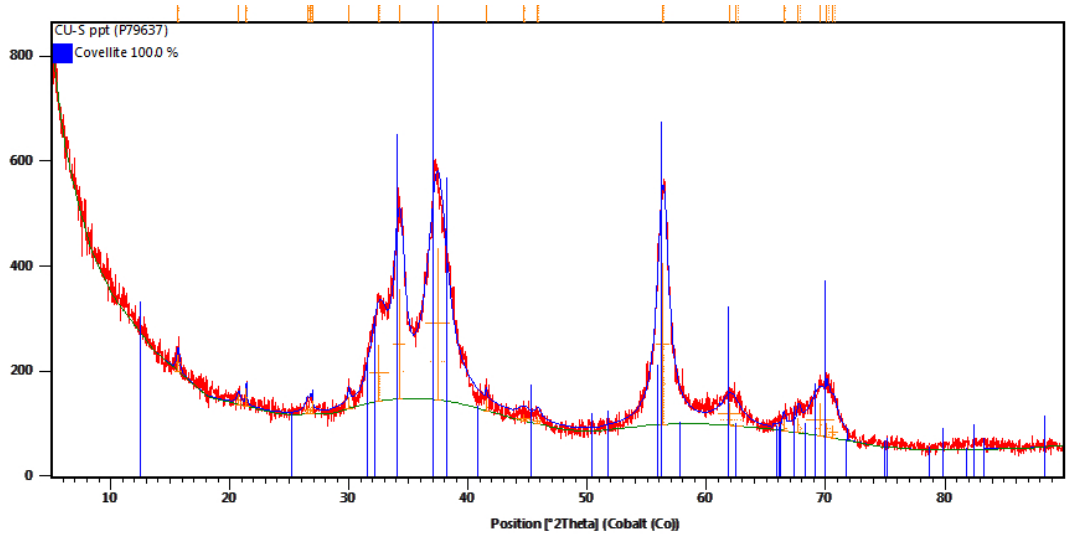

Figure 7.4 XRD pattern of precipitate produced from NaSH precipitation of copper glycinate solution

After precipitation and separation, a portion of the precipitate was immediately analysed by laser diffraction (Malvern) to determine the particle size distribution. The distribution pattern in Figure 7.5 illustrates that P_{80} of the precipitate is 66.96 µm. The significant diameter of the particles account for the observed good settling and filtering properties of the precipitate.

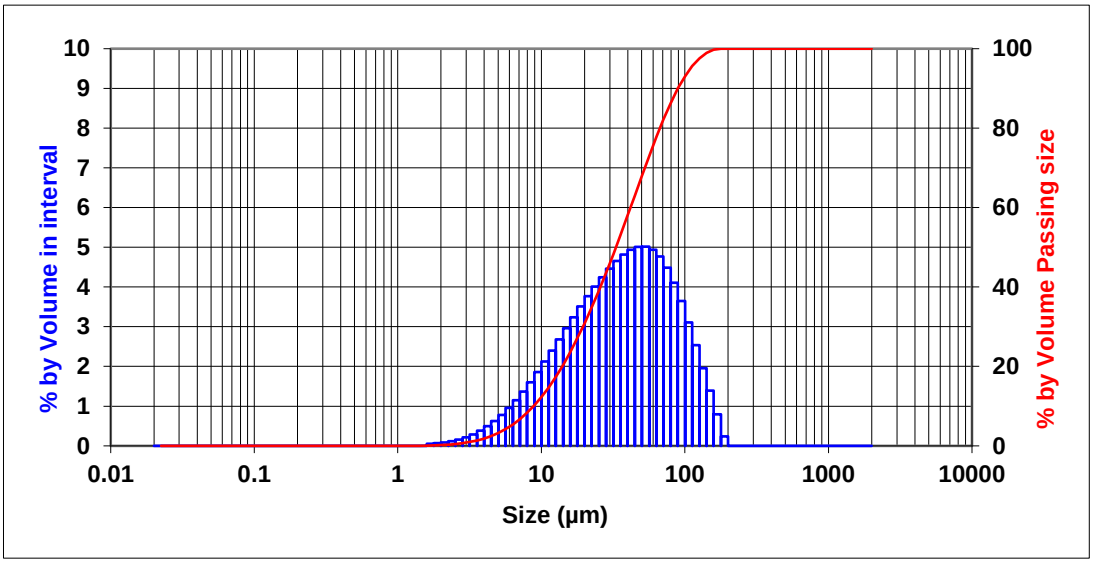

Figure 7.5 Particle size distribution of copper precipitate (CuS) from a copper glycinate solution

7.8 Copper Precipitation from a Malachite Ore Leachate

The leachate obtained from the leaching of a malachite specimen with mineralogy as reported in Section 4.31 was used for the copper precipitation test. Sulfide was introduced into the solution by adding a weighed powder of NaSH in order to obtained a predetermined Cu:S molar ratio. Supernatant analysis by AAS noted that 81.37 % copper was precipitated at Cu:S molar ratio of 1:1. At a Cu:S molar ratio of 1:1.1, 98.98 % of Cu was precipitated from solution.

7.9 Copper Precipitation from Chalcopyrite B Leachate

The leachate from chalcopyrite B (same leachate as in 7.4) was precipitated with NaHS at a Cu:S molar ratio of 1:1 at pH 8, 11 and 12. After 5 minutes of precipitation, 93.5 % copper was precipitated at all pHs considered. The Cu:S molar ratio was varied from 1:1 to 1:1.1 at pH 11. At the Cu: S molar ratio of 1:1.1, 99.5 % copper was precipitated. During the leaching of chalcopyrite B (muti-metal specimen), associated metals such as zinc were concurrently leached into solution with copper. Table 7.17 tracks the concentration of copper and various metals leached into solution and their fate after sulfide precipitation with NaHS at a Cu:S molar ratio of 1:1. Copper precipitation was at 93.3 % Cu while those for Zn, Ca, Co and Ni were 10.5, 6.3, 13.9 and 3.3 %, respectively. The calculated percentage precipitation for the

rest of the major metals was negative, indicating that those metals were not precipitated under the studied conditions.

Table 7.17 Precipitation of copper and accompanying metals from a complex multi-element chalcopyrite specimen

Metals	Cu	Zn	Fe	Mg	As	Ca	Si	Co	Ni
Metal concentration before precipitation, mg/L	2287.6	699.2	3.5	1.7	1.8	5.5	0.5	14.9	8.2
Metal concentration after precipitation, mg/L	153	626	4.5	2.14	1.6	5.2	0.8	12.9	7.9

7.10 Copper Precipitation from a Copper-Gold Ore leachate

The Cu-Au solution used in this precipitation is the same as that used in Section 7.5. The leachate copper concentration is 784 mg/L and that of gold is 0.241 mg/L. Copper was precipitated at a Cu:S molar ratio of 1:1 and 1:1.1. The results in Table 7.18 show that 87.44 % Cu was precipitated at the Cu:S ratio of 1:1 while 97.32 % was precipitated at a Cu:S ratio of 1:1.1. On analysing gold concentration in solution after precipitation, a gold loss of 16.18 and 24.07 % was noted at Cu:S ratio of 1:1 and 1:1.1, respectively. Although gold-sulphide compounds have not been reported to form naturally, stable Au-S compounds (Au_2S, AuS_3) have been synthesized (Faltens & Shirley, 1970). These gold sulfides are black, finely divided amorphous material that are sparingly soluble in water. Thus, the loss of gold during the sulfide precipitation of copper could be attributed to the formation of gold sulfide compounds. This may also be attributed to the metallic reduction of gold cause by the reducing environment of sulfide ions or to the adsorption of gold onto the copper sulfide precipitate. The nature of the gold deportment to the CuS precipitate has not yet been determined. From a commercial perspective, gold precipitation along with copper is not lost as the gold could be recovered during the smelting of the covellite precipitate.

Table 7.18 Copper precipitation from a Cu-Au ore leachate using NaSH: 25 °C, 10 mins, 50 rpm.

Cu:S ratio	1:1	1:1.1
Cu precipitated, %	87.14	97.32
Au precipitated, %	16.18	24.07

7.11 Summary

The major objective of this paper was to investigate and evaluate the possibilty of copper recovery from alkaline glycine solutions. Solvent extraction and sulfide precipitation from both synthetic solutions and leachate from leaching natural ores were conducted. This section therefore summarizes the results obtained from the solvent extraction and precipitation experiments.

The extraction of copper from alkaline glycine solutions was investigated using Mextral 84H and Mextral 54-100 extractants using kerosene as a diluent and results show that copper can be efficiently recovered from the alkaline glycinate media and stripped using acidic solutions similar to conventional spent electrolyte from copper electrowinning tank houses.

Copper extraction rates are fast as equilibrium is established in less than two minutes with both extractants. A temperature range of 20–40 °C has no influence on the percentage copper extracted by either extractants. Increasing the aqueous solution pH has no effect on the ability of Mextral 84H to recover copper while a slight improvement from 97.3 to 99.7 % copper extracted was noted for Mextral 54-100. Higher glycine to copper ratio 16:1 reduces the copper extracted by Mextral 54-100 from 97.86 to 93.02 % meanwhile no changes are noted in the case of Mextral 84H. Mextral 54-100 has superior loading capacities to Mextral 84H. With an aqueous solution containing 2 g/L copper, 5 % Mextral 84H extracts 99.90 % copper while 10 % Mextral 54-100 was needed to extracted 95.87 % copper at an A:O ratio of 2:1. In contrast to the cyanide and ammonia complexes of copper, which are solubilised as the complete complex, the glycine lixiviant was not solubilised by any of the organic extractants. All the glycine/glycinate reported to the aqueous raffinate, making recycling and reuse of glycine on the leaching circuit feasible. Using a make-up spent electrolyte solution containing 30 g/L Cu and 180 g/L sulfuric acid at 40°C, complete copper stripping was realised from Mextral 54-100 at an A:O ratio of 10:1 while just 79.95 % was stripped from Mextral 84H under the same conditions.

In order to validate the results obtained from the copper extraction of synthetic solutions, copper extraction from leached ore samples was performed. Copper extractions at O:A of 1:1 from malachite leachate were 99 % for both extractants while no impurity elements were extracted. Copper extraction from a dirty chalcopyrite leachate at O:A ratio of 1:1 resulted in

91.0 % and 86.6% Cu extracted by 10 % Mextral 54-100 and 5 % Mextral 84H, respectively, while the concentration of most impurity elements in the aqueous raffinates increased. The extractants show the ability to extract Cu from alkaline glycinate solutions over impurity elements except zinc under the conditions used in this work. Solvent extraction on the PLS of a Cu-Au ore containing 784 mg/L Cu and 0.241 mg/L Au at pH 10.3 revealed that up to 80.2 and 99.8 % Cu was extracted by Mextral 54-100 and Mextral 84H, respectively, while the gold is rejected into solution. According to Eksteen & Oraby, (2015a), the rejected gold could then be recovered with activated carbon.

One of the particular benefits of this system is the ability of performing the extraction under alkaline conditions and the stripping using conventional spent electrolyte from conventional copper electrowinning tank houses.

Precipitation of copper from the synthetic copper-glycinate solution at pH 11 resulted in 98.8 % precipitation in less than 10 minutes. It was observed that a pH range of 8-12 has no influence on copper precipitation as approximately 94.0 % was precipitated at all pHs. Precipitate analysis by XRD showed that 100 % of the product is covellite while Mavern laser particle analyser showed that P_{80} of the precipitate was 66.96 µm. Copper precipitation from a malachite leachate at a Cu:S molar ratio of 1.1.1 resulted in a 98.8 % copper precipitation. During the precipitation of copper from a dirty multi-metallic chalcopyrite B specimen, it was observed that at 93.3 % Cu precipitation, Zn, Ni and Co were co-precipitated but to a much lesser extent (<10 %)

Chapter 8 Conclusions

This chapter summarizes the major findings that have been discussed in the previous chapters. In section, a retrospective of the research conducted is provided. The next section outlines achievements and enumerates conclusions drawn from the results of the different sections covered in this thesis. Some criticism of the research methodology that could have improved the interpretation of the results is also given. Another section in this chapter proposes possible flowsheets for different types of copper ores and copper-gold ores. The final section then provides some recommendations for further investigations considered worthy towards this research.

8.1 Retrospective and Discussions

The principal objective of this research was to investigate the application of glycine as a lixiviant for low grade copper–gold ores. Processing of copper-gold by the traditional cyanidation method as discussed in Chapter 1 possess challenges to metallurgists at all unit stages of the process. Cyanidation efficiency is limited by the presesence cyanide soluble copper by causing high cyanide demands. Copper found in the cyanide leached solution interferes with the gold recovery process (carbon absorption). Copper forms WAD cyanide that is not easily degradable by sunlight as compared to cyanide and thus makes the process more environmentally un-friendly. Thus, there is the need to search for a new approach that economically extracts and recovers copper and gold from copper-gold resources in an environmentally benign manner.

Gold is generally found in association with primary copper ores. Porphyry copper deposits are an important source of copper-gold ores as they are obtainable in many parts of the world. More than 60 % of 2110 million tons of discovered copper reserves are made up of porphyry deposits. However, porphyry deposits have significant mineralogical variations that require extensive understanding in order to choose a suitable processing technique. Most of these porphyry ore bodies containing copper-gold ores bear very low metal values that must be processed via economical methods such as heap or dump leaching. Traditional cyanide approaches not only have limitations at the level of reagent consumption and proccessing steps, but their applications are highly restricted or banned for use on heaps or dumps due to environmental concerns. An investigation into the use of cyanide alternatives is vital for the extraction of valuable metals from low grade copper-gold ores.

Glycine has been presented as a potential alternative to cyanide not only due to it being environmentally benign but also as a result of it being able to form stable complexes with copper and gold. In alkaline environments, glycine can selectively leach copper and gold over gangue metals such as iron, manganese, aluminium, calcium, magnesium and silicon. Glycine can also be cheaply produced on an industrial scale.

8.2 Enumerated Conclusions

This section details the specific conclusions that have been drawn based on experimental results. Leaching experiments were conducted with copper mineral specimens and copper-gold ore samples with different copper and gold grades. The focus was also on the leaching mechanisms and kinetics of copper leaching from its major minerals and the recovery of copper metals from their PLSs.

Leaching experiments in this project were focused on leaching of mineral samples and ores under different conditions and not much attention was given to the thermodynamics and electrochemical response of copper minerals and gold ores in the alkaline glycine solutions. Information from such such studies are very helpful in the interpretation of results obtained during the bulk mineral ore leaching.

8.2.1 Leaching of Copper Minerals

Investigations into the leaching behaviour of individual copper minerals in alkaline glycine solutions, in order to evaluate the extent of copper dissolution from common copper minerals, were conducted using a bottle roller at different glycine concentrations and at different initial leach solution pHs. At a Gly: Cu molar ratio of 4:1, initial solution pH of 11 at 25 °C, azurite was the easiest mineral to leach with 93.0 % Cu extraction in 6 hours. This was closely followed by malachite with 88.0 % Cu obtained in 24 hours. Cuprite and metallic copper leach rather slower than malachite and a Cu extraction of 91.7 % for both was achieved after 48 hours. Chalcocite leaches fast in the first 24 hours (40.0 % Cu) and then begins to plateaus as just about 44.0 % Cu is dissolved in 48 hours. The dissolution of copper from chrysocolla is very slow with only 19.7 % Cu leached in 48 hours. Chalcopyrite shows the lowest Cu dissolution with 15.1 % Cu extracted in 96 hours.

However, during the leaching kinetic studies of malachite, chalcocite and chalcopyrite conducted using a glass reactor whereby variables such as temperature, dissolved oxygen

concentration, particle size and stirring speed could be controlled, copper extraction rates were significantly improved. Under the following conditions, 50 °C, [Gly] of 0.5 M, stirring speed of 400 rpm, particle size of +53-75 µm, 99.2 % Cu was extracted from malachite in just 30 minutes of leaching. For chalcocite, at 25 °C, 0.5 M Gly, DO 8 ppm, stirring speed of 400 rpm, particle size of P_{80} 18.9 µm, 78.2 % Cu was extracted in 48 hours. The leaching of minus 10 µm size fraction of chalcopyrite at 50 °C, DO of 15 ppm, stirring speed of 400 rpm, and a glycine concentration of 0.5 M resulted in 90.1 % Cu extraction after 96 hours.

The extent to which the different copper minerals leach in the alkaline glycine solution is similar their leaching behaviours in other alkaline solutions such as cyanide (Hedley & Tabachnick, 1968) and ammonium thiosulfate (Molleman & Dreisinger, 2002). In these solutions, the oxide minerals show high copper leaching rates and secondary sulfides leach to a limited extent, while primary sulfides such as chalcopyrite leach slowest. In industrial applications whereby the ore to be leached contains a multitude of minerals, leaching conditions should be chosen in order to maximise the leaching of the primary sulfides.

8.2.2 Mechanisms and Kinetics of Leaching Malachite, Chalcocite and Chalcopyrite

In order to determine if Cu (I) and/or Cu (II) ions form the copper glycinate complex during leaching of the different copper minerals, copper speciation was determined using UV-Vis and AAS. The UV-Vis spectrum from leachates of azurite, malachite, cuprite, metallic copper, chrysocolla, chalcocite and chalcopyrite showed a peak at 630 nm which is characteristic of the Cu^{2+} of $CuSO_4 \cdot 5H_2O$ (as standard) in alkaline glycine solution. Copper concentration in the leachates determined by UV-Vis (cupric) and AAS (total copper) confirmed that all the copper in the leachates occurs as Cu^{2+} ions which then form the stable copper glycinate complex.

The fate of sulfur during the leaching of copper mineral sulfides was investigated by performing sulfur speciation on the leachate of chalcopyrite. It was shown that about 90 % of sulfur in the sample was converted to sulfate in the alkaline glycine solution.

Chalcocite leaching occurs in two stages. The chalcocite is quickly converted to Cu-glycinate complex and covellite in the first stage. The second stage then involves the slow leaching of the formed covellite. The kinetics of chalcocite investigated using equations of the shrinking core model indicated that chalcocite leaching is controlled by diffusion through the product layer. The apparent activation energy was calculated to be 43.92 kJ/mol.

Copper leaching rate from a malachite mineral sample was established to be controlled by diffusion through the product layer. The calculated activation energy was 48.26 kJ/mol.

The shrinking core model equations were also used to predict the rate controlling steps during the leaching of chalcopyrite. Applying the constrained multi-linear regression analysis using the least square technique, the contributions of the different rate controlling shrinking core models towards the overall leaching reaction could be predicted. As a consequence of the significant difference in the dissolution regime of +20-38 µm size fraction of chalcopyrite to that of the <10 µm size fraction, rate controlling step determination was on both size fractions. The copper dissolution rate from +20-38 µm chalcopyrite fraction is limited by a mixed diffusion regime. Diffusion through the product layer and liquid film both contribute to limiting the leaching process. However, diffusion through the product layer is quite dominant and its model equation was used to calculate the apparent activation energy for the process to be 36.25 kJ/mol. On the other hand, the leaching rate from the < 10 µm chalcopyrite is also controlled by diffusion through the product layer with an apparent activation energy of 29.62 kJ/mol.

The leaching kinetics and activation energies reported for the minerals above are for the given experimental conditions since disparities in leaching kinetics can occur due to different experimental conditions (Nicol et al., 2010).

8.2.3 Leaching of Copper- Gold Ores

Copper-gold ore samples (oxides and sulfides) were leached to investigate the effect of process variables on the dissolution of copper and gold in alkaline glycine solutions.

Copper dissolution from the gold-copper oxide ore was generally independent of glycine concentration, initial solution pH from 8-12, temperature, oxygen flow rate and galvanic interactions as the overall copper extracted after 96 hours was about 75 %. Gold dissolution from the oxide ores was improved at 60 °C with 32.2 % Au obtained against 0.5 % at 25 °C. Galvanic interactions in alkaline glycine solutions markedly improve the dissolution of gold as up to 60.4 % was extracted with 20 kg/t pyrite addition.

Copper and gold from the copper-gold sulfide ores are both influenced by glycine concentration. Higher Gly:Cu ratios favour both copper and gold dissolution while pH 11 was found to be the optimum pH for both copper and gold leaching. Copper and gold are simultaneously leached from the copper-gold sulfide ores at room temperature. The leaching

of gold at room temperature from the sulfide ores was attributed to galvanic interactions between pyrite in the ore and gold. However, the dissolution rate of both were significantly higher at 60 °C.

The influence of galvanic interactions on the leaching of gold from Cu-Au ores was quite a significant observation. Finely ground pyrite could be added to gold-copper oxide ores to improve the leaching rates of gold. However, the added pyrite should be controlled to avoid reactions that may have a counter influence on the either copper or gold.

8.2.4 Recovery of Metals from Leach Solutions

The solvent extraction/stripping and sulfide precipitation methods investigated in this thesis were focused on copper recovery only.

During the solvent extraction of copper from synthetic Cu-glycinate solution, 5 % Mextral 84H extracted 99.9 % Cu while 10 % Mextral 54-100 extracted 97.0 % Cu at an A:O ratio of 2:1. Glycine concentration in the raffinate was 100 %, indicating that the investigated extractants selectively extract copper leaving behind the glycine solution that can be recycled to the leach circuit. Spent electrolyte (30 g/L Cu, 180 g/L H_2SO_4) at 40 °C stripped 100 % copper from the loaded Mextral 54-100 at an A:O ratio of 1:10 while only 79.8 % copper was stripped from Mextral 84H under the same conditions.

Copper solvent extraction on pregnant leach solutions of natural mineral specimens showed a similar trend to that observed with the synthetic solutions. Solvent extraction from a multi-metallic component PLS such as that from chalcopyrite A showed the co-extraction of Cu, Zn, Co and Ni. However, the impurities were extracted to a much lower extent as compared to copper. These impurities were tracked during stripping and low concentrations were detected in the stripping solution. Other metals such as Fe, Mg, Ca, Si, and As were rejected by the extracts. Because gold from the copper-gold ores was also noted to be concurrently leached with copper, solvent extraction of copper from the leachate revealed that gold was not transferred by either extractant. Gold in solution could then be recovered by activated carbon adsorption.

Sulfide precipitation of copper from a synthetic copper glycinate solution using NaHS precipitated up to 99.0 % Cu in less than 10 minutes at a Cu:S ratio of 1:1. Filtration of the precipitate was found to be easy given that the precipitate particle size had a P_{80} of 66 µm. XRD analysis of the precipitate reported that it was 100 % covellite (CuS).

Copper precipitation from the multi-metallic PLS showed that about 93.0 % Cu precipitation was achieved. Impurity metals such as Zn, Ni, As and Co were also precipitated by the NaHS addition though to a lesser extent (< 10 %).

At a 1:1 Cu:S molar ratio, Cu precipitation by NaHS from a Cu-Au leachate was 87.1 %, while the concentration of gold in solution reduced by 16.2 %. It is supposed that the gold losses are as a result of Au sulphide formation or adsorption of reduced metallic gold on to CuS precipitate. The gold can then be recovered as a by-product of CuS smelting.

It was experimentally confirmed in this chapter that during the recovery of copper from leach solutions containing copper and gold by solvent extraction, gold is rejected in solution. Recently, Eksteen and Oraby (2015a) reported that gold can be efficiently recovered from alkaline leach solutions by adsorption onto activated carbon. This research therefore claims that a process flowsheet for Cu-Au ores in which both metals are concurrently leached into solution should incoporate the solvent extraction of copper and then gold recovery by activated carbon. However, the scope of this current thesis did not include experiments in which gold was directly absorbed onto the activated carbon after copper solvent extraction. It needs to be confirmed that gold could be recovered from copper depleted solution by activated carbon absorption with or without modification of the raffinate.

8.3 Proposed Process Flowsheets for Different Copper or Copper and Gold Ores

The results obtained in this research project can lead to the development of a conceptual flowsheet for the industrial production of copper and gold depending on the type of ore being processed. Different flowsheets have been proposed for different copper or gold-copper types.

8.3.1 Large Deposit of Low Grade Gold-Copper Ore

In the case of a typical large deposit containing low grade copper sulfide ore such as chalcopyrite with gold mineralisation whereby the size of the deposit justifies the construction of a L/ SX/EW plant, the process will consist of the following steps:

I. Crushing of mined ore (agglomerate if necessary) and stacking on a prepared heap leaching pad

II. Reagent make-up by adding the required amount of pH modifier (NaOH or $Ca(OH)_2$) and glycine to the predetermined water volume (Equation 8.1)

$$NaOH(aq) + NH_2CH_2COOH(aq) \rightarrow Na^+(aq) + NH_2CH_2COO^-(aq) + H_2O(l) \quad (8.1)$$

III. Leaching is conducted by spraying the leach solution on top of the heap. As the solution percolates through the heap, copper leaching occurs as per Equation 8.2 while gold is leached according to Equation 8.3:

$$CuFeS_2 + 2NH_2CH_2COO^- + 4.5O_2 + 2OH^- \rightarrow Cu(NH_2CH_2COO)_2(aq) + H_2O \; FeO(OH) + 2SO_4^{2-}(aq) \quad (8.2)$$

$$Au + 2NH_2CH_2COO^- + 0.5O_2 + H_2O \rightarrow Au(NH_2CH_2COO)_2] + 2OH^- \quad (8.3)$$

IV. The PLS collected at the bottom of the heap is clarified to remove any solids (which may aid in crud formation during solvent extraction):

V. Copper recovery from solution (through solvent extraction) and glycinate regeneration: copper is removed from solution using LIX Mextral 54-100 (or similar)

$$2RH(Org) + Cu(NH_2CH_2COO)_2(aq) \rightarrow R_2Cu(Org) + 2NH_2CH_2COOH(aq) \quad (8.4)$$

The loaded organic is stripped with a conventional electrowinning (EW) spent electrolyte

$$R_2Cu(Org) + 2H^+(aq) \rightarrow 2RH(Org) + Cu^{2+}(aq) \text{ with } SO_4^{2-} \text{ as spectator ion;} \quad (8.5)$$

Copper is recovered by electrowinning from the rich electrolyte with acid regeneration:

$$Cu^{2+}(aq) + 2e^- \rightarrow Cu\,(s) \quad \text{at cathode} \quad (8.6)$$

$$2H_2O\,(l) \rightarrow O_2(g) + 4H^+(aq) + 4e^- \quad \text{at anode} \quad (8.7)$$

VI. pH re-establishment and precipitation of sulfite/sulfate species or dissolved silicates, phosphates or aluminates by lime addition (only sulfate shown below as predominant species);

$$2NH_2CH_2COO^-(aq) + Ca(OH)_2(aq) + SO_4^{2-}(aq) \rightarrow CaSO_4 \cdot 2H_2O(s) + 2NH_2CH_2COO^-(aq) \quad (8.8)$$

VII. Gold recovery: after the solid/liquid separation of the precipitate, the solution is pumped into columns containing activated carbon for gold adsorption. The barren solution is reconstituted by adding lost glycine and adjusting to the required pH. The solution is solar heated up to 60 °C which is optimum for leaching gold and copper sulfide.

The proposed high level flowsheet for a possible industrial process is given in Figure 8.1.

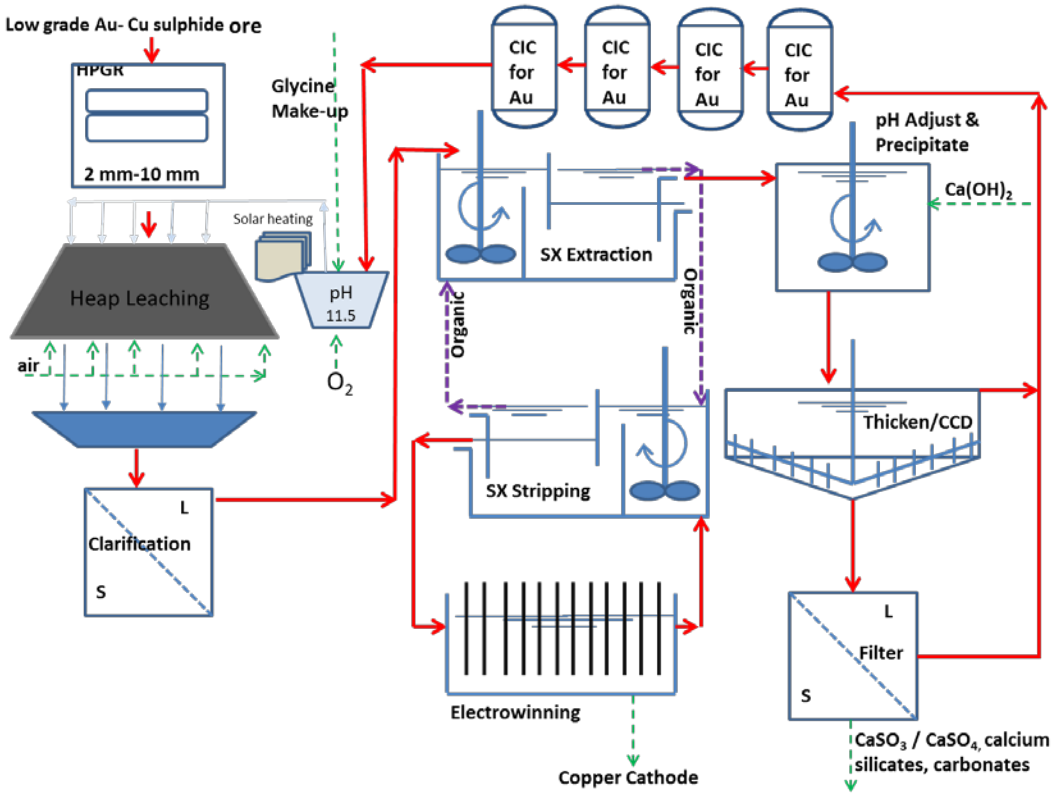

Figure 8.1 Process flow diagram for glycine based leaching of a low Au-Cu ore in an alkaline environment (copper is recovered by solvent extraction and electrowinning while gold recovery is by carbon-in-column)

8.3.2 Lean Deposit of High Grade Copper Oxide Ore

In the case of a typical lean deposit containing high grade copper oxide ore such as malachite (with no gold content), the ore is crushed, milled and atmospherically leached in an agitated tank at room temperature. The capital expenditure needed for the construction of a solvent extraction and an electrowinning plant for copper is not justified copper for such a small

deposit. Leached copper can be recovered from the PLS by precipitating with NaHS or NaS or H_2S. Results from such precipitation experiments revealed that 100 % of the precipitate is covellite. The covellite can be easily transported and sold to smelters. Figure 8.2 illustrates the steps for the possible industrial processing of such an ore.

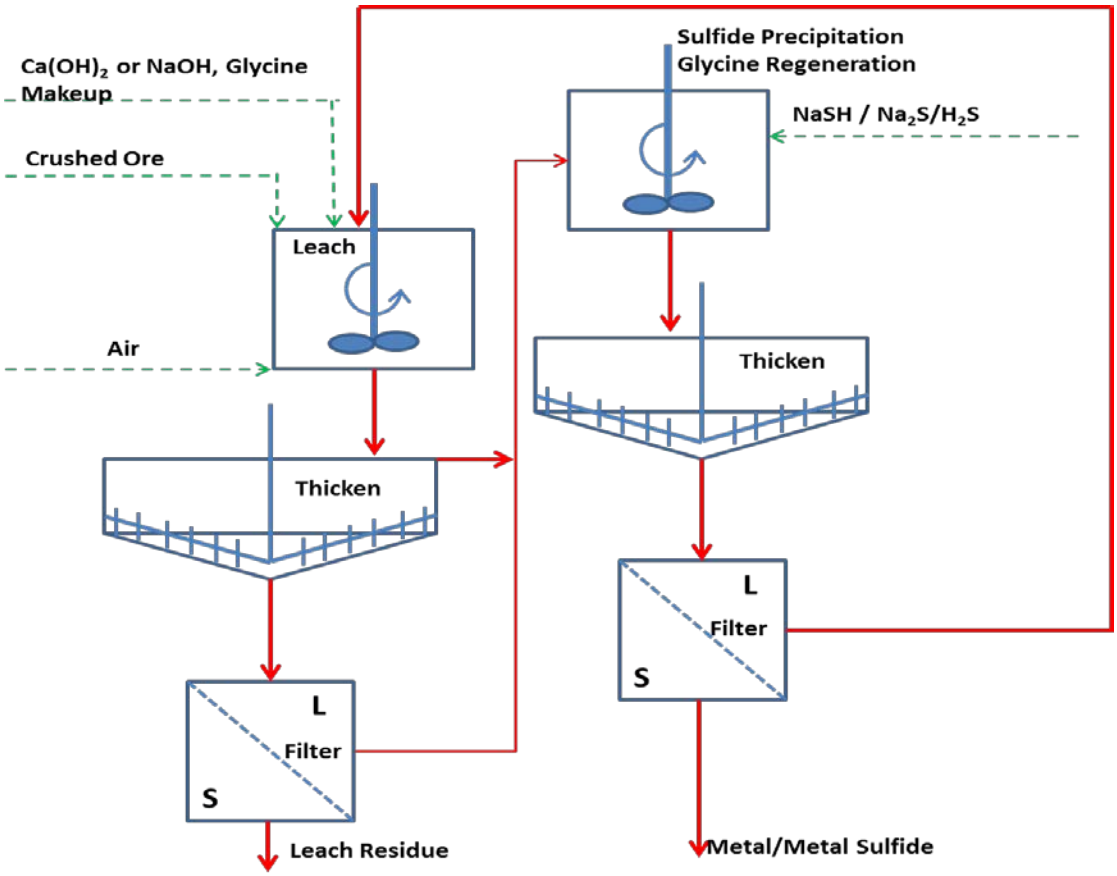

Figure 8.2 Process flow diagram for glycine based leaching of a high grade lean copper oxide deposit in an alkaline environment (copper is recovered by sulfide precipitation)

8.3.3 Copper Sulfide Flotation Concentrate with Gold Mineralization

The major difference between the processing of the flotation concentrate and a large deposit of low grade gold-copper ore is that the concentrate can undergo ultrafine grinding (P80 <10 µm) and then leached in an agitated tank under elevated temperature (60 °C) in an oxidising environment. Leach slurry also has to be filtered and the filtrate forwarded to the SX-EW stage for copper recovery. Gold recovery is through a carbon-in-column stage. A proposed process flowsheet for possible industrial application is shown in Figure 8.3.

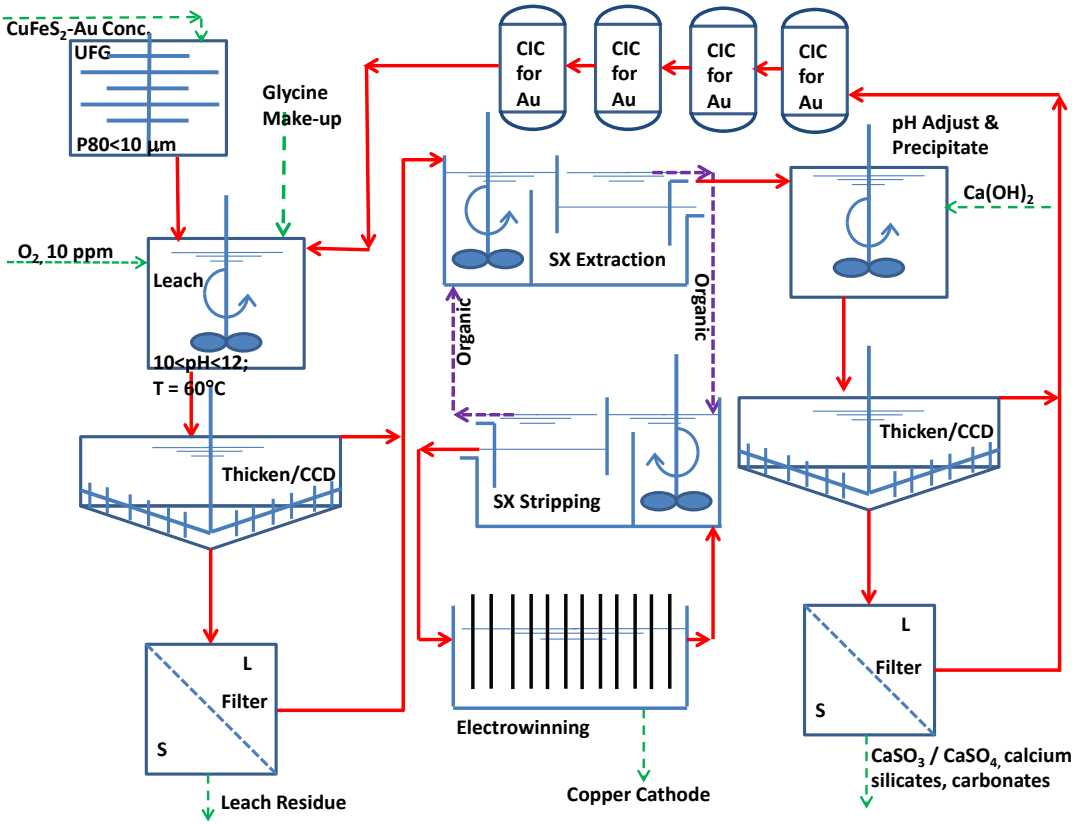

Figure 8.3 A process flow diagram for the glycine based leaching of copper sulfide ore and concentrates (with a gold content) in an alkaline environment (with concentrate ultrafine grinding, copper recovery by SX-EW and gold recovery by carbon-in-column included).

8.4 Recommendations for Further Research

The following topics have been identified as being worthy of further research:

- A more extensive study of the mechanism and leaching kinetics of gold, and the influence of copper minerals during gold leaching in order to increase the gold leaching rate;
- Focus on optimising the leaching of sulfide minerals in the alkaline glycine solution;
- Detailed investigations on glycine degradation during high temperature leaching;
- Dedicated research into impurity deportment (from alkaline glycinate solutions) should be performed to optimise the extraction and stripping conditions for a given leach system;

- Characterise nature of Au deportment during sulfide precipitation as being either Au-S compounds adsorbed gold or reduced gold and;
- Extensive column leaching experiments on a variety of copper-gold ores should be carried out to determine optimum conditions that would enhance heap leaching of low grade copper-gold ores.

Bibliography

Abbruzzese, C., Fornari, P., Massidda, R., Vegliò, F., & Ubaldini, S. (1995). Thiosulphate Leaching for Gold Hydrometallurgy. *Hydrometallurgy, 39*(1–3), 265-276.

Adams, M., Lawrence, R., & Bratty, M. (2008). Biogenic Sulphide for Cyanide Recycle and Copper Recovery in Gold–Copper Ore Processing. *Minerals Engineering, 21*(6), 509-517.

Aghamirian, M. M., & Yen, W. T. (2005). Mechanisms of Galvanic Interactions between Gold and Sulfide Minerals in Cyanide Solution. *Minerals Engineering, 18*(4), 393-407.

Aksu, S., & Doyle, F. M. (2001). Electrochemistry of Copper in Aqueous Glycine Solutions. *Journal of the Electrochemical Society, 148*(1), B51-B57.

Aksu, S., & Doyle, F. M. (2002). The Role of Glycine in the Chemical Mechanical Planarization of Copper. *Journal of the Electrochemical Society, 149*(6), G352-G361.

Aksu, S., Wang, L., & Doyle, F. M. (2003). Effect of Hydrogen Peroxide on Oxidation of Copper in Cmp Slurries Containing Glycine. *Journal of The Electrochemical Society,, 150*(11), 4505–4512.

Alexander V. Naumkin, Anna Kraut-Vass, Stephen W. Gaarenstroom, & Powell, C. J. (2012). X-Ray Photoelectron Spectroscopy Database from National Institute of of Standards and Technology. Retrieved from: http:/srdata.nist.gov/xps/.

Alonso-González, O., Nava-Alonso, F., & Uribe-Salas, A. (2009). Copper Removal from Cyanide Solutions by Acidification. *Minerals Engineering, 22*(4), 324-329.

Amari, K. E., Jdid, E.-A., & Blazy, P. (2013). Copper Recovery from Chalcopyrite Concentrate Acid Leach Solutions by Acorga M5397. *Physicochem. Probl. Miner. Process, 49*(1), 329-339.

Aminian, H., & Bazin, C. (1999). Rate of Crud Formation in a Copper Pilot Plant Settler. *Minerals Engineering, 12*(8), 985-990.

AMIRA International. (2014). Amira's Low Grade Copper Portfolio. Retrieved from: http://www.amirainternational.com/web/documents/newsletter/events/20140220_Newsflash.html#p1134.

Anthony, J. W., Bideaux, R. A., Bladh, K. W., & Nichols, M. C. (1995). *Handbook of Mineralogy*

*(*Vol. 2*)*: Mineral Data Publishing, Tucson, USA, 446 pp.

Anthony, J. W., Bideaux, R. A., Bladh, K. W., & Nichols, M. C. (2001). *Handbook of Mineralogy* (Vol. 1): Mineralogical Society of America,.

Antonijević, M. M., & Bogdanović, G. D. (2004). Investigation of the Leaching of Chalcopyritic Ore in Acidic Solutions. *Hydrometallurgy, 73*(3–4), 245-256.

Antonijević, M. M., Dimitrijević, M., & Janković, Z. (1997). Leaching of Pyrite with Hydrogen Peroxide in Sulphuric Acid. *Hydrometallurgy, 46*(1–2), 71-83.

Arzutug, M. E., Kocakerim, M. M., & Copur, M. (2004). Leaching of Malachite Ore in Nh3-Saturated Water. *Industrial & Engineering Chemistry, 43*, 4118-4123.

Ata, O. N., Çolak, S., Ekinci, Z., & Çopur, M. (2001). Determination of the Optimum Conditions for Leaching of Malachite Ore in H_2so_4 Solutions. *Chemical Engineering & Technology, 24*(4), 409-413.

Avraamides, J. (1982). *Prospects for Alternative Leaching Systems for Gold: A Review.* Paper presented at the Symposium on carbon-in-pulp technology for extraction of gold, Melbourne.369-391.

Avraamides, J., Jones, K., Staunton, W. P., & Sceresini, B. (1992). Gold Hydrometallurgy Research at the Mineral Processing Laboratory of the Department of Mines, Western Australia. *Hydrometallurgy, 30*(1–3), 163-175.

Awakura, Y., Hirato, T., Kagawa, A., Yamada, Y., & Majima, H. (1991). Dissolution of Malachite in Aqueous Ethylenediaminetetraacetate Solution. *Metallurgical Transactions B, 22*(5), 569-574.

Aylmore, M. G. (2005). Alternative Lixiviants to Cyanide for Leaching Gold Ores. In: D. A. Mike & B. A. Wills (Eds.), *Developments in Mineral Processing* (Vol. 15, pp. 501-539): Elsevier.

Baba, A. A., Adekola, F. A., Toye, E. E., & Bale, R. B. (2009). Dissolution Kinetics and Leaching of Rutile Ore in Hydrochloric Acid *Journal of Minerals & Materials Characterization & Engineering, 8*(10), 787-801.

Baker, W. E. (1973). The Role of Humic Acids from Tasmanian Podzolic Soils in Mineral Degradation and Metal Mobilization. *Geochimica et Cosmochimica Acta, 37*(2), 269-281.

Baker, W. E. (1978). The Role of Humic Acid in the Transport of Gold. *Geochimica et Cosmochimica Acta, 42*(6 PART A), 645-649.

Balaž, P. (2000). Chemical Leaching of Mechanically Activated Minerals. In: P. Balaž (Ed.), *Process Metallurgy* (Vol. Volume 10, pp. 143-193): Elsevier.

Baláž, P., Briančin, J., Šepelák, V., Havlík, T., & Škrobian, M. (1992). Non-Oxidative Leaching of Mechanically Activated Stibnite. *Hydrometallurgy, 31*(3), 201-212.

Barbetti, K., & Avraamides, J. (2003). Alternative Lixiviants (Other Than Thiosulfate) for the Extraction of Gold – a Status Review.

Bartlett, R. W. (1998). *Solution Mining :Leaching and Fluid Recovery of Materials* (Second ed.): Gordon and Breach Science Publichers.

Bas, A. D., Yazici, E. Y., & Deveci, H. (2012). Treatment of a Copper - Rich Gold Ore by Ammonia Assisted Cyanide Leaching, New Delhi, 356-365.

Bateman, A. M. (1952). Economic Mineral Deposits. *The Journal of Geology, 60*(2), 193-197.

Batsala, M., Chandu, B., Sakala, B., Nama, S., & Domatoti, S. (2012). Inductively Coupled Plasma Mass Spectrometry (Icp-Ms). *International Journal of Research In Pharmacy And Chemistry, 2*(3), 671-680.

Beckstead, L. W., & Miller, J. D. (1977). Ammonia, Oxidation Leaching of Chalcopyrite — Reaction Kinetics. *Metallurgical Transactions B, 8B*(1), 19-29.

Bell, S. L., Welch, G. D., & Bennett, P. G. (1995). Development of Ammoniacal Lixiviants for the in-Situ Leaching of Chalcopyrite. *Hydrometallurgy, 39*(1), 11-23.

Berger, P., Karpel Vel Leitner, N., Doré, M., & Legube, B. (1999). Ozone and Hydroxyl Radicals Induced Oxidation of Glycine. *Water Research, 33*(2), 433-441.

Bingöl, D., Canbazoğlu, M., & Aydoğan, S. (2005). Dissolution Kinetics of Malachite in Ammonia/Ammonium Carbonate Leaching. *Hydrometallurgy, 76*(1–2), 55-62.

Biswas, A. K., & Davenport, W. G. (1976). *Extractive Metallurgy of Copper* (First Edition): Pergamon Press, Great Britain.

Biswas, A. K., & Davenport, W. G. (1994). Chapter 18 - Hydrometallurgical Copper Extraction:

Introduction and Leaching *Extractive Metallurgy of Copper (Third Edition)* (pp. 358-382). Amsterdam: Pergamon.

Bogdanovskaya, V. A., Safronov, A. Y., Tarasevich, M. R., & Chernyak, A. S. (1986). Adsorption and Anodic Oxidation of Glycylglycine and Some Amino Acids on a Gold Electrode. *Journal of Electroanalytical Chemistry and Interfacial Electrochemistry, 202*(1–2), 147-167.

Böttger, A. J., Delhez, R., & Mittemeijer, E. J. (2000). Advanced Fundamental Parameters Model for Improved Profile Analysis. *Materials Science Forum, 347-349*, 303-308.

Breuer, P. L., & Jeffrey, M. I. (2000). Thiosulfate Leaching Kinetics of Gold in the Presence of Copper and Ammonia. *Minerals Engineering, 13*(10), 1071-1081.

Breuer, P. L., Jeffrey, M. I., & Hewitt, D. M. (2008). Mechanisms of Sulfide Ion Oxidation During Cyanidation. Part I: The Effect of Lead(Ii) Ions. *Minerals Engineering, 21*(8), 579-586.

Briggs, D. F. (2014). What Is a Porphyry Copper Deposit? Retrieved from http://www.libertystaruranium.com/wp-content/uploads/2012/03/What-is-a-Porphyry-Copper-Deposit_David-F-Briggs-TucsonCitizen.com-20140111.pdf.

Brion, D. (1980). Photoelectron Spectroscopic Study of the Surface Degradation of Pyrite (Fes2), Chalcopyrite (Cufes2), Sphalerite (Zns), and Galena (Pbs) in Air and Water Appl Surf Sci, 5, 133-152.

Brook Hunt. Copper. Retrieved from http://www.oracleminingcorp.com/copper/.

Brown, D. H., Smith, W. E., Fox, P., & Sturrock, R. D. (1982). The Reactions of Gold(0) with Amino Acids and the Significance of These Reactions in the Biochemistry of Gold. *Inorganica Chimica Acta, 67*, 27-30.

Bukharov, M. S., Shtyrlin, V. G., Mamin, G. V., Mukhtarov, A. S., & Gilyazetdinov, E. M. (2012). Rotational Dynamics of Copper(Ii) Amino Acid Complexes by EPR and NMR Relaxation Methods. *Journal of Physics: Conference Series, 394*(1).

Bukharov, M. S., Shtyrlin, V. G., Mukhtarov, A. S., Mamin, G. V., Stapf, S., Mattea, C., KrutiKov, A., Il'in, A., Serov, N. Y. (2014). Study of Structural and Dynamic Characteristics of Copper(Ii) Amino Acid Complexes in Solutions by Combined Epr and Nmr Relaxation Methods. *Physical Chemistry Chemical Physics, 16*(20), 9411-9421.

Burkin, A. R. (2001). *Chemical Hydrometallurgy: Theory and Principles*: Imperial College Press.,River Edge, NJ, 414p.

Cai, X.-H., & Xie, B. (2014). Recent Advances on Asymmetric Strecker Reactions. *Archive for Organic Chemistry, 2014*(1), 205-248.

Campbell, L. L. (1955). The Oxidative Degradation of Glycine by a Pseudomonas. *Journal of Biological Chemistry, 217*(2), 669-674.

Carlile, J. C., & Mitchell, A. H. G. (1994). Magmatic Arcs and Associated Gold and Copper Mineralization in Indonesia. *Journal of Geochemical Exploration, 50*(1–3), 91-142.

Chan, W. C., Higton, A., & Davies, J. S. (2006). Amino Acids *Amino Acids, Peptides and Proteins: Volume 35*, pp. 1-73: The Royal Society of Chemistry.

Chemicalland21 (2017). Glycine. Retrieved from http://www.chemicalland21.com/lifescience/foco/GLYCINE.htm.

Chen, H.-Y., Jang, S., Jinn, T.-R., Chang, J.-Y., Lu, H.-F., & Li, F.-Y. (2012). Oxygen Radical-Mediated Oxidation Reactions of an Alanine Peptide Motif - Density Functional Theory and Transition State Theory Study. *Chemistry Central Journal, 6*, 33-33.

Chen, S., Lei, H., & Chen, R. (2013). Effect of Ph on Hard Disk Substrate Polishing in Glycine-Hydrogen Peroxide System Abrasive-Free Slurry (Vol. 562-565, pp. 691-696). Hangzhou.

Cheng, C. Y., & Lawson, F. (1991). The Kinetics of Leaching Chalcocite in Acidic Oxygenated Sulphate-Chloride Solutions. *Hydrometallurgy, 27*(3), 249-268.

Chengyan, W. (2005). *Crud Formation and Its Control in Solvent Extraction* Paper presented at the The 17th International Solvent Extraction Conference Beijing, China. 1066-1071.

Chia, C. L., Taro, U., Chang, C. H., & Masatoshi, O. (2013). Adsorption and Oxidation of Glycine on Au Electrode: An in Situ Surface-Enhanced Infrared Study. *Electrochemistry Communications, 34*(0), 56-59.

Chiacchiarini, P., Fuente, V. d. l., & Donati‡, E. (2003). Pre-Treatment of a Refractory Gold Sulfide Ore by Means of Acidithiobacilli Cells. *Latin American applied research, 33*.

Chin, D., & Achari, R. G. (1982). Analysis of Glycine in Antiperspirant Products by Hpl. *Journal*

of the Society of Cosmetic Chemists, 33, 259-362.

Chmielewski, T., Wódka, J., & Iwachów, Ł. (2009). Ammonia Pressure Leaching for Lubin Shale Middlings. *Physicochemical Problems of Mineral Processing, 43*, 5-10.

Cooper, R. M., Parkinson, G. M., & Newman, O. M. G. (2000). The Precipitation of Silica from Acidic Zinc Leach Liquors. In: B. S. Gupta & S. Ibrahim (Eds.), *Mixing and Crystallization: Selected Papers from the International Conference on Mixing and Crystallization Held at Tioman Island, Malaysia in April 1998* (pp. 163-176). Dordrecht: Springer Netherlands.

Córdoba, E. M., Muñoz, J. A., Blázquez, M. L., González, F., & Ballester, A. (2008). Leaching of Chalcopyrite with Ferric Ion. Part I: General Aspects. *Hydrometallurgy, 93*(3–4), 81-87.

Couriol, C., Fauduet, H., Porte, C., & Delacroix, A. (1999). Setup of Glycine Continuous Synthesis by Ammonolysis of Monochloroacetic Acid. *Laboratory Robotics and Automation, 11*(1), 29-35.

Cox, M. (2004). Solvent Extraction in Hydrometallurgy *Solvent Extraction Principles and Practice* (Second edition). New York: Marcel Dekker, Inc., p480.

Cropp, A. F., Goodall, W. R., & Bradshaw, D. J. (2013). *The Influence of Textural Variation and Gangue Mineralogy on Recovery of Copper by Flotation from Porphyry Ore – a Review.* Paper presented at the The Second AusIMM International Geometallurgy Conference (GeoMet), Brisbane, 279-292.

Crundwell, F. K. (2013). The Dissolution and Leaching of Minerals: Mechanisms, Myths and Misunderstandings. *Hydrometallurgy, 139*(0), 132-148.

Crundwell, F. K., Moats, M. S., Ramachandran, V., Robinson, T. G., & Davenport, W. G. (2011). Extractive Metallurgy of Nickel, Cobalt and Platinum-Group Metals: Amsterdam:Elsevier, p622.

D'Aloya, A., & Nikoloski, A. N. (2012). The Passivation of Iron in Ammoniacal Solutions Containing Copper (Ii) Ions. *Hydrometallurgy, 111–112*(0), 58-64.

Dai, X., Simons, A., & Breuer, P. (2012). A Review of Copper Cyanide Recovery Technologies for the Cyanidation of Copper Containing Gold Ores. *Minerals Engineering, 25*(1), 1-13.

Dalton, R. F., Diaz, G., Price, R., & Zunkel, A. D. (1991). The Cuprex Metal Extraction Process:

Recovering Copper from Sulfide Ores. *JOM, 43*(8), 51-56.

Daniel, M. (2007). Energy Efficient Mineral Liberation Using HPGR Technolog. PhD thesis.University of Queensland, JKMRC, Brisbane, Australia.

Das, R. P., & Anand, S. (1995). Precipitation of Iron Oxides from Ammonia-Ammonium Sulphate Solutions. *Hydrometallurgy, 38*(2), 161-173.

Dasgupta, R., Guan, Y. C., & Han, K. N. (1997). The Electrochemical Behavior of Gold in Ammoniacal Solutions at 75 °C. *Metallurgical and Materials Transactions B, 28*(1), 5-12.

Davenport, W. G., King, M., Schlesinger, M., & Biswas, A. K. (2002a). Chapter 17 - Hydrometallurgical Copper Extraction: Introduction and Leaching. In W. G. Davenport, M. King, M. Schlesinger, & A. K. Biswas (Eds.), *Extractive Metallurgy of Copper* (pp. 289-305). Oxford: Pergamon.

Davenport, W. G., King, M., Schlesinger, M., & Biswas, A. K. (2002b). Chapter 18 - Solvent Extraction Transfer of Cu from Leach Solution to Electrolyte, *Extractive Metallurgy of Copper* (pp. 307-325). Oxford: Pergamon.

Davis, A., Tran, T., & Young, D. R. (1993). Solution Chemistry of Iodide Leaching of Gold. *Hydrometallurgy, 32*(2), 143-159.

de Farias, R. F., Scatena Júnior, H., & Airoldi, C. (1999). Thermoanalytical Investigations About the Metal–Amino Acid Interactions. *Journal of Inorganic Biochemistry, 73*(4), 253-257.

Deng, T. M., Yu. (1995). Enhancing Gold Extraction from Copper Bearing Ores. *Transctions of NFsoc, 5*(3).

Dennis H. Green & Jeffrey J. Mueller, B. C. O. (1999). US Patent No. US 5961833.

Deschênes, G., & Prud'homme, P. J. H. (1997). Cyanidation of a Copper-Gold Ore. *International Journal of Mineral Processing, 50*(3), 127-141.

Deshpande, S., Kuiry, S. C., Klimov, M., Obeng, Y., & Seal, S. (2004). Chemical Mechanical Planarization of Copper: Role of Oxidants and Inhibitors. *Journal of the Electrochemical Society, 151*(11), G788-G794.

DeVries, F. W., & Hiskey, J. B. (1992). *Environmental Impact of Lixiviants : An Overview That*

Includes Noncyanide Chemistry. Paper presented at the Randol Gold Forum, Randol, CO, USA. 89-92

Dougherty, D. A., & Anslyn, E. (2005). *Modern Physical Organic Chemistry.* Sausalito-California: University Science Books, Sausalito, CA, 2006. 1104 pp.

Drauz, K., Grayson, I., Kleemann, A., Krimmer, H. P., Leuchtenberger, W., & Weckbecker, C. (2000). Amino Acids *Ullmann's Encyclopedia of Industrial Chemistry*: Wiley-VCH Verlag GmbH & Co. KGaA., Weinheim, Germany.

Drauz, K., Grayson, I., Kleemann, A., Krimmer, H.P., Leuchtenberger, W., & Weckbecker, C. (2007). Amino Acids, Ullmann's Encyclopedia of Industrial Chemistry 6th Ed: Wiley-VCH Verlag GmbH & Co. KGaA., Weinheim, Germany.

Dreisinger, D., & Abed, N. (2002). A Fundamental Study of the Reductive Leaching of Chalcopyrite Using Metallic Iron Part I: Kinetic Analysis. *Hydrometallurgy, 66*(1–3), 37-57.

Du, T., Luo, Y., & Desai, V. (2004). The Combinatorial Effect of Complexing Agent and Inhibitor on Chemical–Mechanical Planarization of Copper. *Microelectronic Engineering, 71*(1), 90-97.

Duda, L. L., & Bartecki, A. (1982). Dissolution of Cu_2S in Aqueous Edta Solutions Containing Oxygen. *Hydrometallurgy, 8*(4), 341-354.

Dun-Fang, L., Cheng-Yan, W., Yin Fei, Yong-Qiang, C., & Xiao-Wu, J. (2009). Effect of Additive on Copper Removal from Spent Lithium-Ion Batteries by Ammoniacal Leaching. *Chinese Journal of Power Sources, 33*(6).

Dunne, R. (1991). *Auriferous Sulphide Flotation in Australia*. Paper presented at the Randol Gold Forum 91, Cairns, Randol International, Golden, Colorado, 239-244.

Dutrizac, J. E. (1978). The Kinetics of Dissolution of Chalcopyrite in Ferric Ion Media. *Metallurgical Transactions B, 9*(3), 431-439.

Dutrizac, J. E. (1981). The Dissolution of Chalcopyrite in Ferric Sulfate and Ferric Chloride Media. *Metallurgical Transactions B, 12*(2), 371-378.

Egerton, R. F. (2005). The Scanning Electron Microscope *Physical Principles of Electron Microscopy: An Introduction to Tem, Sem, and Aem* (pp. 125-151): Springer Science+Business Media, Inc.

Ekmekyapar, A., Aktas, E., Kunkul, A., & Demirkiran, N. (2012). Investigation of Leaching Kinetics of Copper from Malachite Ore in Ammonium Nitrate Solutions. *Metallurgical and Materials Transactions B, 43B*, 764-772.

Ekmekyapar, A., Demirkiran, N., Künkül, A., & Akta, E. (2015). Leaching of Malachite Ore in Ammonium Sulfate Solutions and Production of Copper Oxide. *Brazilian Journal of Chemical Engineering, 32*, 155-165.

Ekmekyapar, A., Oya, R. & Künkül, A. (2003). Dissolution Kinetics of an Oxidized Copper Ore in Ammonium Chloride Solution. *Chemical and Biochemical Engineering Quarterly, 17*(4), 261–266.

Eksteen, J. J., & Oraby, E. A. (2015a). The Leaching and Adsorption of Gold Using Low Concentration Amino Acids and Hydrogen Peroxide: Effect of Catalytic Ions, Sulphide Minerals and Amino Acid Type. *Minerals Engineering, 70*(0), 36-42.

Eksteen, J. J., & Oraby, E. A. (2015b). A Process for Copper and/or Precious Metal Recovery: Google Patents.

Eksteen, J. J., Oraby, E. A., & Tanda, B. C. (2017). A conceptual process for copper extraction from chalcopyrite in alkaline glycinate solutions. *Minerals Engineering, 108*(0), 53-66.

Encyclopædia Britannica. (2016). Chalcocite. Retrieved from http://www.britannica.com/science/chalcocite.

European Innovation Partnership on Raw Materials. (2014). Metal Recovery from Low Grade Ores and Wastes. Retrieved from https://ec.europa.eu/growth/tools-databases/eip-raw-materials/en/content/meal-recovery-low-grade-ores-and-wastes.

Faltens, M. O., & Shirley, D. A. (1970). Mössbauer Spectroscopy of Gold Compounds. *The Journal of Chemical Physics, 53*(11), 4249-4264.

Feng, D., & Van Deventer, J. S. J. (2011). The Role of Amino Acids in the Thiosulphate Leaching of Gold. *Minerals Engineering, 24*(9), 1022-1024.

Feng, Q., Wen, S., Zhao, W., LV, C., & Bai, X. (2015). Leaching of Copper from Malachite with Methane-Sulfonic Acid. *Solvent extraction research and devlopment, Japan, 22*(2), 159-168.

Fetzer, W. G. (1934). Transportation of Gold by Organic Solutions. *Economic Geology, 29*(6),

599-604.

Fetzer, W. G. (1946). Humic Acids and True Organic Acids as Solvents of Minerals. *Economic Geology, 41*(1), 47-56.

Filmer, A., Parker, A. J., Clare, B. W., & Wadley, L. G. B. (1979). Oxidation of Copper Sulfides in Aqueous Ammonia:Kinetic Characteristics *Australian Journal of Chemistry, 32*, 2597-2609.

First Quantum Minerals.(2016) Las Cruces. Retrived from http://www.first-quantum.com/Our-Business/operating-mines/Las-Cruces/default.aspx.

Fleck, M., & Petrosyan, A. M. (2014). Salts of Amino Acids: Crystallization, Structure and Properties: Springer international Press, New York, 574pp.

Fleming, C. A. (2005). Cyanide Recovery. In: D. A. Mike & B. A. Wills (Eds.), *Developments in Mineral Processing* (Vol. 15, pp. 703-727): Elsevier, New York.

Ford, K. J. R., Henderson, R. D., & Fleming, C. A. (2008). Application of the Sart Process to Heap Leaching of Gold-Copper Ores at Maricunga, Chile. SGS Minerals Services Technical Paper, 51. Retrived from http://www.sgsgroup.com.ar/~/media/Global/Documents/Technical%20Documents.

Free, M. L. (2013). Hydrometallurgy; Fundamentals and Applications. *Reference and Research Book News, 28*(6).

Frost, R., Reddy, L., Fayazuddin, M., & Endo, T. (2007). Electron Paramagnetic Resonance and Optical Absorption Spectral Studies on Chalcocite. *Spectrochimica Acta, A*(68), 420-423.

Fujiwara, K., Ueda, N., Matsuu, Y., Kato, H., & Hiai, A. (1993). Reacting Glyconitrile, Ammonia, Carbondioxide and Water to Obtain Reaction Solution, Concentration in Two Steps-Gas Phase and Liquid Phase: Google Patents.

Gill, F. (1997). X-Ray Fluorescence Spectrometry. In R. Gill (Ed.), Modern Analytical Geochemistry: An Introduction to Quantitative Chemical Analysis for Earth, Environmental and Material Scientists (pp. 87-115). UK: Addison Wesley Longman.

Gálvez, E. D., Vega, C. A., Swaney, R. E., & Cisternas, L. A. (2004). Design of Solvent Extraction Circuit Schemes. *Hydrometallurgy, 74*(1–2), 19-38.

Galvin, K. P., Nicol, S. K., & Waters, A. G. (1992). Selective Ion Flotation of Gold. *Colloids and Surfaces, 64*(1), 21-33.

Gardner, J. R., & Woods, R. (1979). An Electrochemical Investigation of the Natural Flotability of Chalcopyrite. *Int. J. Miner. Process, 6*, 1-18.

Geoscience Australia 2007. Australia's Identified Mineral Resources 2007. Geoscience Australia, Canberra, 95 pp.

Ghahremaninezhad, A. (2012). *The Surface Chemistry of Chalcopyrite During Electrochemical Dissolution.* The University of British Columbia, Vancouver, Canada.

Ghorbani, Y., Becker, M., Petersen, J., Mainza, A. N., & Franzidis, J.-P. (2013). Investigation of the Effect of Mineralogy as Rate-Limiting Factors in Large Particle Leaching. *Minerals Engineering, 52*, 38-51.

Gos, S., & Rubo, A. (2001). The Relevance of Alternative Lixiviants with Regard to Technical Aspects, Work Safety and Environmental Safety. *Infomine*.

Green, D. H., & Mueller, J. J. (1999). Method for Separating and Isolating Gold from Copper in a Gold Processing System. from HW Process Technologies, Inc. (Lakewood, CO http://www.freepatentsonline.com/5961833.html.

Greenberg, D. M. (1951). Amino Acids and Proteins: Theory, Methods, Application: Springfield, Illinois, U.S.A. : Charles C. Thomas, 950pp.

Groudev, S. N., Ivanov, I. M., Spasova, I. I., & Groudeva, V. I. (1995). *Pilot Scale Microbial Leaching of Gold and Silver from an Oxide Ore in Elshitza Mine, Bulgaria*, Snowbird, UT, USA.135-144.

Guan, Y. C., & Han, K. N. (1997). The Leaching Kinetics of Chalcopyrite (Cufes2) in Ammonium Lodide Solutions with Iodine. *Metallurgical and Materials Transactions B, 28*(6), 979-985.

Gupta, C. K., & Mukherjee, T. K. (1990). *Hydrometallurgy in Extraction Processes* (Vol. I): CRC Pres. Boston, Massachusetts, USA.

Gylieneé, O. (2001). *Insoluble Compounds of Heavy Metal Complexes.* Paper presented at the XVI-th ARS SEPARATORIA, Borówno, Poland. Rerieved from www.ars_separatoria.chem.uni.torun.pl/2001_Symp/PDF/gylienekars.pdf.

Habashi, F. (1970). *Principles of Extractive Metallurgy* (Vol. 1. general Principles). New York – London – Paris: Gordon & Breach Science Publisher.

Habashi, F. (1980). *Principles of Extractive Metallurgy* (Vol. 2). New York: Gordon and Beach, Science Publishers, Inc.

Habashi, F. (1989). In-Situ and Dump Leaching Technology: Application to Phosphate Rock. *Fertilizer Research*(18), 275-279.

Habashi, F. (2009). Recent Trends in Extractive Metallurgy. *Journal of Mining and Metallurgy, 45 (1) B,* 1-13

Halpern, J. (1953). Kinetics of the Dissolution of Copper in Aqueous Ammonia. *Journal of the Electrochemical Society, 100*(10), 421-428.

Han, K. N., & Fuerstenau, M. C. (2000). Factors Influencing the Rate of Dissolution of Gold in Ammoniacal Solutions. *International Journal of Mineral Processing, 58*, 361-381.

Harmer, S. L., Thomas, J. E., Fornasiero, D., & Gerson, A. R. (2006). The Evolution of Surface Layers Formed During Chalcopyrite Leaching. *Geochimica et Cosmochimica Acta, 70*(17), 4392-4402.

Haver, F. P., & Wong, M. M. (1971). Recovery of Copper, Iron, and Sulfur from Chalcopyrite Concentrate Using a Ferric Chloride Leach. *JOM, 23*(2), 25-29.

Hayes, G. A., & Corrans, I. J. (1992). *Leaching of Gold-Copper Ores Using Ammoniacal Cyanide*, Kalgoorlie, Aust.349-353.

Hedley, N., & Tabachnick, H. (1968). *Chemistry of Cyanidation*: American Cyanamid Company.

Hegyi, G., Kardos, J., Kovács, M., Málnási-Csizmadia, A., Nyitray, L., Pál, G, Radnai, L., Reményi, A., Venekei, I., (2013). Introduction to Practical Biochemistry: Eötvös Loránd University, Hungary.

Henn, U., & Milisenda, C. C. (2004). *Gemmological Tables*: German Gemmological Association.

Hilson, G., & Monhemius, A. J. (2006a). Alternatives to Cyanide in the Gold Mining Industry: What Prospects for the Future? *Journal of Cleaner Production, 14*(12-13 SPEC. ISS.), 1158-

1167.

Hilson, G., & Monhemius, A. J. (2006b). Alternatives to Cyanide in the Gold Mining Industry: What Prospects for the Future? *Journal of Cleaner Production, 14*(12–13), 1158-1167.

Holliday, J. R., & Cooke, D. R. (2007). *Advances in Geological Models and Exploration Methods for Copper ± Gold Porphyry Deposits.* Paper presented at the Proceedings of Exploration 07: Fifth Decennial International Conference on Mineral Exploration.791-809

Howard T. Evans, J. (1979). The Crystal Structures of Low Chalcocite and Djurleite. *Zeitschrift fUr Kristallographie, 150*, 99-320

Hsu, Y. J., Wong, P. L. M., & Nguyen, H. H. (1997). *Copper-Gold Interaction During the Processing of Copper-Gold Ores*. Paper presented at the World Gold '97 Conference (1997 : Singapore) & Australasian Institute of Mining and Metallurgy 1997, World Gold '97 : 1 - 3 September 1997, Singapore, The Institute, Carlton, Vic.

Hu, H.-p., Liu, C.-x., Han, X.-t., Liang, Q.-w., & Chen, Q.-y. (2010). Solvent Extraction of Copper and Ammonia from Ammoniacal Solutions Using Sterically Hindered B-Diketone. *Transactions of Nonferrous Metals Society of China, 20*(10), 2026-2031.

Huang, M., Lv, S., & Zhou, C. (2013). Thermal Decomposition Kinetics of Glycine in Nitrogen Atmosphere. *Thermochimica Acta, 552*, 60-64.

Hunt, B. (1901). Process of Precipitating and Recovering Precious Metals from Their Solutions: Google Patents.

Iasillo, E., Rempel, C., & Holtzapple, A. (2013). Development of Accurate Metal Production Forecasts for a Heap Leach Project Using Metsim Dynamic Simulation and Defensible Column Leach Testing Data. *InfoMine*.

Imamura, T., Hatanaka, C., & Douoou, T. (1978). Preparation of Copper (Ii)-Glycine Complex. *J. Fac. Fish. Anim. Husb, 17*, 35-41.

Insausti, M. J., Mata-perez, F., & Alvarez-Macho, P. (1992). Permanganate Oxidation of Glycine: Influence of Amino Acid on Colloidal Manganese Dioxide. *International Journal of Chemical Kinetics, 24*(5), 411–419.

International Atomic Energy Agency. (2001). *Manual of Acid in Situ Leach Uranium Mining*

Technology Retrieved from: www-pub.iaea.org/MTCD/Publications/PDF/te_1239_prn.pdf.

International Copper Study Group. (2013). *The World Copper Factbook 2013*. Retrieved from

International Cyanide Management Institue. (2009). International Cyanide Management Code for the Gold Industry. Retrieved from https://www.cyanidecode.org/.

Jeffrey, M. I., Linda, L., Breuer, P. L., & Chu, C. K. (2002). A Kinetic and Electrochemical Study of the Ammonia Cyanide Process for Leaching Gold in Solutions Containing Copper. *Minerals Engineering, 15*(12), 1173-1180.

Jeffrey, M. I., Thompson, D., Chu, C. K., & Breuer, P. (2006). Galvanic Interactions between Gold and Sulfides During Thiosulfate Leaching. *ECS Transactions, 2*(3), 133-142.

Jenkins, R. (2000). X-Ray Techniques: Overview *Encyclopedia of Analytical Chemistry* (pp. 13269–13288, John Wiley & Sons Ltd. Chichester, Sussex, England.

Jergensen, G. V. (1999). *Copper Leaching, Solvent Extraction, and Electrowinning Technology*. Littleton, CO, USA: Society for Mining Metallurgy and Exploration.

Jiang, T., Wang, D., Yang, Y. B., & Li, Q. (2013). Effect of Copper and Ammonia on Consumption of Thiosulfate in Gold Leaching Solutions, San Antonio, TX.511-518

Jiang, T., Zhang, Y. Z., Yang, Y. B., & Huang, Z. C. (2001). Influence of Copper Minerals on Cyanide Leaching of Gold. *Journal of Central South University of Technology (English Edition), 8*(1), 24-28.

Jingrong, Z., Jianjun, L., Fan, Y., Jingwei, W., & Fahua, Z. (1996). An Experimental Study on Gold Solubility in Amino Acid Solution and Its Geological Significance. *Chinese Journal of Geochemistry, 15*(4), 296-302.

Juhász, Z., & Opoczky, L. (1990). Mechanical Activation of Minerals by Grinding : Pulverizing and Morphology of Particles. Budapest: Akadémiai Kiadó. 234pp.

Junior, C., Nascimento, M., Yokoyama, L., & O. Cunha. (2012). Experimental Design in Solvent Extraction: A Study for Divalent Metals Separation in D2ehpa/Isoparaffin System. *Engineering Geology, 4* (No. 11), 816-825.

Kadachia, A. N., & Al-Eshaikhb, M. A. (2012). Limits of Detection in Xrf Spectroscopy. *X-ray*

Spectrometry, 41, 350-354.

Kajala, A., & Gupta, O. D. (2009). Determination of Stability Constants of as(Iii) Complexes with Glicine in Dmf and Dmso at Dropping Mercury Electrode. *Rasayan Journal of Chemistry, 2*(4), 833-835.

Karahan, İ. H. (2013). Effects of pH Value of the Electrolyte and Glycine Additive on Formation and Properties of Electrodeposited Zn-Fe Coatings. *Scientific World Journal*, 2013, 7.

Kenney, C. W., Elmore, C. E., & Brison, R. J. (1987). *New Technology for More Efficient Cyanidation of Gold Ores.* Paper presented at the Proceedings of the Metallurgical Society of the Canadian Institute of Mining and Metallurgy, Wnnipeg, Canada. 295-307

Kerrich, R., Goldfarb, R., Groves, D., & Garwin, S. (2000). The Geodynamics of World-Class Gold Deposits: Characteristics, Space–Time Distribution and Origins. *Society of Economic Geologists 13* (0), 501–552.

Kesler, S. E., Chryssoulis, S. L., & Simon, G. (2002). Gold in Porphyry Copper Deposits: Its Abundance and Fate. *Ore Geology Reviews, 21*(1–2), 103-124.

Khorrami, S. A., Bayat, H., Sharifi, S., & Shafai, M. (1996). Stability Constant of Vanadium(V) with Glycine at Different Ionic Strengths. *Journal of Chemical Engineering, 41*, 1322-1324.

Kiss, T., Sovago, I., & Gergely, A. (1991). Critical Survey of Stability Constants of Complexes of Glycine. *Pure and applied chemistry, 63*(4), 597-638.

Klauber, C. (2008). A Critical Review of the Surface Chemistry of Acidic Ferric Sulphate Dissolution of Chalcopyrite with Regards to Hindered Dissolution. *International Journal of Mineral Processing, 86*(1–4), 1-17.

Klauber, C., Parker, A., van Bronswijk, W., & Watling, H. (2001). Sulphur Speciation of Leached Chalcopyrite Surfaces as Determined by X-Ray Photoelectron Spectroscopy. *International Journal of Mineral Processing, 62*(1–4), 65-94.

Koch, D. M., Toubin, C., Peslherbe, G. H., & Hynes, J. T. (2008). A Theoretical Study of the Formation of the Aminoacetonitrile Precursor of Glycine on Icy Grain Mantles in the Interstellar Medium. *The Journal of Physical Chemistry C, 112*(8), 2972-2980.

Kochhar, S., Mouratou, B., & Christen, P. (2002). Amino Acid Analysis by Precolumn

Derivatization with 1-Fluoro-2,4-Dinitrophenyl-5-L-Alanine Amide (Marfey's Reagent). In J. Walker (Ed.), *The Protein Protocols Handbook* (pp. 567-572): Humana Press, New York, United States.

Koleini, S. M. J., Aghazadeh, V., & Sandström, Å. (2011). Acidic Sulphate Leaching of Chalcopyrite Concentrates in Presence of Pyrite. *Minerals Engineering, 24*(5), 381-386.

Konishi, H. (2007). Selective Separation and Recovery of Copper from Iron and Copper Mixed Waste by Ammonia Solution. *ISIJ International, 36*, 73-79.

Konishi, Y., Katoh, M., & Asai, S. (1991). Leaching Kinetics of Copper from Natural Chalcocite in Alkaline Na4edta Solutions. *Metallurgical Transactions B, 22*(3), 295-303.

Kordosky, G. A. (2002). Copper Recovery Using Leach/Solvent Extraction/Electrowinning Technology:Forty Years of Innovation, 2.2 Million Tonnes of Copper Annually. *The Journal of The South African Institute of Mining and Metallurgy*, 445-450.

Kordosky, G. A., Sudderth, R. B., & Virnig, M. J. (1999). Evolutionary Development of Solvent Extraction Reagents: Real-Lve Experiences. In: G. V. J. II (Ed.), *Copper Leaching, Solvent Extraction, and Electrowinning Technology*: Society for Mining, Metallurgy, and Exploration, Inc. Englewood, Colorado, USA.

Korobushkina, E. D., Cherniak, A. S., & Mineev, G. G. (1974). Dissolution of Gold by Microorganisms and by Products of Their Metabolism (Russian). *Mikrobiologiya, 43*(1), 49-54.

Korte, F., & Coulston, F. (1998). Some Considerations on the Impact on Ecological Chemical Principles in Practice with Emphasis on Gold Mining and Cyanide. *Ecotoxicology and Environmental Safety, 41*(2), 119-129.

Korte, F., Spiteller, M., & Coulston, F. (2000). The Cyanide Leaching Gold Recovery Process Is a Nonsustainable Technology with Unacceptable Impacts on Ecosystems and Humans: The Disaster in Romania. *Ecotoxicology and Environmental Safety, 46*(3), 241-245.

Koyama, K., Tanaka, M., & Lee, J.-c. (2006). Copper Leaching Behavior from Waste Printed Circuit Board in Ammoniacal Alkaline Solution. *Materials Transactions, 47*(7), 1788 -1792.

Künkül, A., Gülezgin, A., & Demİrkiran, N. (2013). Investigation of the Use of Ammonium Acetate as an Alternative Lixiviant in the Leaching of Malachite Ore *Chemical Industry &*

Chemical Engineering Quarterly 19 (1) 25–35, 19(1), 25-35.

Künkül, A., Muhtar Kocakerim, M., Yapici, S., & Demirbağ, A. (1994). Leaching Kinetics of Malachite in Ammonia Solutions. *International Journal of Mineral Processing, 41*(3), 167-182.

La Brooy, S. R., Komosa, T., & Muir, D. M. (1991a). *Selective Leaching of Gold from Copper-Gold Ores Using Ammonia-Cyanide Mixtures.* Paper presented at the Fifth AusIMM Extractive Metallurgy Conference, Perth. , Perth.127-132

La Brooy, S. R., Komosa, T., & Muir, D. M. (1991b). Selective Leaching of Gold from Copper-Gold Ores Using Ammonia-Cyanide Mixtures.127-132

La Brooy, S. R., Linge, H. G., & Walker, G. S. (1994). Review of Gold Extraction from Ores. *Minerals Engineering, 7*(10), 1213-1241.

Lacoste-Bouchet, P., Deschênes, G., & Ghali, E. (1998). Thiourea Leaching of a Copper-Gold Ore Using Statistical Design. *Hydrometallurgy, 47*(2–3), 189-203.

Lane, W., & Mcdonal, H. J. (1946). Reaction Kinetics of Copper and Aqueous Ammonia. *Journal of American Chemical Society, 68*, 1699-1704.

Langhans Jr, J. W., Lei, K. P. V., & Carnahan, T. G. (1992). Copper-Catalyzed Thiosulfate Leaching of Low-Grade Gold Ores. *Hydrometallurgy, 29*(1-3), 191-203.

Lawrence, J. F. (1987). Advantages and Limitations of Hplc in Environmental Analysis. *Chromatographia, 24*(1), 45-50.

Levenspiel, O. (1999). *Chemical Reaction Engineering* (Third ed.): John Wiley & Sons, Inc., New York, USA, 688 p.

Levison, R. *Atomic Absorption Spectrometry*. The Royal Society of Chemistry, Piccadilly, London, 4 p

Lewis, A., & van Hille, R. (2006). An Exploration into the Sulphide Precipitation Method and Its Effect on Metal Sulphide Removal. *Hydrometallurgy, 81*(3–4), 197-204.

Lewis, A. E. (2010). Review of Metal Sulphide Precipitation. *Hydrometallurgy, 104*(2), 222-234.

Li, J., Kawashima, N., Kaplun, K., Absolon, V. J., & Gerson, A. R. (2010). Chalcopyrite Leaching:

The Rate Controlling Factors. *Geochimica et Cosmochimica Acta, 74*(10), 2881-2893.

Li, N., Zhang, Y., Kong, D., Zhou, Q., Chen, X., & Hui, S. (2013a). Fluid Particle Group Reaction Model and Experimental Verification. *Advanced Powder Technology, 24*(1), 200-206.

Li, Y., Chandra, A. P., & Gerson, A. R. (2014). Scanning Photoelectron Microscopy Studies of Freshly Fractured Chalcopyrite Exposed to O2 and H2o. *Geochimica et Cosmochimica Acta, 133*(0), 372-386.

Li, Y., Kawashima, N., Li, J., Chandra, A. P., & Gerson, A. R. (2013b). A Review of the Structure, and Fundamental Mechanisms and Kinetics of the Leaching of Chalcopyrite. *Advances in Colloid and Interface Science, 197–198*(0), 1-32.

Liedberg, B., Lundström, I., Wu, C. R., & Salaneck, W. R. (1985). Adsorption of Glycine on Hydrophilic Gold. *Journal of Colloid and Interface Science, 108*(1), 123-132.

Liu, Z.-x., Yin, Z.-l., Hu, H.-p., & Chen, Q.-y. (2012a). Dissolution Kinetics of Malachite in Ammonia/Ammonium Sulphate Solution. *Journal of Central South University, 19*(4), 903-910.

Liu, Z.-x., Yin, Z.-l., Hu, H.-p., & Chen, Q.-y. (2012b). Leaching Kinetics of Low-Grade Copper Ore Containing Calcium-Magnesium Carbonate in Ammonia-Ammonium Sulfate Solution with Persulfate. *Transactions of Nonferrous Metals Society of China, 22*(11), 2822-2830.

Liu, Z.-x., Yin, Z.-l., Hu, H.-p., & Chen, Q.-y. (2012c). Leaching Kinetics of Low-Grade Copper Ore with High-Alkality Gangues in Ammonia-Ammonium Sulphate Solution. *Journal of Central South University, 19*(1), 77-84.

Llames, C. R., & Fontaine, J. (1994). Determination of Amino Acids in Feeds: Collaborative Study. *Journal of AOAC International*(77), 1362-1402.

Logsdon, M. J., Hagelstein, K., & Mudder, T. I. (1999). *The Management of Cyanide in Gold Extraction*, International Council on Metals and the Environment, Ottawa, Canada, 37p.

Lombardi, J. A. (2008). The HWPT Engineered Membrane Separation® (Ems®) Method for the Cyanide Treatment of Copper-Gold Ore, Hydrometallurgy 2008: Proceedings of the Sixth International Symposium, Young, Courtney A. Taylor, Patrick R. Anderson, Corby G. Choi, Yeonuk, SME Inc, Colorado, USA, pp. 724-730.

Lorenzen, L., van Deventer, J. S. J., & van Meersbergen, M. T. (1994). Interrelationship

between Lixiviants and Galvanic Interaction During Dissolution of Gold *Hydrometallurgy '94: Papers Presented at the International Symposium 'Hydrometallurgy '94' Organized by the Institution of Mining and Metallurgy and the Society of Chemical Industry, and Held in Cambridge, England, from 11 to 15 July, 1994* (pp. 483-499). Dordrecht: Springer Netherlands.

Lowell, D. J. (1989). Gold Mineralization in Porphyry Copper Deposits Discussed, Mining Engineering; 41, 4; 227-231.

Lower, G. W., & Booth, R. B. (1965). *Cyanidation Studies: Recovery of Copper by Cyanidation*: Min.Eng., November,56.

Lu, J., Dreisinger, D. B., & Cooper, W. C. (2002). Thermodynamics of the Aqueous Copper–Cyanide System. *Hydrometallurgy, 66*(1–3), 23-36.

Lwambiyi, M., Maweja, K., Kongolo, K., Lwambiyi, N. M., & Diyambi, M. (2009). Investigation into the Heap Leaching of Copper Ore from the Disele Deposit. *Hydrometallurgy, 98*(1–2), 177-180.

Macchiarola, K., Koenig, U., Gobbo, L., Campbell, I., McDonald, A. M., & Cirelli, J. (2007). *Modern X-Ray Diffraction Techniques for Exploration and Analysis of Ore Bodies.* Paper presented at the Fifth Decennial International Conference on Mineral Exploration, Toronto.1007-1011.

Maeda, M., Tanaka, Y., & Nakagawa, G. (1979). Potentiometric Investigation of Complex Formation of Lead(Ii) with Glycine and Dl-Alanine. *Journal of Inorganic and Nuclear Chemistry, 41*(5), 705-709.

Mahajan, V., Misra, M., Zhong, K., & Fuerstenau, M. C. (2007). Enhanced Leaching of Copper from Chalcopyrite in Hydrogen Peroxide–Glycol System. *Minerals Engineering, 20*(7), 670-674.

Malcolm, D. E., Leahy, G. J., Neville, T. M., & Stuart, K. N. (1991). *Selective Ion Flotation of Gold from Alkaline Cyanide Solutions*. Paper presented at the World Gold '91, Second AusIMM -SME Joint Conference, Cairns, 1991, AIME. Parkville, Australia. p. 121.

Marangoni, D. G., Smith, R. S., & Roscoe, S. G. (1988). Surface Electrochemistry of the Oxidation of Glycine at Pt *Canadian Journal of Chemistry, 67*, 921-926.

Marangoni, D. G., Smith, R. S., & Roscoe, S. G. (1989). Surface Electrochemistry of the Oxidation of Glycine at Pt. *Canadian Journal of Chemistry, 67*(5), 921-926.

Marsden, J., & House, I. (1992). The Chemistry of Gold Extraction (2nd edition) John O Marsden and C Iain House SME Littleton, Colorado, USA, 682pp.

Marsden, J. O. (2008). Energy efficiency and copper hydrometallurgy. In: Proceedings of the Sixth International Symposium, Hydrometallurgy, Phoenix, August 2008, pp. 29–42.

McDonald, R. G., & Muir, D. M. (2007). Pressure Oxidation Leaching of Chalcopyrite. Part I. Comparison of High and Low Temperature Reaction Kinetics and Products. *Hydrometallurgy, 86*(3–4), 191-205.

McIntyre, N. S., & Zetaruk, D. G. (1977). X-Ray Photoelectron Spectroscopic Studies of Iron Oxides. *Analytical Chemistry, 49*(11), 1521-1529.

McMaster, M. C. (2006). Advantages and Disadvantages of HPLC, In: HPLC: A Practical User's Guide, Second Edition (pp. 1-13): John Wiley & Sons, Inc., Hoboken, NJ, USA.

Mellado, M. E., Cisternas, L. A., & Gálvez, E. D. (2009). An Analytical Model Approach to Heap Leaching. *Hydrometallurgy, 95*(1–2), 33-38.

Meng, X., & Han, K. N. (1996). The Principles and Applications of Ammonia Leaching of Metals—a Review. *Mineral Processing and Extractive Metallurgy Review, 16*(1), 23-61.

MetaLeach Limited. (2017). Ammleach. Retrieved from https://www.metaleach.com/ammleach.

Mindat.org. (2016). Malachite. Retrieved from http://www.mindat.org/show.php?id=2550&ld=1#themap.

Mineev, G. G., & Syrtlanova, T. S. (1984). Scientific and Technological Principles of the Leaching of Gold by Microbiological and Chemical Solvents. *Tsvet.Met.N.Y.*(12), 74-76.

Molleman, E., & Dreisinger, D. (2002). The Treatment of Copper–Gold Ores by Ammonium Thiosulfate Leaching. *Hydrometallurgy, 66*(1–3), 1-21.

Moore, S., & Stein, W. (1954). A Modified Ninhydrin Reagent for the Photometric Determination of Amino Acids and Related Compounds. *Journal of Biological Chemistry,*

211(2), 907-913.

Mousavi, S. M., Yaghmaei, S., Vossoughi, M., Roostaazad, R., Jafari, A., Ebrahimi, M., . . . Turunen, I. (2008). The Effects of Fe(II) and Fe(III) Concentration and Initial pH on Microbial Leaching of Low-Grade Sphalerite Ore in a Column Reactor. *Bioresource Technology, 99*(8), 2840-2845.

Moyo, T., & Petersen, J. (2016). Study of the Dissolution of Chalcopyrite in Solutions of *Different Ammonium Salts*. Journal of the Southern African Institute of Mining and Metallurgy, Vol. 116, 509-516.

Muir, D. M. (2011). A Review of the Selective Leaching of Gold from Oxidised Copper–Gold Ores with Ammonia–Cyanide and New Insights for Plant Control and Operation. *Minerals Engineering, 24*(6), 576-582.

Muir, D. M., La Brooy, S. R., & Cao, C. (1989). *Recovery of Gold from Copper-Bearing Ores.* Paper presented at the Gold Forum on Technology and Practices - ”World Gold '89”, Reno, NV, USA, 363-374.

Mukutuma, A., Schwarz, N., & Feather, A. (2008). *Operation of a Flottweg Tricanter® Centrifuge for Crud Treatment at Bwana Mkubwa Solvent Extraction Plant*. In: Proceedings of the International Solvent Extraction Conference 2008, Tucson, Arizona, USA, 15-19 September 2008.

Murray, C., Platzer, W., & Petersen, J. (2017). Potential for Solar Thermal Energy in the Heap Bioleaching of Chalcopyrite in Chilean Copper Mining. *Minerals Engineering, 100*, 75-82.

Naderi, H., Abdollahy, M., Mostoufi, N., Koleini, M. J., Shojaosadati, S. A., & Manafi, Z. (2011). Kinetics of Chemical Leaching of Chalcopyrite from Low Grade Copper Ore: Behavior of Different Size Fractions. *International Journal of Minerals, Metallurgy, and Materials, 18*(6), 638-645.

National Institute for Occupational Safety and Health (1992). *Occupational Safety and Health Guideline for Ammonia*, Retrived from https://www.cdc.gov/niosh/docs/81-123/pdfs/0028-rev.pdf.

Naumkin, A. V., Kraut-Vass, A., Gaarenstroom, S. W., & Powell, C. J. (2012). X-Ray Photoelectron Spectroscopy Database from National Institute of of Standards and

Technology http:/srdata.nist.gov/xps/.

Näveke, R. (1986). Bacterial Leaching of Ores and Other Materials, Retrieved from https://www.scribd.com/document/179482048/Bacterial-Leaching-of-Ores-and-Other-Materials.

Nazari, G., Dixon, D. G., & Dreisinger, D. B. (2011). Enhancing the Kinetics of Chalcopyrite Leaching in the Galvanox™ Process. *Hydrometallurgy, 105*(3–4), 251-258.

Nazemi, M. K., Rashchi, F., & Mostoufi, N. (2011). A New Approach for Identifying the Rate Controlling Step Applied to the Leaching of Nickel from Spent Catalyst. *International Journal of Mineral Processing, 100*(1–2), 21-26.

Nelson, D. L., & Cox, M. M. (2013). *Principles of Biochemistry (6th edit)*: W.H.Freeman & Co Ltd, New York, USA, 1158 pp.

Nicol, M., Miki, H., & Velásquez-Yévenes, L. (2010). The Dissolution of Chalcopyrite in Chloride Solutions: Part 3. Mechanisms. *Hydrometallurgy, 103*(1-4), 86-95.

Nicolia, A., Ferradini, N., Molla, G., Biagetti, E., Pollegioni, L., Veronesi, F., & Rosellini, D. (2014).Expression of an Evolved Engineered Variant of a Bacterial Glycine Oxidase Leads to Glyphosate Resistance in Alfalfa. *Journal of Biotechnoloy, 184, 201-208*.

Norgate, T., & Haque, N. (2010). Energy and Greenhouse Gas Impacts of Mining and Mineral Processing Operations. *Journal of Cleaner Production, 18*(3), 266-274.

Norgate, T., & Jahanshahi, S. (2010). Low Grade Ores – Smelt, Leach or Concentrate? *Minerals Engineering, 23*(2), 65-73.

Nunn, P. B., O'Brien, P., Pettit, L. D., & Pyburn, S. I. (1989). Complexes of Zinc, Copper, and Nickel with the Nonprotein Amino Acid L-A-Amino-B-Methylaminopropionic Acid: A Naturally Occurring Neurotoxin. *Journal of Inorganic Biochemistry, 37*(2), 175-183.

O'Brien, P., & Nunn, P. B. (1982). Metal Ion Complexes of Amino Acids. Part Ii [1]. The Copper Complexes of the A- and B-Isomers of N-Oxalyl-L-A,B-Diaminopropionic Acid. *Inorganica Chimica Acta, 66*(0), 185-188.

O'Brien, T. F. (2012). Salt, Chlor-Alkali, and Related Heavy Metals. In J. A. Kent (Ed.), *Handbook of Industrial Chemistry and Biotechnology* (12 ed., Vol. 1). New York: Springer.

Oishi, T., Yaguchi, M., Koyama, K., Tanaka, M., & Lee, J. C. (2008). Effect of Phosphate on Lead Removal During a Copper Recycling Process from Wastes Using Ammoniacal Chloride Solution. *Hydrometallurgy, 90*(2–4), 161-167.

Olanipekun, E. (1999). A Kinetic Study of the Leaching of a Nigerian Ilmenite Ore by Hydrochloric Acid. *Hydrometallurgy, 53*(1), 1-10.

Olesik, J. W. (1996). Fundamental Research in Icp-Oes and Icpms. *Analytical Chemistry, 68*(15), 469A-474A.

Olubambi, p. A., Ndlovu, s., Potgieter, j. H., & Borode, j. O. (2006). Influence of Applied Mineralogy in Developing an Optimal Hydrometallurgical Processing Route for Complex Sulphide Ores. *Mineral Processing & Extractive Metall.*(27), 143-158.

Oraby, E. A., & Eksteen, J. J. (2013). *The Leaching and Adsorption of Gold and Silver in Aqueous Glycine-Peroxide Environments*. Metallurgical and Minerals Engineering. Curtin University.

Oraby, E. A., & Eksteen, J. J. (2015). The Leaching of Gold, Silver and Their Alloys in Alkaline Glycine-Peroxide Solutions and Their Adsorption on Carbon. *Hydrometallurgy,* 152(0), 199-203.

Oraby, E. A., & Eksteen, J. J. (2014). The Selective Leaching of Copper from a Gold–Copper Concentrate in Glycine Solutions. *Hydrometallurgy, 150*, 14-19.

Oudenne, P., & Olson, F. (1983a). Leaching Kinetics of Malachite in Ammonium Carbonate Solutions. *Metallurgical Transactions B, 14*(1), 33-40.

Oudenne, P. D., & Olson, F. A. (1983b). Leaching Kinetics of Malachite in Ammonium Carbonate Solutions. *Metallurgical Transactions B, 14B*, 33-40.

Pakiari, A. H., & Jamshidi, Z. (2007). Interaction of Amino Acids with Gold and Silver Clusters. *The Journal of Physical Chemistry A, 111*(20), 4391-4396.

Parga, J. R., Valdés, J. V., Valenzuela, J. L., Gonzalez, G., Pérez, L. M. d. J., & Cepeda, T. F. (2015). New Approach for Lead, Zinc and Copper Ions Elimination in Cyanidation Process to Improve the Quality of the Precipitate. *Materials Sciences and Applications, 6*, 117-129.

Parija, C., & Sarma, B. (2000). Separation of Nickel and Copper from Ammoniacal Solutions through Co-Extraction and Selective Stripping Using Lix84 as the Extractant. *Hydrometallurgy,*

54(2–3), 195-204.

Park, J. Y., & Levenspiel, O. (1975). The Crackling Core Model for the Reaction of Solid Particles. *Chemical Engineering Science, 30*(10), 1207-1214.

Park, K.-H., Mohapatra, D., Reddy, B. R., & Nam, C.-W. (2007). A Study on the Oxidative Ammonia/Ammonium Sulphate Leaching of a Complex (Cu–Ni–Co–Fe) Matte. *Hydrometallurgy, 86*(3–4), 164-171.

Parker, A., Klauber, C., Kougianos, A., Watling, H. R., & van Bronswijk, W. (2003). An X-Ray Photoelectron Spectroscopy Study of the Mechanism of Oxidative Dissolution of Chalcopyrite. *Hydrometallurgy, 71*(1–2), 265-276.

Parson, A. B. (1957). *The Porphyry Coppers in 1956* (1st ED). Rocky mountain fund series, American Institute of Mining, Metallurgical and Petroleum Engineers, New York, USA.

Paynter, J. C. (1973). A Review of Copper Hydrometallurgy. *Journal of South African Institute of Mining and Metallurgy, 74*(04), 158-170.

Peters, E. (1992). *Hydrmetallurgical Process Innovation*. Hydrometallurgical Process Innovation. Hydrometallurgy, 29(1), 431-459.

Petruk, W. (2000). Chapter 7 - Applied Mineralogy: Porphyry Copper Deposits. In: W. Petruk (Ed.), *Applied Mineralogy in the Mining Industry* (pp. 135-147). Amsterdam: Elsevier.

Pilśniak, M., & Trochimczuk, A. W. (2007). Synthesis and Characterization of Polymeric Resins with Aliphatic and Aromatic Amino Ligands and Their Sorption Behavior Towards Gold from Ammonium Hydroxide Solutions. *Reactive and Functional Polymers, 67*(12), 1570-1576.

Pilśniak, M., Trochimczuk, A. W., & Apostoluk, W. (2009). The Uptake of Gold(I) from Ammonia Leaching Solution by Imidazole Containing Polymeric Resins. *Separation Science and Technology, 44*(5), 1099-1119.

Ping, Z., ZeYun, F., Jie, L., Qiang, L., GuangRen, Q., & Ming, Z. (2009). Enhancement of Leaching Copper by Electro-Oxidation from Metal Powders of Waste Printed Circuit Board. *Journal of Hazardous Materials, 166*(2–3), 746-750.

Platte, J. A. (1968). Analysis of Industrial Waters by Atomic Absorption *Trace Inorganics in Water* (Vol. 73, pp. 247-252): American Chemical Society.

Pokrovsky, O. S., Golubev, S. V., & Schott, J. (2005). Dissolution Kinetics of Calcite, Dolomite and Magnesite at 25 °C and 0 to 50 Atm Pco2. *Chemical Geology, 217*(3–4), 239-255.

Pourghahramani, P., & Forssberg, E. (2006). Microstructure Characterization of Mechanically Activated Hematite Using Xrd Line Broadening. *International Journal of Mineral Processing, 79*(2), 106-119.

Prasad, S., & Pandey, B. D. (1998). Alternative Processes for Treatment of Chalcopyrite —a Review. *Minerals Engineering, 11*(8), 763-781.

Qi-wen, L., Hui-ping, H., Weng, F., Ting, Y., & Qi-yuan, C. (2011). Recovery of Copper from Simulated Ammoniacal Spent Etchant Using Sterically Hindered Beta-Diketone. *Transactions of Nonferrous Metals Society of China, 21*, 1840-1846.

Qiu, T.-s., Nie, G.-h., Wang, J.-f., & Cui, L.-f. (2007). Kinetic Process of Oxidative Leaching of Chalcopyrite under Low Oxygen Pressure and Low Temperature. *Transactions of Nonferrous Metals Society of China, 17*(2), 418-422.

Radmehr, V., Koleini, S. M. J., Khalesi, M. R., & Tavakoli Mohammadi, M. R. (2013). Ammonia Leaching: A New Approach of Copper Industry in Hydrometallurgical Processes. *Journal of The Institution of Engineers (India): Series D, 94*(2), 95-104.

Reed, R., Rao, A. G., L., Nash, K., Bond, A., (2004). Oxidative Alkaline Leaching of Americium from Simulated High-Level Nuclear Waste Sludges. *Separation Science and Technology, 40*(5), 1029-1046.

Rega, N., Cossi, M., & Barone, V. (1998). Structure and Magnetic Properties of Glycine Radical in Aqueous Solution at Different Ph Values. *Journal of the American Chemical Society, 120*(23), 5723-5732.

Reilly, I. G., & Scott, D. S. (1977). The Leaching of a Chalcopyrite Concentrate in Ammonia. *The Canadian Journal of Chemical Engineering, 55*(5), 527-533.

Remko, M., & Rode, B. M. (2006). Effect of Metal Ions (Li+, Na+, K+, Mg2+, Ca2+, Ni2+, Cu2+, and Zn2+) and Water Coordination on the Structure of Glycine and Zwitterionic Glycine. *J Phys Chem A, 110*(5), 1960-1967.

Ritcey, G. M. (2004). Development of Industrial Solvent Extraction Process. In: *Solvent Extraction Principles and Practice*, Rydberg, Michael Cox, Claude Musikas and Gregory R.

Choppin (Ed.), (Vol. second, Marcel Dekker, New York, pp. 283.

Rosen, H. (1957). A Modified Ninhydrin Colorimetric Analysis for Amino Acids. *Archives of Biochemistry and Biophysics, 67*(1), 10-15.

Rowan, A. M., Moughan, P. J., & Wilson, M. N. (1992). Effect of Hydrolysis Time on the Determination of the Amino Acid Composition of Diet, Ileal Digesta, and Faeces Samples on the Determination of Dietary Amino Acid Digestibility Coefficients. *Agricultural and Food Chemistry*(40), 981-985.

Rubino, J. T., & Franz, K. J. (2012). Coordination Chemistry of Copper Proteins: How Nature Handles a Toxic Cargo for Essential Function. *Journal of Inorganic Biochemistry, 107*(1), 129-143.

Ryan, E. T., Xiang, T., Johnston, K. P., & Fox, M. A. (1997). Absorption and Fluorescence Studies of Acridine in Subcritical and Supercritical Water. *The Journal of Physical Chemistry A, 101*(10), 1827-1835.

Rydberg, J., Choppin, G. R., Musikas, C., & Sekine, T. (2005). Solvent Extraction Principles and Practice. In J. Rydberg (Ed.), *Solvent Extraction Principles and Practice, Revised and Expanded*. New York: Taylor & Francis Group, LLC.

Safronov, A. Y., Tarasevich, M. R., Bogdanovskaya, V. A., & Chernyak, A. S. (1983). Electrooxidation of Glycylglycine, Cysteine, and Histidine on a Gold Electrode. *Soviet electrochemistry, 19*(3), 378-381.

Sakata, K., Yamada, N., Midorikawa, R., Wirfel, J. C., Potter, D. L., & Martinez, A. G. G. (2001). Inductively Coupled Plasma Mass Spectrometer and Method: Google Patents.

Salvador, A. S. (1978). A Kinetic Study of Chalcocite Dissolution in the Low-Pressure Oxygen-Ammonia System. Thesis, University of Arizona, Tucson, Arizona.

Sand, W., Gehrke, T., Jozsa, P.-G., & Schippers, A. (2001). (Bio)Chemistry of Bacterial Leaching—Direct Vs. Indirect Bioleaching. *Hydrometallurgy, 59*(2–3), 159-175.

Sandhibigraha, A., & Bhaskara Sarma, P. V. R. (1997). Co-Extraction and Selective Stripping of Copper and Nickel Using Lix87qn. *Hydrometallurgy, 45*(1–2), 211-219.

Sarangi, K., Parhi, P. K., Padhan, E., Palai, A. K., Nathsarma, K. C., & Park, K. H. (2007).

Separation of Iron(Iii), Copper(Ii) and Zinc(Ii) from a Mixed Sulphate/Chloride Solution Using Tbp, Lix 84i and Cyanex 923. *Separation and Purification Technology, 55*(1), 44-49.

Sarathi, T. V. N. P., Kumar, A. K., Kishore, K. K., & Vani, P. (2005). Kinetics and Mechanism of Oxidation of Glycine by Iron(Iii)–1,10-Phenanthroline Complex in Perchloric Acid Medium *J. Chem. Sci, 117*(4), 329–332.

Sarveswara Rao, K., Paramguru, R. K., Das, R. P., & Ray, H. S. (1992). The Role of Galvanic Interaction During Ammonia Leaching of Multi Metal Sulphides. *Mineral Processing and Extractive Metallurgy Review, 11*(1-2), 21-37.

Saxena, N. N., & Mandre, N. R. (1992). Mixed Control Kinetics of Copper Dissolution for Copper Ore Using Ferric Chloride. *Hydrometallurgy, 28*(1), 111-117.

Sceresini, B. (2005). Gold-Copper Ores. In D. A. Mike & B. A. Wills (Eds.), *Developments in Mineral Processing* (Vol. Volume 15, pp. 789-824): Elsevier.

Scott, J. S. (1987). Removal of Cyanide From Gold Mill Effluents: Proc., Canadian MineralProcessors Thirteenth Ann. Mtg., Jan. 1981, Ottawa, ON.

Seal, S., Kuiry, S. C., & Heinmen, B. (2003). Effect of Glycine and Hydrogen Peroxide on Chemical–Mechanical Planarization of Copper. *Thin Solid Films, 423*(2), 243-251.

Senanayake, G. (2004). Gold Leaching in Non-Cyanide Lixiviant Systems: Critical Issues on Fundamentals and Applications. *Minerals Engineering, 17*(6), 785-801.

Senanayake, G. (2007). Chloride Assisted Leaching of Chalcocite by Oxygenated Sulphuric Acid Via Cu(II)–Oh–Cl. *Minerals Engineering, 20*(11), 1075-1088.

Senanayake, G. (2009). A Review of Chloride Assisted Copper Sulfide Leaching by Oxygenated Sulfuric Acid and Mechanistic Considerations. *Hydrometallurgy, 98*(1–2), 21-32.

SGS Minerals Services. (2013). Cyanide Recovery. In SGS (Ed.), Retrieved from www.sgs.co.nz/~/.../SGS-MIN-WA016-Cyanide-Recovery-Comparison-EN-11.pdf.

Shantz, R., & Reich, J. (1978). A Review of Copper-Cyanide Metallurgy. *Hydrometallurgy, 3*(2), 99-109.

Sillitoe, R.H., (1995), Exploration of porphyry copper lithocaps, In: Pacific Rim Congress 95,

19-22 November 1995, Auckland, New Zealand, proceedings: Carlton South, The Australasian Institute of Mining and Metallurgy, p. 527-532.

Sillitoe, R. H. (2000). Gold-Rich Porphyry Deposits: Descriptive and Generic Models and Their Role in Exploration and Discovery, *Seg Reviews* (Vol. 13), pp. 325-345.

Sillitoe, R. H. (2010a). Porphyry Copper Systems. *Economic Geology, 105*(1), 3-41.

Sillitoe, R. H. (2010b). Porphyry Copper Systems. *Society of Economic Geology, 103*, 3-41.

Sinclair, W.D., 2007, Porphyry deposits, in Goodfellow, W.D., ed., Mineral Deposits of Canada: A Synthesis of Major Deposit-Types, District Metallogeny, the Evolution of Geological Provinces, and Exploration Methods: Geological Association of Canada, Mineral Deposits Division, Special Publication No. 5, p. 223-243.

Smith, R. M., & Martell, A. E. (1989). *Critical Stability Constants* (Vol. 6), Springer Science+Business Media, New York, USA, 640p.

Sobel, S., Haigney, A., Concepcion, T., & Kim, M. (2008). The Complexation of Aqueous Metal Ions Relevant to Biological Applications. 1. Poorly Soluble Zinc Salts and Enhanced Solubility with Added Amino Acid. *Chemical Speciation and Bioavailability, 20*(2), 93-97.

Sokić, M. D., Marković, B., & Živković, D. (2009). Kinetics of Chalcopyrite Leaching by Sodium Nitrate in Sulphuric Acid. *Hydrometallurgy, 95*(3–4), 273-279.

Sorensen, P. F. (1988a). Gold Recovery from Carbon-in-Pulp Eluates by Precipitation with a Mineral Acid Ii. Gold Bullion Production from Precipitate, Treatment of Barren Solution, the Settling Rate of Precipitate and Assisting Precipitation by Addition of $CuSO_4 \cdot H_2O$ in a Recalcitrant Eluate. *Hydrometallurgy, 21*(2), 243-248.

Sorensen, P. F. (1988b). Gold Recovery from Carbon-in-Pulp Eluates by Precipitation with a Mineral Acid Iii. The Acid Precipitation Step in Applications. *Hydrometallurgy, 21*(2), 249-254.

Sparrow, G. J., & Woodcock, J. T. (1995). Cyanide and Other Lixiviant Leaching Systems for Gold with Some Practical Applications. *Mineral Processing and Extractive Metallurgy Review, 14*(3-4), 193-247.

Srivastava, R. R., Kim, M.-s., Lee, J.-c., & Ilyas, S. (2015). Liquid–Liquid Extraction of Rhenium(Vii) from an Acidic Chloride Solution Using Cyanex 923. *Hydrometallurgy, 157*, 33-

38.

Stadler, A. (2015, August 2015). Unlocking the Energy Productivity Proposition. *The AusIMM Bulletin*. Retrived from https://www.ausimmbulletin.com/feature/unlocking-the-energy-productivity-value-proposition/.

Stankova, A., Gilon, N., Dutruch, L., & Kanicky, V. (2011). Comparison of La-Icp-Ms and La-Icp-Oes for the Analysis of Some Elements in Fly Ashes. *Journal of Analytical Atomic Spectrometry, 26*(2), 443-449.

Strizhko, L. S., Boboev, I. R., Gurin, K. K., & Rabiev, F. B. (2013). Development of Hydrometallurgical Processing Technology for the Oxidized Gold-Containing Ore from Taror Deposit. *Tsvetnye Metally*(4), 46-49.

Sultana, U. K., Gulshan, F., & Kurny, A. S. W. (2014). Kinetics of Leaching of Iron Oxide in Clay in Oxalic Acid and in Hydrochloric Acid Solutions. *Materials Science and Metallurgy Engineering, 2*(1), 5-10.

Sun, S.-W., Lin, Y.-C., Weng, Y.-M., & Chen, M.-J. (2006). Efficiency Improvements on Ninhydrin Method for Amino Acid Quantification. *Journal of Food Composition and Analysis, 19*(2–3), 112-117.

Sutulov, A. (1975). *Copper Porphyries*: Miller Freeman Publications, Inc., San Francisco, USA. 206 p.

Suzuki, I. (2001). Microbial Leaching of Metals from Sulfide Minerals. *Biotechnology Advances, 19*(2), 119-132.

Syed, S. (2012). Recovery of Gold from Secondary Sources—a Review. *Hydrometallurgy, 115–116*(0), 30-51.

Tanda, B. C., Eksteen, J. J., & Oraby, E. A. (2017). An Investigation into the Leaching Behaviour of Copper Oxide Minerals in Aqueous Alkaline Glycine Solutions. *Hydrometallurgy, 167*, 153-162.

Thimann, H. B. A. K. V. (1932). The Cupric Complexes of Glycine and of Alanine. William G. Kerckhoff Laboratom'es of the Biological Sciences, California Institute of Technology, Pasadena, retieved from http://citeseerx.ist.psu.edu/viewdoc/download?doi=10.1.1.550.5547&rep=rep1&type=pdf.

Thompson, L., Davidowski, L., Grosser, Z. A., & Neubauer, K. (2008). A Comparison of ICP-OES and ICP-MS for the Determination of Metals in Food. *Spectroscopy*, Retrieved from http://www.spectroscopyonline.com/comparison-icp-oes-and-icp-ms-determination-metals-food.

Tianbao, D., Vijayakumar, A., & Desai, V. (2004). Effect of Hydrogen Peroxide on Oxidation of Copper in Cmp Slurries Containing Glycine and Cu Ions. *Electrochimica Acta, 49*(25), 4505-4512.

Tiang, M., Ballantyne, G. R., & Powell, M. S. (2012). *Proportion of Energy Attributed to Comminution*. Paper presented at the Mill Operators' Conference, Hobart, Tas., pp 25-30.

Titley, S. R. (1982). Advances in Geology of the Porphyry Copper Deposits: Southwestern North America: University of Arizona Press, Tucson, AZ, 560 p.

Tornos, F., Velasco, F., Slack, J. F., Delgado, A., Gomez-Miguelez, N., Escobar, J. M., & Gomez, C. (2017). The High-Grade Las Cruces Copper Deposit, Spain: A Product of Secondary Enrichment in an Evolving Basin. *Mineralium Deposita, 52*(1), 1-34.

Tortonda, F. R., Pascual-Ahuir, J. L., Silla, E., & Tuñón, I. (1996). Why Is Glycine a Zwitterion in Aqueous Solution? A Theoretical Study of Solvent Stabilising Factors. *Chemical Physics Letters, 260*(1–2), 21-26.

Tran, T., & Hsu, Y. J. (1996). Selective Removal of Gold from Copper-Gold Cyanide Liquors by Cementation Using Zinc. *Minerals Engineering, 9*(1), 1-13.

Tran, T., Lee, K., Fernando, K., & Rayner, S. (2000). Use of Ion Exchange Resin for Cyanide Management During the Processing of Copper-Gold Ores. 207-215

Tripathi, S., Doyle, F. M., & Dornfeld, D. A. (2010). *Fundamental Mechanisms of Copper Cmp-Passivation Kinetics of Copper in Cmp Slurry Constituents.* Paper presented at the Materials Research Society Symposium Proceedings.79-84

Trivedi, N. C., & Tsuchiya, H. M. (1975). Microbial Mutualism in Leaching of Cu−Ni Sulfide Concentrate. *International Journal of Mineral Processing, 2*(1), 1-14.

Tsai, G., Yang, P., Chung, L.-C., Lange, N., & Coyle, J. T. (1998). D-Serine Added to Antipsychotics for the Treatment of Schizophrenia. *Biological Psychiatry, 44*(11), 1081-1089.

Turan, M. D., & Altundoğan, H. S. (2013). Leaching of Chalcopyrite Concentrate with Hydrogen Peroxide and Sulfuric Acid in an Autoclave System. *Metallurgical and Materials Transactions B, 44*(4), 809-819.

Turkmen, Y., & Kaya, E. (2009). Acidified Ferric Chloride Leaching of Chalcopyrite Concentrate. *The Journal of Ore Dressing, 11*(22), 16-24.

Tyler, G. ICP-OES, ICP-MS and AAS Techniques Compared, ICP Optical Emission Spectroscopy. *Technical note 05.* Retrieved from http://www.jobinyvon.com/usadivisions/Emission/applications/TN05.pdf.

Uchida, S., Takemura, I., Tokuda, M., & Osseo-Asare, K. (1996). The Kinetics of Dissolution of Copper and Iron in Aqueous Cupric Ammine Solutions. *ISIJ International, 36*(5), 522-527.

United States Geological Survey. (2014). Estimate of Undiscovered Copper Resources of the World, Retrieved from https://pubs.usgs.gov/fs/2014/3004/pdf/fs2014-3004.pdf.

United States International Trade Commission. (2008). *Glycine from Japan and Korea*. Retrieved from Washington, DC 20436: www.usitc.gov.

Unland, G., & Szczelina, P. (2004). Coarse Crushing of Brittle Rocks by Compression. *International Journal of Mineral Processing, 74, Supplement*, S209-S217.

Uvdal, K., Bodo, P., Ihs, A., Liedberg, B., & Salaneck, W. R. (1990). X-Ray Photoelectron and Infrared Spectroscopy of Glycine Adsorbed Upon Copper. *Journal of Colloid and Interface Science, 140*, 207-216.

Vaikuntam, I. L., Raja, R., Ramachandran, V. (2016). Innovative Process Development in Metallurgical Industry-Concept to Commission. Springer International Publishing AG Switzerland, 428 pp.

Vignes, A. (2013). *Extractive Metallurgy 2: Metallurgical Reaction Processes*. Hoboken, NJ 07030 USA: Willey & Sons, Inc.

Vračar, R. Ž., Parezanović, I. S., & Cerović, K. P. (2000). Leaching of Copper(I) Sulfide in Calcium Chloride Solution. *Hydrometallurgy, 58*(3), 261-267.

Vračar, R. Ž., Vučković, N., & Kamberović, Ž. (2003). Leaching of Copper(I) Sulphide by Sulphuric Acid Solution with Addition of Sodium Nitrate. *Hydrometallurgy, 70*(1–3), 143-151.

VTT, T. R. C. o. F. (2016). Recovering Critical, Economically Important Metals from Low-Grade Ores and Waste. Retrieved January 15, 2017 www.sciencedaily.com/releases/2016/11/161107112629.htm

Vukcevic, S. (1997). The Mechanism of Gold Extraction and Copper Precipitation from Low Grade Ores in Cyanide Ammonia Systems. *Minerals Engineering, 10*(3), 309-326.

Wade, L. G. (2011). Amino Acids, Peptides, and Proteins *Organic Chemistry* (8 ed., pp. 1153-1199): Pearson Custom Publishing, London, England.

Wang, W. K., Cui, Y. Q., Tong, X., Dong, P., Meng, Q., (2013). Study on the Optimal Condition of a Copper-Bearing Gold Ore Cyanide Leaching Using Orthogonal Design. Advanced Materials Research, Vols. 734-737, pp. 1006-1009

Wang, X., Chen, Q., Hu, H., Yin, Z., & Xiao, Z. (2009). Solubility Prediction of Malachite in Aqueous Ammoniacal Ammonium Chloride Solutions at 25 °C. *Hydrometallurgy, 99*(3–4), 231-237.

Warren, I. H., & Devuyst. (1973). *Leaching of Metal Oxides*. Paper presented at the International symposium on hydrometallurgy, New York, pp 95-110.

Watling, H. R. (2006). The Bioleaching of Sulphide Minerals with Emphasis on Copper Sulphides — a Review. *Hydrometallurgy, 84*(1–2), 81-108.

Watling, H. R. (2013). Chalcopyrite Hydrometallurgy at Atmospheric Pressure: 1. Review of Acidic Sulfate, Sulfate–Chloride and Sulfate–Nitrate Process Options. *Hydrometallurgy, 140*(0), 163-180.

Wei, L., Mo-tang, T., Chao-bo, T., Jing, H., Sheng-hai, Y., & Jian-guang, Y. (2010). Dissolution Kinetics of Low Grade Complex Copper Ore in Ammonia-Ammonium Chloride Solution. *Transactions of Nonferrous Metals Society of China, 20*(5), 910-917.

Wissing, F. (1974). Cyanide Formation from Oxidation of Glycine by a Pseudomonas Species. *Journal of Bacteriology, 117*(3), 1289-1294.

Woźniak, B., Apostoluk, W., & Wódka, J. (2008). Sorption of Gold(I) from Ammoniacal Solutions into ∝-Zirconium(Iv) Bismonohydrogenphosphate (∝-Zrp) Intercalated with Butylamine. *Solvent Extraction and Ion Exchange, 26*(6), 699-721.

Wu, A., Yin, S., Qin, W., Liu, J., & Qiu, G. (2009). The Effect of Preferential Flow on Extraction and Surface Morphology of Copper Sulphides During Heap Leaching. *Hydrometallurgy, 95*(1–2), 76-81.

X-ray Photoelectron Spectroscopy (XPS) Reference Pages. (2016). Copper Sulphides, Cu_2S and CuS. Retrieved from http://www.xpsfitting.com/search/label/Copper.

Xi, W., Qi-yuan, C., Zhou-lan, Y., Hui-ping, H., & Zhong-liang, X. (2011). Real-Solution Stability Diagrams for Copper-Ammonia-Chloride-Water System *Journal of Central South University of Technology (English Edition), 18*, 48-55.

Xiang, T., & Johnston, K. P. (1994). Acid-Base Behavior of Organic Compounds in Supercritical Water. *The Journal of Physical Chemistry, 98*(32), 7915-7922.

Xie, F., & Dreisinger, D. (2009). Recovery of Copper Cyanide from Waste Cyanide Solution by Lix 7950. *Minerals Engineering, 22*(2), 190-195.

Xie, F., Dreisinger, D., & Doyle, F. (2013). A Review on Recovery of Copper and Cyanide from Waste Cyanide Solutions. *Mineral Processing and Extractive Metallurgy Review, 34*(6), 387-411.

Xie, F., & Dreisinger, D. (2010). Copper Solvent Extraction from Alkaline Cyanide Solution with Guanidine Extractant Lix 7950. *Transactions of Nonferrous Metals Society of China, 20*(6), 1136-1140.

Xie, H.-J., Lei, Q.-F., & Fang, W.-J. (2012). Intermolecular Interactions between Gold Clusters and Selected Amino Acids Cysteine and Glycine: A Dft Study. *Journal of Molecular Modeling, 18*(2), 645-652.

Xu, B., Yang, Y., Li, Q., Li, G., & Jiang, T. (2014). Fluidized Roasting-Stage Leaching of a Silver and Gold Bearing Polymetallic Sulfide Concentrate. *Hydrometallurgy, 147–148*, 79-82.

Yartaşi, A., & Çopur, M. (1996). Dissolution Kinetics of Copper(Ii) Oxide in Ammonium Chloride Solutions. *Minerals Engineering, 9*(6), 693-698.

Yildirim, B. G., Bradshaw, D., Powell, M., Evans, C., & Clark, A. (2014). Development of an Effective and Practical Process Alteration Index (Pai) for Predicting Metallurgical Responses of Cu Porphyries. *Minerals Engineering, 69*, 91-96.

Yin, Q., Kelsall, G. H., Vaughan, D. J., & England, K. E. R. (1995). Atmospheric and Electrochemical Oxidation of the Surface of Chalcopyrite (Cufes2). *Geochimica et Cosmochimica Acta, 59*(6), 1091-1100.

Yokoyama, S., & Hiramatsu, J.-I. (2003). A Modified Ninhydrin Reagent Using Ascorbic Acid Instead of Potassium Cyanide. *Journal of Bioscience and Bioengineering, 95*(2), 204-205.

You-Cai, L., Wei, Y., Jian-Gang, F., Li-Feng, L., & Dong, Q. (2013). Leaching Kinetics of Copper Flotation Tailings in Aqueous Ammonia/Ammonium Carbonate Solution. *The Canadian Journal of Chemical Engineering, 91*(4), 770-775.

Zachwieja, J. B., McCarron, J. J., Walker, G. W., & Buckley, A. N. (1989). Correlation between the Surface Composition and Collectorless Flotation of Chalcopyrite. *Journal of Colloid and Interface Science, 132*(2), 462-468.

Zammit, C. M., Cook, N., Brugger, J., Ciobanu, C. L., & Reith, F. (2012). The Future of Biotechnology for Gold Exploration and Processing. *Minerals Engineering, 32*(0), 45-53.

Zanbak, C. (2012). *Heap Leaching Technique in Mining*. Retrieved from www.euromines.org/.../mining.../mining-techniques/batforheapleaching-feb2013-c.za.

Zarate, G., & Torres, M. (2016, September 11 to 15). *Solvent Extraction Plant Modifications at Anglo American Copper.* Paper presented at the XXVIII International Mineral Processing Congress, Quebec City, Quebec.

Zhang, L., & Shankar, R. (2001). A Model of Abrasive-Free Removal of Copper Films Using an Aqueous Hydrogen Peroxide–Glycine Solution. *Thin Solid Films, 397*(1–2), 143-151.

Zhang, S. (2004). Oxidation of Refractory Gold Concenrates and Simulataneous Dissolution of Gold in Aerated Alkaline Solutions. (Thesis), Murdoch University. Murdoch, Australia.

Appendices

Appendix A: XRD Patterns

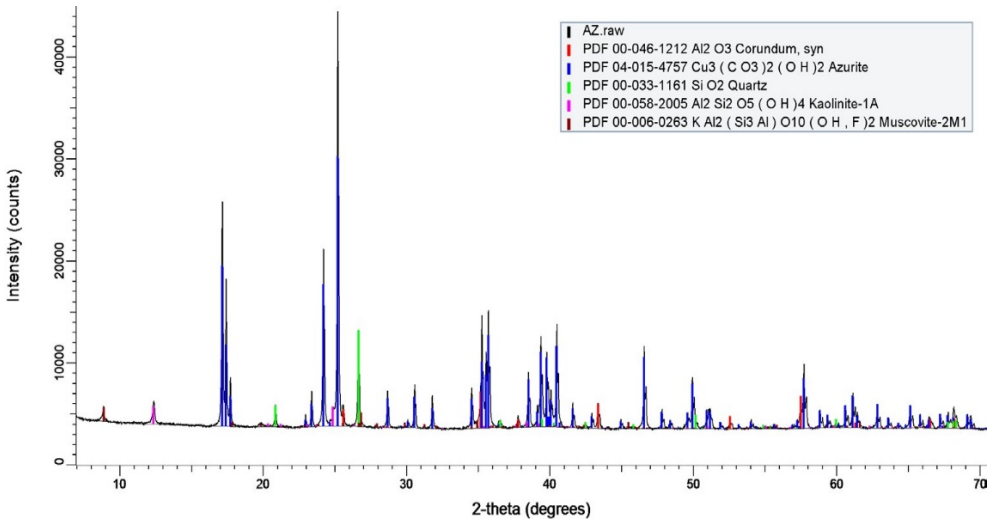

Appendix A1 XRD pattern for azurite mineral specimen

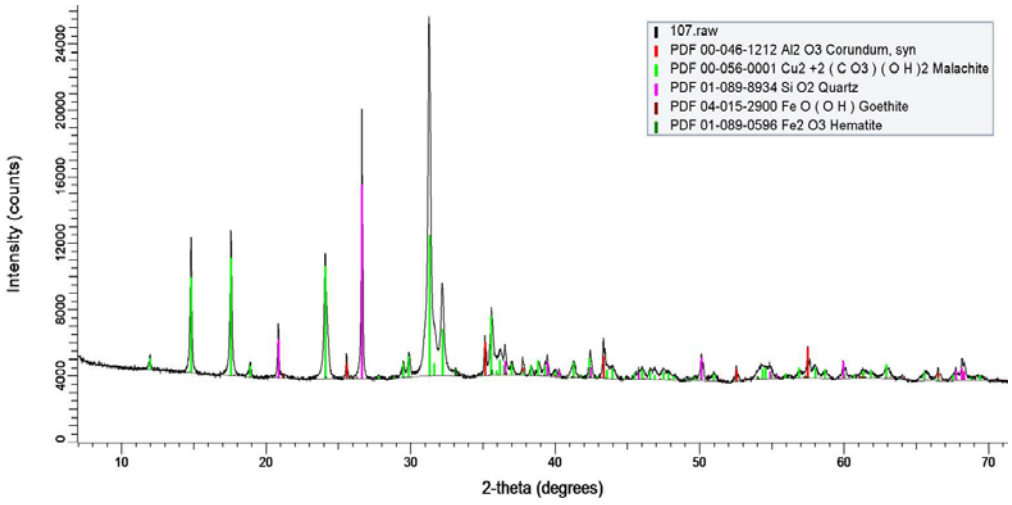

Appendix A2 XRD pattern for malachite A mineral specimen

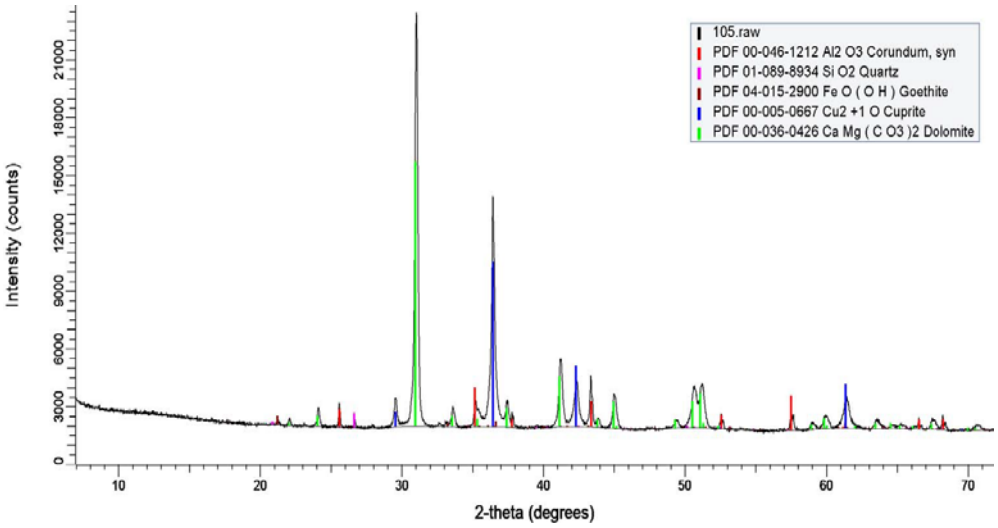

Appendix A3 XRD pattern for cuprite mineral specimen

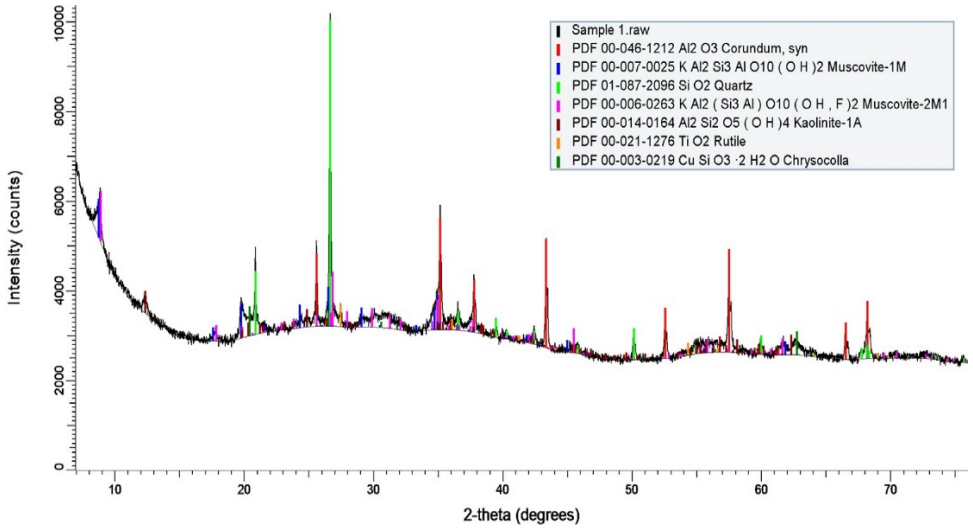

Appendix A4 XRD pattern for Chrysocolla mineral specimen

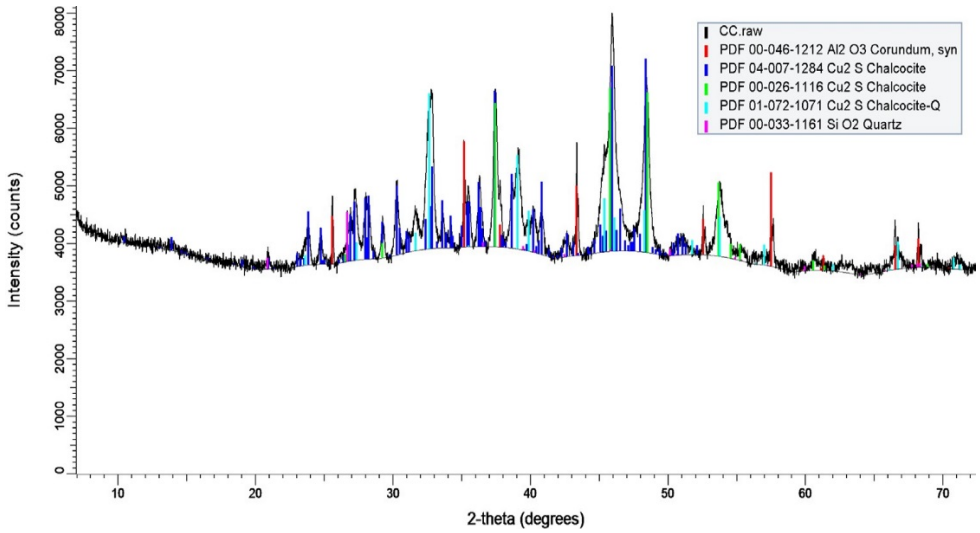

Appendix A 5 XRD pattern for chalcocite A mineral specimen

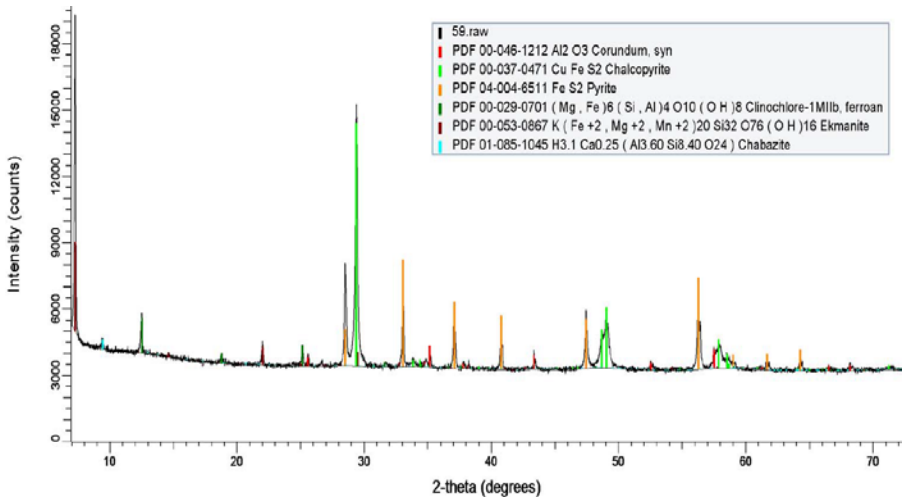

Appendix A6 XRD pattern for chalcopyrite A mineral specimen

Appendix B: Instrumental Detection Limits

.

Appendix B1 Elemental detection limits of XRF: Extended Iron Ore Suite, Fused with 12:22 Lithium Borate flux. LOI determined by RTGA. Detection limits in ppm

Fe (100)	SiO_2 (100)	Al_2O_3 (100)	MnO (10)	TiO_2 (10)	CaO (100)
MgO (100)	K_2O (10)	P (10)	S (10)	Na_2O (100)	Cu (10)
Sn (10)	Sr (10)	Zr (10)	Ba (10)	V (10)	Cl (10)
LOI (0.01%)					

Appendix B 2 Fused Bead Laser Ablation ICP-MS: ppb otherwise detection limits are ppm

Ag (0.1)	As (0.2)	Ba (0.5)	Be (0.2)	Bi (0.2)	Cd (0.1)
Ce (0.02)	Co (0.1)	Cr (1)	Cs (0.01)	Cu (2)	Dy (0.01)
Er (0.01)	Eu (0.01)	Ga (0.1)	Gd (0.01)	Ge (0.05)	Hf (0.01)
Ho (0.01)	In (0.05)	La (0.01)	Lu (0.01)	Mn (1)	Mo (0.2)
Nb (0.01)	Nd (0.01)	Ni (2)	Pb (1)	Pr (0.01)	Rb (0.05)
Re (0.01)	Sb (0.1)	Sc (0.1)	Se* (5)	Sm (0.01)	Sn (0.2)
Sr (0.1)	Ta (0.01)	Tb (0.01)	Te (0.2)	Th (0.01)	Ti (1)
Tl (0.2)	Tm (0.01)	U (0.01)	V (0.1)	W (0.05)	Y (0.02)
Yb (0.01)	Zn (5)	Zr (0.5)			

**partially volatilized*

Appendix B 3 Lead Collection Fire Assay – ICP-MS: Nominal 40g charge analysed. Silver used as secondary collector, Au, Pt, Pd determined with ICP quantification. Nature of the sample and/or lower sample weights may compromise detection limits. Detection limits in ppb.

Au (1)	Pt (1)	Pd (1)

Appendix C: Particle size Distribution

Appendix C 1 Particle size distribution ultrafine Chalcocite B

Dispersant:	Ethanol	**RI/ABS:**	2.74 / 1
Additives:	0 ml Calgon	**Analysis Model:**	General purpose
Sonication:	15 minutes in ultrasonic bath	**Result units:**	Volume

Concentration:	0.01 % vol	**Vol. Weighted Mean D[4,3]:**	13.761	µm	**d(0.1):**	2.811	µm
Obscuration:	12.25 %	**Surface Weighted Mean D[3,2]:**	6.031	µm	**d(0.5):**	8.395	µm
Weighted Residual:	0.846 %	**Specific Surface Area:**	0.995	m^2/cc	**P80:**	18.883	µm

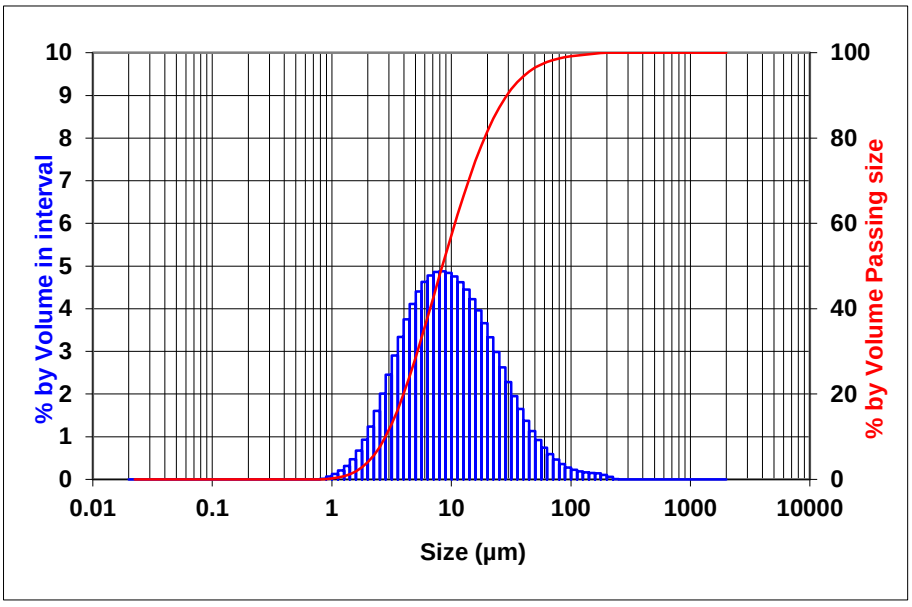

Appendix C 2 Particle size distribution ultrafine Chalcopyrite B

Dispersant:	Water	**RI/ABS:**	2.74 / 1
Additives:	10 ml Calgon	**Analysis Model:**	General purpose
Sonication:	20 minutes in ultrasonic bath	**Result units:**	Volume

Concentration:	0.0039 % vol	**Vol. Weighted Mean D[4,3]:**	5.272	µm	**d(0.1):**	0.838	*µm*
Obscuration:	16.87 %	**Surface Weighted Mean D[3,2]:**	1.848	µm	**d(0.5):**	3.392	*µm*
Weighted Residual:	0.891 %	**Specific Surface Area:**	3.25	m^2/cc	**P80:**	8.56	*µm*
					d(0.9):	12.67	*µm*

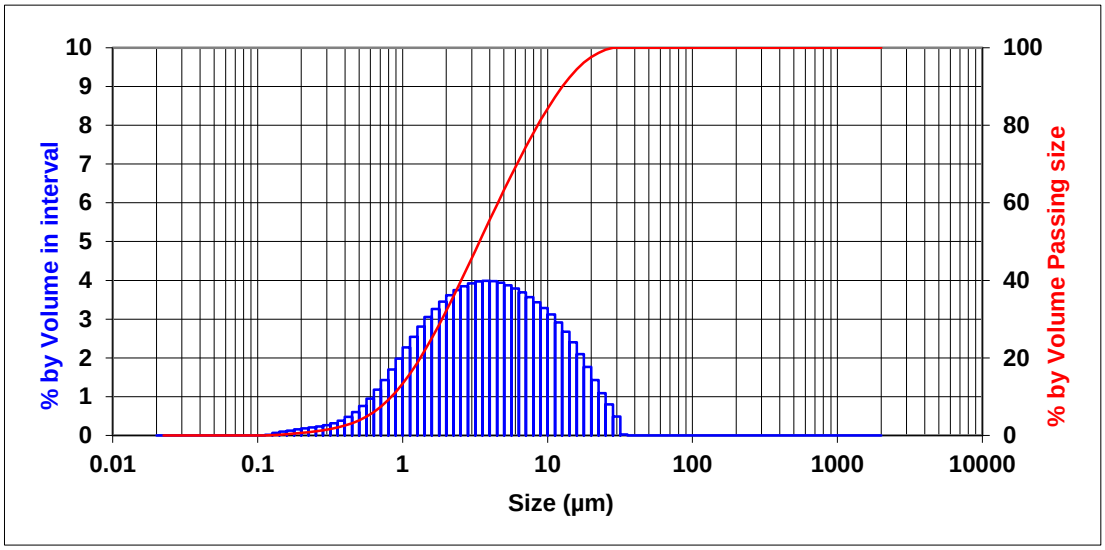

Appendix D: XPS Spectra

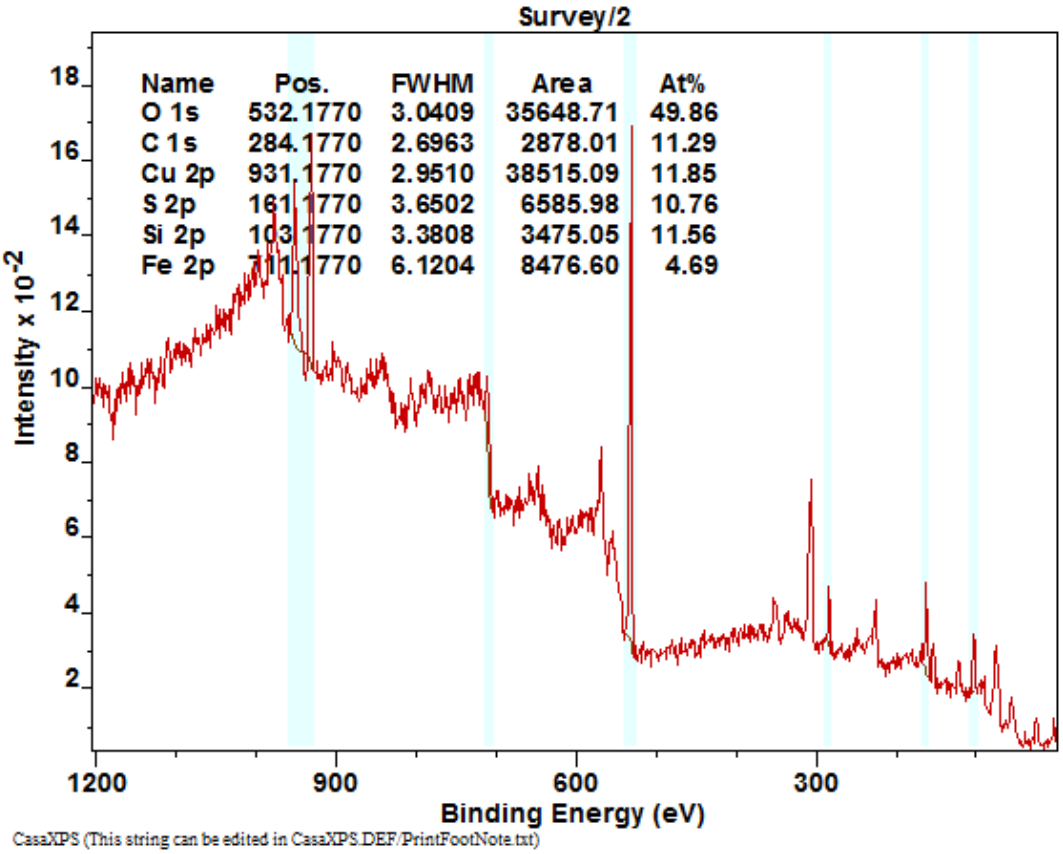

Appendix D1The XPS survey spectrum for unleached chalcopyrite B

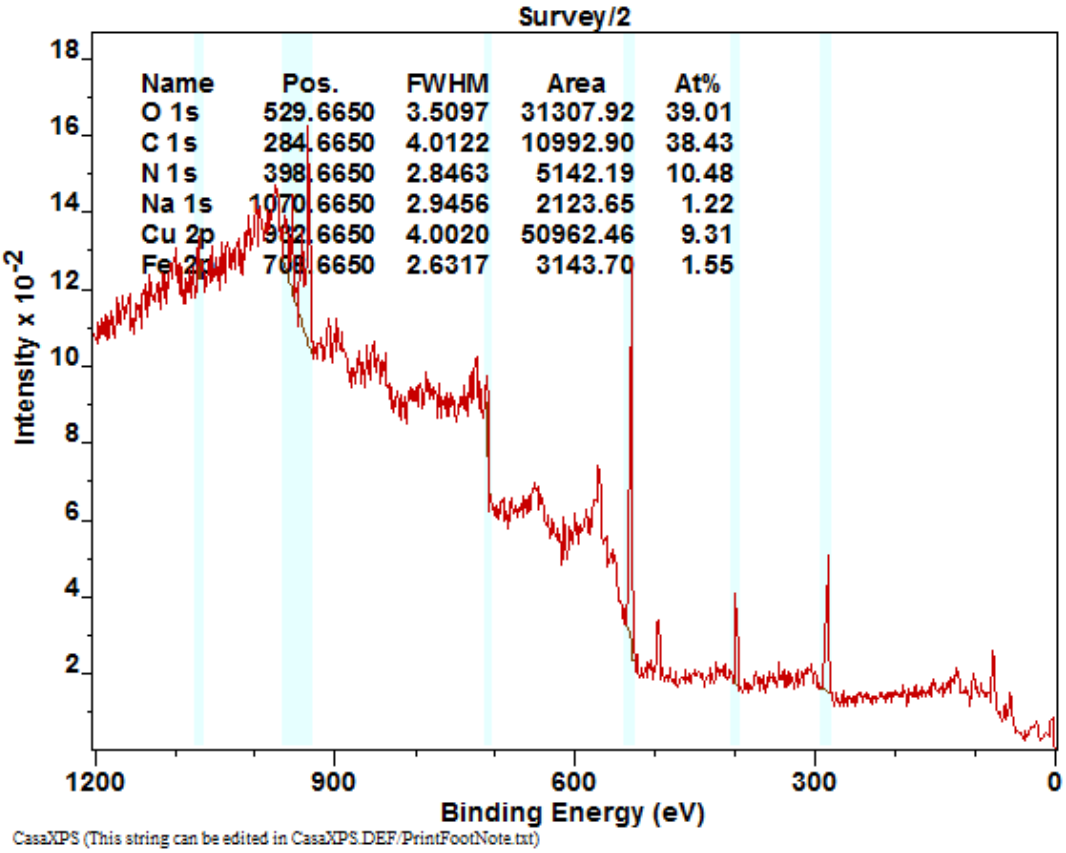

Appendix D2 XPS survey spectrum for leached chalcopyrite B

Appendix E: Properties of Reagents

Appendix E1 Properties of Glycine (Chemicalland21, 2017)

PRODUCT IDENTIFICATION	
CAS NO.	56-40-6
EINECS NO.	200-272-2
FORMULA	H_2NCH_2COOH
MOL WT.	75.07
H.S. CODE	2922.49
TOXICITY	Oral rat LD50 7930 mg/kg
SYNONYMS	
Aminoacetic Acid; Glycocoll; Athenon; Gly; G salt; Iconyl; Monazol; glycosthene; p-Hydroxyphenylaminoacetic Acid; Aminoethanoic Acid; p-Hydroxyanilinoacetic Acid; para-Oxyphenyl Glycocoll; Sucre De Gelatine;	
PHYSICAL AND CHEMICAL PROPERTIES	
PHYSICAL STATE	White crystals, Odorless
MELTING POINT	245 C (Decompose)
BOILING POINT	

SPECIFIC GRAVITY	1.6
SOLUBILITY IN WATER	25g/100 ml
pH	5.97 (Isoelectric point)
VAPOR DENSITY	
REFRACTIVE INDEX	
AUTOIGNITION	
NFPA RATINGS	Health: 0 Flammability: 1 Reactivity: 0
FLASH POINT	145 C
STABILITY	Stable under ordinary conditions
APPLICATIONS:	
Flavor enhancers and maskers, pH buffers and stabilizers, an ingredient in pharmaceutical products, food and personal care products and as a chemical intermediate.	
SALES SPECIFICATION	
TECHNICAL GRADE	
APPEARANCE	white to off-white crystalline powder
ASSAY (DRY BASIS)	98.5% min
LOSS ON DRYING	0.5% max
CHLORIDE	0.5% max
Fe	0.003% max
FEED GRADE	
APPEARANCE	white to off-white crystalline powder
ASSAY (DRY BASIS)	98.5% min
CHLORIDE	0.5% max
HEAVY METALS	20ppm max
ARSENIC	3ppm max
LOSS ON DRYING	0.2% max
FOOD GRADE	
BIBLIOGRAPHY	FCC IV
APPEARANCE	white, odorless, crystalline powder
ASSAY (DRY BASIS)	99.0% min
IDENTIFICATION	passes test
LOSS ON DRYING	0.2% max
CHLORIDE	0.002% max
HEAVY METALS	20ppm max
SULPHATE	50ppm max

pH	5.5 - 7.0
RESIDUE ON IGNITION	0.05% max
As	3ppm max
Pb	5ppm max
USP/BP GRADE	
BIBLIOGRAPHY	USP 24 / BP 93
APPEARANCE	white, odorless, crystalline powder
ASSAY (DRY BASIS)	99.0 -101.0%
IDENTIFICATION	passes test
LOSS ON DRYING	0.2% max
CHLORIDE	70ppm max
HEAVY METALS	20ppm max
SULPHATE	65 ppm
pH	5.5 - 6.5
RESIDUE ON IGNITION	0.1% max
As	3ppm max
Pb	5ppm max
HYDROLYZABLE SUBSTANCES	passes test
PYROGEN CONTENT	meets the requirements
ALUMINUM	meets the requirements
ORGANIC VOLATILES	meets the requirements
TRANSPORTATION	
PACKING	25kgs in Fiber Drum
HAZARD CLASS	Not regulated
UN NO.	
GENERAL PROPERTIES OF GLYCINE	
Glycine is a white, crystalline amino acid; dissolve in water and. As also known as aminoacetic acid, it is the simplest amino acid. It has acid group as well as amino group which both groups act as a base. It is not optically active, i.e., it does not have d- and l-stereoisomers as two hydrogens are bonded to the central carbon atom. It is nonessential amino acids for mammals; i.e., they can synthesize it from amino acids serine and threonine and from other sources and do not require dietary sources. It is commercially synthesis from ammonia. It is also prepared from bromoethanoic acid by reaction with potassium phthalimide. It helps to improve glycogen storage utilized in the synthesis of hemoglobin, collagen, and glutathione, and facilitates the amelioration of high blood fat and uric acid levels.	

Appendix E2 Appendix D1 Properties of Mextral 54-100

Item	Index
Extractant Appearance	Clear light yellow liquid, free from visible impurities
Maximum Copper Loading (g/1 Cu)	100

Viscosity(cP) (@ (kinematic))	10
Specific Gravity(250/)	0.95-0.98
Flash Point (°C)	90
Extraction Isotherm Point, Organic (g/1 Cu)	14
Extraction Isotherm Point, aqueous (g/1 Cu)	0.5
Stripping Isotherm Point ,Organic (g/1 Cu)	0.1
Stripping Isotherm Point, aqueous (g/1 Cu)	54
Extraction Kinetics, 30sec (%)	95
Strip Kinetics, 30sec (%)	95
1200r/min Extraction Phase Separation (s)	120
1200r/min Strip Phase Separation (s)	90
Extraction Cu/Fe Selectivity	2000
Copper Net Transfer (g/1 Cu)	14
Complex solubility (g/1 Cu)	40

Appendix E 3 Properties of Mextral 84H

Item	Index
Extractant Appearance	fluid amber liquid, free from visible
Maximum Copper Loading (g/1 Cu)	4.7
Viscosity(cP) at 25 "C	40
Specific Gravity(25 "C)	0.900.92
Flash Point ("C)	70
Extraction Isotherm Point, Organic (g/1 Cu)	3.65
Extraction Isotherm Point ,aqueous (g/1 Cu)	3
Strip Isotherm Point ,Organic (g/1 Cu)	0.5
Strip Isotherm Point ,aqueous (g/1 Cu)	38
Extraction Kinetics,30sec(%)	90
Strip Kinetics,30sec (%)	90
1200r/min Extraction Phase Separation (s)	60
1200r/min Strip Phase Separation (s)	80
Extraction Cu/Fe Selectivity	2000
Copper Net Transfer (g/1 Cu)	3
Complex solubility (g/1 Cu)	30

Appendix F Examples of Metal leaching Calculations

Appendix F1 Copper extraction calculations from chalcopyrite A: 25 °C, Gly:Cu 4:1, pH 11 and 100 rpm.

Measurements					Removed from soln			Calaculations		
Time (hours)	Ore (g)	Sol vol (mL)	sol ,L	[C],g/L	vol(mL)	Cu (g)	Cumm Cu (g)	Cu leach vessel (g)	Cu extrn total(g)	Soln Cu extrn,%
	14.81									
0					0					
3		500	0.5	0.159	3	0.000	0.000	0.080	0.080	3.800
29		497	0.497	0.270	3	0.001	0.001	0.134	0.135	6.419
97		494	0.494	0.643	3	0.002	0.003	0.318	0.321	15.231
192		491	0.491	0.995	3	0.003	0.006	0.488	0.495	23.467
266		488	0.488	1.506	3	0.005	0.011	0.735	0.746	35.387
435		485	0.485	2.056	3	0.006	0.017	0.997	1.014	48.119
600		482	0.482	2.278	3	0.007	0.024	1.098	1.122	53.225
864		479	0.479	2.399		0.000	0.024	1.149	1.173	55.651
Total						**0.024**				
Product	Qty	grade	cu mass,g							
Solids	10.833	8.63	0.9348879							
Sol(L)	0.479	2.399	1.149121							
Total Cu removed			0.02372415							
cal'ted Cu in sample			**2.10773305**							

Appendix F2 Copper and gold extraction calculations from Cu-Au ore C: [Gly] 0.5M, 60°C, O_2 0.05 l/min, 50% w/v % solids, Stirring, 250 rpm.

Measurements						Cu removed from soln						AU removed from soln				
Time (hours)	Ore (g)	Solution volume (mL)	sol ,L	[Cu],g/L	Au, ppm	vol(mL)	Cu (g)	Cumm Cu (g)	Cu leach vessel (g)	Cu extrn total(g)	Soln Cu extrn %	Au (µg)	Cumm Au (µg)	Au leach vessel (µg)	Au extrn total(µg)	Soln Au extrn %
	500															
1		500	0.5	0.0629	0.0113	5	0.00031	0.00031	0.03145	0.03145	4.702	0.057	0.0565	5.65	5.65	2.374
3		495	0.495	0.12425	0.0314	5	0.00062	0.00094	0.06150	0.06182	9.243	0.157	0.21350	15.543	15.60	6.554
6		490	0.49	0.206575	0.0404	5	0.00103	0.00197	0.10122	0.10216	15.274	0.202	0.41550	19.796	20.01	8.407
24		485	0.485	0.347575	0.0729	5	0.00174	0.00371	0.16857	0.17054	25.498	0.365	0.78000	35.357	35.77	15.029
48		480	0.48	0.6039	0.122	5	0.00302	0.00673	0.28987	0.29358	43.893	0.61	1.39000	58.56	59.34	24.931
72		475	0.475	0.586975	0.209	5	0.00293	0.00966	0.27881	0.28554	42.691	1.045	2.43500	99.275	100.67	42.293
102		475	0.475	0.494	0.22				0.23465	0.24431	36.527			104.5	106.94	44.927
						30	**0.00935**					**2.435**				

Cu			
Product	Quantity	grade	mass,g
Solids	518.11	0.082	0.42485
Solution	0.475	0.494	0.23465
Removed			0.009346
Total			0.668847

GOLD EXTRACTION CALCULATIONS				
PRODUCT	Quantity	GRADE (ppm)	GOLD MASS (µg)	DISTn. (%)
SOLIDS	518.1	0.253	131	55.07
SOLUTION	475.00	0.220	105	43.90
REMOVED			2.435	1.02
TOTAL	993.1		238	100.00
CALC'd HEAD		0.46		

Appendix G SEM Images of Un-leached and Leached Mineral Specimens

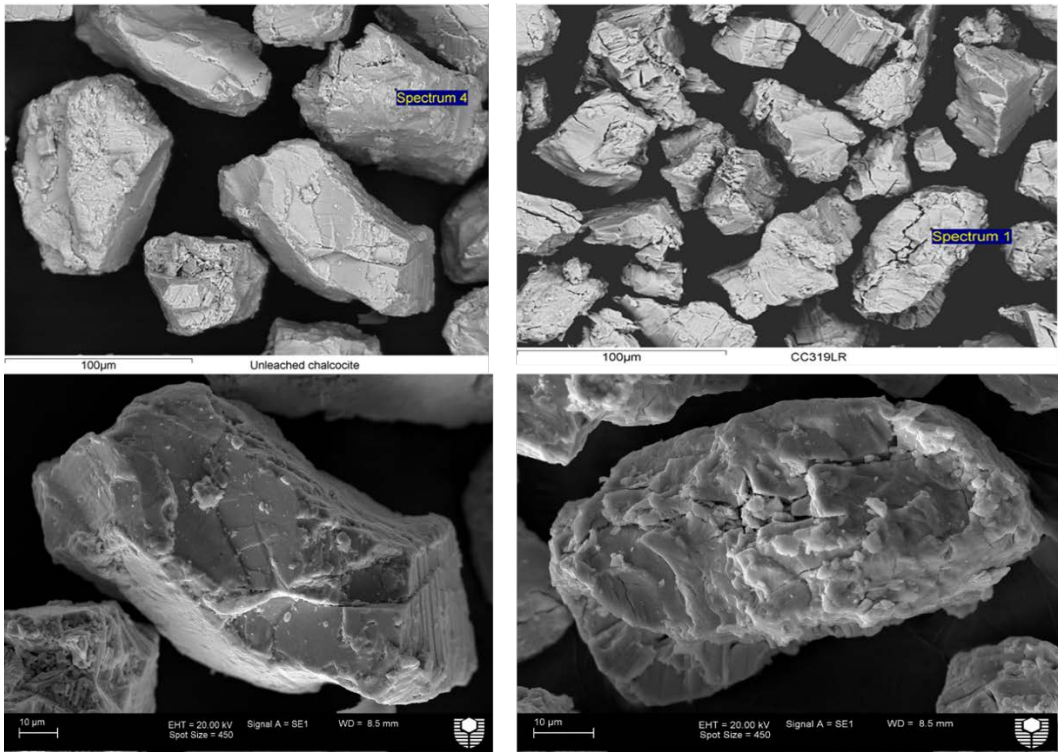

Appendix G 1 SEM Images of un-leached and leached chalcocite B

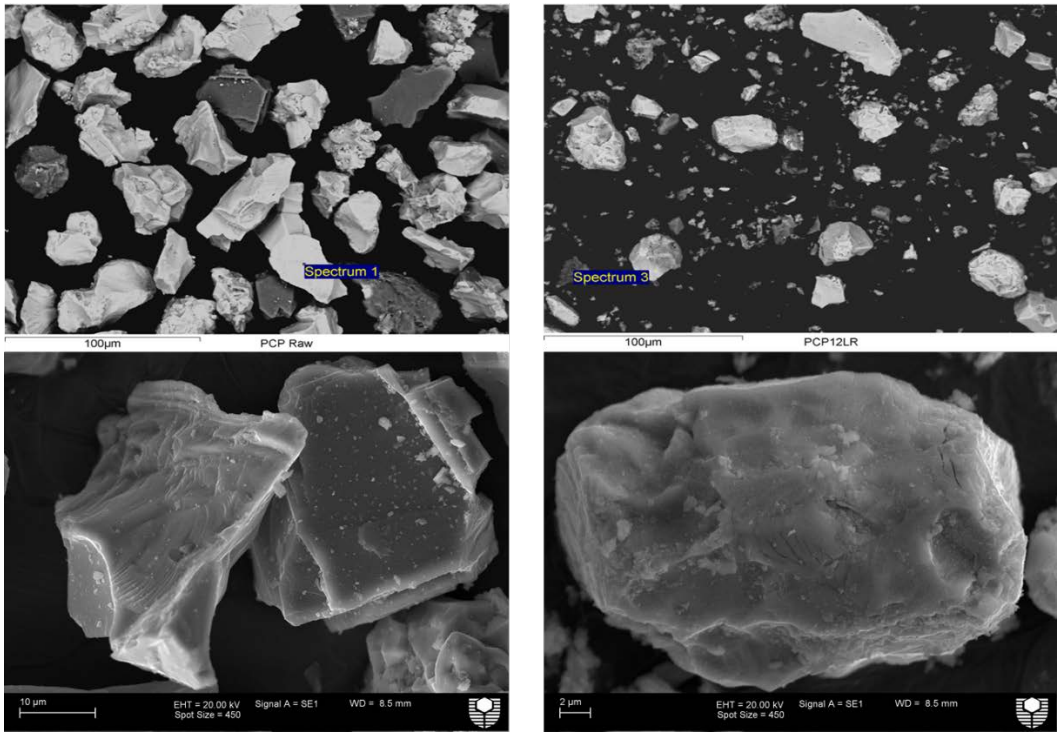

Appendix G 2 SEM Images of un-leached and leached chalcopyrite B

Appendix H Experimental Leaching Data

Appendix H 1 Azurite leaching data

Leaching Conditions	Time,hrs	pH	Eh, mV	[Cu], g/l	% Cu extraction
Gly:Cu 2:1	1	12.02	-1	1.679	41.98
mass sample= 4.750g	3	12.07	14	2.385	59.63
Gly: Cu= 2:1=4.725 g	6	12.06	24	2.526	63.15
DI = 500m l	24	12.06	42	2.771	69.28
Starting pH 11.09	48	11.96	53	2.922	73.05
Gly:Cu 3:1	1	11.99	7	2.308	57.70
mass sample= 4.750g	3	12.04	29	2.939	73.48
Gly: Cu= 3:1= 7.088g	6	12.11	25	3.245	81.13
DI = 500m l	24	12.14	48	3.6	90.00
Starting pH 11.04	48	12.09	50	3.902	97.55
Gly:Cu 4:1	1	11.99	40	2.65	66.25
mass sample= 4.750g	3	12.1	20	3.521	88.03
Gly: Cu 4:1 9.450g	6	12.14	27	3.735	93.38
DI = 500m l	24	12.16	42	3.874	96.85
Starting pH 11.01	48	12.09	46	3.878	96.95
Gly:Cu 8:1	1	11.72	-10	3.65	91.25
mass sample= 4.750g	3	11.87	-5	3.939	98.48

Gly: Cu= 8:1 =18.900g	6	11.92	8	3.988	99.70
DI = 500m l	24	11.93	23	4	100.00
Starting pH 11.00	48	11.83	29	4	100.00
pH 10	1	10.15	24	3.107	77.68
mass sample= 4.750g	3	10.23	40	3.595	89.88
Gly: Cu= 4:1= 9.450g	6	10.25	46	3.617	90.43
DI = 500m l	24	10.27	57	2.506	62.65
Starting pH 10	48	10.27	62	2.475	61.88

Appendix H 2 Malachite A leaching data

Leaching Conditions	Time,hrs	pH	Eh, mV	[Cu], g/l	% Cu extrn
Gly:Cu 2:1	1	12.16	1	2.085	52.13
mass sample= 4.813g	3	12.14	21	2.192	54.80
Gly: Cu= 2:1=4.725 g	6	12.11	21	2.308	57.70
DI = 500m l	24	12.13	28	2.326	58.15
Starting pH 11.00	48	12.04	28	2.379	59.48
	72	11.99	42	2.393	59.83
	96	11.98	41	2.599	64.98
Gly:Cu 3:1	1	12.23	-3	2.881	72.03
mass sample= 4.813g	3	12.22	-14	3.178	79.45
Gly: Cu= 3:1= 7.088g	6	12.21	14	3.303	82.58
DI = 500m l	24	12.22	18	3.39	84.75
Starting pH 11.17	48	12.15	31	3.433	85.83
Gly:Cu 4:1	1	12.26	12	3.091	77.28
mass sample= 4.813g	3	12.32	12	3.255	81.38
Gly: Cu 4:1 9.450g	6	12.25	18	3.365	84.13
DI = 500m l	24	12.27	34	3.546	88.65
Starting pH 11.01	48	12.12	23	3.581	89.53
Gly:Cu 4:1	1	12.17	-15	3.483	87.08
mass sample= 4.813g	3	12.18	-14	3.518	87.95
Gly: Cu= 8:1 =18.900g	6	12.17	-3	3.626	90.65
DI = 500m l	24	12.07	15	3.692	92.30
Starting pH 11.07	48	11.63	22	3.715	92.88
pH 9.5	1	9.33	71	2.756	68.90
mass sample= 4.813g	3	9.28	68	2.705	67.63
Gly: Cu= 4:1= 9.450g	6	9.26	70	2.809	70.23
DI = 500m l	24	9.31	69	2.004	50.10
Starting pH 9.50	48	9.28	76	1.532	38.30

Appendix H 3 Cuprite leaching data

Leaching Conditions	Time,hrs	pH	Eh, mV	[Cu], g/l	% Cu extraction
Gly:Cu 2:1	1	12.25	-80	1.15	28.75
mass sample= 4.750g	3	12.39	-47	1.74	43.50
Gly: Cu= 2:1=4.725 g	6	12.45	-39	1.755	43.88
DI = 500m l	24	12.55	-21	2.722	68.05
Starting pH 11.14	48	12.49	-10	2.833	70.83
	72	12.33	-6	2.986	74.65
	96	11.94	15	3.114	77.85
Gly:Cu 3:1	1	12.29	-93	1.198	29.95
mass sample= 4.750g	3	12.44	-63	1.647	41.18
Gly: Cu= 3:1= 7.088g	6	12.5	-52	2.232	55.80
DI = 500m l	24	12.6	-34	3.036	75.90
Starting pH 11.03	48	12.52	-26	3.409	85.23
Gly:Cu 4:1	1	12.31	-124	1.339	33.48
mass sample= 4.750g	3	12.46	65	2.058	51.45
Gly: Cu 4:1 9.450g	6	12.55	-55	2.452	61.30
DI = 500m l	24	12.64	-33	3.369	84.23
Starting pH 11.06	48	12.58	-25	3.732	93.30
Gly:Cu 8:1	1	12.28	-219	1.459	36.48
mass sample= 4.750g	3	12.49	-74	2.328	58.20
Gly: Cu= 8:1 =18.900g	6	12.58	-53	2.822	70.55
DI = 500m l	24	12.64	-28	3.425	85.63
Starting pH 11.09	48	12.36	-7	3.755	93.88
pH 9.0	1	8.97	-176	1.615	40.38
mass sample= 4.750g	3	8.99	77	2.441	61.02
Gly: Cu= 4:1= 9.450g	6	8.99	105	2.968	74.20
DI = 500m l	24	9.11	104	2.122	53.05
Starting pH 9	48	9.1	86	1.812	45.30
pH 10.0	1	10.31	-181	1.923	48.08
mass sample= 4.750g	3	10.78	-3	2.473	61.83
Gly: Cu= 4:1= 9.450g	6	11.19	-6	3.282	82.05
DI = 500m l	24	11.62	8	3.665	91.63
Starting pH 10	48	11.4	-5	3.888	97.20

Appendix H 4 Chrysocolla leaching data

Leaching conditions	Time, hrs	pH	Eh,mV	[CU], g/L	% Copper extrn
Gly:Cu 2:1	1	11.07	9	0.274	6.85
sample = 2g Cu = 8.097g	3	11.07	-1	0.346	8.65
DI= 500mL	6	11.12	-3	0.39	9.75
Gly:Cu 2:1 (4.725g)	24	11.13	17	0.472	11.80
Initial pH 11	48	11.17	14	0.475	11.88
Gly:Cu 2:1	1	11.01	6	0.388	9.70
sample = 2g Cu = 8.097g	3	11.02	-9	0.424	10.60
DI= 500mL	6	11.05	-14	0.437	10.93
Gly:Cu 3:1 (7.088g)	24	11.09	3	0.479	11.98
Initial pH 11	48	11.13	13	0.631	15.78
Gly:Cu 2:1	1	11.13	-10	63	7.88
sample = 2g Cu = 8.097g	3	11.17	-28	-10	12.18
DI= 500mL	6	11.16	13	-28	12.75
Gly:Cu 4:1 (9.450g)	24	11.17	-2	13	18.98
Initial pH 11	48	11.36	4	-2	19.13
pH 8	1	8.16	211	0.444	11.10
sample = 2g Cu = 8.097g	3	8.06	211	0.534	13.35
DI= 500mL	6	8.05	201	0.573	14.33
Gly:Cu 4:1 (9.450g)	24	8.02	130	0.762	19.05
Initial pH 8.01	48	8.14	107	1.075	26.88
pH9.5	1	9.48	119	0.561	14.03
sample = 2g Cu = 8.097g	3	9.47	117	0.651	16.28
DI= 500mL	6	9.47	114	0.671	16.78
Gly:Cu 4:1 (9.450g)	24	9.5	49	0.813	20.33
Initial pH 9.57	48	9.55	70	0.89	22.25

Appendix H 5 Chalcocite A leaching data

Leaching Conditions	Time,hrs	pH	Eh, mV	[Cu], g/L	% Cu extraction
Gly:Cu 2:1	**1**	**11.96**	**-121**	**0.537**	13.43
sample = 2g Cu = 2.538g	3	11.74	-86	0.661	16.53
DI= 500mL	6	11.58	-62	0.801	20.03
Gly:Cu 2:1 (4.725g)	24	11.47	-52	1.05	26.25
0.5% peroxide= 8.33mL	48	11.13	-37	1.269	31.73
Initial pH 11					
Gly:Cu 3:1	1	11.76	-111	0.68	17.00
sample = 2g Cu = 2.538g	3	11.6	-66	0.827	20.68
DI= 500mL	6	11.46	-67	0.951	23.78
Gly:Cu 3:1 (7.088g)	24	11.34	-49	1.316	32.90
0.5% peroxide= 8.33mL	48	11.1	-61	1.504	37.60
Initial pH 11					
Gly:Cu 4:1	1	11.62	-117	0.773	19.33
sample = 2g Cu = 2.538g	3	11.58	-65	0.922	23.05
DI= 500mL	6	11.51	-55	1.069	26.73
Gly:Cu 4:1 (9.450g)	24	11.35	-43	1.538	38.45
0.5 % peroxide= 8.33mL	48	11.14	-47	1.663	41.58
Initial pH 11					
Gly:Cu 8:1	1	11.52	-148	0.896	22.40
sample = 2g Cu = 2.538g	3	11.56	-94	1.082	27.05
DI= 500mL	6	11.57	-93	1.277	31.93
Gly:Cu 8:1 (18.900g)	24	11.39	-58	1.696	42.40
0.5% peroxide =8.33mL	48	11.17	-68	1.858	46.45
pH 11					
pH 9	1	8.15	101	1.529	38.225
sample = 2g Cu = 2.538g	3	7.84	74	1.581	39.525
DI= 500mL	6	7.9	56	1.552	38.8
Gly:Cu 4:1 (9.450g)	24	8.24	37	1.544	38.6
0.5% peroxide =8.33mL	48	8.42	30	1.573	39.325
Initial pH 9.06					
pH 10	1	9.84	-21	1.644	41.1
sample = 2g Cu = 2.538g	3	9.83	-29	1.601	40.025
DI= 500mL	6	9.8	-37	1.532	38.3
Gly:Cu 4:1 (9.450g)	24	9.8	-25	1.676	41.9
0.5% peroxide =8.33mL	48	9.78	-24	1.678	41.95
Initial pH 10.08					
0% peroxide	1	11.19	-140	0.288	7.2
sample = 2g Cu = 2.538g	3	11.36	-134	0.532	13.3
DI= 500mL	6	11.61	-63	1.071	26.775
Gly:Cu 4:1 (9.450g)	24	12.32	-62	1.615	40.375
0% peroxide	48	12.27	-49	1.751	43.775
Initial pH 11					

Leaching Conditions	Time,hrs	pH	Eh, mV	[Cu], g/L	% Cu extraction
sample = 2g Cu = 2.538g	3	11.58	-65	0.922	23.05
DI= 500mL	6	11.51	-55	1.069	26.725
Gly:Cu 4:1 (9.450g)	24	11.35	-43	1.538	38.45
0.5 % peroxide= 8.33mL	48	11.14	-47	1.663	41.575
Initial pH 11					

Appendix H 6 Chalcopyrite A leaching data

Leaching condition	Time, hrs	pH	Eh,mV	[Cu], g/L	% Copper extraction
Gly:Cu 2:1	3	11.1	-49	0.037	1.679
Sample 14.81g= 2.19 g Cu	29	10.85	-54	0.104	4.750
DI=500mL	97	10.4	-22	0.319	14.535
Gly:Cu 2:1	192	10.02	-17	0.463	21.106
0.5% peroxide	266	9.49	11	0.621	28.279
pH 11.22	435	8.99	50	0.686	31.277
Calculated head= 2.068g	600	8.71	63	0.896	40.825
	864	8.22	91	0.937	42.708
Gly:Cu 3:1	3	11.05	-42	0.040	1.829
Sample 14.81g= 2.19 g Cu	24	10.97	-82	0.095	4.355
DI=500mL	97	10.73	-50	0.256	11.779
Gly:Cu 3:1 (7.088g)	192	10.57	-18	0.473	21.737
0.5 % peroxide	266	10.29	-14	0.485	22.313
pH 11	435	9.73	4	0.708	32.555
Calculated head= 2.174g	534	9.55	18	0.754	34.662
	864	9.14	57	0.996	45.814
Gly:Cu 4:1	3	11.14	-67	0.072	3.262
Sample 14.81g= 2.19 g Cu	29	10.98	-67	0.121	5.536
DI=500mL	97	10.7	-57	0.363	16.551
Gly:Cu 4:1	192	10.44	-34	0.587	26.734
0.5% peroxide	266	10.11	-13	0.836	38.115
pH 11.16	435	9.69	3	1.058	48.222
Calculated head= 2.195%	600	9.25	20	1.105	50.382
	864	9.01	45	1.209	55.128
Gly:Cu 8:1	3	11.01	-68	0.108	4.834
Sample 14.81g= 2.19 g Cu	29	10.94	-81	0.213	9.498
DI=500mL	97	10.78	-58	0.410	18.299
Gly:Cu 8:1	192	10.6	-55	0.653	29.104
0.5% peroxide	266	10.32	-43	0.968	43.169
pH 11.00	435	10.16	-14	1.320	58.857
Calculated head= 2.242g	600	9.75	-5	1.491	66.480

Leaching condition	Time, hrs	pH	Eh,mV	[Cu], g/L	% Copper extraction
	864	9.35	14	1.599	71.291
pH 9	3	8.93	12	0.057	2.760
Sample 14.81g= 2.19 g Cu	29	8.89	2	0.080	3.888
DI=500mL	97	8.66	21	0.175	8.476
Gly:Cu 4:1	192	8.53	14	0.209	10.097
0.5% peroxide	266	8.39	24	0.271	13.068
pH 9.02	435	8.28	34	0.345	16.646
Calculated head= 2.070g	600	8.12	41	0.389	18.785
	864	7.92	54	0.417	20.145
EXPT 9	3	9.99	-22	0.068	2.924
Sample 14.81g= 2.19 g Cu	29	9.93	-41	0.093	4.023
DI=500mL	97	9.81	-18	0.209	9.005
Gly:Cu 4:1	192	9.64	-22	0.351	15.134
0.5% peroxide	266	9.41	1	0.563	24.282
pH 10.08	435	9.15	22	0.834	35.965
Calculated head= 2.319g	600	8.93	31	0.941	40.561
	864	8.87	47	1.029	44.370
No peroxide	3	10.99	-14	0.080	3.800
Sample 14.81g	29	10.86	-47	0.135	6.419
DI=500mL	97	10.65	-53	0.321	15.231
Gly:Cu 4:1	192	10.43	-35	0.495	23.467
0% peroxide	266	10.15	-23	0.746	35.387
pH 11.01	435	9.78	4	1.014	48.119
Calculated head= 2.108%	600	9.34	18	1.122	53.225
	864	9.08	34	1.173	55.651
0.1 % peroxide	3	11.03	-58	0.045	2.027
Sample 14.81g= 2.19 g Cu	29	10.89	-49	0.114	5.108
DI=500mL	97	10.67	-51	0.307	13.708
Gly:Cu 4:1	192	10.45	-25	0.515	22.981
0.1% peroxide	266	10.15	-27	0.751	33.548
pH 11.05	435	9.79	-2	0.968	43.241
Calculated head= 2.260%	600	9.34	14	1.132	50.529
	864	9.18	27	1.196	53.423
1 % peroxide	3	11.14	-67	0.072	3.262
Sample 14.81g= 2.19 g Cu	29	10.98	-67	0.121	5.536
DI=500mL	97	10.7	-57	0.363	16.551
Gly:Cu 4:1	192	10.44	-34	0.587	26.734
1% peroxide	266	10.11	-13	0.836	38.115
pH 11.16	435	9.69	3	1.058	48.222
Calculated head= 2.195%	600	9.25	20	1.105	50.382
	864	9.14	45	1.209	55.128

Appendix H 7 Malachite B leaching data

leaching conditions		Time, mins	pH	Eh, mV	[Cu], g/L	Cu extrn, %
% Cu in ore	56	5	9.98	144	0.1136	5.64
sample , g	1.799	15	10.07	124	0.2479	12.30
Di, mL	500	30	10.14	110	0.4156	20.63
Gly, M	0.1	60	10.26	96	0.7227	35.87
Temp, degrees	25	120	10.36	96	1.0911	54.15
Expected total copper in soln, g/L	2.015	180	10.45	80	1.3618	67.59
Stirring speed, RPM	350					
Particle size, µm	+53-75					
% Cu in ore	56	5	10.39	91	0.2398	11.90
sample , g	1.799	15	10.46	89	0.5885	29.21
Di, mL	500	30	10.52	70	0.8511	42.24
Gly, M	0.2	60	10.62	70	1.3119	65.11
Temp, degrees	25	120	10.76	78	1.6690	82.83
Expected total copper in soln, g/L	2.015	180	10.83	56	1.8361	91.13
Stirring speed, RPM	350					
% Cu in ore	56	5	10.06	-19	0.4488	22.27
sample , g	1.799	15	10.08	1	0.9048	44.91
Di, mL	500	30	10.13	22	1.3823	68.60
Gly, M	0.4	60	10.16	27	1.8040	89.53
Temp, degrees	25	120	10.18	172	1.9507	96.81
Expected total copper in soln, g/L	2.015	180	10.29	-27	2.0141	99.96
Particle size, µm	+53-75					
Stirring speed, RPM	350					
% Cu in ore	56	5	10.14	-18	0.5230	25.96
sample , g	1.799	15	10.15	-12	0.8907	44.21
Di, mL	500	30	10.14	-6	1.3451	66.76
Gly, M	0.8	60	10.17	5	1.7570	87.20
Temp, degrees	25	120	10.14	14	1.9777	98.15
Expected total copper in soln, g/L	2.015	180	10.11	18	2.0120	99.86
Stirring speed, RPM	350					
% Cu in ore	56	5	10.01	N/A	0.6833	33.91
sample , g	1.799	15	10.02	42	1.3800	68.49
Di, mL	500	30	10.07	36	1.6271	80.75
Gly, M	0.4	60	10.16	34	1.9536	96.96
Temp, degrees	30	120	10.18	28	1.9874	98.64
Expected total copper in soln, g/L	2.015	180	10.22	28	2.0120	99.86
Stirring speed, RPM	350					
Particle size, µm	+53-75					
% Cu in ore	56	5	10.01	58	0.9933	0.28
sample , g	1.799	15	10.08	28	1.6953	0.48
Di, mL	500	30	10.22	15	1.9500	0.56
Gly, M	0.4	60	10.29	14	1.9855	0.57

Temp, degrees	40	120	10.32	42	2.0141	0.58
Expected total copper in soln, g/L	2.015	180	10.23	17	2.0145	0.58
Stirring speed, RPM	350					
Particle size, µm	+53-75					
% Cu in ore	56	5	10.04	15	1.6840	3.01
sample , g	1.799	15	10.15	9	1.9537	3.49
Di, mL	500	30	10.26	-1	1.9981	3.57
Gly, M	0.4	60	10.16	3	2.0070	3.58
Temp, degrees	50	120	10.31	9	2.0145	3.60
Expected total copper in soln, g/L	2.015	180	10.34	5	2.0146	3.60
Stirring speed, RPM	350					
Particle size, µm	+53-75					
% Cu in ore	56	5	10.29	39	0.3321	16.48
sample , g	1.799	15			0.6782	33.66
Di, mL	500	30	10.3	33	1.0159	50.42
Gly, M	4	60	10.31	26	1.3783	68.41
Temp, degrees	25	120	10.4	36	1.7360	86.16
Expected total copper in soln, g/L	2.015	180	40.39	42	1.9281	95.69
Stirring speed, RPM	150					
Particle size, µm	+53-75					
% Cu in ore	56	5	10.27	53	0.5591	0.16
sample , g	1.799	15	10.31	63	0.9775	0.28
Di, mL	500	30	10.25	-29	1.4339	0.41
Gly, M	0.4	60	10.32	5	1.8328	0.52
Temp, degrees	25	120	10.37	14	1.9509	0.56
Expected total copper in soln, g/L	2.015	180	10.21	-1	2.0146	0.58
Stirring speed, RPM	550					
Particle size, µm	+53-75					
% Cu in ore	56	5	10.15	32	0.4830	0.86
sample , g	1.799	15	10.2	15	1.1953	2.13
Di, mL	500	30	10.33	29	1.5339	2.74
Gly, M	0.4	60	10.43	8	1.8630	3.33
Temp, degrees	25	120	10.19	21	2.0106	3.59
Expected total copper in soln, g/L	2.015	180	10.19	45	2.0147	3.60
Stirring speed, RPM	800					
Particle size, µm	+53-75					
% Cu in ore	56	5	10.1	-29	0.8025	39.83
sample , g	1.799	15	10.14	12	1.3425	66.63
Di, mL	500	30	10.17	27	1.7150	85.12
Gly, M	4	60	10.15	-17	1.9847	98.50
Temp, degrees	25	120	10.34	-22	1.9995	99.24
Expected total copper in soln, g/L	2.015	180			2.0148	100.00
Stirring speed, RPM	350					
Particle size, µm	+20-38					
% Cu in ore	56	5	10.04	-3	0.8590	42.63
sample , g	1.799	15	10.06	-4	1.3081	64.92

Di, mL	500	30	10.28	15	1.6837	83.56
Gly, M	0.4	60	10.32	11	1.9982	99.17
Temp, degrees	30	120	10.36	35	2.0146	99.99
Expected total copper in soln, g/L	2.015	180	10.2	5	2.0148	100.00
Stirring speed, RPM	350					
Particle size, µm	+38-53					
% Cu in ore	56	5	10.31	58	0.3598	17.86
sample , g	1.799	15	10.37	35	0.6894	34.22
Di, mL	500	30	1043	41	1.1569	57.42
Gly, M	0.4	60	10.51	44	1.6686	82.81
Temp, degrees	50	120	10.52	40	1.9035	94.47
Expected total copper in soln, g/L	2.015	180	10.32	10	1.9156	95.07
Stirring speed, RPM	350					
Particle size, µm	+75-106					

Appendix H 8 Chalcocite B leaching data

leaching conditions		Time, hours	pH	Eh, mV	[Cu], g/L	Cu extrn, %
% Cu in ore	78.5	0.5	10.04	-121	0.084	4.20
sample , g	1.274	1	10.06	-122	0.1088	5.44
Di, mL	500	3	10.01	-113	0.163	8.15
Gly, M	0.1	6	10.06	-36	0.2979	14.89
Temp, degrees	25	24	10.49	-11	0.555	27.75
Expected total copper in soln, g/L	2.000	48	10.4	-28	0.6304	31.52
Stirring speed, RPM	400					
Particle size, µm	+38-53					
DO, ppm	8					
% Cu in ore	78.5	0.5	10.03	-188	0.151	7.55
sample , g	1.274	1	10.04	-114	0.1576	7.88
Di, mL	500	3	10.05	-82	0.2267	11.33
Gly, M	0.3	6	10.05	-57	0.3949	19.74
Temp, degrees	25	24	10.14	-73	0.6561	32.80
Expected total copper in soln, g/L	2.000	48	9.59	7	0.7434	37.17
Stirring speed, RPM	400					
Particle size, µm	+38-53					
DO, ppm	8					
% Cu in ore	78.5	0.5	10.19	-227	0.1351	6.75
sample , g	1.274	1	10.15	-228	0.1461	7.30
Di, mL	500	3	10.18	-132	0.2542	12.71
Gly, M	0.5	6	10.27	-164	0.4826	24.13
Temp, degrees	25	24	10.21	-106	0.7996	39.98

Expected total copper in soln, g/L	2.000	48	10.21	-58	0.8667	43.33
Stirring speed, RPM	400					
Particle size, µm	+38-53					
DO, ppm	8					
% Cu in ore	78.5	0.5	10.05	-55	0.1411	7.05
sample , g	1.274	1	10.09	-128	0.1485	7.42
Di, mL	500	3	10.04	-180	0.264	13.20
Gly, M	1	6	10.05	-40	0.5043	25.21
Temp, degrees	25	24	10.16	-77	0.7983	39.91
Expected total copper in soln, g/L	2.000	48	10.09	-72	0.8633	43.16
Stirring speed, RPM	400					
Particle size, µm	+38-53					
DO, ppm	8					
% Cu in ore	78.5	0.5	10.25	-123	0.102	5.10
sample , g	1.274	1	10.2	-16	0.132	6.60
Di, mL	500	3	10.23	26	0.2	10.00
Gly, M	0.5	6	10.21	71	0.273	13.65
Temp, degrees	25	24	10.29	54	0.351	17.55
Expected total copper in soln, g/L	2.000	48	10.31	-75	0.477	23.85
Stirring speed, RPM	200					
Particle size, µm	+38-53					
% Cu in ore	78.5	0.5	10.23	-161	0.117	5.85
sample , g	1.274	1	10.23	-175	0.155	7.75
Di, mL	500	3	10.21	-148	0.312	15.60
Gly, M	0.5	6	10.2	-93	0.596	29.80
Temp, degrees	25	24	10.3	-74	0.959	47.95
Expected total copper in soln, g/L	2.000	48	10.4	-56	1.048	52.40
Stirring speed, RPM	600					
Particle size, µm	+38-53					
% Cu in ore	78.5	0.5	10.33	-155	0.118	5.90
sample , g	1.274	1	10.26	109	0.166	8.30
Di, mL	500	3	10.06	-87	0.299	14.95
Gly, M	0.5	6	10.03	-117	0.46	23.00
Temp, degrees	25	24	10.1	-41	0.818	40.90
Expected total copper in soln, g/L	2.000	48	10.08	-45	0.882	44.10
Stirring speed, RPM	800					
Particle size, µm	+38-53					
% Cu in ore	79.2	0.5	10.28	-86	0.1316	6.52
sample , g	1.274	1	10.28	-99	0.1808	8.96
Di, mL	500	3	10.24	-57	0.424	21.01
Gly, M	4	6	10.27	-97	0.5989	29.68
Temp, degrees	25	24	10.31	-81	0.7986	39.57

Expected total copper in soln, g/L	2.018016	48	10.42	-12	0.8735	43.29
Stirring speed, RPM	350					
Particle size, µm	+20-38					
% Cu in ore	78.6	0.5	10.31	-200	0.1119	5.59
sample , g	1.274	1	10.26	-153	0.1157	5.78
Di, mL	500	3	10.33	-46	0.2181	10.89
Gly, M	0.4	6	10.24	-113	0.3208	16.02
Temp, degrees	25	24	10.39	-66	0.5681	28.37
Expected total copper in soln, g/L	2.002728	48	10.47	-200	0.6356	31.74
Stirring speed, RPM	350					
Particle size, µm	+53-75					
% Cu in ore	77.6	0.5	10.12	-97	0.0467	2.36
sample , g	1.274	1	10.37	-107	0.0949	4.80
Di, mL	500	3	10.06	-75	0.1878	9.50
Gly, M	0.4	6	9.83	-168	0.2837	14.35
Temp, degrees	25	24	9.97	-55	0.5275	26.68
Expected total copper in soln, g/L	1.977248	48	9.97	-10	0.6235	31.53
Stirring speed, RPM	350					
Particle size, µm	+75-106					
% Cu in ore	77.6	0.5	10.7	-93	0.351975	17.80
sample , g	1.274	1	10.66	-81	0.533525	26.98
Di, mL	500	3	10.91	-61	0.847775	42.88
Gly, M	0.4	6	10.9	-50	0.96905	49.01
Temp, degrees	25	24	10.87	-37	1.331	67.32
Expected total copper in soln, g/L	1.977248	48	10.66	-9	1.54645	78.21
Stirring speed, RPM	350					
pH	10.5					
Particle size, µm	P80 18.88					
% Cu in ore	78.5	0.5	9.86	-151	0.167	8.35
sample , g	1.274	1	9.88	-73	0.209	10.45
Di, mL	500	3	9.82	-46	0.442	22.10
Gly, M	0.5	6	9.98	-68	0.635	31.75
Temp, degrees	35	24	10.06	-71	0.887	44.35
Expected total copper in soln, g/L	2.000	48	10.09	-68	0.946	47.30
Stirring speed, RPM	400					
Particle size, µm	+38-53					
DO, ppm	8					
% Cu in ore	78.5	0.5	10.4	-161	0.237	11.85
sample , g	1.274	1	10.39	-152	0.241	12.05
Di, mL	500	3	10.27	-98	0.436	21.80
Gly, M	0.5	6	10.33	-75	0.642	32.10
Temp, degrees	45	24	10.38	-91	0.879	43.95

Expected total copper in soln, g/L	2.000	48	10.47	-82	1.047	52.35
Stirring speed, RPM	400					
Particle size, µm	+38-53					
DO, ppm	8					
% Cu in ore	78.5	0.5	9.93	-183	0.222	11.10
sample , g	1.274	1	10.02	-132	0.278	13.90
Di, mL	500	3	10.06	-110	0.566	28.30
Gly, M	0.5	6	9.92	-91	0.759	37.95
Temp, degrees	55	24	10.36	-84	0.91	45.50
Expected total copper in soln, g/L	2.000	48	10.1	-64	1.1	55.00
Stirring speed, RPM	400					
Particle size, µm	+38-53					
DO, ppm	8					
% Cu in ore	78.5	0.5	10.17	-65	0.2363	11.81
sample , g	1.274	1	10.11	-126	0.2578	12.89
Di, mL	500	3	10.02	-75	0.5067	25.33
Gly, M	0.5	6	10.08	-83	0.7652	38.26
Temp, degrees	25	24	10.12	-71	0.9831	49.15
Expected total copper in soln, g/L	2.000	48	10.22	-19	0.9968	49.84
Stirring speed, RPM	400					
Particle size, µm	+38-53					
DO, ppm	15					
% Cu in ore	78.5	0.5	11.1	-136	0.307	15.35
sample , g	1.274	1	11.1	-152	0.487	24.35
Di, mL	500	3	11.24	-162	0.633	31.65
Gly, M	0.5	6	11.34	-152	0.744	37.20
Temp, degrees	25	24	11.48	-103	0.998	49.90
Expected total copper in soln, g/L	2.000	48	11.42	-86	1.081	54.05
Stirring speed, RPM	400					
Particle size, µm	+38-53					
DO, ppm	20					
% Cu in ore	78.5	0.5	10.14	-152	0.287	14.35
sample , g	1.274	1	10.15	-119	0.36	18.00
Di, mL	500	3	10.17	-46	0.682	34.10
Gly, M	0.5	6	10.2	88	0.841	42.05
Temp, degrees	25	24	10.24	-6	0.893	44.65
Expected total copper in soln, g/L	2.000	48	10.26	-16	0.891	44.55
Stirring speed, RPM	400					
Particle size, µm	+38-53					
DO, ppm	25					

Appendix H 9 Chalcopyrite B leaching data

leaching conditions		Time, hours	pH	Eh, mV	[Cu], g/L	Cu extrn, %
Gly, M	0.1	1	11.04	-35	0.0073	0.35
sample mass, g	3.8	3	11.03	-36	0.0145	0.70
% Cu in sample	27.2	6	10.96	-60	0.0279	1.35
DI, L	0.5	24	10.51	-11	0.1182	5.72
PS, um	20-38	48	0	-3	0.2154	10.42
SS	400	72	10.03	0	0.3008	14.55
Temp, degrees Celsius	50	96	9.77	22	0.3592	17.37
[O2],ppm	15					
expected Cu in sol, g/L	2.0672					
Gly, M	0.3	1	11.6	-35	0.0116	0.56
sample mass, g	3.8	3	11.29	-36	0.0282	1.37
% Cu in sample	27.2	6	11.19	-60	0.0538	2.60
DI, L	0.5	24	10.81	-11	0.1469	7.10
PS, µm	20-38	48	10.37	-3	0.2277	11.01
SS	400	72	0	0	0.3958	19.15
Temp, degrees Celsius	50	96	10.22	22	0.5080	24.57
[O2],ppm	15					
expected Cu in sol, g/L	2.0672					
Gly, M	0.5	1	11.3	-4	0.0121	0.59
sample mass, g	3.801	3	11.17	1	0.0133	0.64
% Cu in sample	27.2	6	11.06	-5	0.0410	1.98
DI, L	0.5	24	10.66-11.03	-9	0.1350	6.53
PS, um	20-38	48	10.85	3	0.2698	13.05
SS	400	72	10.5	4	0.4478	21.65
Temp, degrees Celsius	50	96	10.51	24	0.5823	28.16
[O2],ppm	15					
expected Cu in sol, g/L	2.0677					
Gly, M	1	1	11.01	-28	0.0198	0.96
sample mass, g	3.8	3	10.91	-15	0.0405	1.96
% Cu in sample	27.2	6	10.9	-12	0.0760	3.68
DI, L	0.5	24	10.85	-19	0.2018	9.76
PS, um	20-38	48	10.83	-29	0.3388	16.39
SS	400	72	10.8	-23	0.4795	23.20
Temp, degrees Celsius	50	96	10.43	-16	0.5888	28.48
[O2],ppm	15					
expected Cu in sol, g/L	2.0672					
Gly, M	0.5	1	10.6	-40	0.0219	1.06
sample mass, g	3.804	3	10.71	-39	0.0246	1.19
% Cu in sample	27.2	6	10.93	-7	0.0450	2.17
DI, L	0.5	24	10.91	-1	0.1797	8.68
PS, µm	20-38	48	10.87	8	0.3109	15.02
SS	200	72	10.8	10	0.4135	19.98

Temp, degrees Celsius	50	96	10.65	17	0.5145	24.86
[O2],ppm	15					
expected Cu in sol, g/L	2.0694					
Gly, M	0.5	1	11.02	2	0.0176	0.85
sample mass, g	3.8	3	10.86	-6	0.0330	1.60
% Cu in sample	27.2	6	10.83	-8	0.0642	3.11
DI, L	0.5	24	10.73	-2	0.2614	12.64
PS, um	20-38	48	10.72	23	0.3977	19.24
SS	400	72	10.42	-7	0.5207	25.19
Temp, degrees Celsius	50	96	10.2	13	0.6527	31.57
[O2],ppm	15					
expected Cu in sol, g/L	2.0672					
Gly, M	0.5	1	10.92	-53	0.0059	0.29
sample mass, g	3.8	3	10.8	-35	0.0285	1.41
% Cu in sample	26.6	6	10.78	-27	0.0588	2.91
DI, L	0.5	24	10.75	-20	0.2342	11.58
PS, um	20-38	72	10.42	-7	0.5631	27.85
SS	600	96	10.38	5	0.6643	32.86
Temp, degrees Celsius	50					
[O2],ppm	15					
expected Cu in sol, g/L	2.0216					
Gly, M	0.5	1	11.05	-54	0.0259	1.25
sample mass, g	3.804	3	11.04	-43	0.0310	1.50
% Cu in sample	27.2	6	10.9	-41	0.0502	2.42
DI, L	0.5	24	10.79	-46	0.2006	9.69
PS, µm	20-38	48	10.52	-27	0.4494	21.72
SS	800	72	10.47	-7	0.6441	31.12
Temp, degrees Celsius	50	96	10.16	-3	0.8123	39.25
[O2],ppm	15					
Gly, M	0.5	1	10.96	-27	0.26158	12.94
sample mass, g	3.8	3	10.81	-17	0.6245	30.89
% Cu in sample	26.6	6	10.6	-13	0.9468	46.83
DI, L	0.5	24	10.17	1	1.4825	73.33
PS, µm	-10	48	10.29	8	1.66308	82.27
SS	400	72	10.1	21	1.729	85.53
Temp, degrees Celsius	50	96	9.88	27	1.82173	90.11
[O2],ppm	15					
expected Cu in sol, g/L	2.0216					
Gly, M	0.5	1	11.02	2	0.01765	0.85
sample mass, g	3.8	3	10.86	-6	0.03299	1.60
% Cu in sample	27.2	6	10.83	-8	0.06419	3.11
DI, L	0.5	24	10.73	-2	0.26138	12.64
PS, um	20-38	48	10.72	23	0.39769	19.24
SS	400	72	10.42	-7	0.52071	25.19
Temp, degrees Celsius	50	96	10.2	13	0.65267	31.57
[O2],ppm	15					

expected Cu in sol, g/L	2.0672					
Gly, M	0.5	1	10.92	-35	0.0092	0.44
sample mass, g	3.804	3	10.88	-33	0.01568	0.76
% Cu in sample	27.2	24	10.82	-35	0.13873	6.70
DI, L	0.5	48	10.62	-14	0.31208	15.08
PS, µm	53-75	72	10.49	7	0.49423	23.88
SS	400	96	10.31	-6	0.6263	30.27
Temp, degrees Celsius	50					
[O2],ppm	15					
expected Cu in sol, g/L	2.0694					
Gly, M	0.5	1	10.94	-33	0.0123	0.61
sample mass, g	3.804	3	10.91	-44	0.01718	0.85
% Cu in sample	26.6	6	10.87	-44	0.03385	1.67
DI, L	0.5	24	10.78	-9	0.1926	9.52
PS, µm	75-106	48	10.58	-13	0.38913	19.23
SS	400	72	10.57	-9	0.52968	26.17
Temp, degrees Celsius	50	96			0.64968	32.10
[O2],ppm	15					
expected Cu in sol, g/L	2.0237					
Gly, M	0.5	1	10.96	-19	0.0105	0.51
sample mass, g	3.8	3	10.89	-12	0.023	1.11
% Cu in sample	27.2	6	10.85	-13	0.03775	1.83
DI, L	0.5	24	10.66	-14	0.17975	8.70
PS, um	20-38	48	10.55	-10	0.2925	14.15
SS	400	72	0	0	0.4785	23.15
Temp, degrees Celsius	50	96	10.3	9	0.65325	31.60
[O2],ppm	8					
expected Cu in sol, g/L	2.0672					
Gly, M	0.5	1	10.99	4	0.01875	0.91
sample mass, g	3.8	3	10.93	-1	0.03675	1.78
% Cu in sample	27.2	6	10.8	4	0.06775	3.28
DI, L	0.5	24	10.7	-8	0.26075	12.61
PS, um	20-38	48	10.5	20	0.51225	24.78
SS	400	72	10.01	10	0.52575	25.43
Temp, degrees Celsius	50	96	10	40	0.55425	26.81
[O2],ppm	25					
expected Cu in sol, g/L	2.0672					
Gly, M	0.5	1	11.02	2	0.01765	0.853655
sample mass, g	3.8	3	10.86	-6	0.03299	1.595963
% Cu in sample	27.2	6	10.83	-8	0.06419	3.105324
DI, L	0.5	24	10.73	-2	0.26138	12.64399
PS, um	20-38	48	10.72	23	0.39769	19.23816
SS	400	72	10.42	-7	0.52071	25.189
Temp, degrees Celsius	50	96	10.2	13	0.65267	31.57285
[O2],ppm	15					
expected Cu in sol, g/L	2.0672					

Gly, M	0.5	1	11.15	-15	0.00928	0.448203
sample mass, g	3.804	3	11.1	-42	0.01563	0.755059
% Cu in sample	27.2	6	11.07	-19	0.02545	1.229839
DI, L	0.5	24	0	0	0.07753	3.746298
PS, µm	20-38	48	10.94	-33	0.1492	7.209903
SS	400	72	10.93	-36	0.21948	10.60585
Temp, degrees Celsius	40	96	10.85	-32	0.2912	14.07187
[O2],ppm	15					
expected Cu in sol, g/L	2.0694					
Gly, M	0.5	1	10.96	-27	0.02018	0.997972
sample mass, g	3.8	3	10.81	-17	0.05195	2.569747
% Cu in sample	26.6	6	10.6	-13	0.093	4.600317
DI, L	0.5	24	10.17	1	0.273	13.50416
PS, um	20-38	72	10.1	21	0.6172	30.53027
SS	400	96	9.88	27	0.78958	39.05694
Temp, degrees Celsius	60					
[O2],ppm	15					
expected Cu in sol, g/L	2.0216					
Gly, M	0.5	1	0	0	0.02198	1.061914
sample mass, g	3.804	3	10.35	-34	0.05403	2.61069
% Cu in sample	27.2	6	10.3	-31	0.09018	4.357594
DI, L	0.5	24	9.95-10.63	-7	0.27148	13.11869
PS, µm	20-38	48	9.91-11.19	-6	0.50875	24.58471
SS	400	72	9.38-11.30	11	0.70325	33.98367
Temp, degrees Celsius	70	96	9.08	78	0.8826	42.65054
[O2],ppm	15					
expected Cu in sol, g/L	2.0694					
Gly, M	0.5	0.5	11.82	-51	0.03446	1.727433
sample mass, g	3.7	1	11.82	-70	0.06281	3.148579
% Cu in sample	26.2	3	11.69	-46	0.15728	7.884231
DI, L	0.5	6	11.58	-40	0.26838	13.45352
PS, um	10	24	11.32	-4	0.72016	36.10063
SS	500	48	11.13	30	0.99615	49.93563
Temp, degrees Celsius	30					
[O2],ppm	8					
expected Cu in sol, g/L	1.9388					
Gly, M	0.5	0.5	11.71	-83	0.06887	3.452359
sample mass, g	3.8	1	11.7	-79	0.11753	5.891618
% Cu in sample	27.2	3	11.34	-53	0.28529	14.3012
DI, L	0.5	6	11.25	-39	0.4699	23.55544
PS, um	10	24	10.97	-6	1.059	53.08622
SS	500	48	10.77	-10	1.18408	59.35631
Temp, degrees Celsius	40					
expected Cu in sol, g/L	2.0672					
Gly, M	0.5	1	11.4	-55	0.17999	9.022652

sample mass, g	3.804	3	10.95	-43	0.40387	20.24545
% Cu in sample	27.2	6	10.64	-34	0.64885	32.52596
DI, L	0.5	24	10.34	-14	1.09768	55.02519
PS, µm	10	48	10.14	-3	1.27891	64.11001
SS	400					
Temp, degrees Celsius	50					
[O2],ppm	15					
expected Cu in sol, g/L	2.0694					
Gly, M	0.5	0.5	11.22	-78	0.15885	7.962933
sample mass, g	3.8	1	10.75	-73	0.25971	13.01891
% Cu in sample	26.6	3	10.54	-45	0.66144	33.15708
DI, L	0.5	6			0.95744	47.99516
PS, um	10	24	10.04	-16	1.4491	72.6414
SS	400	48	10.03	-9	1.51172	75.78045
Temp, degrees Celsius	60					
[O2],ppm	15					
expected Cu in sol, g/L	2.0216					

Appendix H 10 Copper-Gold ore A leaching data

leaching Conditions		Time,h	pH	Eh, mV	[Cu],g/L	[Au], mg/L	% cu extrn (recal'ted h'grade	% Au extrn (recal'ted h'grade)
Peroxide,%	0	6	11.2	-47	0.174		2.41	
pH (NaoH)	11	24	11.1	-61	0.455		6.28	
DI 500 mL		120	10.6	-24	2.01		27.57	
Sample mass, g (% Cu 3.56, Au 1.96ppm)	100	168	10.4	-34	2.538	0.275	37.37	50.34
Cu:Gly 1:2								
Peroxide, %	0	6	11	-18	0.235		3.21	
pH (NaoH)	11	24	11	-25	0.628		8.54	
DI 500 mL	500	120	10.7	-42	2.505		33.87	
Sample mass, g 100g (% Cu 3.56, Au	100	168	10.6	-35	3.372	0.211	46.68	42.33
Cu:Gly 1:4								
0% peroxide	0	6	11.1	72	0.309		4.12	
pH (NaoH)	11	24	11.1	-86	0.874		11.60	
DI 500 mL	500	120	10.8	-64	2.85		37.61	
Sample mass, g (% Cu 3.56, Au 1.96ppm)	100	168	10.7	-58	3.787	0.244	50.44	40.54
Cu:Gly 1:8								
Peroxide, %	0	6	10.1	-6	0.18		2.45	
pH	10	24	10	-25	0.542		7.35	
DI, mL	500	120	9.73	-22	1.762		23.77	
Sample mass,g (% Cu 3.56, Au 1.96ppm)	100	168	9.55	-9	2.267	0.258	31.36	51.44
Cu:gly 1:4								
Peroxide,%	0	6	11	-18	0.235		3.21	
pH	11	24	11	-25	0.628		8.54	
DI,mL	500	120	10.7	-42	2.505		33.87	
Sample mass,g (% Cu 3.56, Au 1.96ppm)	100	168	10.6	-35	3.372	0.211	46.68	42.33
Cu:gly 1:4								
Peroxide, %	0	6	11	-52	0.243		3.22	
pH 12		24	11	-61	0.614		8.10	
DI mL	500	120	10.6	-42	2.468		32.34	
Sample mass,g (% Cu 3.56, Au 1.96ppm)	100	168	10.5	-32	3.268	0.238	46.53	39.61
Cu:gly 1:4								
Peroxide, %	1	6	12.1	-80			5.75	
pH (NaoH)		24	11.8	-81			11.82	
DI ,mL	500	120	10.9	-51			38.71	
Sample mass, g (% Cu 3.56, Au 1.96ppm)	100	168	10.3	-26			45.93	4.17
Cu:gly 1:4								

Appendix H 11 Copper-Gold ore B leaching data

Leaching conditions		Time, h	pH	Eh, mV	[Cu], g/L	Cu extrn, % (from re-caltd h'grade)	[Au], mg/L	Au Extrn,% (from re-caltd h'grade)
		3	10.51	63	0.019	1.63	0	0.00
sample, g (0.134 Cu = 0.67g Cu in sample)	500	6	10.47	44	0.025	2.21	0	0.00
DI, mL	500	24	10.54	52	0.047	4.11	0.002	0.43
glycine,M	0.1	96	10.22	15	0.106	9.14	0.005	1.07
pH	11.06	192	10.24	36	0.152	13.03	0.008	1.71
Bottl roll, rpm	100	361	9.56	86	0.211	17.96	0.019	4.03
		528	941	135	0.246	20.85	0.026	5.45
		3	10.88	-20	0.026	2.16	0.001	0.20
sample, g (0.134 Cu = 0.67g Cu in sample)	500	6	10.79	-22	0.035	2.98	0.002	0.40
DI, mL	500	24	10.9	-7	0.066	5.56	0.004	0.79
glycine,M	0.3	96	10.64	-32	0.169	14.02	0.011	2.16
pH	11.06	192	10.63	-12	0.273	22.48	0.024	4.66
Bottl roll, rpm	100	361	10.48	40	0.444	36.24	0.058	11.13
		528	10.44	71	0.567	46.03	0.082	15.66
		3	10.94	-29	0.031	2.63	0.002	0.47
sample, g (0.134 Cu = 0.67g Cu in sample)	500	6	10.85	-40	0.04	3.46	0.002	0.47
DI, mL	500	24	10.97	-44	0.077	6.58	0.004	0.93
glycine,M	0.5	96	10.8	-57	0.202	17.01	0.017	3.89
pH	11.06	192	10.75	-23	0.335	28.00	0.034	7.72
Bottl roll, rpm	100	361	10.63	8	0.526	43.60	0.103	23.09
		528	10.58	49	0.675	55.64	0.169	37.63
		3	10.94	-64	0.041	3.51	0.003	0.69
sample, g (0.134 Cu = 0.67g Cu in sample)	500	6	10.95	-65	0.057	4.91	0.004	0.93
DI, mL	500	24	11.08	-70	0.108	9.28	0.009	2.07
glycine,M	1	96	10.94	-87	0.261	22.12	0.028	6.33
pH	11.06	192	10.86	-45	0.41	34.49	0.06	13.44
Bottl roll, rpm	100	361	10.83	-14	0.66	55.03	0.183	40.47
		528	10.85	-3	0.784	65.10	0.241	53.08
		3	7.81	82	0.019	1.61	0	0.00
sample, g (0.134 Cu = 0.67g Cu in sample)	500	6	7.83	74	0.025	2.19	0	0.00
DI, mL	500	24	7.94	99	0.084	7.23	0.001	0.24
glycine,M	0.5	96	7.89	69	0.095	8.16	0.001	0.24
pH	8	192	8.1	92	0.132	11.26	0.003	0.71
Bottl roll, rpm	100	361	7.92	163	0.188	15.90	0.005	1.27
		528	8.23	167	0.225	18.93	0.01	2.33

		3	9.05	47	0.028	2.37	0	0.00
sample, g (0.134 Cu = 0.67g Cu in sample)	500	6	8.93	19	0.042	3.53	0	0.00
DI, mL	500	24	9.1	36	0.048	4.07	0	0.00
glycine,M	0.5	96	9.05	27	0.194	16.06	0.003	0.61
pH	9	192	9.06	47	0.288	23.70	0.005	1.01
Bottl roll, rpm	100	361	8.92	83	0.404	33.03	0.015	3.04
		528	8.95	128	0.514	41.78	0.022	4.36
		3	9.97	19	0.039	3.35	0.001	0.22
sample, g (0.134 Cu = 0.67g Cu in sample)	500	6	9.94	-3	0.055	4.80	0.002	0.43
DI, mL	500	24	10.03	-19	0.114	9.82	0.004	0.85
glycine,M	0.5	96	10.02	5	0.267	22.72	0.008	1.69
pH	10	192	9.97	7	0.359	30.39	0.014	2.93
Bottl roll, rpm	100	361	9.91	45	0.51	42.84	0.03	6.23
		528	9.96	50	0.62	51.82	0.038	7.83
sample mass, g	500	1	10.02-11.11	-4	0.076	6.99	0.001	0.17
DI, mL	500	3	10.6	-25	0.146	13.43	0.01	1.64
glycine, M	0.5	6	10.62-11	-22	0.232	21.22	0.02	3.25
pH (lime)	11.22	24	9.87-10.5	-149	0.364	33.05	0.021	3.41
Temp, degrees celsius	60	48	9.22-11	34	0.62	55.77	0.093	14.83
Oxygen flow, L/min	0.3	99.5	8.59	52	0.777	65.96	0.103	15.38
Stirring speed, RPM	250							
sample mass, g	500	1	10.81	50	0.031	2.68	0.007	2.20
DI, mL	500	3	10.71	51	0.051	4.33	0.01	3.01
glycine, M	0.5	6	10.73	46	0.077	6.52	0.01	3.04
pH (lime)	11.22	24	10.66	56	0.205	17.10	0.011	3.25
Temp, degrees celsius	25	48	10.73	34	0.323	26.79	0.012	3.49
Oxygen flow, L/min	0.3	72	10.66	39	0.408	33.71	0.015	4.53
Stirring speed, RPM	250	95.5	10.08	30	0.495	40.67	0.029	8.52
sample mass, g	500	1	10.07-11.03	-9	0.074	4.44	0.008	3.35
DI, mL	500	3	10.77	-20	0.149	7.20	0.014	5.63
glycine, M	0.5	6.6	10.19-11.07	-9	0.267	10.83	0.021	8.45
pH (lime)	11.22	24	9.71-11.14	11	0.5	28.42	0.037	14.40
Temp, degrees celsius	60	48	9.51-11.07	33	0.682	44.51	0.05	19.48
Oxygen flow, L/min	0.05	72	9.17-11.08	32	0.691	56.01	0.062	23.95
Stirring speed, RPM	250	96	9.4	45	0.716	43.70	0.101	24.91
sample mass, g	500	1	10.27		0.142	9.63	0.023	4.09
DI, mL	500	3	9.96-11.27	-3	0.23	15.56	0.04	7.08
glycine, M	0.5	6	10.88	-10	0.308	20.77	0.065	11.44
pH (lime)	11.22	24	9.82-11.20	46	0.641	42.70	0.109	19.03
Temp, degrees celsius	60	48	9.45-11.09	23	0.798	52.94	0.136	23.64
Oxygen flow, L/min	0.05	72	9.00-11.38	43	0.841	55.71	0.154	26.69
Stirring speed, RPM	250	96	8.96	53	0.897	59.32	0.172	29.70
pyrite, g	4							
sample mass, g	500	1.5	10.32-11.68	5	0.101	8.88	0.016	1.83

DI, mL	500	3	10.39		0.138	12.10	0.023	3.08
glycine, M	0.5	6	10.48	-27	0.236	20.57	0.044	4.62
pH (lime)	11.22	24	9.96-11.53	37	0.482	41.49	0.085	7.88
Temp, degrees celsius	60	48	9.87-11.30	-6	0.652	55.90	0.134	10.67
Oxygen flow, L/min	0.05	72	9.96-11.20	34	0.7	59.84	0.158	13.11
Stirring speed, RPM	250	96			0.618	53.64	0.168	21.35
pyrite, g	2							
No pyrite		1	10.73	-12	0.063	4.70	0.011	2.37
sample mass, g	500	3	10.75	-7	0.124	9.24	0.031	6.55
DI, mL	500	6	10.21-11.5	5	0.207	15.27	0.04	8.41
glycine, M	0.5	24	10.08-11.46	-5	0.348	25.50	0.073	15.03
pH (lime)	11.7	48	9.48-11.56	19	0.604	43.89	0.122	24.93
Temp, degrees celsius	60	72	9.81-11.52	15	0.587	42.69	0.209	42.29
Oxygen flow, L/min	0.05	96	10.15	47	0.494	36.53	0.22	44.93

Appendix H 12 Copper- Gold ore C leaching data

leaching conditions		Time, h	pH	Eh, mV	[Cu], g/L	Cu extrn, % (from re-caltd h'grade)	[Au], mg/L	Au Extrn,% (from re-caltd h'grade)
		3	10.51	63	0.019	1.63	0	0.00
sample, g (0.134 Cu = 0.67g Cu in sample)	500	6	10.47	44	0.025	2.21	0	0.00
DI, mL	500	24	10.54	52	0.047	4.11	0.002	0.43
glycine,M	0.1	96	10.22	15	0.106	9.14	0.005	1.07
pH	11.06	192	10.24	36	0.152	13.03	0.008	1.71
Bottl roll, rpm	100	361	9.56	86	0.211	17.96	0.019	4.03
		528	941	135	0.246	20.85	0.026	5.45
		3	10.88	-20	0.026	2.16	0.001	0.20
sample, g (0.134 Cu = 0.67g Cu in sample)	500	6	10.79	-22	0.035	2.98	0.002	0.40
DI, mL	500	24	10.9	-7	0.066	5.56	0.004	0.79
glycine,M	0.3	96	10.64	-32	0.169	14.02	0.011	2.16
pH	11.06	192	10.63	-12	0.273	22.48	0.024	4.66
Bottl roll, rpm	100	361	10.48	40	0.444	36.24	0.058	11.13
		528	10.44	71	0.567	46.03	0.082	15.66
		3	10.94	-29	0.031	2.63	0.002	0.47
sample, g (0.134 Cu = 0.67g Cu in sample)	500	6	10.85	-40	0.04	3.46	0.002	0.47
DI, mL	500	24	10.97	-44	0.077	6.58	0.004	0.93
glycine,M	0.5	96	10.8	-57	0.202	17.01	0.017	3.89
pH	11.06	192	10.75	-23	0.335	28.00	0.034	7.72
Bottl roll, rpm	100	361	10.63	8	0.526	43.60	0.103	23.09
		528	10.58	49	0.675	55.64	0.169	37.63
		3	10.94	-64	0.041	3.51	0.003	0.69

sample, g (0.134 Cu = 0.67g Cu in sample)	500	6	10.95	-65	0.057	4.91	0.004	0.93
DI, mL	500	24	11.08	-70	0.108	9.28	0.009	2.07
glycine,M	1	96	10.94	-87	0.261	22.12	0.028	6.33
pH	11.06	192	10.86	-45	0.41	34.49	0.06	13.44
Bottl roll, rpm	100	361	10.83	-14	0.66	55.03	0.183	40.47
		528	10.85	-3	0.784	65.10	0.241	53.08
		3	7.81	82	0.019	1.61	0	0.00
sample, g (0.134 Cu = 0.67g Cu in sample)	500	6	7.83	74	0.025	2.19	0	0.00
DI, mL	500	24	7.94	99	0.084	7.23	0.001	0.24
glycine,M	0.5	96	7.89	69	0.095	8.16	0.001	0.24
pH	8	192	8.1	92	0.132	11.26	0.003	0.71
Bottl roll, rpm	100	361	7.92	163	0.188	15.90	0.005	1.27
		528	8.23	167	0.225	18.93	0.01	2.33
		3	9.05	47	0.028	2.37	0	0.00
sample, g (0.134 Cu = 0.67g Cu in sample)	500	6	8.93	19	0.042	3.53	0	0.00
DI, mL	500	24	9.1	36	0.048	4.07	0	0.00
glycine,M	0.5	96	9.05	27	0.194	16.06	0.003	0.61
pH	9	192	9.06	47	0.288	23.70	0.005	1.01
Bottl roll, rpm	100	361	8.92	83	0.404	33.03	0.015	3.04
		528	8.95	128	0.514	41.78	0.022	4.36
		3	9.97	19	0.039	3.35	0.001	0.22
sample, g (0.134 Cu = 0.67g Cu in sample)	500	6	9.94	-3	0.055	4.80	0.002	0.43
DI, mL	500	24	10.03	-19	0.114	9.82	0.004	0.85
glycine,M	0.5	96	10.02	5	0.267	22.72	0.008	1.69
pH	10	192	9.97	7	0.359	30.39	0.014	2.93
Bottl roll, rpm	100	361	9.91	45	0.51	42.84	0.03	6.23
		528	9.96	50	0.62	51.82	0.038	7.83
sample mass, g	500	1	10.02-11.11	-4	0.076	6.99	0.001	0.17
DI, mL	500	3	10.6	-25	0.146	13.43	0.01	1.64
glycine, M	0.5	6	10.62-11	-22	0.232	21.22	0.02	3.25
pH (lime)	11.22	24	9.87-10.5	-149	0.364	33.05	0.021	3.41
Temp, degrees celsius	60	48	9.22-11	34	0.62	55.77	0.093	14.83
Oxygen flow, L/min	0.3	99.5	8.59	52	0.777	65.96	0.103	15.38
Stirring speed, RPM	250							
sample mass, g	500	1	10.81	50	0.031	2.68	0.007	2.20
DI, mL	500	3	10.71	51	0.051	4.33	0.01	3.01
glycine, M	0.5	6	10.73	46	0.077	6.52	0.01	3.04
pH (lime)	11.22	24	10.66	56	0.205	17.10	0.011	3.25
Temp, degrees celsius	25	48	10.73	34	0.323	26.79	0.012	3.49
Oxygen flow, L/min	0.3	72	10.66	39	0.408	33.71	0.015	4.53
Stirring speed, RPM	250	95.5	10.08	30	0.495	40.67	0.029	8.52
sample mass, g	500	1	10.07-11.03	-9	0.074	4.44	0.008	3.35

DI, mL	500	3	10.77	-20	0.149	7.20	0.014	5.63
glycine, M	0.5	6.6	10.19-11.07	-9	0.267	10.83	0.021	8.45
pH (lime)	11.22	24	9.71-11.14	11	0.5	28.42	0.037	14.40
Temp, degrees celsius	60	48	9.51-11.07	33	0.682	44.51	0.05	19.48
Oxygen flow, L/min	0.05	72	9.17-11.08	32	0.691	56.01	0.062	23.95
Stirring speed, RPM	250	96	9.4	45	0.716	43.70	0.101	24.91
sample mass, g	500	1	10.27		0.142	9.63	0.023	4.09
DI, mL	500	3	9.96-11.27	-3	0.23	15.56	0.04	7.08
glycine, M	0.5	6	10.88	-10	0.308	20.77	0.065	11.44
pH (lime)	11.22	24	9.82-11.20	46	0.641	42.70	0.109	19.03
Temp, degrees celsius	60	48	9.45-11.09	23	0.798	52.94	0.136	23.64
Oxygen flow, L/min	0.05	72	9.00-11.38	43	0.841	55.71	0.154	26.69
Stirring speed, RPM	250	96	8.96	53	0.897	59.32	0.172	29.70
pyrite, g	4							
sample mass, g	500	1.5	10.32-11.68	5	0.101	8.88	0.016	1.83
DI, mL	500	3	10.39		0.138	12.10	0.023	3.08
glycine, M	0.5	6	10.48	-27	0.236	20.57	0.044	4.62
pH (lime)	11.22	24	9.96-11.53	37	0.482	41.49	0.085	7.88
Temp, degrees celsius	60	48	9.87-11.30	-6	0.652	55.90	0.134	10.67
Oxygen flow, L/min	0.05	72	9.96-11.20	34	0.7	59.84	0.158	13.11
Stirring speed, RPM	250	96			0.618	53.64	0.168	21.35
pyrite, g	2							
No pyrite		1	10.73	-12	0.063	4.70	0.011	2.37
sample mass, g	500	3	10.75	-7	0.124	9.24	0.031	6.55
DI, mL	500	6	10.21-11.5	5	0.207	15.27	0.04	8.41
glycine, M	0.5	24	10.08-11.46	-5	0.348	25.50	0.073	15.03
pH (lime)	11.7	48	9.48-11.56	19	0.604	43.89	0.122	24.93
Temp, degrees celsius	60	72	9.81-11.52	15	0.587	42.69	0.209	42.29
Oxygen flow, L/min	0.05	96	10.15	47	0.494	36.53	0.22	44.93
Stirring speed, RPM	250							

Appendix H 13 Copper-Gold ore C column leaching data

Leaching conditions		Time, days	pH	Eh (mV)	[Cu], mg/L	Cu extrn ,%	[Au], mg/L	Au extrn, %
Sample mass, g	5000	0.063	10.56	55	5	0.32		
DI, L	3	0.15	11.05	45	7.3	0.46		
[Cu] in ore, %	0.095	0.25			14.9	0.94		
expected Cu in soln, g/L	1.5833	1	10.95-11.12	33	20.5	1.29		
[Au] in ore, %	8E-05	3	11.2	55	26.17	1.65		
expected Au in soln	0.0013	10	10.48-11.30	27	35.5	2.24		
solution flow, ml/min	3.5	28	10.96	-32	42.25	2.67		
[Gly], M	0.1	39	10.39	33	56.175	3.55		
		56			88.075	5.56		
		60			88.875	5.61		
		87			101	6.38	0.007	0.54
		111			115	7.26	0.019	1.46
		125	9.89-11.45		121	7.64		0.00
		159			147.25	9.30	0.009	0.68
		166			148	9.35	0.023	1.76
mass sample, g	5000	1	10.46	9	22.4	1.41		0.00
DI, L	3	4	10.42	65	24.95	1.58		0.00
[Cu] in ore, %	0.095	8			32.05	2.02		0.00
expected Cu in solution	1.5833	30			80	5.05		0.00
[Au] in ore, %	8E-05	36			94.375	5.96	0.004	0.31
expected Au in soln	0.0013	60			105	6.63	0.007	0.54
solution flow, ml/min	3.5	74	10.44-11.21		110.425	6.97		
[Gly], M	0.5	103			152.125	9.61	5E-04	0.04
		115			156	9.85	0.013	1.00

Appendix H 14 Copper-Gold D column leaching data

Leaching conditions		Time, days	pH	[Cu], g/L	Cu extrn, %	[Au], mg/L	Au extrn, %
Total sample mass, g	2698.7	1	9.39	0.348	7.07		
minus 2mm, g	1553.3	3	9.24	0.498	10.11		
plus 2 mm, g	1145.4	7	8.99	0.912	18.52		
Soln vol, L	2	14	8.87	1.3825	28.07		
Soln pH	11.04	24	9.97	0.9741	39.56		
slon flow rate, mL/min	14.4	40		1.15	46.70	0.022	5.03
% Cu in sample	0.365	49	9.5	1.32	53.60	0.033	7.55
expexted Cu in soln b4 19/04/16, g/L	4.92513						
expexted Cu in soln, g/L	2.46256						
on 19/04/2016, (14 days) leaching solution was diluted with 2L of same composition							
Au in ore , %	6.5E-05						
[Au] in soln, g/L	0.00044						

Appendix H 15 Example of copper and gold leaching rates from recalculated head grades- leaching Cu-Au ore C with 0.5 M [Gly]

				Recordings		Cu removed from soln						U removed from sol				
Time (hours)	Ore (g)	Solution volume (mL)	sol ,L	[Cu],g/L	Au, ppm	vol(mL)	Cu (g)	Cumm Cu (g)	Cu leach vessel (g)	Cu extrn total(g)	Soln Cu extrn %	Au (µg)	Cumm Au (µg)	Au leach vessel (µg)	Au extrn total(µg)	Soln Au extrn %
	500															
0		500	0.5			0					0					0
3		490	0.49	0.0305	0.002	10	0.00031	0.00031	0.01495	0.01495	2.626	0.02000	0.02000	0.98000	0.98000	0.469
6		485	0.485	0.04	0.002	5	0.00020	0.00051	0.01940	0.01971	3.462	0.01000	0.03000	0.97000	0.99000	0.474
24		480	0.48	0.077	0.004	5	0.00039	0.00089	0.03696	0.03747	6.583	0.02000	0.05000	1.92000	1.95000	0.934
96		475	0.475	0.202	0.017	5	0.00101	0.00190	0.09595	0.09684	17.015	0.08500	0.13500	8.07500	8.12500	3.892
192		470	0.47	0.335	0.034	5	0.00168	0.00358	0.15745	0.15935	27.998	0.17000	0.30500	15.98000	16.11500	7.720
361		465	0.465	0.526	0.103	5	0.00263	0.00621	0.24459	0.24817	43.602	0.51500	0.82000	47.89500	48.20000	23.090
528		460	0.46	0.675	0.169				0.31050	0.31671	55.645			77.74000	78.56000	37.634
						35	**0.00621**					**0.82000**				

Cu			
Product	Qty	grade	mass,g
Solids	495	0.051	0.25245
Solution	0.46	0.675	0.3105
Removed			0.006205
Total			0.569155

GOLD EXTRACTION CALCULATIONS				
PRODUCT	Quantity		GOLD	
		GRADE (ppm)	MASS (µg)	DISTn. (%)
SOLIDS	495.0	0.263	130	62.37
SOLUTION	460.0	0.169	78	37.24
REMOVED			0.82	0.39
GRAVITY				
TOTAL	955.0		209	100.00
CALC'd HEAD		0.42		